GEOSPATIAL ANALYSIS OF TOTAL MERCURY CONCENTRATIONS IN STREAM AND LAKE SEDIMENTS ACROSS CANADA

by

Mina Nasr

MSc Forestry and Environmental Management, University of New Brunswick, 2007

A Dissertation Submitted in Partial Fulfillment
of the Requirements for the Degree of

Doctor of Philosophy

in the Graduate Academic Unit of Forestry and Environmental Management

Supervisor: Paul A. Arp, PhD, Forestry and Environmental Management

Examining Board: Michelle Gray, PhD, Forestry and Environmental Management
Charles Bourque, PhD, Forestry and Environmental Management
Bruce Broster, PhD, Earth Sciences

External Examiner: David Lean, PhD, University of Ottawa

This dissertation is accepted by the
Dean of Graduate Studies

THE UNIVERSITY OF NEW BRUNSWICK

September, 2015

Abstract

This study focused on geospatially analyzing and mapping total mercury concentrations (THg) in stream and lake sediments across Canada, as compiled by the sediment surveys of the Geological Survey of Canada, Quebec, and Nova Scotia (total number of samples = 254,133). The objective was to quantify how sediment THg varies by atmospheric Hg deposition, climate, geology, topography, stream and lake morphology, vegetation/land cover type, and sediment composition pertaining to other elements and to organic matter (determined through loss on ignition: LOI).

On average, upland sediments have slightly but still significantly higher THg values (streams: 97.8 ± 1.4 SE; lakes: 113.2 ± 1.1 SE, ppb) than lowland sediments (streams: 90.1 ± 2.2 SE; lakes: 90.4 ± 0.2 SE, ppb). Lake sediment THg increases with increasing lake depth and decreasing lake area (p–value < 0.0001). Stream sediment THg increases with increasing stream depth and decreasing flow rate, order, and width (p–value < 0.0001).

Mean sediment THg decreases from forests to tundra, barrens, and ice– and snow–covered basins (p–value < 0.0001). In wetland-dominated basins, sediment THg decreases by approximately a factor of two as the wet–area portion per basin increases from 0 to 40 %. Swamp dominated basins have higher sediment THg than marsh and bog/fen dominated basins (p–value < 0.0001). Highest sediment THg occurs downstream from high Hg–containing geogenic and anthropogenic sources, with sediment THg related to other heavy metals such as copper and zinc (p–value < 0.0001).

The examination of 10^{th}, 25^{th}, 50^{th}, 75^{th} and 90^{th} percentiles of sediment THg displays parallel trends with increasing LOI, being lowest at LOI = 0 and highest at 30 to 50 %. This suggests that geogenic THg contributions to sediments decrease as the organic THg contributions increase. The latter relates positively to mean annual atmospheric Hg deposition and precipitation rates, and more so for lakes than for streams. The regression coefficient between lake sediment THg and mean atmospheric Hg deposition and precipitation rates amounts to 0.432 (p–value < 0.0001) per National Topographic System (NTS, 1:250,000) tile.

The standardized fish Hg concentration of the Fish Mercury Datalayer for Canada (FIMDAC) relate positively to lake sediment THg, but negatively to mean annual July temperature. This association explains 38.2 % of the mean fish Hg concentration variations per NTS tile. Hence, the climate and atmospheric Hg variations across Canada not only contribute to the Hg concentration variations in sediments but also in fish.

Dedication

To my beloved family Ali & Abtin Hozouri

Acknowledgements

It is with immense gratitude that I acknowledge the continuous guidance of my supervisor Dr. Paul Arp, whose expertise and dedication added much to my PhD study. I am so thankful that the insightful comments and encouragement from my other advisory committee, Drs. Dave MacLean and Andy Rencz, widened the perspectives of my research. The diligent effort from my examiners, Drs. David Lean, Michelle Gray, Charles Bourque, and Bruce Broster, in reviewing my thesis added a great value to the delivery of my research findings.

This study would not have been possible without the generous financial support from Environment Canada through the Clean Air Regulatory Agenda (CARA) Science Program, as facilitated by Dr. Heather Morrison and additional support from the Forest Watershed Research Center of the Faculty of Forestry and Environmental Management at UNB.

In preparation for this study, I received access to many data: (i) the Geological Survey of Canada open files for the sediment surveys across Canada, including Quebec and Nova Scotia (c/o Dr. Andy Rencz, Natural Resources Canada); (ii) the Global/Regional Atmospheric Heavy Metals Model (GRAHM) for atmospheric mercury deposition data (c/o Dr. Ashu Dastoor, Environment Canada); and (iii) the Fish Mercury Datalayer for Canada (FIDMAC; c/o Dr. Linda Campbell, Saint Mary's university). Technical assistance in GIS, computer programming, data analysis, and IT services was provided in a great extent by Jae Ogilvie, Mark Castonguay, John Paul Arp, Marie-France Jones, and Duc Banh from UNB.

In addition, I would like to express my great appreciation to the unconditional love and patience of my husband and son, Ali and Abtin Hozouri, during my study. Without the emotional support, attention, and encouragement from my parents, Mounes and Mostafa, my siblings, especially Danial, and my very special friends, Phillis and George Farrell, I would not be able to accomplish this journey smoothly.

Table of Contents

List of Tables

List of Figures

List of Abbreviations, Acronyms, and Conventions

Area:

A_B	Area of Basin (Watershed)
AW	Area of Wet-area

Climate:

atm.Hgdep	Atmospheric Mercury Deposition
ppt	Precipitation
T	Temperature
$T_{Jan.}$	January Temperature
T_{July}	July Temperature

Element:

Ag	Silver
As	Arsenic
Au	Gold
C	Carbon
Ca	Calcium
Cd	Cadmium
Co	Cobalt
Cu	Copper
F	Fluorine
Fe	Iron
Ge	Germanium
Mn	Manganese
Ni	Nitrogen
Ni	Nickel
Pb	Lead
S	Sulphur
Sb	Antimony
Zn	Zinc
U	Uranium

THg	Total Mercury Concentration
CH_3Hg^+	Methyl Mercury Cation/MeHg
HgS	Mercuric Sulphide/Cinnabar
Hg^0	Gaseous Mercury

Statistic:

Critic. Diff.	Critical Difference
Eq.	Equation
Std. Dev., SD	Standard Deviation
Std. Err., SE	Standard Error
Coeff.	Regression Coefficient

Units:

˚	Degree

Geospatial Analysis:

DEM	Digital Elevation Model
DTW	Depth to Water Index
WAM	Wet Area Mapping

Organic Substance:

DOC	Dissolved Organic Carbon
DOM	Dissolved Organic Matter
LOI	Loss on Ignition
POC	Particulate Organic Carbon
POM	Particulate Organic Carbon

Province/Territory:

AB	Alberta
BC	British Colombia
Lab	Labrador
MB	Manitoba
NB	New Brunswick
NL	Newfoundland and Labrador
NWT	Northwest Territories
NS	Nova Scotia
NU	Nunavut
ON	Ontario
QC	Quebec
SK	Saskatchewan
YT	Yukon Territory

Quebec Geological Survey Zone:

Abitibi A	Abitibi Pontiac A
Minto B	Minto Bienville Ashuanipi B
Opatica	Opatica La Grande Opinaca
	Nemiscau
	Minto A

˚C	Degree Centigrade
Bya	Billion Years Ago
ha	Hectare
m a^{-2}	Meter per Year (annual)
µg m^{-2} a^{-1}	Microgram per Square Meter per Year
Mya	Million Years Ago
ppb	Parts per Billion
ppm	Parts per Million
%	Percentage

Conventions:

AAS	Atomic Absorption Spectrometry
CANCP	Canadian Northern Contaminants Program
CARA	Clean Air Regulatory Agenda
COMERN	Collaborative Mercury Research Network
FIMDAC	Fish Mercury Datalayer for Canada
GME	Geospatial Modelling Environment
GSC	Geological Survey of Canada
GRAHM2005	2005 Global/Regional Atmospheric Heavy Metals Model
ICMGP	Mercury as a Global Pollutant
ICP-MS	Inductive Coupling Mass Spectrometry
METAALICUS	Mercury Experiment to Assess Atmospheric Loading in Canada and
USA NGR	National Geochemical Reconnaissance
NRC	National Resources Canada
NTDB	National Topographical Database
NTS	National Topographic System
PRISM	Parameter-elevation Regressions on Independent Slopes
SRTM	Shuttle Radar Topography
URP	Uranium Reconnaissance Program
USEPA	US Environmental Protection Agency
VMS	Volcano-massive sulphide

Chapter 1 General Introduction

Scope and Objectives

The main objective of this study was to quantify how the survey data of the Geological Survey of Canada (GSC), Quebec (QC) and Nova Scotia (NS) for total mercury concentration (THg) in stream and lake sediments relate to:

- sediment-external variables (geology, climate, topography, stream and lake morphologies, and vegetation/land cover type), and
- sediment-internal variables that pertain to sediment composition including organic matter and other elemental contents across Canada.

The second objective was to use the resulting quantified relationships for the mapping of sediment THg, as influenced specifically by atmospheric Hg deposition and by climate, as represented by mean annual precipitation rate and January and July temperatures, to reflect the maximum and minimum annual temperature excursions across Canada. Both objectives were aligned with other concurrent Canadian Hg study objectives, namely:

- To advance Hg related policy formulations in terms of quantifiable relationships between atmospheric Hg deposition rate and sediment Hg in the context of long-range Hg transport and climate change (Kirk *et al.*, 2011; Braun *et al.*, 2014; Chételat *et al.*, 2014).
- To assemble baseline sediment data for the purpose of modelling and mapping Hg accumulations in sediments (Morrison, 2011).

- To model and map how various anthropogenic, geogenic, climatic, vegetative, and topographic factors influence actual sediment Hg loadings (Morrison, 2011).
- To provide Canada-wide data layers that should be proven useful for estimating (i) the extent of Hg mobilization from soils towards streams and lakes, (ii) the extent of Hg re-mobilization from stream and lake sediments through various process such as volatilization and Hg methylation, (iii) and subsequent Hg bioaccumulation and uptake of Hg by fish (Depew *et al.*, 2013a, b).

The study of this Thesis was done in support of the Mercury Science Program of the Clean Air Regulatory Agenda of Canada (CARA; Morrison, 2011). The Phase 1 goal of that program was: "… to enhance and advance on-going and past research and monitoring efforts to develop a cohesive national description of Hg pollution in Canada" (Morrison, 2011). With this mandate, and focusing on stream and lake sediment THg in particular, the aim of this study was to provide integrative representations and interpretations of how sediment THg varies across Canada, and how this variation could be mapped and linked to evaluate potential Hg bioaccumulation risks in streams and lakes.

Thesis Structure

This thesis is structured as follows:

Chapter 1 describes the scope of the study, objectives, and the thesis structure.

Chapter 2 provides sediment related literature reviews on Hg and related processes.

Chapter 3 illustrates the methods of (i) data gathering, sorting, compilation, and statistical analysis and (ii) geospatial analysis including upland/lowland sampling point divisions, and drainage basin and wet-area delineations above each sediment sampling point. A number of case studies for basin-specific examinations are also described.

Chapter 4 provides results from an overview of sediment THg across Canada, by highlighting areas with extremely high and low THg, stream versus lake, and upland versus lowland location.

Chapter 5 presents the results on the relationship between sediment THg and atmospheric Hg deposition and precipitation rates and air temperatures.

Chapter 6 provides the results on the sediment THg variation in relation to sediment organic matter content and atmospheric Hg deposition and precipitation rates and air temperatures.

Chapter 7 provides the results on the sediment THg variation by sediment composition (organic matter and other elemental contents), and other factors including geology, topography, and stream and lake morphologies.

Chapter 8 provides illustrations on how sediment THg varies by geological region and elaborates briefly on the regression results of Chapter 7.

Chapter 9 provides results on the relationship between sediment THg and the wet-area proportion of the basins above sediment sampling locations, for selected case studies.

Chapters 10 and 11 provide a general discussion and summary of the results including claims of original contributions and recommendations for further research.

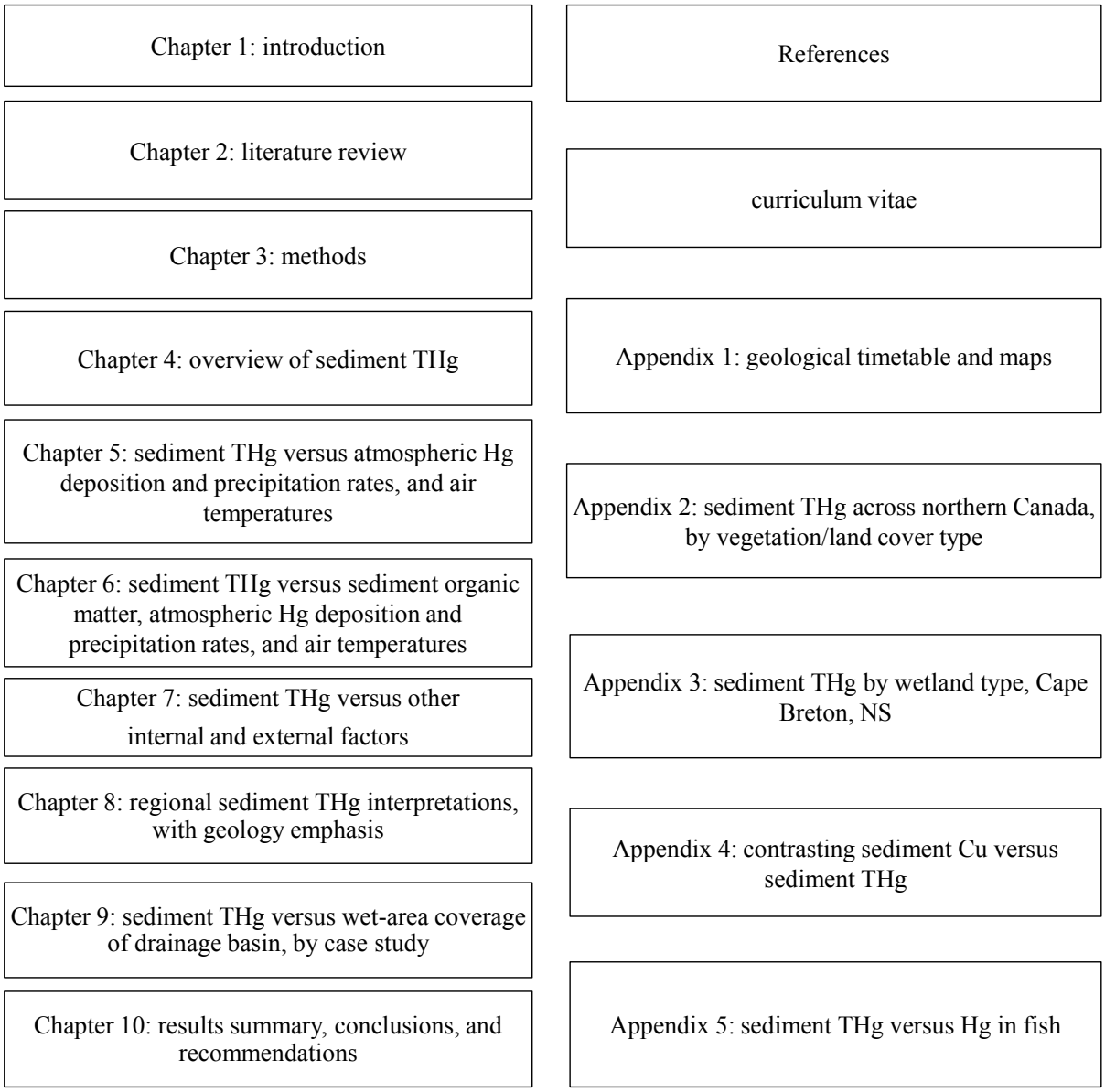

Figure 1.1 Thesis structure.

Appendix 1 contains supplementary materials of geological timetable and bedrock geology maps for NS and YT.

Appendix 2 presents the analysis results on the relationship between sediment THg and vegetation/land cover type and climate conditions.

Appendix 3 presents the analysis results on the relationship between sediment THg and vegetation/land cover and wetland types of Cape Breton, NS.

Appendix 4 provides the analysis results on sediment Cu and organic matter content relationships, similar to the sediment analysis of Chapter 6 for sediment THg.

Appendix 5 presents the extent to which Hg concentrations in fish relates to sediment THg across Canada.

The results of the GSC, QC, and NS sediment survey data are summarized in Chapters 4 to 9, and also in Appendix 2 to 5. Maps that show how sediment THg as well as sediment LOI vary regionally across Canada and for selected areas are presented in Chapters 4 to 9. For earlier sediment THg summaries across Canada, see Rasmussen (1998a) and Nasr *et al. (*2011).

Much of what is described in Chapters 4, and in combination with the YT component of Chapter 8, can be found in Nasr M., Ogilvie J., Castonguay M., Rencz A., Arp P.A: total Hg concentrations in stream and lake sediments: discerning geospatial patterns and controls across Canada. Applied Geochemistry 2011; 26: 1818-1831.

A preceding version of Appendix 2 appears in Nasr M. and Arp P.A.: spatial analysis of Hg levels in bulk sediment from Arctic streams and lakes. In book: Mercury in Canada's North, Chapter 5: Freshwater Environment. Editors: Chételat J., Braune. Aboriginal Affairs and Northern Development 2011; 110-111.

A further summation of Appendix 2 appears in Chételat J., Amyot M., Arp P., Blais J.M., Depew D., Emmerton C.A., Evans M., Gamberg M., Gantner N., Girard C., Graydon J., Kirk J., Lean D., Lehnherr I., Muir D., Nasr M., Poulain A., Power M.,

Roach P., Stern G., Swanson H., van der Velden S. 2014. Science of the Total Environ: Special Issue: Mercury in Canada's North 2015; 509-510: 41-66.

A combination of Chapter 4, 7 and 8 results will appear in Nasr M. and Arp P.A.: total mercury concentrations in stream and lake sediments across Canada. Environment Canada Report: Canadian Mercury Science Assessment 2015 Chapter 3b. In print.

Chapter 2 Literature Review

Primary Hg Concerns

The primary concern about sediment THg is based on many earlier studies alerting about the bioaccumulation of toxic methyl Hg (MeHg) in fish and other aquatic biota, as reviewed by, e.g. Rasmussen *et al. (*1998b), Chen *et al. (*2014), and Wentz *et al. (*2014). These reviews were in part centered on the following initiatives:

- the Mercury Experiment to Assess Atmospheric Loadings in Canada and the US (METAALICUS-1999; US Department of Interior and US Geological Survey, 2013);
- the Collaborative Mercury Research Network (COMERN, Université du Québec à Montréal, 2001);
- the Canadian Arctic Northern Contaminants Program (CANCP-1992; Government of Canada, Environment Canada, 2013a);
- the Clean Air Regulatory Agenda of Canada CARA-2006 (Government of Canada, 2013b).

It is now known that Hg bioaccumulation within streams, lakes, and other surface water bodies occurs through the methylation of Hg, with sulfate- and iron-reducing bacteria being the primary methylation agents (Fleming *et al.*, 2006; Kerin *et al.*, 2006). The subsequently low turn-over rate of organism-ingested MeHg leads to a trophic build-up of MeHg in muscle and brain tissues, with highest levels in top predatory fish, fish-eating otter, seals, and birds such as loons, gulls and eagles (Wong *et al.*, 1997;

Chen *et al.*, 2005; Kainz and Mazumder, 2005; Otorowkski, 2005; Kainz *et al.*, 2008; Spencer *et al.,* 2011). On land, Hg bioaccumulation starts with the sequestration of atmospheric Hg. At the base of terrestrial Hg bioaccumulation are litter-digesting soil organisms (USEPA, 2009). On land and in water bodies, accumulating Hg and MeHg contribute to sediment THg.

Sediment Hg Accumulation Pathway

To determine how THg varies in stream and lake sediments, it is important to consider the transfer processes of Hg from its sources to sediment accumulation locations (Figure 1.1). These processes involve sequestration of atmospheric Hg deposition and retention of geologically/anthropogenic Hg release and emissions (Government of Canada, Environment Canada, 2014). A part of terrestrial retained Hg is gradually released into streams and lakes through (i) litter inputs (detritus), (ii) upslope soil and streambed erosion, and (iii) by dissolved organic matter (DOC; Grigal, 2002; Meng *et al.,* 2005; Demers, *et al.,* 2007; Dittman *et al.,* 2010). With regard to detrital Hg inputs, tree foliage, twigs, branches, bark, and wood have lower Hg concentrations than mosses, fungi, and lichens (Nasr and Arp, 2015a).

In soils, Hg concentrations decrease with increasing depth from the organic litter layers on the surface to the subsoil layers below (Nasr, 2007; Nasr *et al.*, 2011). Downstream, the total amount of Hg generally increases with increasing organic matter transfer (Schuster *et al.*, 2008), which then leads to increasing Hg and organic matter accumulations in stream and lake sediments (Sanei and Goodarzi, 2006; Ghorpade *et al.,* 2009; Riscassi and Scanlon, 2011; Zhang *et al.,* 2014).

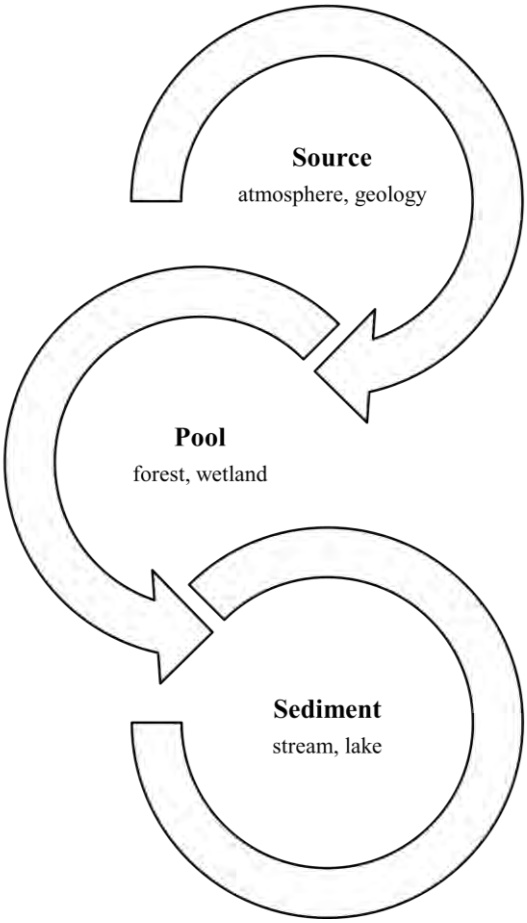

Figure 2.1 Accumulation pathway of Hg in stream and lake sediments.

In comparison, streams and lakes downslope from forested and wetland dominated watersheds have higher THg and dissolved and particulate organic matter content than elsewhere (Jutras *et al.,* 2011; Teisserenc *et al.,* 2011; Demers *et al.,* 2011; Dick, *et al.,* 2015; Mei *et al.,* 2014).

Sediment Hg Sources

Sediments at the bottom of streams and lakes contain Hg from atmospheric, geologic, and/or anthropogenic sources (Donovan *et al.*, 2014; Parsons *et al.*, 2014).

Geologic or "geogenic" sources refer to the release of Hg from surface-exposed Hg minerals. These are usually associated with heavy metal mineralization in local bedrock formations. Anthropogenic sources refer to human activities that involve retrieving, processing, using, emitting, discarding and discharging Hg and Hg-containing compounds as part of industrial, medical or residential processes (Strode *et al.,* 2009; Pirrone *et al.*, 2010). Examples include artisanal (small scale, using traditional methods) to industrial use of Hg in Au mining, releasing Hg containing wastewater from chloralkali electrolysis, pulp and paper plants, mine tailing ponds, and emitting Hg from incinerators, smelters, coal burning power plants, Au and Ag mines.

Atmospheric, geogenic and anthropogenic contributions to sediment THg vary locally by the strength of local Hg sources. These sources are mostly atmospheric in small upland basins on Hg-free bedrock formations (Paulson, 2004), mostly geogenic in areas with considerable Hg mineralization (Plouffe, 1997; Friske and Coker, 1995), and mostly anthropogenic downslope and downwind from past and present locations where Hg is being discarded (Gray *et al.*, 2000; Ashley and Rytuba, 2008).

Geological Processes

Geological processes such as volcanic eruptions, geothermal activities, glacial dispersal, and bedrock weathering all affect the extent to which Hg accumulates in sediments, from past to present (Coker *et al.*, 1995; Jebrak *et al.*, 2002; Gustin, 2003; Smith *et al.*, 2008; Bagnatoa *et al.*, 2009; Qingua and Mingcai, 2009). For example, black shale, a fine grained sedimentary rock, rich in organic C and S, contains 4-15 times higher Hg concentrations (200-800 ppb) than marble, sandstone, gneiss, granite, mica

schist, and quartzite (Friske and Coker, 1995; Loukola-Ruskeeniemi *et al.*, 2003). In bedrock formations, heavy metal mineralization with high S content have high Hg contents. Examples are phyllite and argillite bedrocks with high pyrite (FeS_2) and elevated Hg contents (Franzen *et al.*, 2004). Subsequently, the oxidation and weathering of black shales, phyllites, and argillites contribute to the release of Hg into soil, water, wetlands, and stream and lake sediments (Loukola-Ruskeeniemi *et al.*, 2003).

Apart from geological sources, areas disturbed by past and present mining activities, reservoir development, industrial, residential and agricultural activities, and forest fire further elevate the transfer of upland Hg to streams and lakes, often through enhanced rates of soil erosion (Louchouarn *et al.*, 1993; Caldwell *et al.,* 2000; Gelinas *et al.*, 2000; Ashley and Rytuba, 2008; Caron *et al.*, 2008).

Atmospheric Hg Deposition

Recent developments in regional and global circulation modelling of air pollutants, including Hg, have produced Canada-wide annual and monthly atmospheric Hg deposition maps, with local Hg deposition rates generally increasing with increasing precipitation rates, and decreasing with increasing remoteness towards the east, west and north of Canada (Dastoor and Larocque, 2004; Dastoor and Davignon, 2009). This mapping effort is based on a systematic inventory and tracking of industrial and residential Hg emissions. It accounts for wet and dry Hg deposition including vegetative Hg sequestration according to spatially and temporally varying ground and surface conditions. Additional mapping efforts address natural Hg emissions (Gbor *et al.*, 2007)

as well as the depletion of atmospherically-deposited Hg through season and climate influenced re-volatilization (Dastoor *et al.*, 2008; Zhang *et al.*, 2009).

Geographic Location and Climate

Across Canada, the presence of Hg in stream and lake sediments varies by geographic location (Nasr *et al.*, 2011). For example, while atmospheric Hg deposition can be extensive in the Arctic during short periods following polar sunrise, only small amounts of the deposited Hg remain on snow and ice-covered ground (Bidleman *et al.*, 2003; Steffen *et al.*, 2008; Canuel *et al.*, 2009). The remaining Hg, however, can contribute significantly to stream and lake THg during snowmelt (Lahoutifard *et al.*, 2005, 2006), and to subsequent bioaccumulation (Bidleman *et al.*, 2003). Mean THg of the arctic sediments remain quite low at < 170 ppb (Lockhart, 2003), but an increasing trend for sediment THg has been noted for the eastern Arctic (Diamond *et al.*, 2003; Muir *et al.*, 2009). Moore *et al. (*2014) changing air and ground temperature as the result of climate affect the atmospheric Hg deposition on arctic land surfaces.

Under subarctic to boreal conditions, longer growing seasons and less extensive snow and ice-cover intensify atmospheric Hg scavenging by vegetation on land and in water (Outridge *et al.*, 2007). Regardless of the local/regional/global source of Hg, at mid-latitude locations (49-60˚ N), sediment THg accumulation varies widely dependent on topographic conditions, geological processes, vegetation type, local landuse, industrial and residential developments, and recreational traffic (Bubb *et al.*, 1994; Coker *et al.*, 1995; Mills *et al.*, 2009). In addition, extensive wetland cover filters, retains, and transforms much of the incoming Hg as it arrives in mineral, organic, particulate or

dissolved form (Driscoll *et al.*, 1998; Hintelmann *et al.*, 2002; Hissler and Probst, 2006; Bash and Miller, 2007; Caron *et al.*, 2008; Yu *et al.*, 2008; Kolker *et al.*, 2010). Similar to the Artic, Hg re-volatilization from snow (Lalonde *et al.*, 2002) and from other open water surfaces (Bash *et al.*, 2007) lowers the net Hg accumulation in stream and lake sediments in other regions of Canada.

Stream and Lake *in situ* Processes

Hg loads and retention in sediments depend on *in situ* physical, chemical, and biological processes (Bengtsson and Picado, 2008; Hintelmann and Harris, 2004; ten Hulscher *et al.*, 1992). Some of these processes refer to Hg methylation, the formation of gaseous Hg (Hg^0), and other Hg species (O'Driscoll *et al.*, 2007; Boszke *et al.*, 2003). All of this is further affected by:

- the physical and chemical properties of water (pH, temperature, chemical composition, etc.) that influence the fate of Hg in water with regard to biological uptake, re-precipitation and settling, methylation, demethylation, and volatilization (Vaidya *et al.,* 2000; Chadwick *et al.,* 2006; Skyllberg, 2008);
- the organic matter content and mineral composition of the sediments (El Bilali *et al., 2002;* Kainz *et al.,* 2003; Kainz and Lucotte, 2006; Sanei and Goodarzi, 2006): typically, sediment THg increases with sediment organic matter, and also increases when other heavy elements such as Cu, Pb, and Zn are present; and
- time, with techniques being used to discern the gradual build-up and depth profiles of sediment THg by way of:

- sediment flux estimation (Lockhart *et al.*, 1998 ; Muir *et al.*, 2009);
- sediment Hg fractionation (Wu *et al.,* 2013);
- chemical Hg speciation (He *et al.,* 2007);
- isotope analyses (Jackson *et al.,* 2004);
- Hg enrichment factor and geoaccumulation index (Wu *et. al.,* 2008; Olubunmi and Olorunsola, 2010).

Synopsis

The study objectives of this Thesis were built on the above review in terms of quantifying and interpreting the Canada-wide stream and lake survey data for sediment THg. Actual mechanisms and processes that contribute to sediment THg accumulation through specific Hg release, metabolic uptake, and retention processes were not addressed. Such details are and have been subject to many investigations, as reported, e.g., at the annual International Conferences on Mercury as a Global Pollutant (ICMGP).

Chapter 3 Methods

Data Sources and Compilation

The bulk stream and lake sediment data used in this study were obtained from the open geochemical survey files of Natural Resources Canada (NRC; GSC, 2008), Government of Quebec (personal communication: Andy Rencz, August, 2010), and Province of Nova Scotia (2006). These files provide information about:

- the geographic location (longitude, latitude) of each stream and lake sampling location;
- water and sediment characteristics of the sampled streams and lakes (notably, lake area and depth, stream channel width and depth, stream order and flow rate, water and sediment colour);
- terrain type and landform;
- elemental composition, listing up to 36 elements including heavy metals, notably Hg, Cu, Zn, Pb, Cd, As, and Au and other elements such as Fe, Mn, Se, and S; however Se and S data were sparse;
- loss of ignition at 500˚C (LOI), as an estimate of sediment organic matter content (Sanei and Goodarzi, 2006).

Sediment data collection followed the protocol of the GSC's National Geochemical Reconnaissance (NGR) and Uranium Reconnaissance Program (URP), done in cooperation with provincial/territorial governments (GSC, 2008). That protocol involved

standardized sampling, sample preparation and treatment, and laboratory analysis techniques (Friske and Hornbrook, 1991). Stream sediments mostly consisted of silt and clay materials collected from active stream channels. Lake sediments were collected with hollow pipe samplers down to a sediment depth of 30 cm. This depth corresponds to about 100 years of sediment accumulation (Lockhart *et al.*, 2000). The muddy portion of the sediment samples (a few top centimeters) was discarded. The field collected samples were placed into paper bags, air-dried, and sieved to obtain their 80-mesh fractions for laboratory analysis. For NS, sample preparations for THg analysis varied by stream versus lake samples (DP ME 132, 133, 136; Nova Scotia Department of Natural Resources, 2006a, b, c). Stream samples were passed through a 1 mm nylon grid followed by air-drying for 2 to 3 days and sieving; lake samples were oven dried at 80 ˚C and then ground to fine powder.

The samples were analyzed for THg using Atomic Absorption Spectrometry (AAS) and/or inductive coupling mass spectrometry (ICP-MS; GSC, 2008; Ressources naturelles et de la Faune Québec, 2012). Also determined was the loss on ignition (LOI) by weighing dried sediment samples before and after heating at 500˚C for 24 hrs. For one survey zone in QC, total elemental S was included in the analyses as well. Quality control included the insertion of control samples and duplicate samples as part of the batch-processing procedures. The THg data were reported on a dry-weight basis in parts per billion (ppb). LOI and S contents were reported in %. Other elements were reported in parts per million (ppm, dry weight).

The sampling locations were referenced by latitude and longitude (x and y coordinates). These were additionally characterized as follows: (i) National Topographic

System (NTS) map sheet (tile) identification number, (ii) province/territory, (iii) geographically distinct survey zone (1-30), (iv) lake area (km^2) and depth (m), (v) stream width and depth (m), (vi) terrain relief (low, medium, high), (vii) sediment colour and suspended material (none, light, heavy), and (viii) water source (ground, spring) and colour. Stream flow rates were reported by class as stagnant, slow, moderate, fast and torrential. Stream order (Strahler) was reported from 1^{st} to 4^{th} order.

Compiling the data produced a total of 254,133 THg sampling points, all surveyed from 1960 to 2008. Each sample represented a one-time sampling effort from each sampling location. By adding the data of NS and QC, the new dataset provided an update of the earlier sediment THg presentation by Rasmussen *et al. (*1998a). The compiled data were organized into data rows and columns using Excel spreadsheets, with each row representing a sampling point. Each column represented attributes provided in the original datasets and additional data/information obtained through geospatial cross-referencing via ArcMap, as detailed below.

Geospatial Analysis: Additional Information

In ArcMap, mapping projects were generated and populated with a series of overlaying Canada-wide data layers, as follows:

- The compiled sediment THg data as point shapefile (THg shapefile).
- Bedrock geology polygon shapefile, including rock type, age, formation, and faults (Fulton, 1995; Wheeler *et al.,* 1997; for geological time table, see Figure A1.1);.

- Ecological land classification (vegetation/land cover), terrestrial and ecological ecozone, and NS wetland classification polygon shapefiles (Province of Nova Scotia, 2014; Geobase, Natural Resources Canada, 2006; Ecological Stratification Working Group, 1995). The cover types were classified as snow/ice (glacial, non-glacial), sparse vegetation, barren (bare ground with no vegetation), frost worked-soil (cryptogam crust, frost boils with sparsely graminoids and cryptogam plants), tundra (graminoid, shrub), wetlands (bog, fen, swamp, marsh), and forest (broadleaf, conifer, mixedwood).

- Mean annual net atmospheric Hg deposition rate (Global/Regional Atmospheric Heavy Metals Model; GRAHM2005 atm.Hg_{dep}, μg m^{-2} a^{-1}; Dastoor and Moran, 2010), a raster grid at 25 x 25 km^2 grid resolution.

- The 1961-1990 rasters (4 km^2 grids) for mean annual precipitation rate (ppt, m a^{-1}) and July and January air temperatures (T_{July}, $T_{Jan.,}$ ˚C; Parameter-elevation Regressions on Independent Slopes Model (PRISM) climate group; Daly *et al.*, 2002).

- Digital elevation models in raster layers:

    - National Digital Elevation Model (DEM) grid at 300 m (Natural Resources Canada, 2007).

    - Canadian National Topographical Database at 30 m (NTDB: YT; Government of Yukon, 2014).

    - Enhanced DEM at 20 m (2006; NS; Province of Nova Scotia, 2013).

- Shuttle Radar Topography Mission (SRTM: NU, QC, NWT; Geobase, Natural Resources Canada, 2011) at 90 m resolution.

Using the ArcMap Spatial Analysis routine, information contained in the polygon shapefiles were spatially joined to the THg shapefile, resulted in adding descriptive (nominal) values for each sediment point (Chapters 7, 8; Appendix 3) . In addition, the raster-based data were extracted for each sediment point, using the "Extract by Point" function of the Spatial Analyst Tool Kit. This enabled some of the analyses in Chapters 5 and 6, and Appendix 4. The THg attribute tables of the shapefiles were also saved and exported as text files, to enable data quality control, statistical analysis and plotting in Excel and other software such Statview and ModelMaker.

Map illustrations were created based on overlying the THg data on the National Geographic Basemap in ArcMap (Chapter 8). Also overlaid were geological faults and dominant bedrock formations. The main bedrock formations were classified as extrusive (volcanic rocks) and intrusive (or plutonic) rocks, sedimentary and metamorphic rocks. The age of the bedrock formations (Figure A1.1) was specified as part of the text. Map layers of surface water features, roads, and provincial boundaries (Geobase, Natural Resources Canada, 2006) were used for inspection and visualizing purposes, and for the the topographic analysis described below.

Geospatial Analysis: Topographic Analysis based on DEMs

Topographic analysis was done by developing Cartographic Depth to Water index (DTW) using the above-listed available DEMs and mapped surface-water features

(Figure 3.1; Wet Areas Mapping: WAM; Murphy *et al.*, 2008, 2011; Forest Watershed Research Center, University of New Brunswick University, 2015).

The conformance between the geo-referenced stream sediment sampling locations and the DEM-derived sample locations was inspected. The latter locations fell within 40 m of the actual sampling location, 7 times out of 10. This precision generally increased with increasing terrain complexity, but decreased towards flat areas such as flood plains with meandering streams. The x,y specifications for the stream sediment locations were snapped to the nearest mapped channel locations as mapped. The x,y locations of lake sampling points were generally consistent with surface water feature map, and with ArcMap basemaps. The upland (DTW > 10 m) versus lowland (DTW ≤ 10 m) assignment for each sampling locations was done in reference to the nearest mapped streams, rivers, lakes and coast lines, and using the 300 m resolution national DEM (Chapter 4; Murphy *et al.,* 2011). The DTW = 10 m threshold approximates the extent floodplains.

Upslope basin borders and wet-area delineations were done for selected case studies by using 20, 30, and 90 m resolution DEMs described above (Chapters 8, 9; Appendix 3). These DEMs were all spatially interpolated to a resolution of 10 m. The basin areas were determined by using ArcMap flow accumulation process for continuous flow convergence (D8 algorithm) for each sediment sampling location of the selected case studies. The DTW that was associated with a 4 ha flow initiation for stream networks and with open water features such as pools, ponds, and lakes, for which DTW was set to zero. Generally, the wet-areas with DTW < 0.5 m were characterized by very poor to imperfect soil drainage (Murphy *et al.*, 2007, 2008).

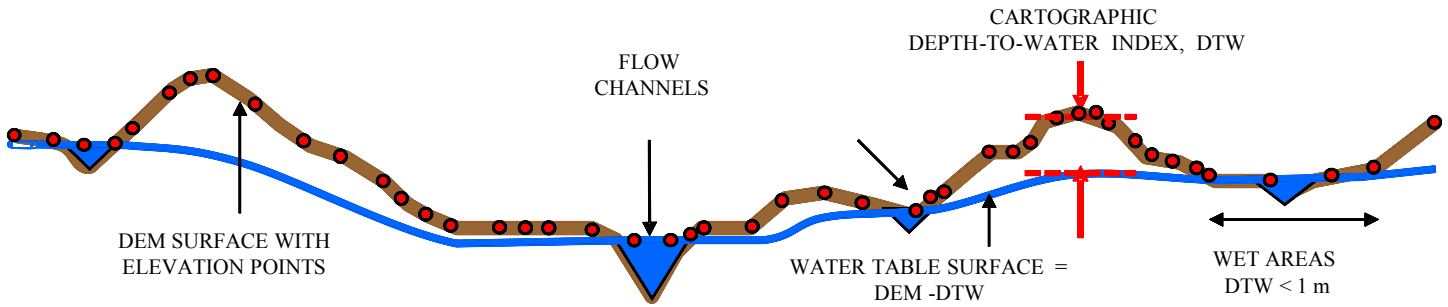

1. Prepare bare ground DEM surface from digital elevation points (red dots) through nearest neighbour interpolation.
2. Delineate stream channels based on filled DEM, flow direction, flow accumulation and flow initiation. The threshold area for flow initiation was 100 ha or 4 ha, depending on the 300 m or higher resolution national and regional DEM used, respectively.
3. Delineate cartographic depth-to-water index (DTW) across Canada, using DEM delineated flow channels.
4. Delineate upland/lowland (based on 300 m resolution national DEM) and wet-areas (based on regional high resolution (20-90 m) interpolated DEM to 10 m resolution) by DTW classification: lowlands: (DTW < 10m); wet-areas: DTW <0.5 m).
5. Overlay the resulting DEM derived digital layers on the bare ground DEM surface, surface images, and existing mapped flow channels and wetlands for inspection, mapping, and analysis.
6. Locate sediment sampling points and delineate above points basin borders by watershed delineation function (D8 algorithm).

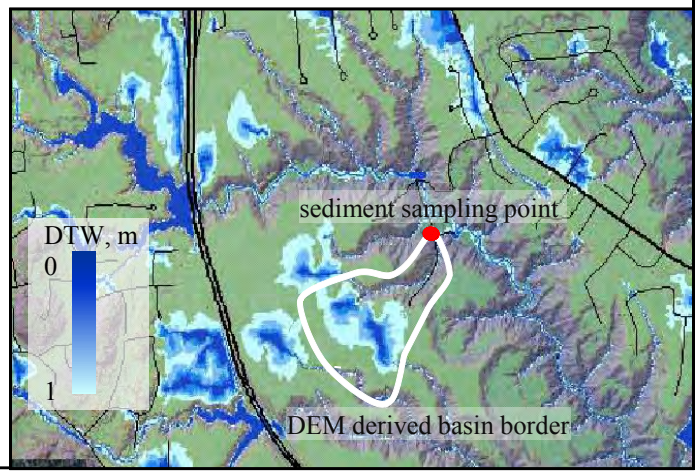

Figure 3.1 Overview of upland/lowland and wet-area delineation processes.

Once the basin boundaries and we-area coverages were delineated, Geospatial Modelling Environment (GME) software (Beyer, 2001-2002) was used for automated quantification of the A_B (ha) and A_W (ha) per basin. The resulting A_W/A_B ratios were compiled for each sediment sampling location in a single spreadsheet, with the following data columns (fields): name of study location, latitude and longitude, A_W, A_B, A_W/A_B, and sediment THg and $\log_{10}$THg. Specifically, the data were used to plot $\log_{10}$THg versus A_W/A_B and determine the mean and range of $\log_{10}$THg by A_W/A_B (Chapter 9, Appendix 3). The mean $\log_{10}$THg were regressed against A_W/A_B, by medium type (stream, lake) and by study location (Chapter 9).

Data Processing and Statistical Analysis

For data quality assurance, all compiled data were inspected for (i) correct data alignments within and across individual files, (ii) numerical and typographical inconsistencies within each column, (iii) data flags such as symbols denoting no data, values below analytical resolution, and zeros, (iv) the numerical distribution pattern within each column. These were done by drawing frequency distributions (grouped and ungrouped), and grouping data by sediment medium type, NTS tile, province/territory, survey zone, local landform, sediment colour, stream order and network pattern, upland/lowland location, water origin, and type of suspended materials in the water. After inspection, faulty data entries were replaced by empty cells, misspellings were corrected, and misplaced sampling points, e.g. offshore longitudes and latitudes were removed.

A number of categorical variables were numerically re-coded into sets of dummy variables (e.g. bedrock types, with each type coded 0 when absent and 1 when present)

and simple ordination (e.g. Strahler stream order = 1, 2, 3 4; flow rate = 0, 1, 2, 3, 4, 5, if stagnant, slow, moderate, fast, and torrent, respectively). Each adjusted numerical data column were then inspected for the order and magnitude of outliers with and without $\log_{10}$ transformation by way of boxplots (showing the 10^{th}, 25^{th}, 50^{th}, 75^{th}, and 90^{th} percentiles) with and without splitting by categorical grouping. The numerical columns were also regressed against each other to (i) locate and ascertain the nature of these outliers and (ii) determine faulty zero data entries, as these together with the outliers cause strong and erroneous deviations from the trend lines of the resulting y versus x scatterplots. Further data cleaning was done by correcting and/or eliminating any data entries such as misalignments, typographical errors, data flags, and erroneous entries (i.e. negative concentration values).

The statistical procedures involved: (i) basic statistics (mean, minimum, maximum, standard deviation, standard error) with and without splitting by groups, (ii) the 10^{th}, 25^{th}, 50^{th}, 75^{th}, and 90^{th} percentiles summary with and without splitting by groups; (iii) the statistical significance among the grouping ranks, using post-hoc comparisons (pairwise Fisher's Protected Least Significant Difference: PLSD).

Further procedures involved determining the relationships between variables by simple and multiple regression analyses of actual or $\log_{10}$ transformed data. Re-coding of categorical values to dummy variables and simple ordination were used to permit their use as stepwise backward regression variables.

The multiple regression analysis results were reported by compiling the least-squares fitted intercepts (if applicable), the regression coefficients, their standard errors of estimates, and corresponding t and p-values. The least-squares model results were also

examined in terms of the actual versus best-fit scatter plots of the dependent variables. The aim was to check the influence of outliers on the regression results and the associated R^2 values. All of this was done to identify the least set of independent variables for which the least-squares regression coefficients:

- were significantly different from zero;
- were as precisely estimated as possible, as judged by their standard errors of estimates and associated t and p-values; and
- did not lead to negative estimates for dependent variables when these variables should not attain negative numbers (such as THg, LOI).

Variables with significant influence were selected when t-value was > 4.0, p-value < 0.0001, and the R^2 value of the multivariable regression model was noticeably improved.

The quality of best-fit values was further evaluated by examining the resulting plots of actual versus best-fit values for (i) outliers with disproportional influence on the analysis outcome, (ii) linearity, and (iii) heteroscedasticity. In some cases, outliers with undue influence on the regression results were excluded to determine how the majority of the data influences the dependent variable without the extraordinary influence of specific outliers. Conformance plots were generated by plotting the cumulative frequencies of the best-fit absolute residual differences between estimated and actual values versus these differences.

LOI Analysis

For Chapter 6**,** the compiled stream and lake sediment data for THg, LOI, GRAHM2005 mean annual net atmospheric Hg deposition rate and climate variables (annual precipitation rate, July and January air temperatures) were used. The combined data were grouped, plotted and analysed by NTS tile, survey zone (QC only), and province/territory. Not all of the THg data were accompanied by LOI data. For example, there were no LOI data for NS stream sediments. The statistical analysis of Chapter 6 involved:

- a basic summary of the data;
- comparing the frequency distributions for $\log_{10}$THg and LOI;
- plotting sediment $\log_{10}$THg against LOI by individual streams and lakes;
- regressing the mean THg and LOI by NTS tile against means values of (a) GRAHM2005 mean annual net atmospheric Hg deposition rate, (b) mean annual precipitation rate, and (c) mean annual July and January air temperatures;
- estimating THg and LOI across Canada by regression analyses based on the rasterized climate variables. These estimates were overlaid with the mean THg and LOI values per NTS tile for inspection and comparison;
- generating the 10^{th}, 25^{th}, 50^{th}, 75^{th} and 90^{th} $\log_{10}$THg percentiles of these plots within the 0-10, 10-20, 20-30 % … LOI classes.

The resulting $\log_{10}$THg percentile values were then subjected to least-squares model fitting, using the following equations:

$$\log_{10}\text{THg (ppb, stream)} = (a + i\, e_{stream}) + b_{stream} \sin (c_{stream}\, \pi\, \text{LOI (\%)} / 100)^{d} \quad \text{Eq. 3.1}$$

$$\log_{10}\text{THg (ppb, lake)} = (a + i\, e_{lake}) + (b_{lake} - i\, f_{lake}) \sin (c_{lake}\, \pi\, \text{LOI (\%)} / 100)^{d} \quad \text{Eq. 3.2}$$

where i = 0, 1, 2, 3 , 4 refers to the 10^{th}, 25^{th}, 50^{th}, 75^{th} and 90^{th} percentile, respectively, and a, d, b_{stream}, c_{stream}, b_{lake}, c_{lake} are the regression coefficients, with a and d to be held the same for streams and lakes, based on preliminary examinations.

The 10^{th} and 90^{th} THg percentiles were further analyzed by province/territory and QC geological survey zone, and by considering that (i) the mineral component of sediment THg needs to decrease from 100 to 0 % as organic matter increases from 0 to 100 % and (ii) the organic component of sediment THg increases towards saturation with increasing organic matter content. Quantitatively, this was formulated as follows:

$$\log_{10}\text{THg}_{i,j}\,\text{(ppb)} = a_{ij}\,(1 - \text{LOI (\%)}\,/100) + b_{ij}\,[1 - \exp(-\,c_j\,\text{LOI (\%)} / 100)] \quad \text{Eq. 3.3}$$

where “i” refers to each of the 1-30 numbered survey zone, “j” refers to stream (j = 1) and lake (j = 2), a_{ij}, b_{ij} and cj are coefficients, and LOI refers to the midpoint of each LOI class, i.e. 5, 15, 25… %, etc. The best-fit values for the a_{ij}, b_{ij} and c_j, coefficients were obtained using a non-linear least-squares fitting routine (ModelMaker). The resulting coefficient values were then regressed against the mean annual rate estimates for atmospheric Hg deposition and precipitation for each of the 30 survey zones. The same procedures applied to the Cu versus LOI data analysis of Appendix 4.

Fish Hg Analysis

The Fish Mercury Data layer for Canada (FIMDAC) provided 387,872 fish Hg concentration estimates, acquired from data collected from 1,936 non-contaminated Hg lakes (Depew *et al.*, 2013 a, b; Little *et al.*, 2014). The data were collected from 1970 to

2010 and were standardized for one fish species (yellow perch) and one fork length (12 cm). The analyses in Appendix 5 involved regressing the standardized values for fish $\log_{10}$Hg against lake sediment $\log_{10}$THg, mean GRAHM2005 annual net atmospheric Hg deposition rate, mean annual precipitation rate, and mean July and January air temperatures. Correlation, factor, and conformance analyses were done to enable the data interpretations.

Case Studies

Nine case studies were selected for conducting climate and terrain representative basin analyses (Figure 3.2):

- **The NS locations** were selected because of extensive past to present Au prospecting and mining activities throughout the province and because of considerable concerns about Hg bioaccumulation in fish, loons, and otter (Environment Canada Atlantic Region, 1998, 2001). The aim was to determine the sediment THg and A_W/A_B relationship (Chapter 9), and how land cover (forest versus non-forest), wetland (Appendix 3), and bedrock type (Chapters 7, 8) affect sediment THg. Three study locations were selected: (i) northcentral mainland (n = 913 lakes), (ii) southern-western mainland, centered around Kejimkujik National Park (n = 431 lakes), and (iii) Cape Breton (n = 2,627 streams, n = 351 lakes).

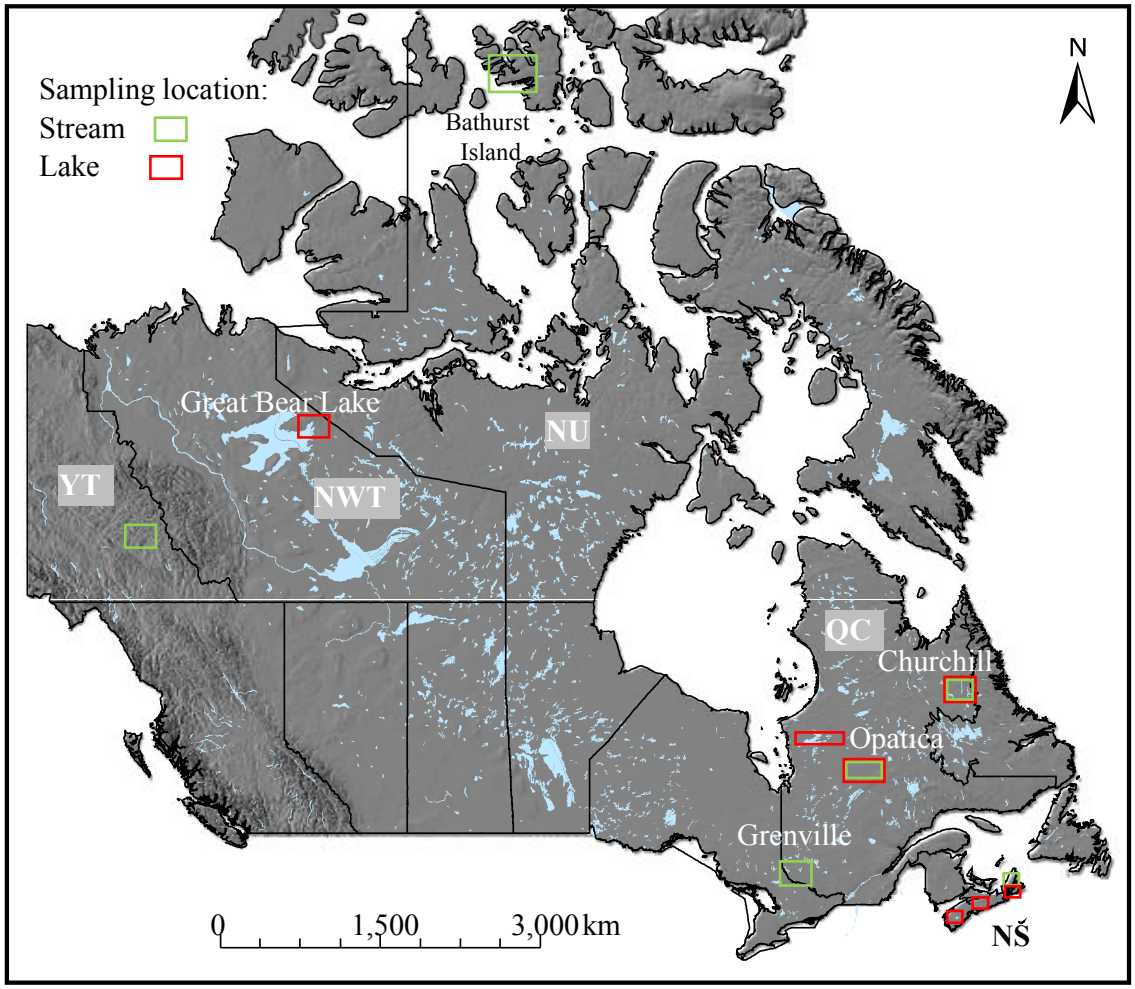

Figure 3.2 Selected case studies for geospatial basin analysis.

- **The QC locations** were selected because of diverse climatic and geological gradients and dense clusters of high sediment THg. The aim was to determine to what extent sediment THg was affected by increasing A_W/A_B from low to high geogenic Hg source areas (Chapter 9). The locations are (i) Grenville A located in southern Laurentiens in Témiscamingue/Temiscaming area (n = 2,936 streams), (ii) Opatica in James Bay region central Superior Province (n = 881 streams, n = 690

lakes), and (iii) Churchill A close to QC-NFL and Labrador border (n = 510 streams, n = 252 lakes).

- **The Great Bear Lake, NWT and Bathurst Island, NU locations** were selected since these regions have been recognized as high mineral and geogenic metal deposit locations in northern Canada, resulted in extensive mining activities in especially in Great Bear Lake area (McCurdy *et al.*, 1997; Indian and Northern Affairs Canada, 2006). The aim was to determine the sediment THg and A_W/A_B relationship (Chapter 9), and how vegetation and land cover affected sediment THg in northern locations (Appendix 2). The NWT study location was in the northeast of Great Bear Lake (n = 1,298 lakes). The stream sediment samples of Bathurst Island area were scattered across the northern section of the island and across the Massey Island, Alexander Island, and Helen Island in the north (n = 407).
- **Selwyn Basin, YT location** was selected because of a high contrast from low to high geogenic Hg occurrences (Nasr *et al.,* 2011) on mountainous terrain, typified by variations in surface-exposed black shales, and volcanic, intrusive and metamorphosed bedrock formations. The selected case study was located on the central-east section (n = 1,666 streams).

The sediment THg analyses in Chapter 7 and regional illustrations in Chapter 8 pertaining to sediment composition and underlying bedrock formations were centered on individual provinces/ territories and specific NTS tiles as follows:

- **NL:** Sneagamook Lake area, Central Mineral Belt, Labrador (13K);
- **QC:**
    - Churchill A: Schefferville, Labrador Trough (23I-J, 23N-P);
    - Grenville A: Témiscamingue/Temiscaming;
    - Opatica: Sakami, La Grande volcanic belt (34-C, 33F-H);
    - Appalaches B: McGarrigle Mountains - Murdochville, Gaspé Peninsula (22A-B);
- **ON:**
    - Greater Sudbury area (31M, 41I-J, 41O-P);
    - Kenora-Dryden (52E-F);
- **NWT:** northeast of Great Bear Lake area (86 K, L);
- **MB:** La Ronge-Flin Flon, Northern SK-MB (63K-N, 73P, 74A);
- **YT:** Selwyn Basin (105M-N, 105-L)
- **NU:** Bathurst Island (69A-B, 69H-G).

Chapter 4 THg in Stream and Lake Sediments across Canada, Overview

Introduction

The bulk stream and lake sediment data are a reliable and systematic coast-to-coast source for evaluating sediment THg across Canada (Friske *et al.,* 1991). In this chapter, the compiled GSC, QC and NS data were analyzed by province/territory and by the 30 survey zones. The objective was to determine and summarize how sediment THg varies in these zones from east to west and from south to north by upland versus lowland and stream versus lake location. Some of the results of this chapter were already presented in Nasr *et al. (*2011) and Nasr and Arp (2015b).

Results

Across Canada, stream and lake sediment THg range from 5 to 36,000 ppb (Figure 4.1). Sediment THg is generally more variable in streams than in lakes, with NS being a notable exception. THg in lakes is significantly higher than streams, by province/territory (Table 4.1; p-value < 0.0001). Exceptions are (i) significantly higher values for the streams of NWT (p-value < 0.0001), located close to YT-NWT boundary and (ii) no stream and lake significant differences for YT and NU due to small sediment sample size of YT lakes and NU streams.

.

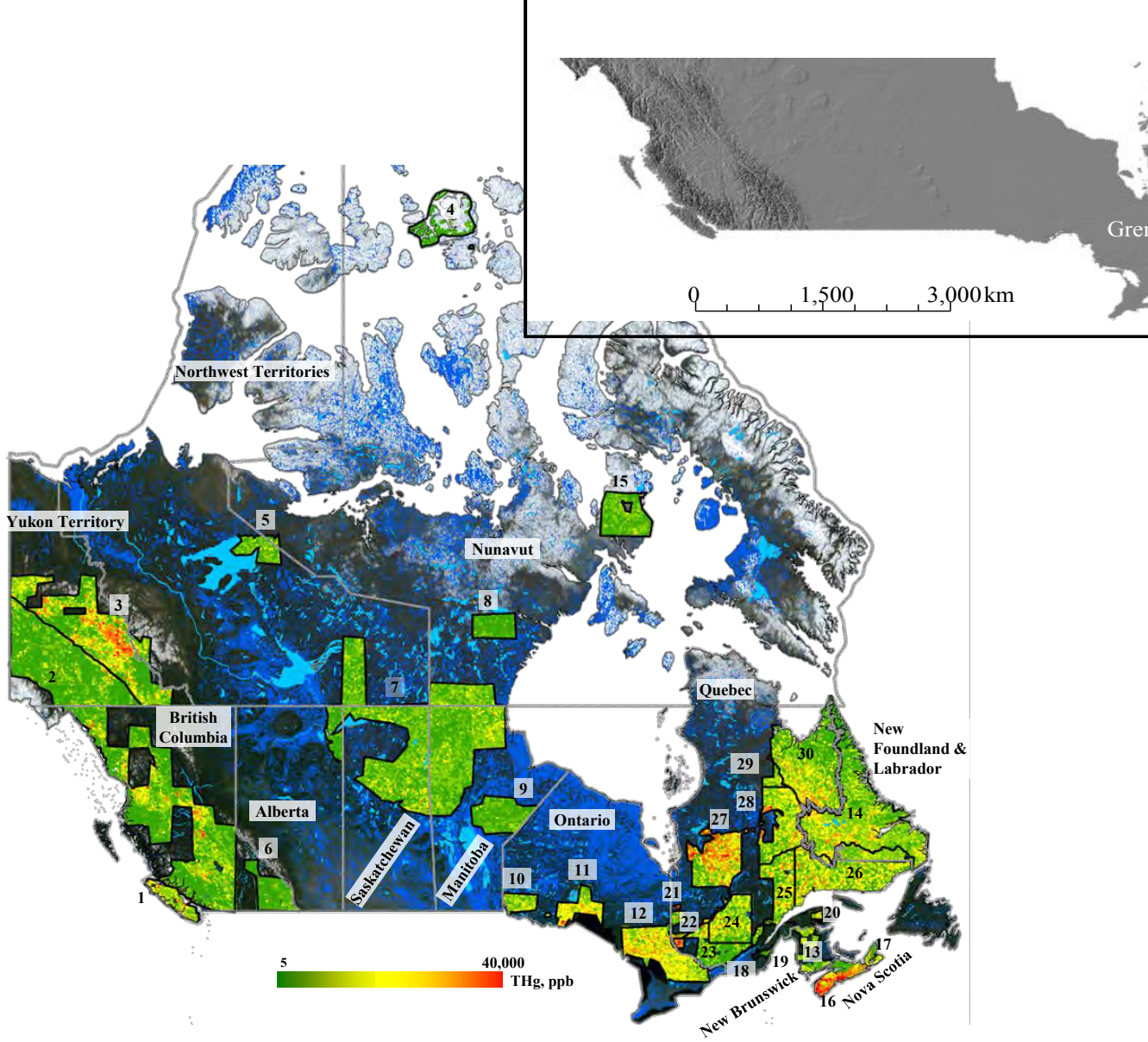

Figure 4.1 Overview of data compiled for stream and lake sediment THg (ppb) from low (green) to high (red) across Canada, by survey zone (1-30). Background: DEM derived lowlands (dark blue) and main surface water features (light blue), based on the national DEM (300 m resolution), also showing provincial/territorial borders.

Table 4.1 Sediment THg (ppb), by province/territory and medium type (stream, lake).

Province/Territory	Lake sediment THg, ppb						Stream sediment THg, ppb					
	n	Mean	Min.	Max.	Std. Dev.	Std. Err.	n	Mean	Min.	Max.	Std. Dev.	Std. Err.
AB	1,147	**35.8**	5	367	19.0	0.6	-	-	-	-	-	-
BC	587	**106.6**	10	960	69.8	2.9	33,509	**74.1**	10	22,690	335.9	1.8
MB	18,057	**51.6**	8	960	26.2	0.2	-	-	-	-	-	-
NB	336	**129.0**	25	270	43.2	2.4	7,435	**81.6**	10	6,830	98.5	1.1
NL	19,295	**84.9**	8	900	57.3	0.4	1,254	**32.0**	10	410	30.4	0.9
NS	3,776	**379.6**	10	36,000	746.7	12.2	8,148	**101.1**	10	10,000	274.7	3.0
NU	5,852	**46.3**	10	200	25.6	0.3	403	**25.4**	10	170	16.4	0.8
NWT	4,071	**51.2**	10	525	32.2	0.5	447	**111.5**	30	727	93.5	4.4
ON	14,166	**119.7**	10	21,000	196.0	1.7	187	**42.4**	10	184	36.7	2.7
QC	68,264	**125.2**	5	22,700	183.4	0.7	31,916	**140.4**	5	9,392	277.1	1.6
SK	12,155	**57.8**	6	1,560	40.1	0.4	-	-	-	-	-	-
YT	204	**85.1**	6	720	83.6	5.9	22,924	**75.0**	5	5,950	121.7	0.8
Total*	147,910	**105.4**	5	36,000	139.0	1.0	106,223	**96.2**	5	22,690	244.3	1.6

* Weighted mean, standard deviation (Std. Dev.), and standard error (Std. Err.).

Stream and lake sediment THg varies in each survey zone (Figure 4.2). Mean ± SE THg is lowest on Bathurst Island, NU (25.4 ± 0.8, ppb; zone 4) and highest in the Grenville A, QC (223.8 ± 4.4, ppb; zone 21) and NS mainland (216.2 ± 5.8, ppb; zone 16). THg outliers ≥ 1,500 ppb refers to 468 sampling points (n = 344 streams, n = 124 lakes), and were scattered across several zones. The sediment THg values for NWT and QC are higher for streams than for lakes due to geogenic Hg anomalies, especially for the Selwyn Basin (NWT) and Témiscamingue areas (QC).

As summarized in Table 4.2 by survey zone, overall mean ± SE THg is higher for upland lakes (113.2 ± 1.1, ppb) and streams (97.8 ± 1.4, ppb) than for lowland lakes (90.4 ± 0.2, ppb) and streams (90.1 ± 2.2, ppb). Post-host analysis indicate a significant drop in mean THg from lakes to streams (critical mean = 1.8, p-value < 0.0001), from upland to lowland lakes (critical mean = 2.1, p-value < 0.0001), and from upland to lowland streams (crit. mean = 4.0, p-value < 0.0001).

While the standard deviation about the mean values in Tables 4-1 and 4-2 are large, the significant differences between upland and lowland sediment values of streams and lakes arise from high sample sizes. As the result, the standard errors of the mean values amount to only a small percentage of the mean, thereby indicating that the mean values by upland versus lowland streams and lakes are indeed statistically significant.

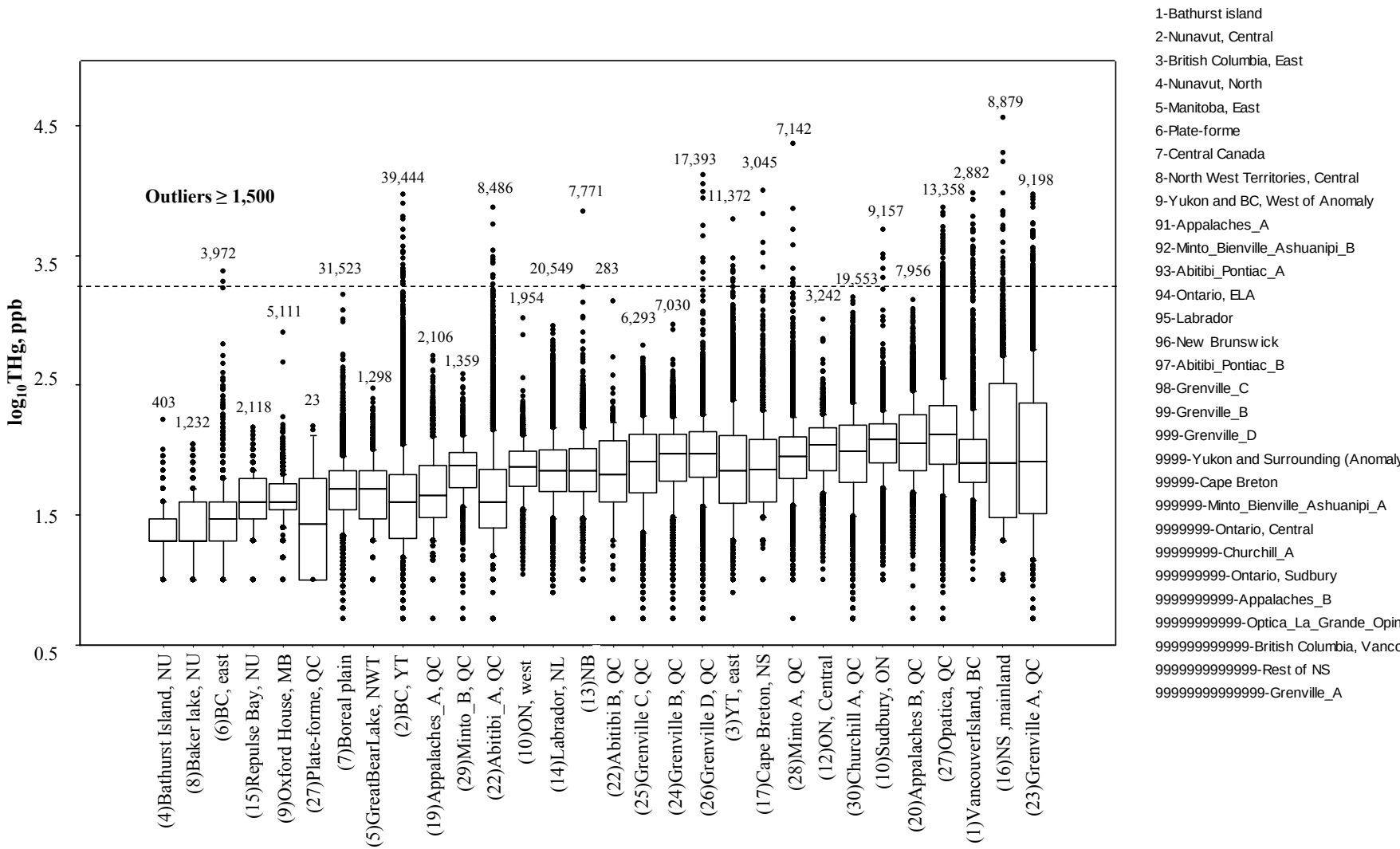

Figure 4.2 Box plots for stream and lake sediment $\log_{10}$THg (ppb), by survey zone (Figure 4.1). The line inside each box is the median, the upper and lower edges of the box are the 75th and 25th percentiles, and the upper and lower error bars are the 90th and 10th percentiles. The dashed horizontal line identifies THg outliers ≥ 1,500 ppb. Left to right: increasing mean THg per survey zone.

Table 4.2 Sediment THg (ppb), by survey zone (1-30), upland/lowland location, and medium type (stream, lake).

Survey zone	Terrain	Lake sediment THg, ppb					
		n	Mean	Std. Dev.	Std. Err.	Crit. Diff.*	p-value*
Sudbury, ON (11)	Upland	5,735	**132.8**	100.8	1.3	4.3	<0.0001
	Lowland	3,235	**119.1**	100.5	1.8		
NB (13)	Upland	299	**128.9**	41.9	2.4	14.8	0.9886
	Lowland	37	**129.1**	53.6	8.8		
YT, east (3)	Upland	72	**123.2**	111.3	13.1	47.8	0.4716
	Lowland	24	**105.8**	66.7	13.6		
ON, central (12)	Upland	2,263	**123.1**	61.8	1.3	4.6	<0.0001
	Lowland	979	**97.1**	62.1	2.0		
BC, west & north; YT, west (2)	Upland	542	**103.5**	73.1	3.1	12.3	0.0004
	Lowland	153	**81.4**	49.6	4.0		
Labrador, NL (14)	Upland	13,789	**86.9**	59.1	0.5	1.8	<0.0001
	Lowland	5,506	**80.0**	52.1	0.7		
ON, west (10)	Upland	953	**86.8**	38.5	1.2	4.1	<0.0001
	Lowland	1,001	**73.7**	52.1	1.6		
Great Bear Lake north-east, NWT (5)	Upland	906	**59.7**	36.7	1.2	4.2	<0.0001
	Lowland	392	**50.0**	32.2	1.6		
Boreal Plain (7)	Upland	16,330	**58.3**	33.7	0.3	0.7	<0.0001
	Lowland	15,193	**50.5**	32.4	0.3		
Oxford House, MB (9)	Upland	1,195	**48.9**	28.6	0.8	1.3	<0.0001
	Lowland	3,916	**44.4**	17.5	0.3		
Repulse Bay Peninsula, NU (15)	Upland	1,539	**44.7**	19.8	0.5	1.9	0.0701
	Lowland	579	**42.9**	21.7	0.9		
Baker Lake, Nunavut (8)	Upland	546	**32.9**	19.4	0.8	2.0	<0.0001
	Lowland	686	**25.9**	16.7	0.6		
Cape Breton, NS (17)	Upland	245	**119.7**	45.5	2.9	12.5	0.6403
	Lowland	110	**122.7**	72.8	6.9		
NS, mainland (16)	Upland	2,322	**409.5**	919.8	19.1	56.0	0.7414
	Lowland	1,099	**400.1**	321.6	9.7		
QC (18-30)	Upland	50,053	**127.9**	153.2	0.7	3.1	<0.0001
	Lowland	18,211	**118.0**	248.0	1.8		
Zones with stream & lake data	Upland	73,057	**129.9**	155.0	1.3	3.2	<0.0001
	Lowland	28,375	**121.8**	218.2	2.0		
Total**		**101,432**	**127.6**	**172.7**	**1.5**		
All zones	Upland	96,789	113.2	125.1	1.1	2.1	<0.0001
	Lowland	51,121	90.4	121.5	0.2		
Total**		**147,910**	**105.3**	**123.8**	**0.8**		

Table 4.2 Continued:

Survey zone	Stream sediment THg, ppb						Lake versus stream	
	n	Mean	Std. Dev.	Std. Err.	Crit. Diff.*	p-value*	Crit. Diff.	p-value
Vancouver Island, BC (1)	2,448	**209.4**	1016.0	20.5	99.0	0.3146	-	-
	434	**158.6**	649.3	31.2			-	-
Sudbury, ON (11)	117	**42.4**	36.7	3.4	11.0	0.9949	18.3	<0.0001
	70	**42.5**	37.1	4.4			23.6	<0.0001
NB (13)	5,716	**84.2**	108.4	1.4	5.3	0<.0001	12.3	<0.0001
	1,719	**73.0**	53.3	1.3			17.4	<0.0001
YT, east (3)	9,557	**112.7**	153.4	1.6	7.7	0<.0001	35.5	0.5646
	1,719	**95.7**	127.4	3.1			51.1	0.7004
BC, west & north; YT, west (2)	31,550	**59.4**	153.3	0.9	4.3	0.4588	12.9	<0.0001
	7,199	**57.8**	213.4	2.5			33.8	0.1726
Labrador, NL (14)	1,116	**32.6**	31.5	0.9	5.4	0.0385	3.5	<0.0001
	138	**27.0**	17.7	1.5			8.7	<0.0001
BC, east (6)	3,012	**35.7**	44.9	0.8	4.7	0.7199	-	-
	960	**34.8**	105.0	3.4			-	-
Bathurst Island, NU (4)	311	**25.7**	16.4	0.9	1..6	0.4210	-	-
	92	**24.1**	16.3	1.7			-	-
Cape Breton, NS (17)	2,056	**110.4**	209.4	4.6	25.6	0.7532	29.9	0.4605
	634	**106.3**	455.4	18.1				
NS, mainland (16)	3,941	**106.0**	282.3	4.5	15.9	<.0001	11.7	<0.0001
	1,517	**73.6**	226.8	5.8				
QC (18-30)	25,062	**141.8**	270.3	1.7	7.4	0.0822	2.6	<0.0001
	6,854	**135.2**	300.7	3.6				
Zones with stream & lake data	79,115	120.2	239.3	1.9	3.4	0.0210	2.2	<0.0001
	19,850	110.8	277.0	4.3			4.4	<0.0001
Total**	**98,965**	**118.3**	**246.9**	**2.4**				
All zones	84,886	98	140.2	1.4	4.0	0.0001	1.8	<0.0001
	21,336	90	126.1	2.6				
Total**	**106,222**	**96.3**	**137.5**	**1.6**				

* Critical difference (Crit. Diff.) and p-value by Fisher's Probable Least Squares Difference (PLSD).

**Weighted mean, standard deviation (Std. Dev.), and standard error (Std. Err.).

No lake samples: Vancouver Island, BC (1); Bathurst Island, NU (4); BC, east (6). No stream samples: Great Bear Lake north-east, NWT (5); Boreal Plain (7); Oxford House, MB (9); ON, west (10).

The majority of sediments (98 %) had THg < 500 ppb (Figure 4.3). The occurrences of sediment THg above 500 and 1,500 ppb are summarized as follows:

Sediments with THg > 500 ppb (n = 3,871), prominent in BC, NS, QC, and YT.

- Western Canada (zones 1 and 2) - There are 314 sediment samples with THg > 500 ppb up to 22,690 ppb on Vancouver Island, i.e. approximately 1 % of the total samples (zone 1). Across mainland BC (zone 2), the highest THg amount to 15,000 (stream) and 960 (lake) ppb. For YT there are only 20 streams with THg > 1,500 ppb, with maximum values of 5,950 ppb (stream) and 720 ppb (lake) in zone 3.
- NS (zones 16 and 17) - There are 947 sediment samples with THg > 500 ppb, approximately 8 % of the total samples. In mainland (zone 17) the highest concentrations were 36,000 ppb (stream) and 16,500 ppb (lake). On Cape Breton, the highest THg was recorded for a stream at 10,000 ppb.
- QC (zones 18-30) - There are 2,337 sediment samples with THg > 500 ppb, approximately 2 % of the total samples (Figure A1.1). The highest concentrations are as follows, by survey zone (Table 4.3):
    - Opatica (zone 27): 7,410 ppb (stream), 6,720 ppb (lake);
    - Abitibi A and B (zones 21 and 22): 7,331 ppb (stream);
    - Grenville A (zone 23): 9,392 ppb (stream);
    - Appalaches B (zone 20): 1,435 ppb (stream);
    - Churchill A (zone 30): 1,500 ppb (stream), 980 ppb (lake);
    - Minto A (zone 28): 1,500 ppb (stream), 980 ppb (lake).

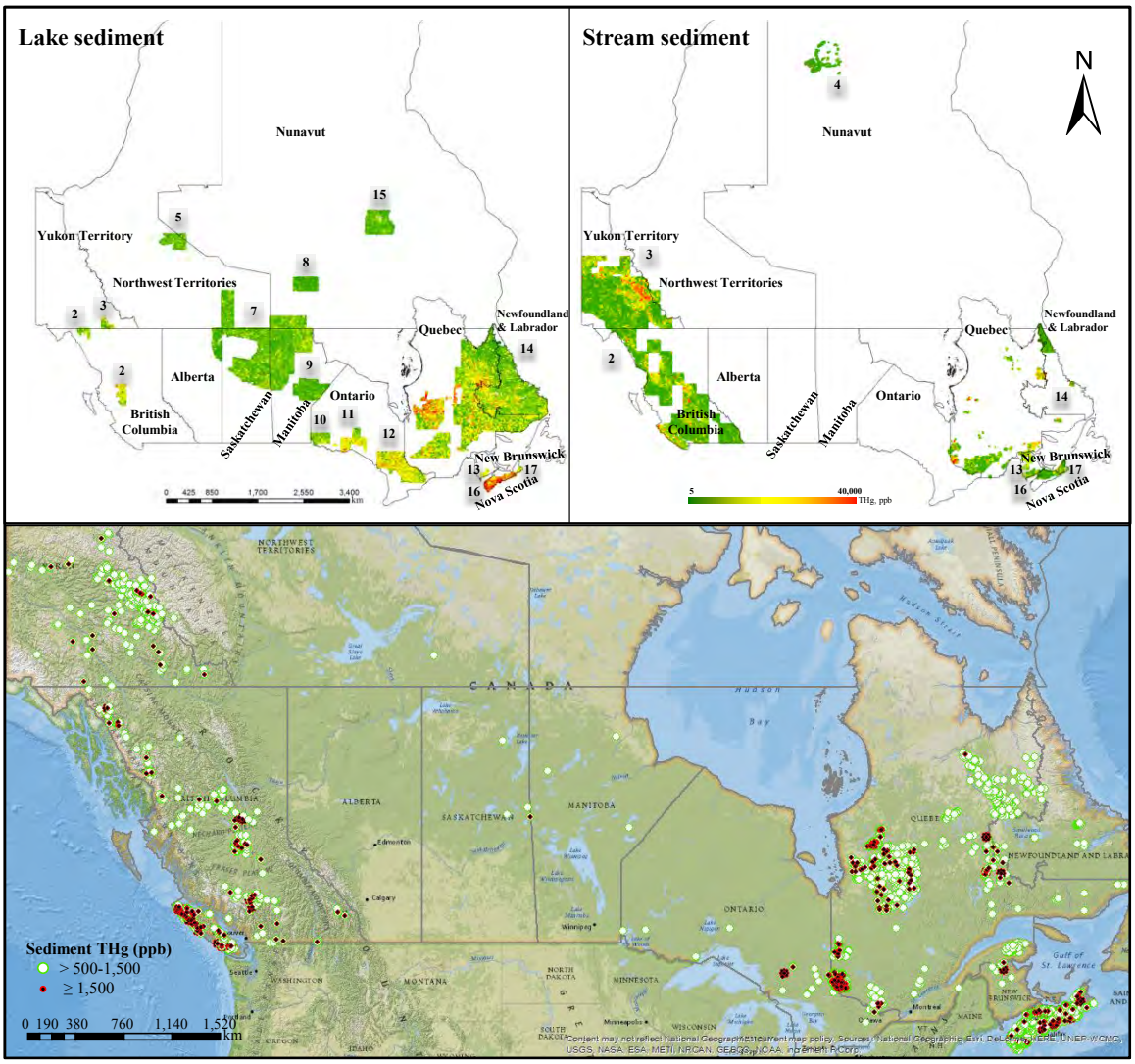

Figure 4.3 Sediment THg: top right: stream; top left: lake; bottom: THg > 500- 1,500 ppb (red) and ≥ 1,500 ppb (green).

Table 4.3 QC sediment THg (ppb), by geological survey zone (18-30), terrestrial and ecological zone (ecozone), upland/lowland location, and medium type (stream, lake).

Quebec	Ecozone	Upland lake sediments THg, ppb				Lowland lake sediments THg, ppb				Upland versus lowland	
Survey zone		n	Mean	Std. Dev.	Std. Err.	n	Mean	Std. Dev.	Std. Err.	Crit. Diff.*	p-value*
Abitibi A (22)	Boreal Shield	156	**108.1**	61.5	4.9	143	**99.9**	75.7	6.3	15.6	0.3036
Abitibi B (21)	Boreal Shield	86	**117.2**	54.2	5.8	46	**84.5**	42.6	6.3	18.3	0.0060
Appalaches A (19)	Atlantic Maritime	2	**169.0**	82.3	61.0	-	-	-	-	-	-
Appalaches B (20)	Atlantic Maritime	-	-	-	-	-	-	-	-	-	-
Churchill A (30)	Arctic Cordillera	630	**35.7**	38.8	1.5	111	**36.6**	33.0	3.1	7.7	0.8112
	Southern Arctic	5	**58.2**	15.0	6.7	2	**62.0**	42.4	30.0	49.9	0.8526
	Taiga Shield	12,648	**126.2**	96.4	0.9	5,100	**110.4**	83.3	1.2	3.0	<0.0001
	Total**	13,283	**121.9**	93.6	0.9	5,213	**108.8**	82.2	1.2		
Grenville A (23)	Boreal Shield	436	**115.9**	57.9	2.8	328	**91.9**	50.6	2.8	7.9	<0.0001
Grenville B (24)	Boreal Shield	4,436	**112.6**	55.4	0.8	1,329	**99.7**	57.9	1.6	3.4	<0.0001
Grenville C (25)	Boreal Shield	3,967	**110.1**	66.4	1.1	864	**86.5**	65.7	2.2	4.9	<0.0001
Grenville D (26)	Boreal Shield	13,760	**113.3**	146.4	1.2	2,573	**91.2**	81.5	1.6	5.8	<0.0001
	Taiga Shield	539	**91.7**	129.9	5.6	232	**64.5**	44.2	2.9	17.2	0.0190
	Total**	14,299	**112.5**	145.8	1.4	2,805	**89.0**	78.5	1.7		
Minto A (28)	Boreal Shield	774	**78.3**	57.4	2.1	347	**74.9**	139.2	7.5	11.5	0.5698
	Taiga Shield	3,756	**118.5**	119.8	2.0	2,264	**111.3**	213.6	4.5	8.4	0.0937
	Total**	4,530	**111.7**	109.2	2.0	2,611	105.1	203.7	4.9	-	-
Minto B (29)	Taiga Shield	1,037	**82.5**	39.1	1.2	288	**71.2**	39.4	2.3	5.1	<0.0001
Opatica (27)	Boreal Shield	4,028	**154.5**	199.5	3.1	2,972	**130.9**	163.9	3.0	8.8	<0.0001
	Hudson Plain	426	**244.0**	341.0	16.5	391	**224.3**	474.0	24.0	56.4	0.4913
	Taiga Shield	3,355	**246.9**	276.1	4.8	1,217	**218.3**	247.4	7.1	17.6	0.0015
	Total**	7,809	**199.1**	240.1	4.6	4,580	**162.1**	212.6	5.9		
Plate-forme (18)	Boreal Shield	8	**96.4**	44.0	15.6	2	**43.5**	24.7	17.5	76.73	0.1507
Total zones with stream & lake data**		8,051	**196.4**	234.7	4.6	6,962	**139.0**	160.9	4.6	2.8	<0.0001
Total all zones**		50,049	**127.6**	125.6	164.2	18,209	**116.1**	127.9	3.2	2.5	<0.0001

Table 4.3 Continued:

Quebec	Upland stream sediment THg, ppb				Lowland stream sediment THg, ppb				Upland versus lowland		Lake versus stream	
Survey zone	**n**	**Mean**	**Std. Dev.**	**Std. Err.**	**n**	**Mean**	**Std. Dev.**	**Std. Err.**	**Crit. Diff.***	**p-value***	**Crit. Diff.**	**p-value**
Abitibi A (22)	5,561	**78.5**	197.1	2.6	2,626	**77.8**	176.0	3.4	8.8	0.8647	21.7	0.0194
Abitibi B (21)	87	**87.0**	163.0	17.5	64	**45.9**	26.5	3.3	40.7	0.0478	23.2	0.0024
Appalaches A (19)	1,448	**69.2**	55.0	1.4	589	**52.0**	44.6	1.8	5.0	<0.0001	-	-
	36	**34.6**	24.2	4.0	31	**39.4**	56.8	10.2	20.8	0.6501	-	-
Total**	1,484	**68.3**	54.2	1.5	620	**51.4**	45.2	2.3			73.1	0.0046
Appalaches B (20)	7,229	**148.5**	115.9	1.4	727	**107.7**	93.3	3.5	8.7	<0.0001	5.9	<0.0001
Churchill A (30)	876	**135.0**	121.3	4.10	181	**139.0**	138.2	10.3	19.9	0.6923	-	-
Grenville A (23)	6,462	**226.1**	429.9	5.35	1,951	**264.1**	482.7	10.9	22.4	0.0009	-	-
	20	**46.1**	53.1	11.88	1	**10.0**			113.9	0.5151	-	-
Total**	6,482	**225.6**	428.7	5.4	1,952	**263.9**	482.4	10.9			31.4	<0.0001
Grenville B (24)	1,025	**56.5**	52.8	1.65	237	**57.2**	73.5	4.8	8.1	0.8639	3.4	<0.0001
Grenville C (25)	1,296	**63.7**	53.8	1.49	166	**52.4**	46.2	3.6	8.6	0.0099	3.7	<0.0001
Grenville D (26)	268	**79.0**	54.9	3.35	19	**92.2**	59.4	13.6	25.8	0.3160	15.9	0.0004
Minto B (29)	22	**33.4**	38.9	8.30	12	**37.5**	30.0	8.6	26.4	0.7542	13.4	<0.0001
Opatica (27)	31	**86.1**	77.3	13.88	22	**102.0**	54.8	11.7	38.6	0.4094	-	-
	21	**33.0**	40.4	8.81	12	**40.9**	39.1	11.3	29.5	0.5877	-	-
	669	**280.6**	532.2	20.58	214	**196.2**	312.1	21.3	75.2	0.0280	-	-
Total**	743	**258.2**	484.7	19.6	260	**173.8**	264.7	19.5			17.4	<0.0001
Plate-forme (18)	6	**22.2**	18.5	7.55	1	**27.0**			21.3	0.8184	-	-
	5	**13.4**	7.6	3.40	1	**10.0**			23.1	0.7040	-	-
	11	**18.2**	13.5	5.7	2	**18.5**	12.0	8.5			27.6	<0.0001
Total zones with stream & lake data**	5,659	**112.4**	259.8	5.4	5,139	**154.3**	**291.8**	**7.3**	9.6	0.0633		
Total all zones**	25,062	**141.8**	**216.0**	**3.4**	6,854	**135.2**	**236.6**	**6.3**	7.4	0.0822		

*Critical difference (Crit. Diff.) and p-value by Fisher's Probable Least Squares Difference (PLSD).

** Weighted mean, standard deviation (Std. Dev.), and standard error (Std. Err.).

Areas with generally low to medium sediment THg, and occasional THg > 500 ppb in MB, Labrador, NS, NWT, ON, and SK*:*

- MB and SK (zones 7 and 9) - There are sediment samples with THg > 500 ppb, on both sides of the MB-SK provincial border near Flin Flon area and to the northwest of La Ronge Provincial Park in SK (Table 4.2).
- ON (zones 10-12) - Lake sediment THg increases to 21,000 ppb in the Sudbury region (zone 12).
- Cape Breton, NS (zone 17) - There are high THg for a number of areas on this island.
- Labrador (zone 14) - High sediment THg occurs along the QC-Labrador border in Churchill A, up to 900 ppb (lake), and up to 700 ppb (lake) near Snegamook Lake.
- NWT (zone 5) - North-east of Great Bear Lake, the highest lake sediment THg value amounts to 727 ppb.

Discussion and Conclusions

The analysis of GSC open file data for THg in bulk stream and lake sediments of this chapter was done for survey zones across Canada, with emphasis on discerning geographic and topographic terrain effects.

Mean THg values are generally higher for upland streams and lakes than for lowland streams and lakes. Once at the surface, Hg containing minerals combine with atmospherically-sequestered Hg, and are then transported to streams and lakes by way of water, soil, and wind erosion (Dai *et al.*, 2012). This accounts for the trend that uplands

provide greater surface exposure of heavy mineral, while lowland streams and lakes are more distant from these sources.

On average, lakes have higher sediment THg than streams. This was because stream sediments are coarser than lake sediments, and heavy metals including Hg are more associated with fine mineral and organic particles (Rydberg *et al.*, 2012). Furthermore, repeated streambed scouring, wave action and bioturbation lead to a steady refreshment of stream sediments (Sichingabula, 1998; Haschenburger, 2006; Riscassi *et al.*, 2011), while lake sediments remain mostly undisturbed and accumulate Hg and other heavy metals together with organic matter over long periods of time.

Background levels for THg are elevated in the more populated areas along the south, but dropped toward the remote and coldest locations in the east, north and west. In terms of geographic locations, THg varied from alpine to non-alpine and arctic to boreal and temperate climates, and from barrens and open fields to tundra and forests as follows:

Sediment THg by region: Arctic Cordillera and southern Arctic ≈ alpine areas with ice-covered caps < Boreal Shield and Atlantic Maritimes < Taiga Shield < Hudson Bay (Table 4.3).

Sediment THg by vegetation/land cover type: snow/ice < frost-worked soil (sparse vegetation) < non-vegetated < wetland < graminoid Tundra < shrub Tundra < conifer and mixedwood (Appendices 2, 3).

The increasing vegetation cover from arctic to temperate climate areas increases the capturing of atmospheric transported Hg at air-vegetation surface through wet and dry deposition (Muir *et al.,* 2009). This effect is strongest in forested areas because deep

forest canopy layers promote the sequestering, retaining and, transferring atmospheric Hg (Poissant *et al.,* 2008).

Lowest lake sediment THg occurs downslope from alpine ice fields in BC and YT, and from artic snow- and ice-covered areas in the NWT, NU, QC and Labrador (Figure 4.4; Appendix A.2). In part, this could be due to low rates of annual precipitation rate coupled with photochemically-induced Hg evasion from sun-exposed snow/ice and barren surfaces (Steffen *et al.*, 2008; Sanei *et al.*, 2010; Mann *et al.,* 2014). This is evident from the low sediment THg of Baker Lake, NU, northern QC, and Labrador, and occurs in spite of relatively high atmospheric Hg deposition rates (9.1, 12.3, 10.0, μg m^{2-} a^{-1}, respectively). Specifically Bathurst Island, NU, and northern QC and Labrador are mostly covered by barren and none to sparsely covered by vegetation due to their North Arctic and Arctic Cordillera climate condition, respectively. In these regions, cold and harsh climate restrict weathering and erosion release of geogenic Hg to sediments.

The gradually increasing vegetation cover towards the southern region of NWT and NU subsequently results in higher atmospheric deposition and sediment THg, as further explored in Appendix 2. In the Great Bear Lake area, NWT, increased atmospheric Hg sequestration due to increased tree-line vegetation cover adds to sediment THg in combination with increased contributions from geogenic Hg sources (Chapter 8; Macdonald *et al.,* 2004). With climate change and increasing air temperature, one can therefore expect that increasing vegetation cover would enhance sediment THg in northern watersheds, as also suggested by Cook *et al. (*2008), Chételat *et al. (*2014), and Jutras *et al. (*2014).

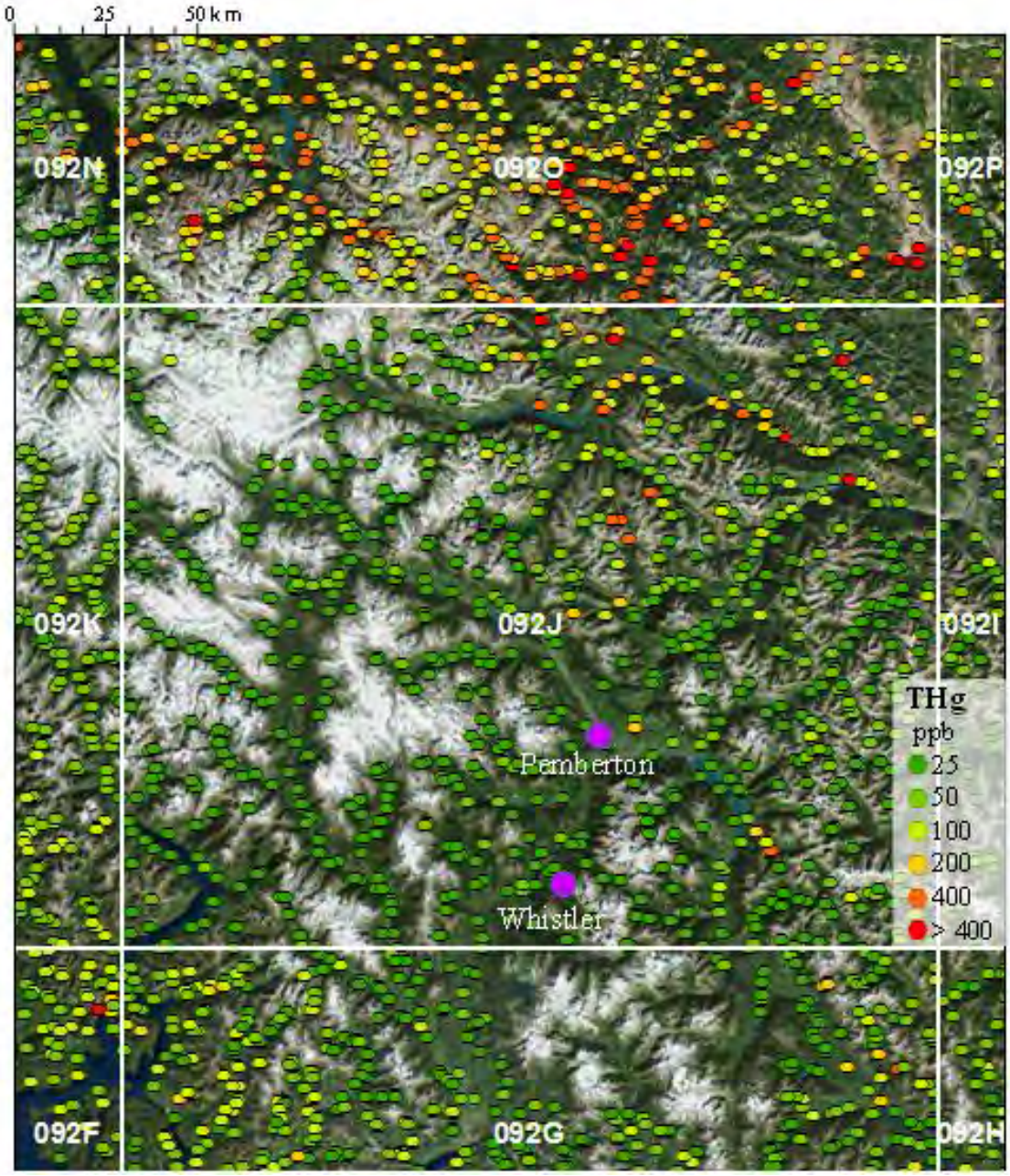

Figure 4.4 Example of low sediment THg (ppb) in streams next to and below alpine ice fields in BC.

.

Chapter 5 Sediment THg versus Atmospheric Hg Deposition and Precipitation Rates, and Air Temperature

Introduction

The objective of this chapter was to determine how sediment THg varies across Canada based on previously modelled geographic variations in atmospheric Hg deposition (Dastoor and Moran, 2010) and climate (Daly *et al.*, 2002). This objective follows the earlier findings by Munthe *et al. (*2007), Muir *et al. (*2009), and Scudder *et al. (*2009) who found direct correlations between sediment THg, climate, and local net flux estimates for atmospheric Hg deposition. In principle, atmospherically-deposited Hg, which includes vegetation-sequestered Hg, becomes a source for terrestrial and aquatic Hg bioaccumulation and therefore a component of stream and lake sediments due to the following reasons:

- **Deposition:** Atmospherically-deposited Hg reaches the ground through litter- and throughfall (St. Louis *et al.*, 2001; Ericksen *et al.*, 2003; Schuster *et al.*, 2008). Also, Hg is directly deposited onto the lake surface (Rada *et al.,* 1989).
- **Accumulation:** Atmospheric Hg is captured by terrestrial and aquatic vegetation on uplands and in wetlands and lakes (Stokes and Dreier, 1983; Rada *et al.*, 1989; Moore *et al.*, 1995; Stamenkovic and Gustin, 2009). The rate of vegetative Hg sequestration (or accumulation) increases with increasing of the rate of atmospheric Hg deposition and Hg exposure time (Lodenius *et al.*, 2003; Yu *et al.*, 2013). The length of growing season exposure time also affects the Hg exposure time of soil, surface waters, and vegetation (Ericksen *et al.*, 2003). Surface induced-

volatilization of Hg decreases the overall amounts of surface deposited and sequestered Hg (Dastoor *et al.,* 2008; Zhang *et al.,* 2009).

- **Transport:** Hydrologically-induced transfer of organically-bound Hg in the form of Hg-DOC or Hg-POC (particulate organic C) releases sequestered Hg to lowland wetlands, streams, and lakes (Schuster *et al.*, 2008). Soil and sediment erosion is also another Hg transportation route (Dai *et al.*, 2012).

- **Availability:** Within the accumulated decaying organic matter, total C is lost faster than organically-bound Hg, with Hg mostly bound by the S component of humic substances (Xia *et al.*, 1999). Therefore, Hg availability for bioaccumulation would gradually decrease with advancing state of organic matter decay and humification (Nasr, 2007). This availability would further decrease as the sediment layers thicken).

Atmospheric Hg Deposition versus Climate Variables, by NTS Tile

The GRAHM2005 mean annual net atmospheric Hg deposition rate per NTS tile ranges from 1 to 40 μg m^{-2} a^{-1} across Canada (Figure 5.1). In detail, this rate increases with (i) increasing mean annual precipitation rates and July temperature and (ii) decreasing mean annual January air temperature, and is further affected by geographic location, as follows (Figure 5.2):

$$\text{atm.Hg}_{dep}\ (\mu g\ m^{-2}\ a^{-1}) = -\ (24.7 \pm 0.8\ SD) + (26.8 \pm 1.0\ SD)\ ppt\ (m\ a^{-1})^{0.5}$$
$$+ (0.80 \pm 0.06\ SD)\ T_{July}\ (^{\circ}C) - (0.25 \pm 0.03\ SD)\ T_{Jan.}\ (^{\circ}C)$$
$$- (7.7 \pm 0.7\ SD)\ \text{Pacific Rim} + (7.5 \pm 1.0\ SD)\ \text{Bathurst Island} \qquad R^2 = 0.803 \qquad \text{Eq. 5.1}$$

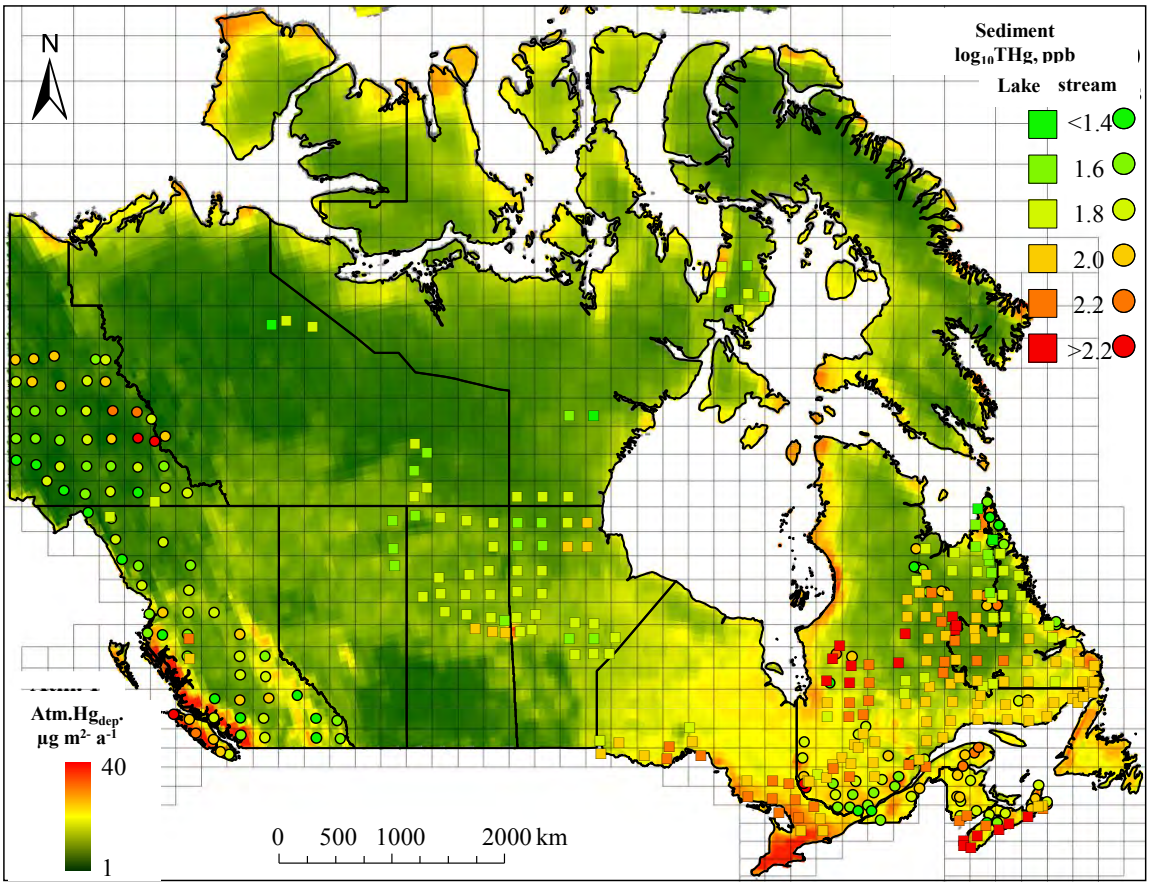

Figure 5.1 GRAHM2005 mean annual net atmospheric Hg deposition rates ($atmHg_{dep}$; µg m^{-2} a^{-1}) from low (green) to high (red), acquired from Environment Canada (Dastoor and Moran, 2010). Overlaid: mean stream and lake sediment $log_{10}THg$ (ppb; points), by NTS tile.

The NTS tiles for the Pacific Rim (coastal zone for BC, coded 1, elsewhere 0) and the Bathurst Island in NU (coded 1, 0 elsewhere) adjust for otherwise under- and over-estimated atmospheric Hg deposition rates, respectively.

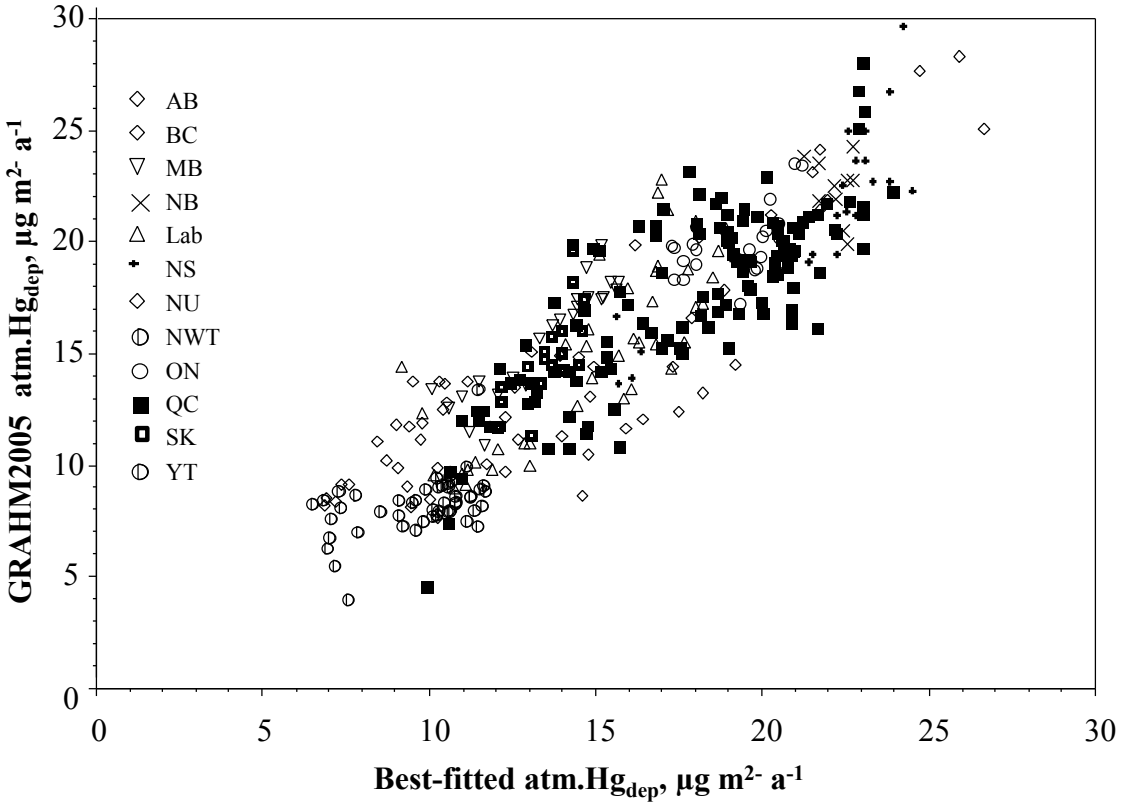

Figure 5.2 Scatterplot of GRAHM2005 mean annual net atmospheric Hg deposition rate 2005 ($atmHg_{dep}$; µg m^{-2} a^{-1}) versus best-fit Hg deposition rate (Eq. 5.1), by NTS tile.

Including the $T_{Jan.}$ and the Bathurst Island locator variables reflects the greater retention of volatile Hg as winter temperatures and the length of the summer period decreases. Including the Pacific Rim locator variable reflects the lower than precipitation estimated atmospheric Hg deposition rate in this area because of orographic dilution, i.e. atmospheric water content increases as air rises over mountainous terrain. In detail, Eq. 5.1 implies that a sustained increase in precipitation by 0.1 m at 1 m per year, on average, adds 2.68 µg m^{-2} to atmospheric Hg deposition rate annually where this increase is experienced. Likewise, an increase of 1 ˚C in July temperature, on average, increases this

rate by 0.80 μg m^{-2} a^{-1}. A parallel increase of 1 ˚C in January air temperature, however, compensates for some of that increase by 0.25 μg m^{-2} a^{-1}, thereby resulting in mean atmospheric annual increase of 0.55 ± 0.09 SD μg m^{-2} where the annual temperature increases throughout the year by 1 ˚C.

Sediment THg versus Atmospheric Hg Deposition, by Survey Zone

Plotting and regressing mean stream and lake sediment THg against the mean GRAHM2005 estimated atmospheric Hg deposition rate by survey zone (Figure 5.3) produced the following equation (p-value < 0.0001):

$$THg\ (ppb) = 2.0\ (atm.Hg_{dep},\ \mu g\ m^{-2}\ a^{-1})^{1.3} \qquad R^2 = 0.870 \qquad \text{Eq. 5.2a}$$

In this equation, all survey zones with very high geogenic and/or anthropogenic Hg sources were excluded, as follows: QC (Appalaches, B; 20; Churchil A, 30; Grenville A, 23; Opatica, 27), NS mainland (16), Selwyn Basin (YT, 3), Great Bear Lake (NWT, 5). Also excluded were survey areas with relatively low sediment THg in the east of BC (6), MB (9), NB (5), and QC: Abitibi A (22); Appalaches A (19), Plate-forme (18). Including all of these locations still produced a positive trend, i.e.:

$$THg\ (ppb) = 14.8 + 4.42\ (atm.Hg_{dep},\ \mu g\ m^{-2}\ a^{-1}) \qquad R^2 = 0.252 \qquad \text{Eq. 5.2b}$$

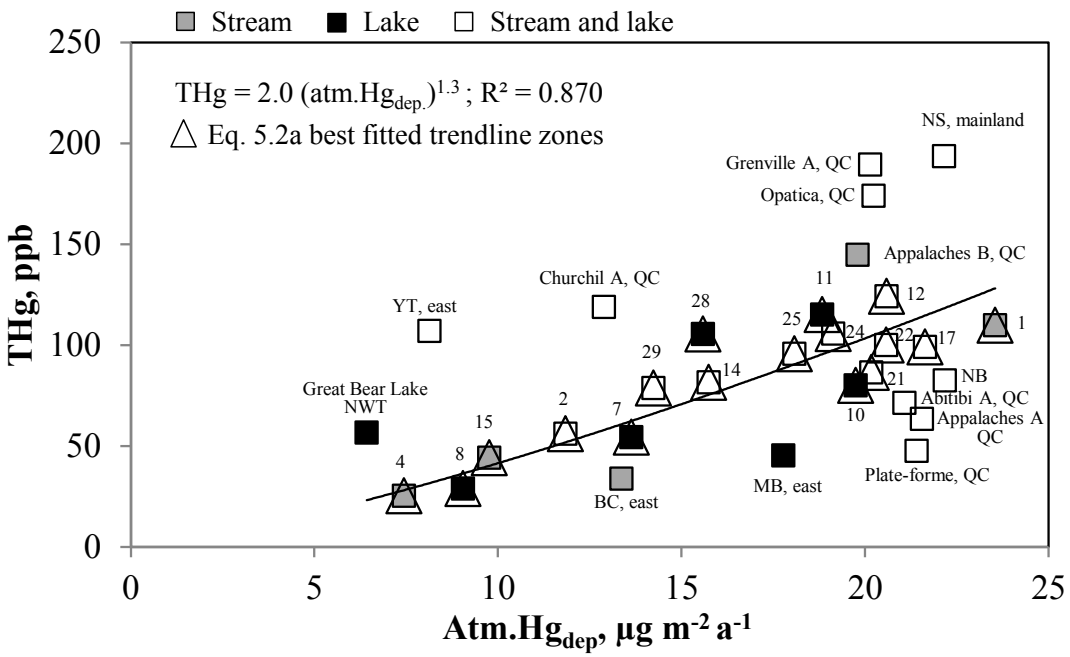

Figure 5.3 Scattergram of stream and lake sediment THg (ppb) versus GRAHM2005 mean annual net atmospheric Hg deposition rate (atm.Hg_{dep}, µg m^{-2} a^{-1}), by survey zones 1 to 30. The trend line (Eq. 5.2) is best-fit to the numbered survey zones; the non-numbered survey zones were excluded due to the dominance of geologic formations of relatively high or very low geogenic Hg content as well as zones with high anthropogenic Hg sources.

Sediment THg versus Atmospheric Hg Deposition and Climate Variables, by NTS Tile

Plotting and regressing the mean lake sediment THg against the GRAHM2005 mean annual net atmospheric Hg deposition rate by NTS (Figure 5.4) produced the following regression equation (p-value < 0.0001):

$\log_{10}$THg (ppb, lake) = (1.37 ± 0.053 SD) + (0.031 ± 0.03 SD) atm.Hg_{dep} (µg m^{-2} a^{-1})

$R^2 = 0.318$ Eq. 5.3

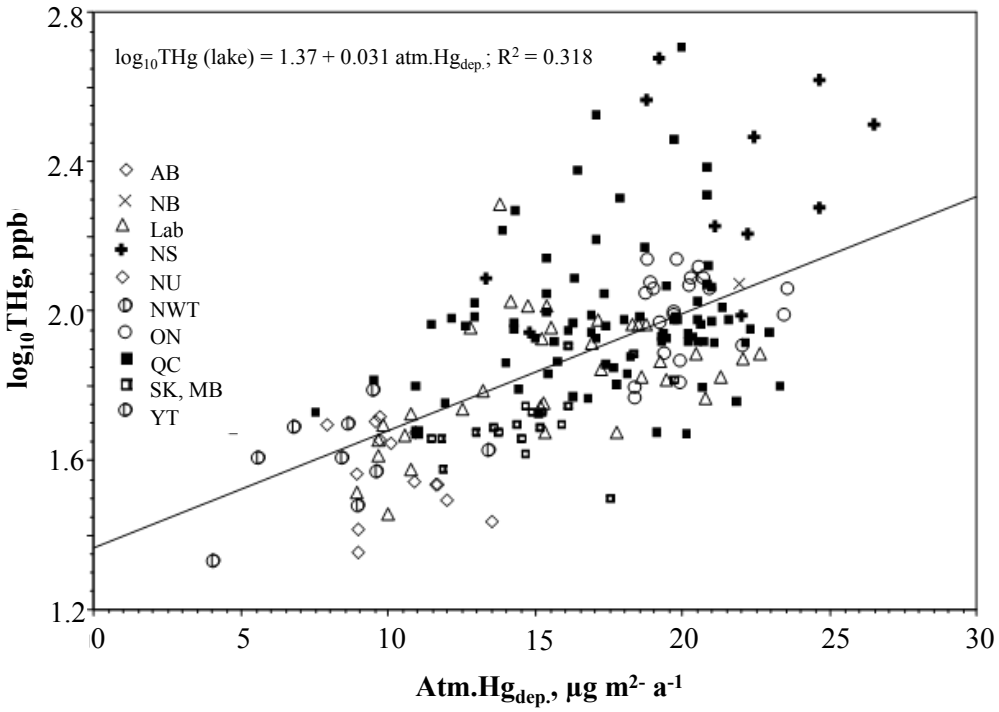

Figure 5.4 Scatterplot of lake sediment $\log_{10}$THg (ppb) versus GRAHM2005 mean annual net atmospheric Hg deposition rate (atm.Hg_{dep}, µg m^{-2} a^{-1}; Eq. 5.3), by NTS tile.

Doing the same for stream sediment THg does not produce a clear trend. In detail Eq. 5.3 implies that an increase in atmospheric Hg deposition rate of 10 µg m^{-2} a^{-1}, on average, increases lake sediment THg by a factor of 2.04. For NTS tiles where atmospheric Hg deposition rate is zero or near zero, mean lake sediment THg is at or near 23.4 ppb. Plotting mean sediment THg against the GRAHM2005 mean annual net atmospheric Hg deposition rates by NTS tile also produces a positive trend for lakes, but again not for streams (Figure 5.5):

$\log_{10}$THg (ppb, lake) = (1.44 ± 0.04 SD) + (0.58 ± 0.04 SD) (ppt, m a^{-1})

$R^2 = 0.407$ Eq. 5.4

$\log_{10}$THg (ppb, stream) = (1.68 ± 0.05 SD) - (0.022 ± 0.060 SD) (ppt, m a^{-1})

$R^2 = 0.001$ Eq. 5.5

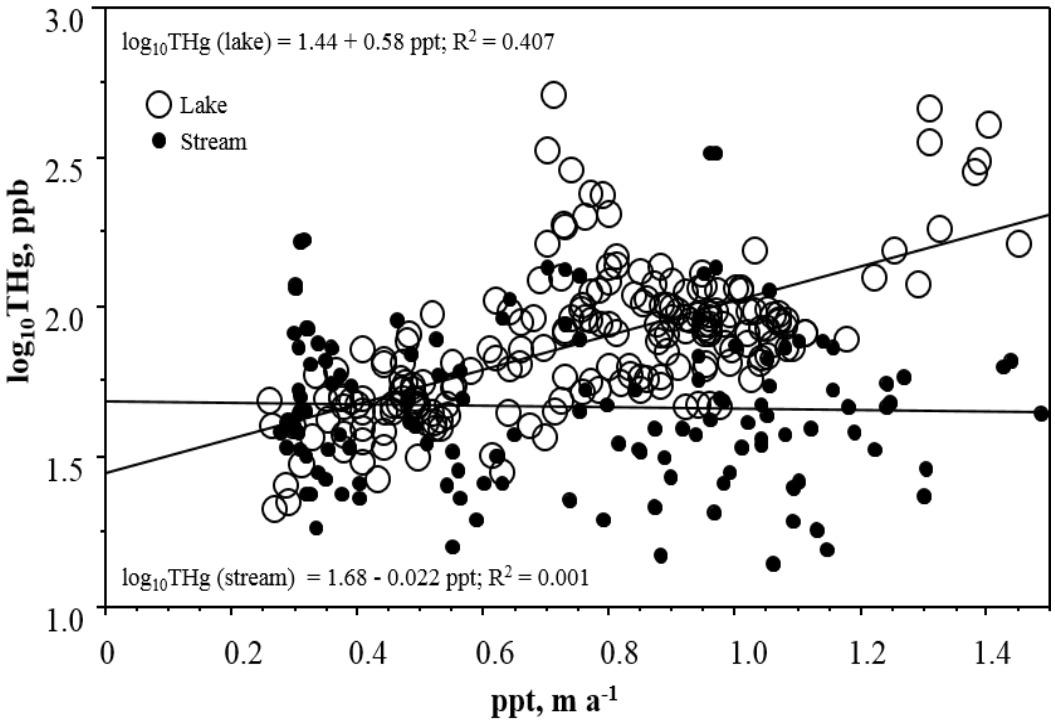

Figure 5.5 Scatterplot of stream and lake sediment $\log_{10}$THg (ppb) versus mean annual precipitation rate (ppt, m a^{-1}; Eqs. 5.4, 5.5), by NTS tile.

Eq. 5.4 implies that an increase of 100 mm of precipitation, on average, increases lake sediment THg by approximately 14 %. For NTS tiles with low precipitation rates, lake sediments has, on average, a THg of as low as 27.6 ppb. In contrast, stream sediments maintain a mean value of approximately 50 ppb across the precipitation rate range from near zero to greater than 1,400 mm.

Eqs. 5.3 and 5.4 were used to produce maps for lake sediment $\log_{10}$THg (Figure 5.6). These maps generally conform to the mean lake sediment $\log_{10}$THg survey values by NTS tile.

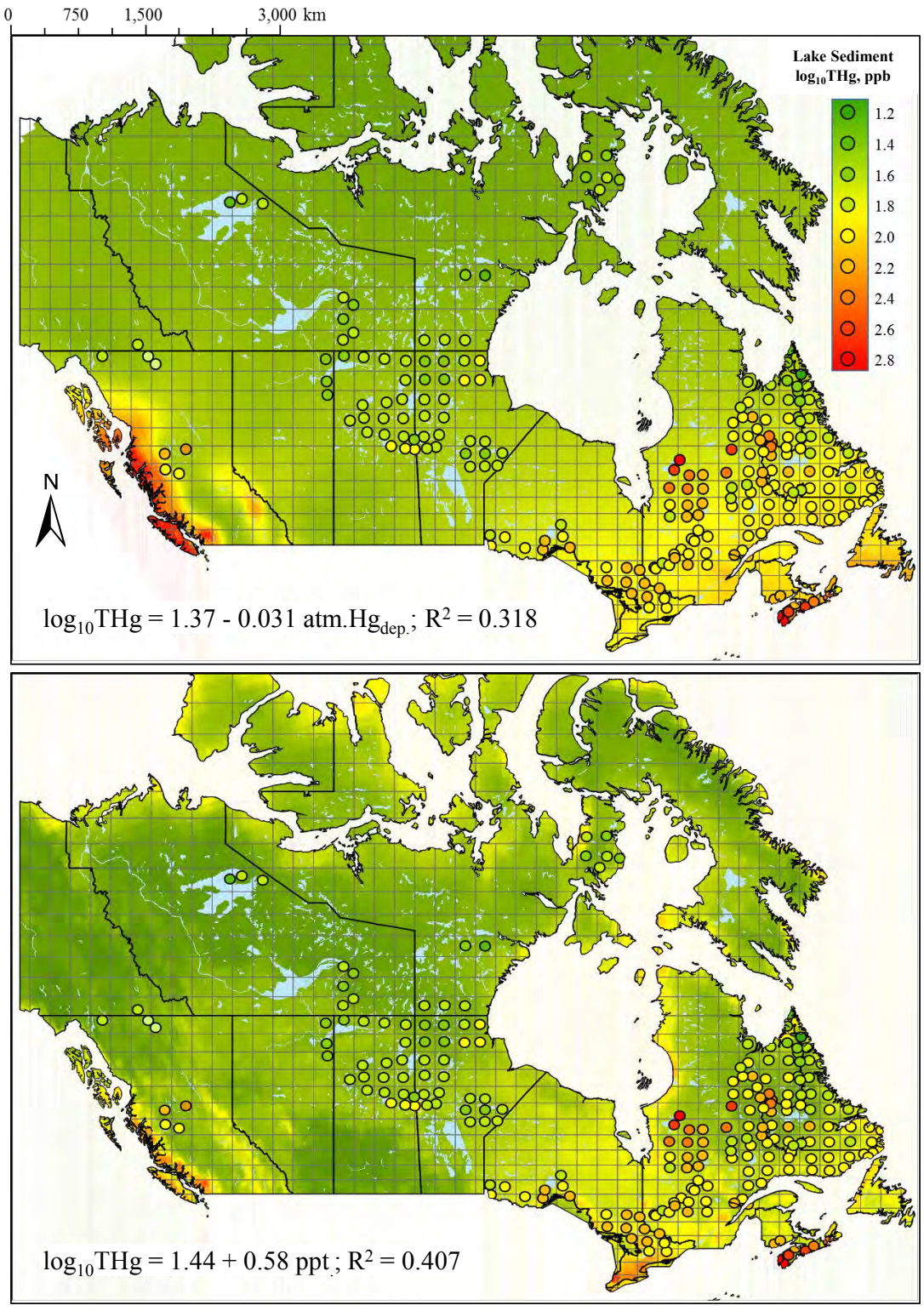

Figure 5.6 Lake sediment log_{10}THg (ppb) estimated from GRAHM2005 mean annual net atmospheric Hg deposition rate (atm.$Hg_{dep.}$, µg m^{-2} a^{-1}; Eq. 5.3, Figure 5.4; top) and mean annual precipitation rates (ppt, m a^{-1}; Eq. 5.4, Figure 5.5; bottom). Overlaid: mean log_{10}THg, by NTS tile (points).

Discussion

The results in Figures 5.1 to 5.6 and the associated equations indicate that both mean annual atmospheric Hg deposition rate and mean lake sediment THg by NTS tile are influenced by climatic conditions. The maps in Figure 5.6 indicate that mean lake sediment THg increases towards northeastern Canada, and is also particularly high on Vancouver Island in northwestern BC. The trend of increasing atmospheric Hg deposition rate with increasing precipitation would be due to the wet component of atmospheric Hg deposition. The positive influence of increasing July temperatures correlates with increasing vegetative cover and increasing length of growing season from arctic and alpine to temperate climate conditions: increased vegetation cover and duration per year means increased sequestration of atmospheric Hg by terrestrial and aquatic vegetation (Moore *et al.*, 1995; Miller *et al.*, 2005). Decreasing January air temperatures means increased retention of surface deposited Hg on the ground due to temperature-reduced Hg volatilization for longer periods of the year.

According to Barrow *et al. (*2004), summer and winter temperatures will increase by approximately 5 to 6 ˚C at, e.g. Resolute Bay (northwest corner of Cornwallis Island; northeast of Bathurst Island, NU) by 2050. Based on Eq. 3.1, this would translate into a net gain in atmospheric Hg deposition rate of approximately 3.0 μg m^{-2} a^{-1}. Lake sediment THg is predicted to increase as well by almost a factor of 10. Further south at Norman Wells (along the Mackenzie river; west of Great Bear Lake, NWT), the corresponding temperature would increase by approximately 2 to 3 ˚C, and the growing season would increase by approximately a month (Barrow *et al.,* 2004).

Note that the lake sediment THg values refer to bulk sediment samples taken from up to the 30 cm depth. This depth would correspond to a sediment accumulation time for a period of 100 years (Lockhart *et al.,* 2000). Hence, the above results do not account for any recent increases in atmospheric Hg deposition to cumulative Hg inputs over at least 100 years or so. For a more consistent analysis, one needs to relate the results of the sediment THg surveys (obtained during the latter half of the 20^{th} century) to the mean atmospheric deposition and climate conditions over the last 100 years or so. While this may change the numeric values of the coefficients in Eqs. 5.1 to 5.5, it would not affect the relative sediment THg trends with respect to changing precipitation rate and July and January air temperatures across Canada and through time.

Mean lake sediment THg is significantly affected by atmospheric Hg deposition and precipitation rate by NTS tile, but mean stream sediment THg is not. This contrast reflects the following lake versus stream differences:

- The lake catchments are generally larger than stream catchments. Therefore, lake sediment THg is more reflective of steady and area-wide atmospheric Hg deposition rates than stream sediment THg.
- Stream sediments are generally closer to local Hg mineralizations and/or anthropogenic activities than lake sediments (Al et al., 2006; Broster et al., 2009, 2013).
- Stream sediments are subject to frequent relocation and scouring and tend to vary from coarse to fine (Fleck *et al.*, 2011; Lin *et al.,* 2011; Riscassi *et al.,* 2011), while lake sedimentation is steady, cumulative, and fine textured and organically-

enriched (Guy, 1970; Yang, 1996; Madsen *et al.*, 2001). In addition, lake sediments remain largely undisturbed (Herschy, 2012).

- Stream sediments may lose some sediment THg by way of DOC and POC, and with the finer particles generally carrying more Hg than larger particles (Gray *et al.*, 2000; Marvin-Dipasquale *et al.*, 2009; Fleck *et al.*, 2011; Riscassi *et al.*, 2011). Once entering lakes, the finer particles (Vernet and Thomas, 1972) and some of the organically-bound Hg settle on the sediment bed, especially after coagulation (Wu *et al.*, 2013).
- Atmospheric deposition to lakes is direct, whereas indirect to streams. While some of the lake deposited Hg volatilize, some of it is sequestered by DOC, POC, and aquatic organisms. In addition, some of the DOC is reallocated by flocculation at the lake bottom that subsequently leads to further settling of the organically-sequestered Hg in sediments (von Wachenfeldt *et al.,* 2008).

The above approach, as it was based on a 25 x 25 km^2 raster grid for atmospheric Hg deposition rate, cannot be used to address small-scale variations in atmospheric Hg deposition rate. The summation of sediment THg by NTS tiles is also too coarse to detect small-scale correlations between Hg emissions, deposition, and sediment accumulation. Even locally, plume dispersal patterns, downwind variations in terrain and vegetation cover, and coal chemical composition often obscure such correlations (Bourque and Arp, 1996; Landis *et al.,* 2014).

Conclusions

This chapter established an empirical approach for relating THg in lake sediments to modelled atmospheric Hg deposition within the context of basic climate variables (annual precipitation rate, July and January air temperatures). While THg in streams should be similarly affected, it is reasonable to suggest that the sedimentation environment in streams is, as discussed, variable and thereby obscures potential relationships between stream sediment THg, atmospheric Hg deposition, and climate. The next Chapter expands this analysis by including sediment organic matter as an additional variable to model and map stream and lake sediment THg trends across Canada as averaged, also by NTS tile.

Chapter 6 Sediment THg versus LOI, Atmospheric Hg Deposition, and Related Climate Conditions

Introduction

Earlier study by Rasmussen *et al. (*1998a) documented a positive relationship between sediment THg and organic matter content. The objective of this chapter was to analyze, quantify and map how stream and lake sediment THg and organic matter content (determined as LOI, Chapter 3) relate to each other, and are affected by the mean annual variations in atmospheric Hg deposition, precipitation, and July and January air temperature across Canada.

LOI and THg: Basic Statistics, by Province/Territory

By individual sampling location, 90 % of all LOI values for the stream sediments fall below 10 %, while lake sediment LOI peaks at approximately 35 %. In contrast, stream and lake sediment THg values occur most frequently at ≈ 100 ppb, with stream sediment THg somewhat lower but more variable than lake sediment (Figure 6.1). By province/territory and QC geological survey zone, mean lake LOI values are higher than stream LOI but not so for THg (Tables 6.1 and 6.2).

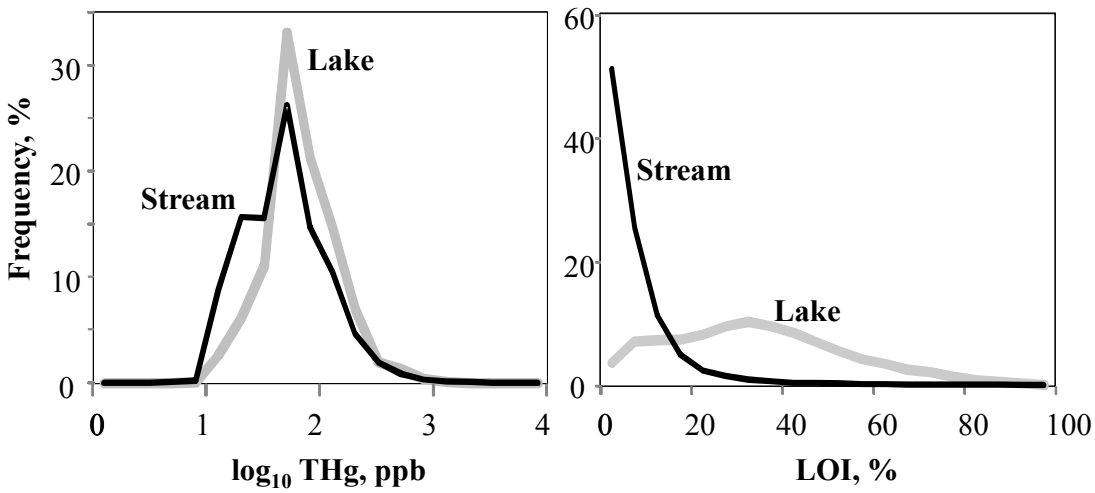

Figure 6.1 Frequency diagram of stream and lake sediment log_{10}THg (ppb) and LOI (%).

Table 6.1 Sediment THg (ppb) and LOI (%), by province/territory and medium type (stream, lake).

Quebec survey zone	Medium	n	Sediment THg, ppb				Sediment LOI, %			
			Mean	Min.	Max.	Std. Dev.	Mean	Min.	Max.	Std. Dev.
Abitibi A (22)	Lake	299	**104.1**	5	422	68.7	**33.6**	2	88	15.9
Churchill A (30)		18,496	**118.2**	5	1,500	93.1	**26.9**	1	98	19.9
Grenville A (23)		764	**105.6**	5	339	56.1	**32.4**	2	80	12.2
Grenville B (24)		5,768	**109.6**	5	490	56.3	**34.8**	2	94	14.6
Grenville C (25)		4,831	**105.9**	5	639	66.9	**27.3**	2	98	14.1
Grenville D (26)		17,104	**108.6**	5	9,820	137.5	**30.2**	1	98	19.1
Minto A (28)		7,141	**109.8**	5	7,180	153.4	**23.1**	2	98	13.1
Minto B (29)		1,325	**80.0**	6	376	39.4	**31.8**	2	92	19.1
Opatica (27)		12,389	**185.4**	10	7,410	243.7	**28.1**	1	98	21.7
Plate-forme (18)		10	**85.8**	26	150	45.5	**28.2**	2	90	28.0
Total *		68,127	**124.6**	5	9,820	131.4	**28.4**	1	98	18.4
Abitibi A	Stream	8,187	**78.3**	5	7,331	190.6	**12.5**	1	92	15.03
Abitibi B (21)		151	**69.6**	5	1,400	126.3	**18.1**	1	91	19.59
Appalaches A (19)		2,104	**63.3**	5	520	52.7	**10.5**	1	95	14.38
Appalaches B (20)		7,956	**144.8**	5	1,435	114.6	**30.5**	1	97	20.00
Churchill A		1,057	**135.7**	5	980	124.3	**30.1**	1	92	18.62
Grenville A		8,434	**234.5**	5	9,392	442.5	**13.4**	1	94	17.18
Grenville B		1,262	**56.6**	5	933	57.2	**10.2**	2	96	11.24
Grenville C		1,462	**62.4**	5	354	53.1	**17.5**	2	100	20.21
Grenville D		287	**79.9**	10	412	55.2	**18.6**	2	92	15.02
Minto B		34	**34.9**	5	150	35.6	**19.7**	1	69	19.90
Opatica		969	**243.4**	5	6,720	470.5	**28.3**	1	90	23.32
Plate-forme		13	**18.2**	10	57	13.8	**2.1**	1	4	0.64
Total*		31,916	**140.4**	5	22,690	222.1	**18.4**	1	100	17.3
Total*		100,043	**129.6**	5	22,690	160.3	**25.2**	1	100	18.0

* Weighted mean and standard deviation (Std. Dev.). This table only includes data with both THg and LOI values.

Table 6.2 Sediment THg (ppb) and LOI (%), by QC geological survey zones (18-30) and medium type (stream, lake).

Quebec survey zone	Medium	n	Sediment THg, ppb				Sediment LOI, %			
			Mean	Min.	Max.	Std. Dev.	Mean	Min.	Max.	Std. Dev.
Abitibi A (22)	Lake	299	**104.1**	5	422	68.7	**33.6**	2	88	15.9
Churchill A (30)		18,496	**118.2**	5	1,500	93.1	**26.9**	1	98	19.9
Grenville A (23)		764	**105.6**	5	339	56.1	**32.4**	2	80	12.2
Grenville B (24)		5,768	**109.6**	5	490	56.3	**34.8**	2	94	14.6
Grenville C (25)		4,831	**105.9**	5	639	66.9	**27.3**	2	98	14.1
Grenville D (26)		17,104	**108.6**	5	9,820	137.5	**30.2**	1	98	19.1
Minto A (28)		7,141	**109.8**	5	7,180	153.4	**23.1**	2	98	13.1
Minto B (29)		1,325	**80.0**	6	376	39.4	**31.8**	2	92	19.1
Opatica (27)		12,389	**185.4**	10	7,410	243.7	**28.1**	1	98	21.7
Plate-forme (18)		10	**85.8**	26	150	45.5	**28.2**	2	90	28.0
Total *		68,127	**124.6**	5	9,820	131.4	**28.4**	1	98	18.4
Abitibi A	Stream	8,187	**78.3**	5	7,331	190.6	**12.5**	1	92	15.03
Abitibi B (21)		151	**69.6**	5	1,400	126.3	**18.1**	1	91	19.59
Appalaches A (19)		2,104	**63.3**	5	520	52.7	**10.5**	1	95	14.38
Appalaches B (20)		7,956	**144.8**	5	1,435	114.6	**30.5**	1	97	20.00
Churchill A		1,057	**135.7**	5	980	124.3	**30.1**	1	92	18.62
Grenville A		8,434	**234.5**	5	9,392	442.5	**13.4**	1	94	17.18
Grenville B		1,262	**56.6**	5	933	57.2	**10.2**	2	96	11.24
Grenville C		1,462	**62.4**	5	354	53.1	**17.5**	2	100	20.21
Grenville D		287	**79.9**	10	412	55.2	**18.6**	2	92	15.02
Minto B		34	**34.9**	5	150	35.6	**19.7**	1	69	19.90
Opatica		969	**243.4**	5	6,720	470.5	**28.3**	1	90	23.32
Plate-forme		13	**18.2**	10	57	13.8	**2.1**	1	4	0.64
Total*		31,916	**140.4**	5	22,690	222.1	**18.4**	1	100	17.3
Total*		100,043	**129.6**	5	22,690	160.3	**25.2**	1	100	18.0

* Calcuated weighted mean and standard deviation (Std. Dev.). This table only includes data with both THg and LOI values.

Sediment LOI versus Climate Variables, by NTS Tile

The best-fit regressing results for stream and lake LOI by NTS tile indicate that LOI is significantly influenced by climate as represented by mean annual precipitation rate and July and January air temperatures (p-value < 0.0001), and there is also a lake versus stream difference, as follows:

$$\log_{10}\text{LOI}\ (\%) = (0.246 \pm 0.028\ \text{SD})\ \text{ppt}\ (\text{m a}^{-1}) + (0.056 \pm 0.003\ \text{SD})\ T_{\text{July}}\ (^{\circ}\text{C}) - (0.020 \pm 0.001\ \text{SD})\ T_{\text{Jan.}}\ (^{\circ}\text{C}) - (0.482 \pm 0.021\ \text{SD})\ \text{medium}$$

$$R^2 = 0.703 \qquad \text{Eq. 6.4}$$

where medium is coded 1 for streams and 0 for lakes. This equation implies that LOI increases with increasing mean annual precipitation rate and July and January temperatures, and that lakes tend to have higher LOI than streams. In principle, increasing precipitation coupled with higher July temperature stimulate terrestrial and aquatic plant growth. Decreasing January temperatures are symptomatic of year-round reduced biological activities including organic matter decomposition. Lower LOI in streams versus lakes originates from a larger mineral content.

Figure 6.2 demonstrates how the actual versus the resulting best-fit LOI is distributed by province/territory and by lake versus stream. Using Eq. 6.4 produced the map in Figure 6.3, with stream and lake sediment LOI decreasing from northeastern to northwestern Canada and increasing again along the Pacific Rim. The overlay of the mean sediment LOI values per NTS tile on the two climate-based LOI maps generated via Eq. 6.4 underscores the general conformance between the Eq. 6.4 estimated and the tile averaged LOI values.

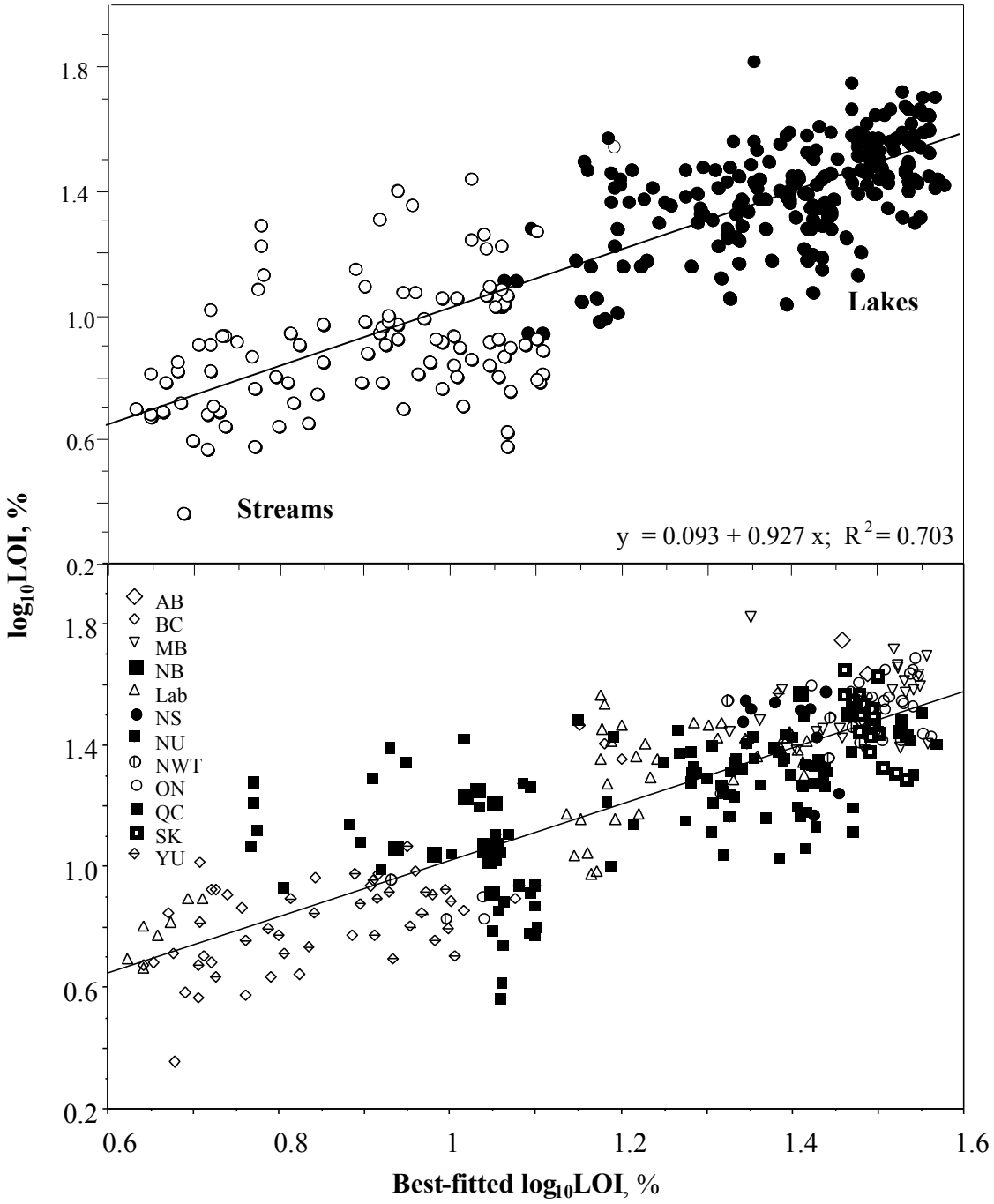

Figure 6.2 Scatterplots of stream and lake sediment $\log_{10}$LOI (%) versus best-fit $\log_{10}$LOI (Eq. 6.1), by medium type (stream, lake; top) and province/territory (bottom).

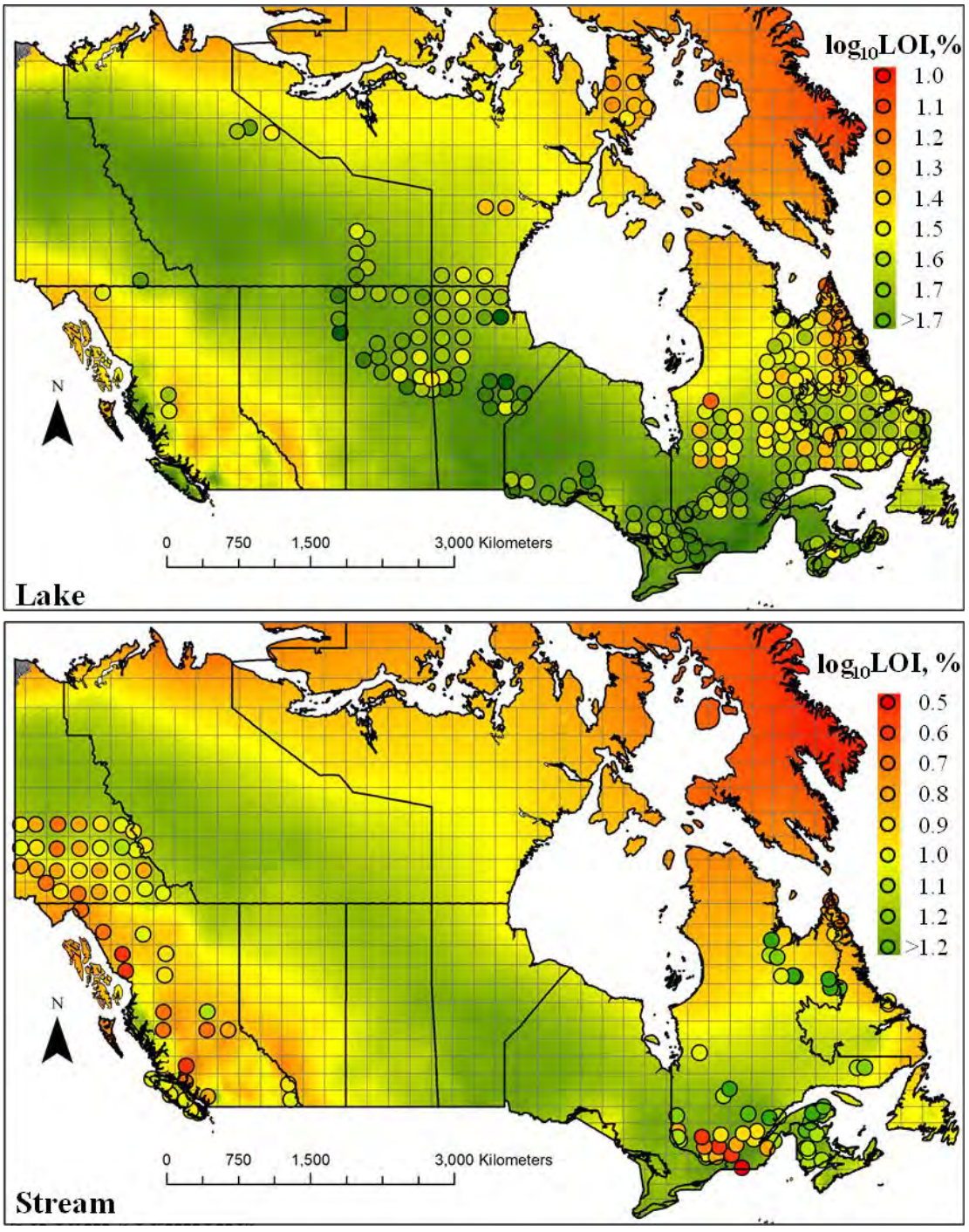

Figure 6.3 Sediment LOI (%), estimated using Eq. 6.1. Overlaid: mean stream and lake sediment $\log_{10}$LOI, by NTS tile (points). Top: lake. Bottom: stream.

Sediment THg versus LOI, Atmospheric Hg Deposition, and Climate Variables, by NTS Tile

Regressing the mean sediment $\log_{10}$Hg values by NTS tile against the corresponding NTS values for mean annual atmospheric Hg deposition and precipitation rates produced the following equations:

$$\log_{10}\text{THg (ppb, lake)} = (1.380 \pm 0.048\ \text{SD}) + (0.406 \pm 0.059\ \text{SD})\ \text{ppt (m a}^{-1}\text{)} + (0.012 \pm 0.004\ \text{SD})\ \text{atm.Hg}_{dep}\ (\mu\text{g m}^{-2}\ \text{a}^{-1}) \qquad R^2 = 0.432 \qquad \text{Eq. 6.2}$$

$$\log_{10}\text{THg(ppb, stream)} = (0.61 \pm 0.14\ \text{SD}) + (0.67 \pm 0.08\ \text{SD})\ \log_{10}\text{LOI (\%)} + (0.031 \pm 0.007\ \text{SD})\ T_{July}\ (^{\circ}\text{C}) \qquad R^2 = 0.434 \qquad \text{Eq. 6.3}$$

Hence, lake sediment THg is most significantly and positively related to the mean annual precipitation and atmospheric Hg deposition rates (p-value < 0.0001). In contrast, stream sediment THg is most significantly and positively related to stream sediment LOI and mean annual July temperature (p-value < 0.0001). The scatterplots in Figure 6.4 show how the actual stream and lake $\log_{10}$THg values per NTS tile are distributed against the corresponding best-fit values.

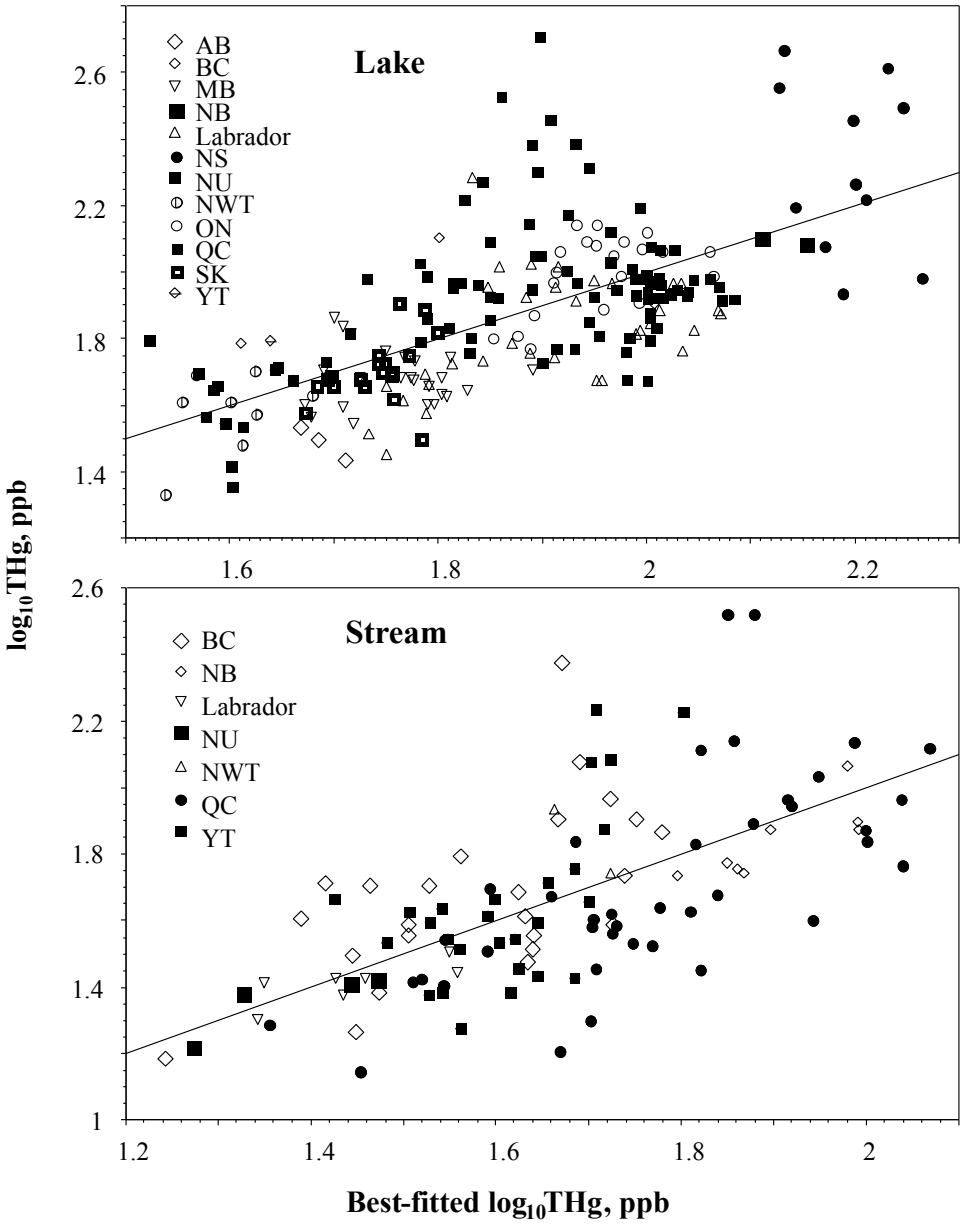

Figure 6.4 Scatterplots of sediment $\log_{10}$THg (ppb) versus best-fit $\log_{10}$THg (Eqs. 6.2, 6.3). Top: lakes. Bottom: streams.

Areas along the Pacific Rim and the northeastern provinces have elevated stream and lake sediment THg, and there is a general high to low THg grading towards north, northwest, and alpine areas (Figure 6.5). A similar directional trend is apparent for the sediment LOI projections (Figure 6.3). The overlay of the mean $\log_{10}$THg and $\log_{10}$LOI per NTS tile on the LOI maps generated with Eq. 6.1, 6.2 and Eq. 6.3 underscores the general conformance between estimated and NTS-tile averaged $\log_{10}$THg (Figure 6.5). The extent of actual versus modelled conformance is demonstrated in Figure 6.6 by way of cumulative frequency plots of the absolute differences between the modelled and the NTS-tile averaged $\log_{10}$THg and $\log_{10}$LOI values. The extent of lake versus stream model conformance is approximately the same, with 80% of the model projections falling within the $\log_{10}$Hg and $\log_{10}$LOI residual range of -0.2 to 0.2.

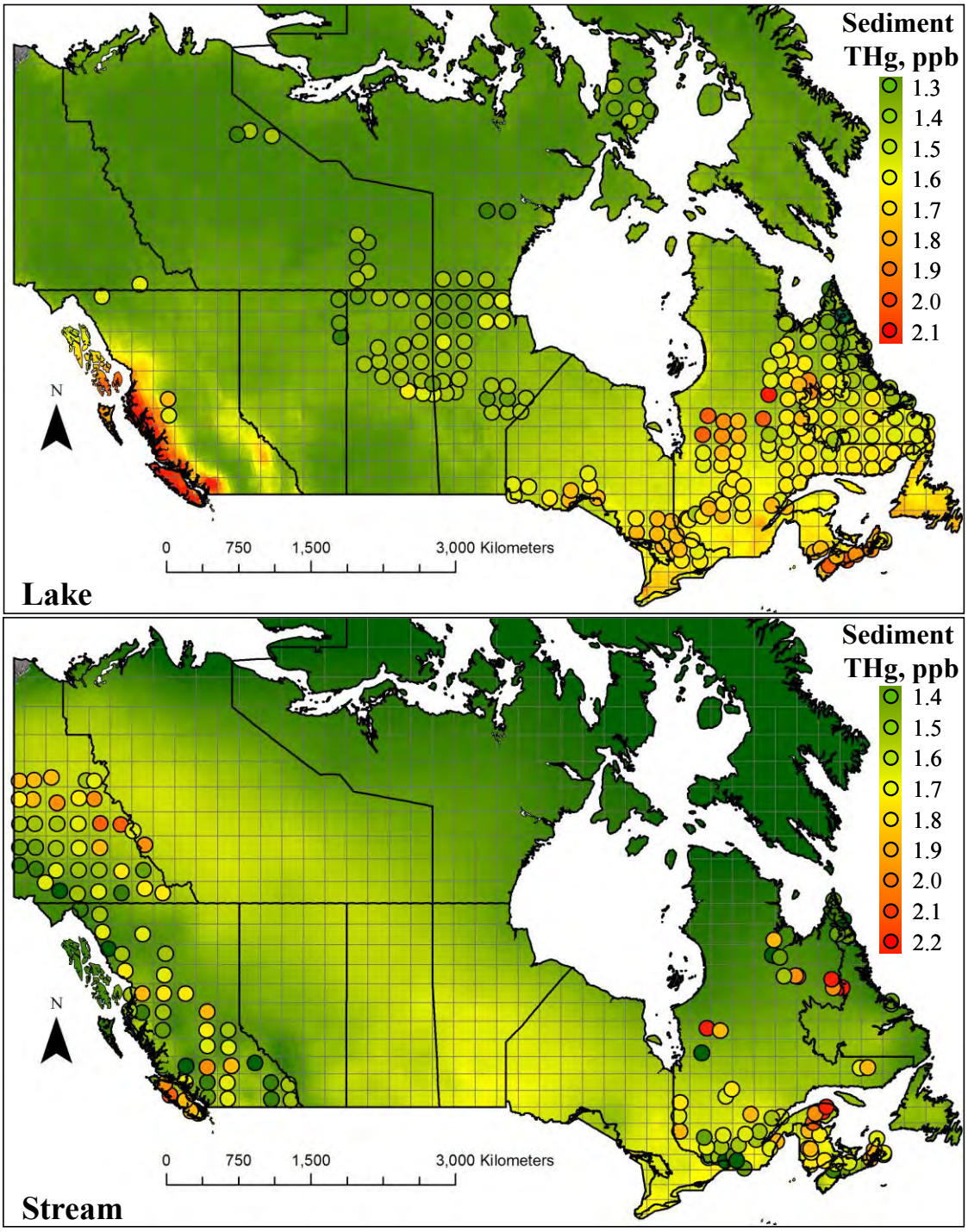

Figure 6.5 Sediment $\log_{10}$THg (ppb), estimated using Eqs. 6.2 and 6.3. Overlaid: mean sediment $\log_{10}$THg, by NTS tile (points). Top: lakes. Bottom: streams.

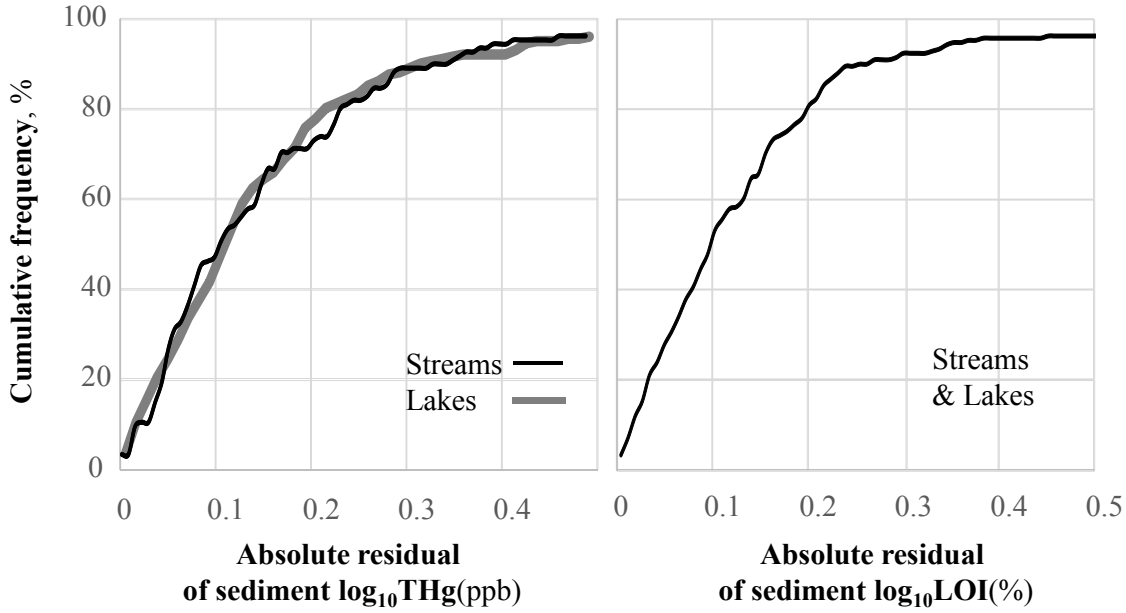

Figure 6.6 Conformance plots: cumulative frequency of the best-fit absolute residual differences between mapped and NTS tile averaged sediment log_{10}THg and log_{10}LOI using Eqs. 6.1- 6.3.

Sediment THg versus LOI, Point by Point, and by Province/Territory

The log_{10}THg versus LOI scatterplots follow curvilinear patterns (Figures 6.7, 6.8; Rasmussen *et al. (*1998a), but the THg versus LOI plots are generally less curved for lakes than for streams. In addition, some of plots for streams have high THg at low LOI, and notably so for BC, YT, and some of the QC geological survey zones. For the Abitibi and Grenville zones, QC, there is a clear separation between high and low stream sediment THg.

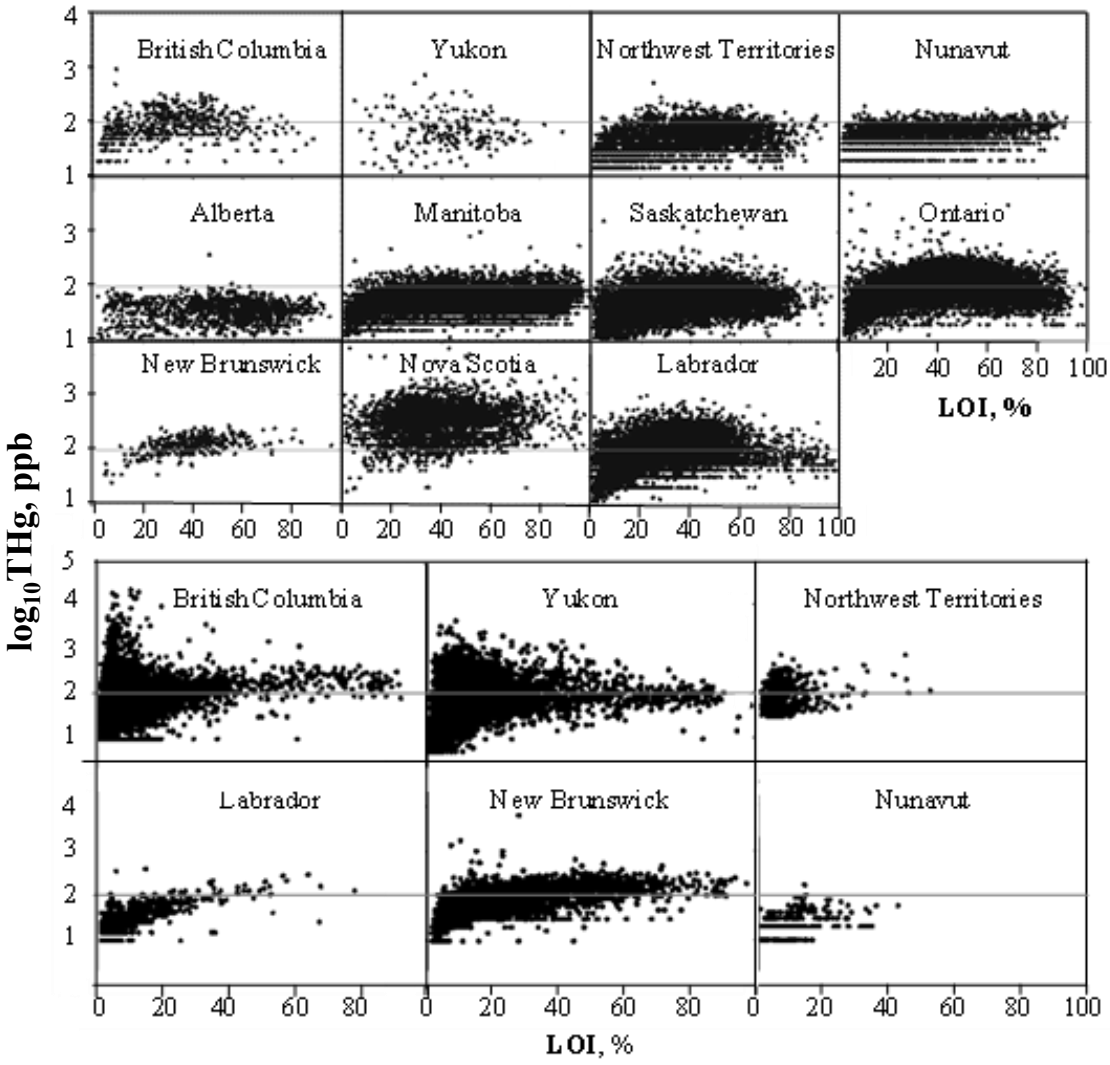

Figure 6.7 Scatterplots of sediment log_{10}THg (ppb) versus LOI (%), by province/territory. Top: lake. Bottom: stream. Grey lines mark sediment THg at 100 ppb.

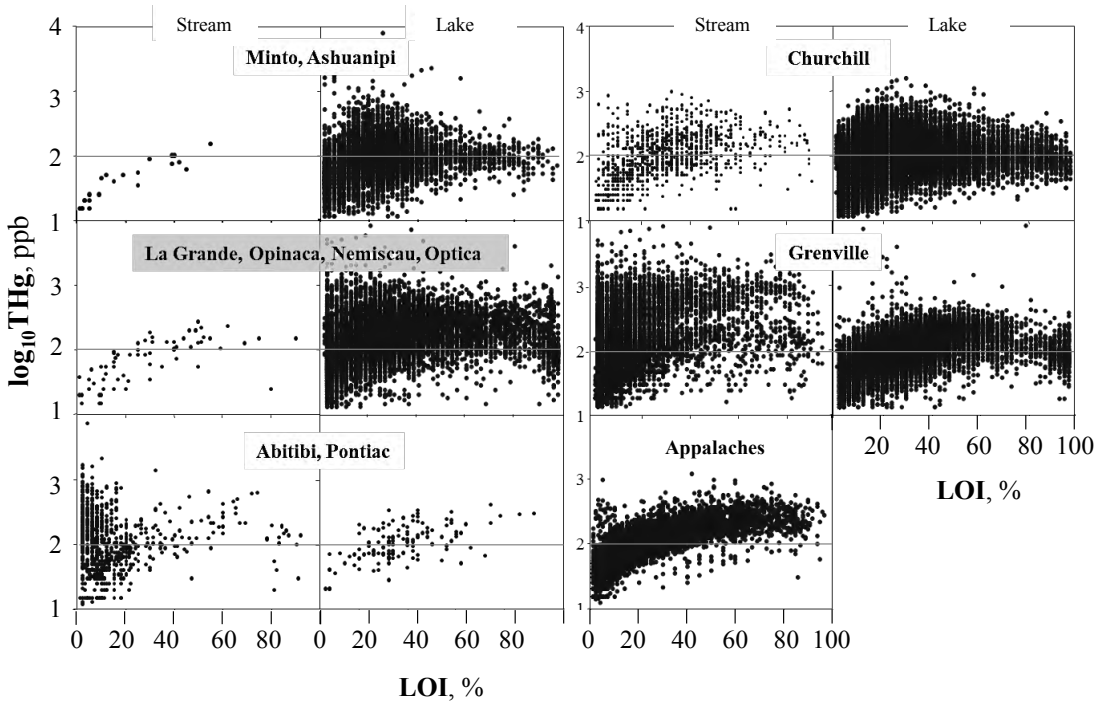

Figure 6.8 Scatterplots of sediment log_{10}THg (ppb) versus LOI (%), by QC geological survey zone (18-30) and medium type (stream, lake). Grey lines mark sediment THg at 100 ppb.

Sediment THg Percentile Distributions versus LOI, across Canada

The plots of 10th, 25th, 50th, 75th to 90th log_{10}THg percentiles for all of the paired THg and LOI across Canada by each 10 % LOI class differ by lake versus stream (Figure 6.9). The log_{10}THg percentiles rise and fall more sharply for the stream than the lake sediments with increasing LOI. These differences are quantified through least-squares fitting of Eqs. 3.1 and 3.2, and the following results were produced:

$a = 0.932 \pm 0.013$ SD, $d = 0.560 \pm 0.029$ SD, $b_{stream} = 0.949 \pm 0.016$ SD, $c_{stream} = 0.727 \pm 0.013$ SD, $e_{stream} = 0.165 \pm 0.004$ SD, $b_{lake} = 0.769 \pm 0.086$ SD, $c_{lake} = 0.803 \pm 0.017$ SD, $e_{lake} = 0.252 \pm 0.01$ SD, and $f_{lake} = 0.128 \pm$ SD 0.012 SD.

The above coefficients and the plots in Figure 6.9 indicate that:

- The 10^{th} percentiles for stream and lake sediment $\log_{10}$THg have the same value at LOI = 0 %.
- The 10^{th}, 25^{th}, 50^{th}, 75^{th} and 90^{th} percentile curves for the streams share the same shape (i.e. c_{stream} is constant at 0.727), but increase in a linear fashion from the 10^{th} to the 90^{th} percentile curves, i.e. a + i e_{Stream} = 0.93, 1.10, 1.26, 1.43, 1.59, hence THg at LOI = 0 % increases accordingly from 8.6 to 12.6, 18.4, 26.9, 39.4 ppb.
- The 10^{th} to the 90^{th} percentile curves for the lakes become narrower, i.e. b_{lake} - i f_{lake} decreases from 0.77, 0.64, 0.51, 0.39, 0.26, and also becomes flatter or more stretched, i.e. c_{lake} 0.803 > c_{stream} = 0.727.

Altogether, the combined best-fit results for Eqs. 3.1 and 3.2 conform to the $\log_{10}$THg percentile values across the 10 % LOI classes, with an R^2 value of 0.947 and an RMSE value of 0.042. While the percentiles for stream sediment THg rises faster than lake sediment THg with increasing LOI, this does not imply that mean stream sediment THg > mean lake sediment THg. This is because (i) LOI values are generally greater for lake than stream sediments, but (ii) THg increases more sharply with increasing LOI for stream than for lake sediments.

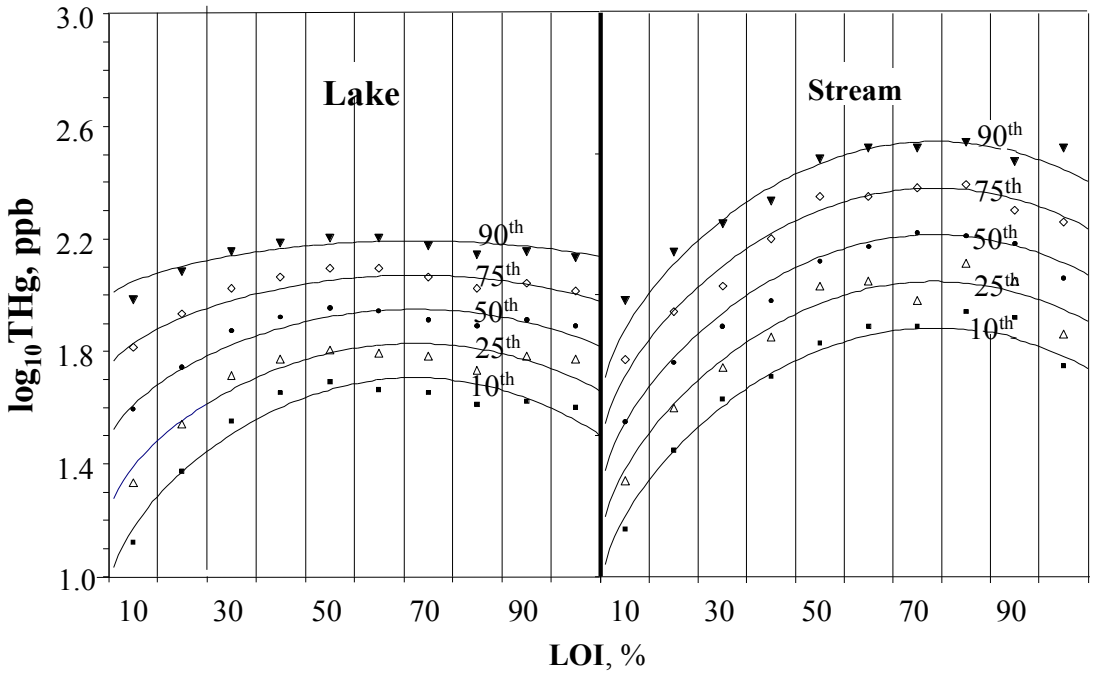

Figure 6.9 Sediment $\log_{10}$THg (ppb) percentiles (10^{th}, 25^{th}, 50^{th}, 75^{th}, 90^{th}; points), overlaid on their best-fit curves (Eqs. 3.1, 3.2: Chapter 3) versus LOI 10 % classes. Right: stream. Left: lake. All data across Canada combined; $R^2 = 0.947$.

Sediment THg Percentile Distributions versus LOI, by Province/Territory and QC Geological Survey Zone

Plotting the 10^{th} and 90^{th} stream and lake sediment $\log_{10}$THg percentiles versus the 10 % LOI classes by province/territory and QC geological survey zone, and overlaying the corresponding best-fit Eq. 3.3 model curves revealed a fairly close correspondence between the actual and best-fit values in Figure 6.10. Note that the shape of these plots are very similar across the provinces/territories, and the QC survey zones. Nevertheless, there are differences, and these differences are quantified by the list of the best-fit a_{ij}, b_{ij} and c_j values in Table 6.3 by survey zone (denoted "i") and medium type (denoted "j").

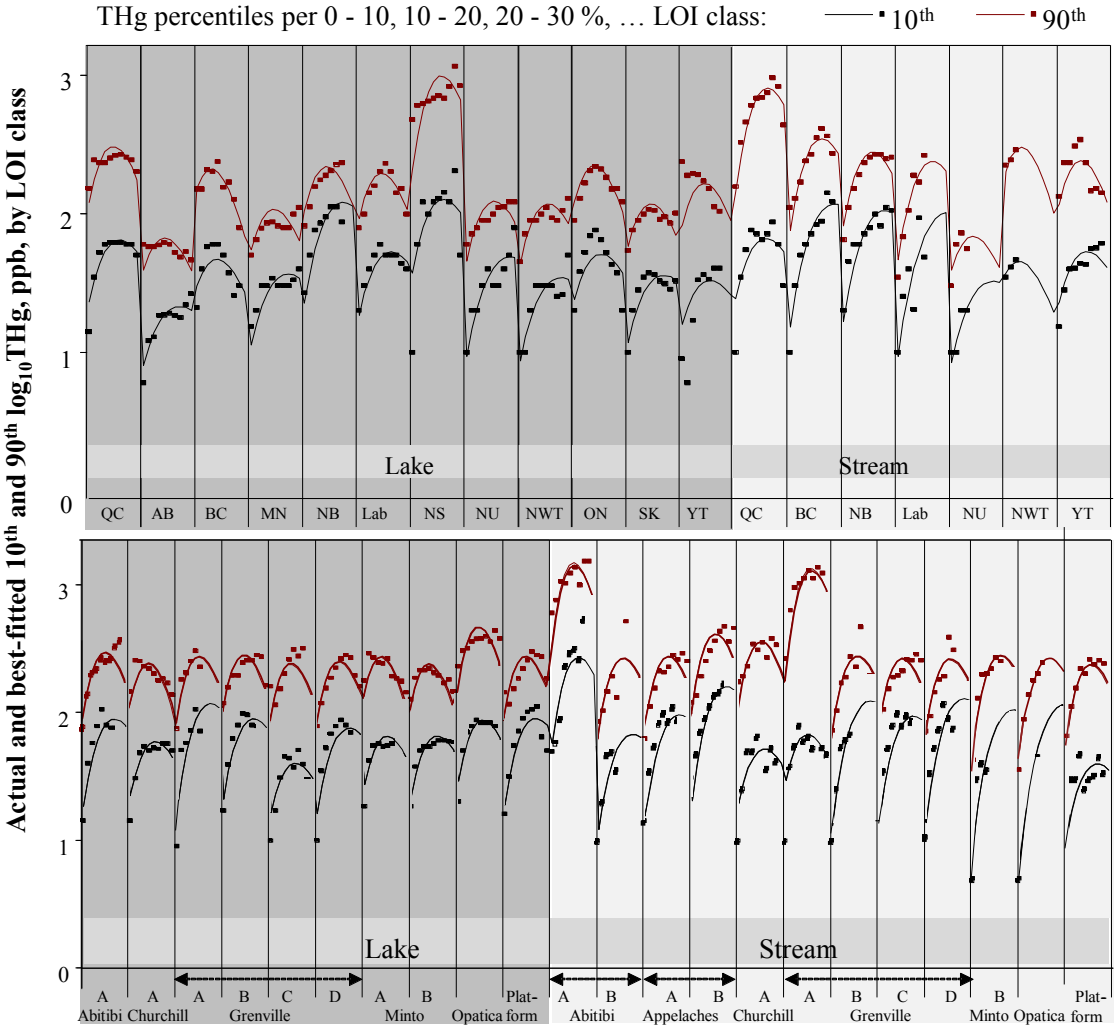

LOI (0 - 100%), by province/territory (top) and Quebec geological region (bottom)

Figure 6.10 Plots of actual versus best-fit (Eq. 3.3: Chapter 3) 10th and 90th percentiles for stream and lake log_{10}THg (ppb) versus LOI (%), by province/territory (top) and QC geological survey zone (bottom).

Regressing the stream and lake a_{ij} coefficients against mean annual atmospheric Hg deposition and precipitation rates produced no significant trends. This means that the mineral component of the stream and lake sediment THg is not influenced by the atmospheric deposition variations as modelled. On average, the a_{ij} values generate the following 10^{th} and 90^{th} percentile values for stream and lake sediment THg when LOI = 0 %:

- for lake sediments, 10^{th} og$_{10}$THg percentile = 1.15 (THg = 14 ppb);
- for lake sediments, 90^{th} log$_{10}$THg percentile = 1.84 (THg = 69 ppb);
- for stream sediments, 10^{th} log$_{10}$THg percentile = 1.08 (THg = 12 ppb);
- for stream sediments, 90^{th} log$_{10}$THg percentile = 1.77 (THg = 59 ppb).

These numbers are generally consistent with the cross-Canada best-fit 10^{th} to 90^{th} THg percentiles for LOI = 0 %, for which the best-fit a + i $e_{stream/lake}$ values via Eq. 3.1 and 3.2 amount to 8 to 40 ppb, respectively.

In contrast to the a_{ij} coefficients, the log$_{10}$THg b_{ij} coefficients for log$_{10}$THg are related to the mean annual atmospheric THg deposition and precipitation rates, with R^2 values near 0.50 for the lakes (Figure 6.11).

Table 6.3 Best-fit a_{ij} and b_{ij} parameter values and sediment THg (ppb) for the 10th and 90th percentiles of THg for LOI = 0 versus LOI = 100 %, by province/territory and QC geological survey zone (18-30), and medium type (stream, lake; Eq. 3.3: Figure 6.10).

Location	Medium	ppt*	atm.Hg$_{dep.}$*	Subscript		log_{10}THg Parameters			Sediment THg, ppb			
						a_{ij}	b_{ij}		LOI = 0 %		LOI = 100 %	
		m a^{-1}	µg m^{-2} a^{-1}	i	j	10th	10th	90th	10th	90th	10th	90th
Abitibi A (22)	**Lake**	0.95	20.0	1	1	1.13	2.25	2.66	**13.4**	**65.1**	**74.6**	**163.5**
Churchill A (30)	QC	0.64	13.0	3		1.24	1.93	2.42	**17.5**	**85.4**	**40.6**	**103.0**
Grenville A (23)		0.96	20.2	6		1.09	2.43	2.64	**12.3**	**59.7**	**104.8**	**157.4**
Grenville B (24)		0.98	20.4	7		1.19	2.23	2.58	**15.6**	**75.9**	**71.4**	**139.7**
Grenville C (25)		0.97	17.9	8		1.12	1.74	2.52	**13.2**	**64.2**	**28.4**	**125.8**
Grenville D (26)		1.05	19.1	9		1.08	2.17	2.58	**12.0**	**58.3**	**64.3**	**140.8**
Minto A (28)		0.76	15.6	10		1.33	1.93	2.42	**21.5**	**104.7**	**40.5**	**103.6**
Minto B (29)		0.61	14.3	11		1.22	2.00	2.42	**16.7**	**81.6**	**46.8**	**104.1**
Opatica (27)		0.82	20.4	12		1.35	2.12	2.82	**22.3**	**108.7**	**57.8**	**223.7**
Plate-forme (18)		1.09	15.7	13		1.14	2.25	2.60	**13.7**	**67.0**	**74.6**	**147.2**
QC	Canada	0.85	17.3	14		1.27	2.16	2.79	**18.4**	**89.8**	**62.7**	**210.3**
AB		0.40	12.1	15		0.82	1.64	1.97	**6.6**	**32.4**	**23.1**	**43.4**
BC		0.79	11.1	16		1.42	1.77	2.25	**26.3**	**128.4**	**30.0**	**74.2**
MB		0.47	15.7	17		0.95	1.93	2.23	**8.9**	**43.5**	**40.8**	**72.7**
NB		1.28	21.8	18		1.22	2.59	2.56	**16.6**	**80.9**	**143.2**	**134.7**
NL		0.88	16.1	19		1.17	2.07	2.51	**14.9**	**72.4**	**53.2**	**123.9**
NS		1.39	24.1	20		1.46	2.51	3.52	**29.0**	**141.3**	**124.2**	**850.3**
NU		0.30	9.8	21		0.86	2.13	2.42	**7.2**	**35.0**	**59.9**	**103.4**
NWT		0.31	9.4	22		0.84	1.93	2.40	**6.9**	**33.6**	**40.7**	**100.5**
ON		0.86	20.1	23		1.30	1.96	2.48	**20.0**	**97.6**	**42.9**	**116.7**
SK		0.46	14.3	24		0.97	1.91	2.28	**9.4**	**45.9**	**39.2**	**79.9**
YT		0.36	9.5	25		1.13	1.77	2.42	**13.4**	**65.2**	**29.6**	**103.5**
Abitibi A	**Stream**	0.88	21.1	1	2	1.61	2.71	3.44	**40.4**	**196.7**	**180.2**	**731.0**
Abitibi B (21)	QC	0.95	19.5	2		0.94	2.15	2.71	**8.8**	**42.9**	**61.3**	**181.1**
Appalaches A (19)		1.16	21.6	3		1.04	2.32	2.67	**11.1**	**53.9**	**86.4**	**167.0**
Appalaches B (20)		0.95	19.8	4		1.15	2.59	2.88	**14.0**	**68.1**	**143.7**	**251.3**
Churchill A		0.69	11.5	5		1.18	1.88	2.76	**15.2**	**74.2**	**36.9**	**199.5**
Grenville A		1.00	20.1	6		1.37	1.93	3.52	**23.4**	**114.1**	**40.2**	**848.6**
Grenville B		1.08	21.2	7		0.95	2.49	2.73	**8.8**	**43.1**	**118.7**	**188.5**
Grenville C		1.08	18.7	8		1.04	2.31	2.64	**10.9**	**53.3**	**84.5**	**159.7**
Grenville D		1.05	19.1	9		0.97	2.50	2.68	**9.4**	**45.6**	**121.9**	**171.7**
Minto B		0.58	12.6	11		0.83	2.42	2.80	**6.8**	**33.3**	**103.4**	**215.9**
Opatica		0.75	18.1	12		0.71	2.41	2.84	**5.1**	**25.0**	**101.8**	**232.2**
Plate-forme		1.07	25.8	13		0.94	1.84	2.64	**8.6**	**42.1**	**33.8**	**159.1**
QC	Canada ***	0.96	20.0	14		1.29	2.16	3.48	**19.6**	**95.3**	**62.9**	**798.3**
BC		1.09	14.3	16		1.04	2.62	3.05	**10.9**	**53.3**	**152.3**	**344.6**
NB		1.15	22.2	18		1.09	2.55	2.86	**12.3**	**59.8**	**132.5**	**239.7**
NL		0.63	11.0	19		0.82	2.56	2.90	**6.6**	**32.3**	**135.5**	**261.4**
NU		0.30	7.4	21		0.82	1.90	1.99	**6.6**	**32.2**	**38.2**	**45.6**
NWT		0.32	8.0	22		1.53	1.57	2.46	**33.8**	**164.8**	**20.4**	**111.9**
YT		0.36	9.49	25		1.28	2.01	2.58	**19.0**	**92.6**	**47.1**	**139.8**

$a_{ij}(90^{th}) = aij(10^{th}) + (0.688 \pm$ SE 0.018); a_{ij} and b_{ij} standard error of estimate (Std. Err.: SE) = ± 0.15; c_j = 0.0180 ± SE 0.0011. * Precipitation rate (ppt, m a^{-1}); GRAHM2005 mean annual net atmospheric Hg deposition rate (atm.Hgdep., µg m^{-2} a^{-1}). *** Excluded: ON stream sediments due to the small sample size (n =287) and insufficient number of values for 10th and 90th percentiles.

The above results suggest that the LOI-based sediment THg contributions increase strongly with increasing atmospheric Hg deposition, and this is especially so for lake sediments. For streams, the LOI contributions to sediment THg have lower R^2 values of approximately 12 to 23 % for the 10^{th} and 90^{th} $\log_{10}$THg percentiles (Figure 6.11). This difference could be due to:

- episodic scouring of stream sediment versus the gradual build-up of lake sediments;
- settling of coarser particles in streams versus the settling of finer particles in lakes;
- decreasing THg from finer to coarser particles;
- stronger binding of Hg by DOC and POC than by mineral particles;
- gradual coagulation and settling of organic matter in lake water;
- direct deposition of atmospheric Hg into lakes.

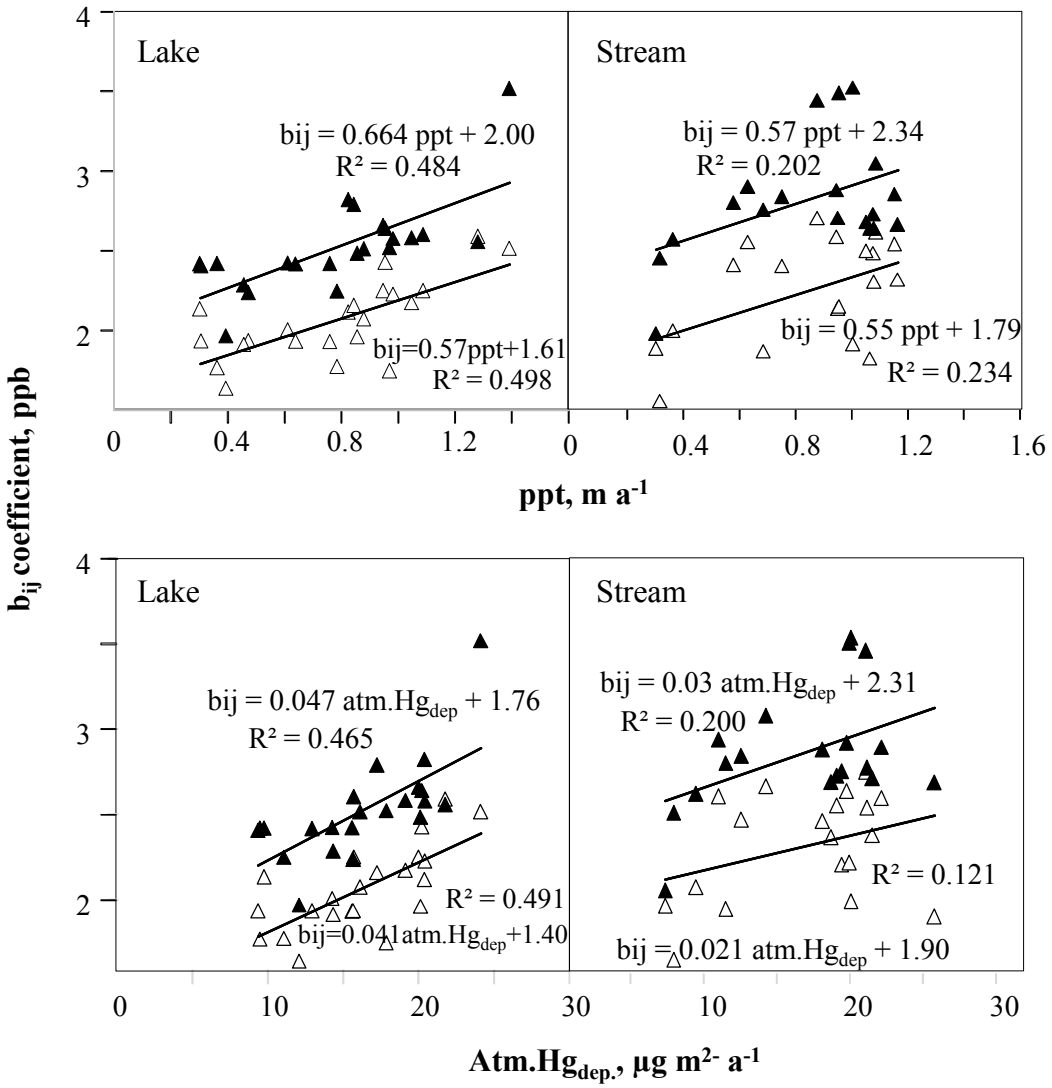

Figure 6.11 Scatterplots of best-fit bij coefficients (ppb) for the 10th and 90th $\log_{10}$THg (ppb) versus mean annual precipitation rate (ppt, m a^{-1}; top) and GRAHM2005 mean annual net atmospheric Hg deposition rate (atm.Hgdep, µg m^{-2} a^{-1}; bottom), by province/territory and QC geological survey zone, with best-fit y versus x trend lines (Table 6.3).

Gain of Atmospherically-Deposited Hg in Sediments, by NTS Tile

The THg gain of sediment organic matter from low to high deposition environments is estimated from the Table 6.3 entries as follows:

$$\text{THg Gain} = 10^{[b_{ij}(x) - b_{ij}(x0)][1 - \exp(-c_j \text{LOI}(\%)/100)]} / 10^{b_{ij}(x0)[1 - \exp(-c_j \text{LOI}(\%)/100)]} \quad \text{Eq. 6.4}$$

where $b_{ij}(x)$ and $b_{ij}(x_0)$ represent the linear trend equations in Figure 6.11, with x and x_0 referring to high and low rates of atmospheric Hg deposition or precipitation rate. This gain amounts to a factor of 3.4 to 5 (Table 6.4) for streams and lakes when based on mean annual precipitation rates from near zero to 1.4 m a^{-1} at LOI = 100 %. When based on mean annual Hg deposition rates from near zero to 26 μg m^{-2} a^{-1}, the estimated gain increases even further at 6.7 to 9.3 for the lake sediments, but decreases somewhat at 1.8 to 3.5 for the stream sediments.

Using the estimated sediment THg gains from low to high atmospheric Hg deposition produced the sediment THg gain maps in Figure 6.12. These maps suggest that there is a high lake sediment THg acquisition susceptibility across southeastern Canada and along the Pacific Rim. This susceptibility would decrease from southeast to north and northwest and towards alpine areas, and would generally be generally lower for stream than lake sediments.

Table 6.4 Trend analysis for the organic matter contributions to sediment THg (ppb) from low to high rates of annual precipitation rate (ppt, m a^{-1}) and low to high GRAHM2005 annual net atmospheric Hg deposition rate (atm.Hg_{dep} µg m^{-2} a^{-1}), by THg 10^{th} and 90^{th} percentiles and medium type (stream, lake).

Percentile	Medium	bij, ppb *			bij, ppb at ppt, m a^{-1} **		Gain of THg in sediment organic matter **
		Intercept	Slope	R^2	0	1.4	
90^{th}	Stream	2.00	0.664	0.484	101.0	602.9	5.0
10^{th}		1.61	0.570	0.498	40.7	188.8	3.6
90^{th}	Lake	2.34	0.570	0.202	218.8	1,014.4	3.6
10^{th}		1.79	0.550	0.234	62.2	273.5	3.4
		b_{ij}			at atm.$Hg_{dep.}$, µg m^{-2} a^{-1} **		
		Intercept	Slope	R^2	0	26	
90^{th}	Stream	1.76	0.0467	0.465	57.9	597.2	9.3
10^{th}		1.40	0.0408	0.491	25.2	193.6	6.7
90^{th}	Lake	2.31	0.0300	0.200	204.2	914.3	3.5
10^{th}		1.90	0.0212	0.121	79.4	229.1	1.9

* Calcualated based on Eqs. of Figure 6.11. ** Precipitation rate (ppt, m a^{-1}); GRAHM2005 mean annual net atmospheric Hg deposition rate (atm.Hgdep, µg m^{-2} a^{-1}). ** Calculated based on Eq. 6.4.

Using Eq. 6.4 would over–estimate the lake sediment THg gains in areas for which Eq. 6.2 predicts consistently high sediment LOI values, as is the case for northern AB, MB, and SK (Figure 6.13). Here, lake-to-lake LOI content varies from high to low depending on lake size and extent of surround wet areas (details not shown). Lower than the Eq. 6.4 expected estimates for stream sediment THg gains would occur in (i) areas with rugged terrain due to frequently scoured streambeds, and (ii) downstream from open non–forested areas where much of the atmospherically–deposited Hg would re–volatize, as would be case in southeastern QC where agriculture and open fields dominate (Figure 6.13). The Eq. 6.4 generated estimates do not apply where geogenic or anthropogenic sources have a major influence on local sediment THg accumulations.

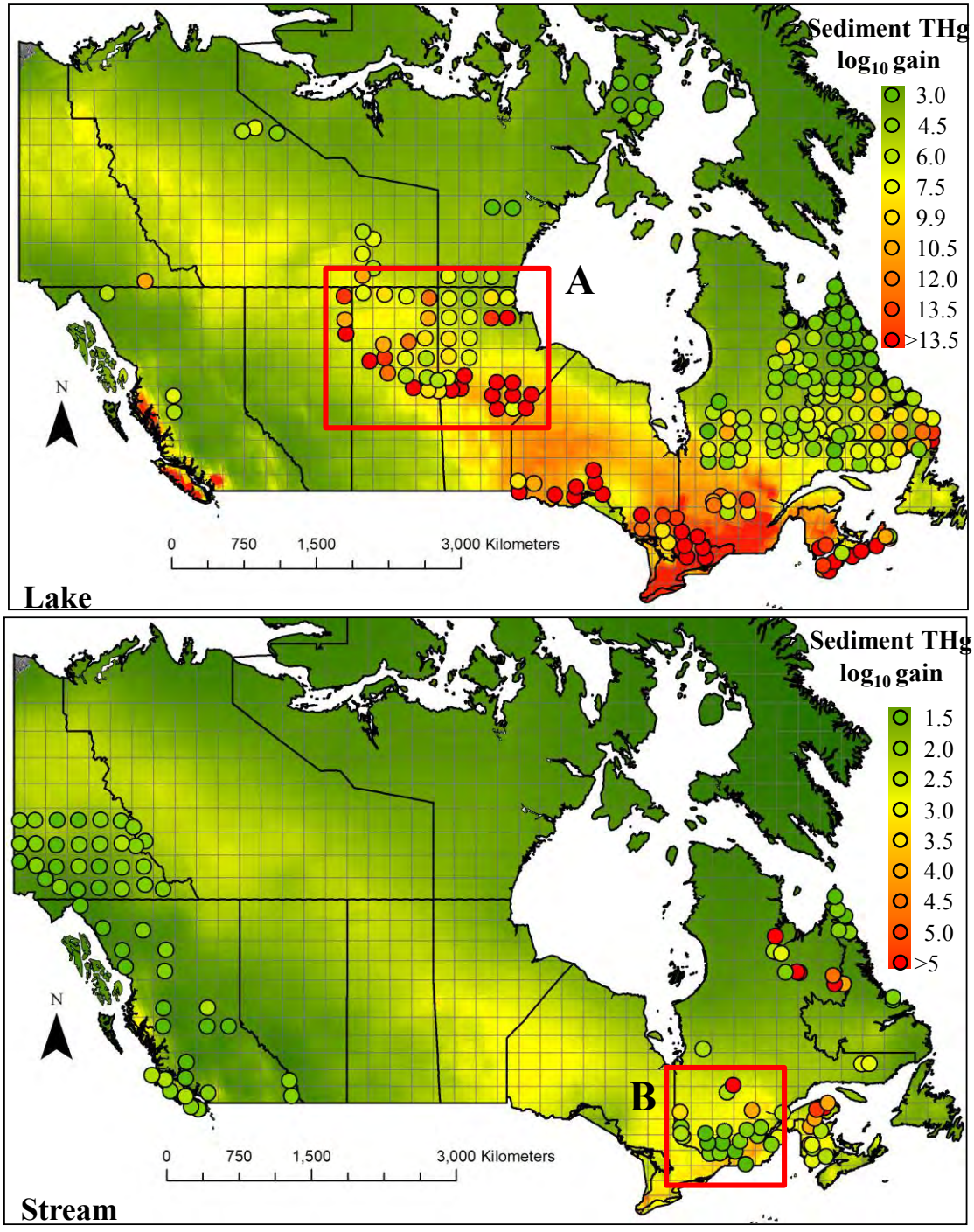

Figure 6.12 Sediment $\log_{10}THg_{gain}$, Eq. 6.4 from low (green) to high (red), based on the climate-based estimates for LOI (%). Overlaid: the corresponding $\log_{10}THg_{gain}$ estimates based on mean LOI per NTS tile (points). Red boxes A and B are expanded in Figures 6.13 and 6.14, respectively. Top: lakes. Bottom: streams.

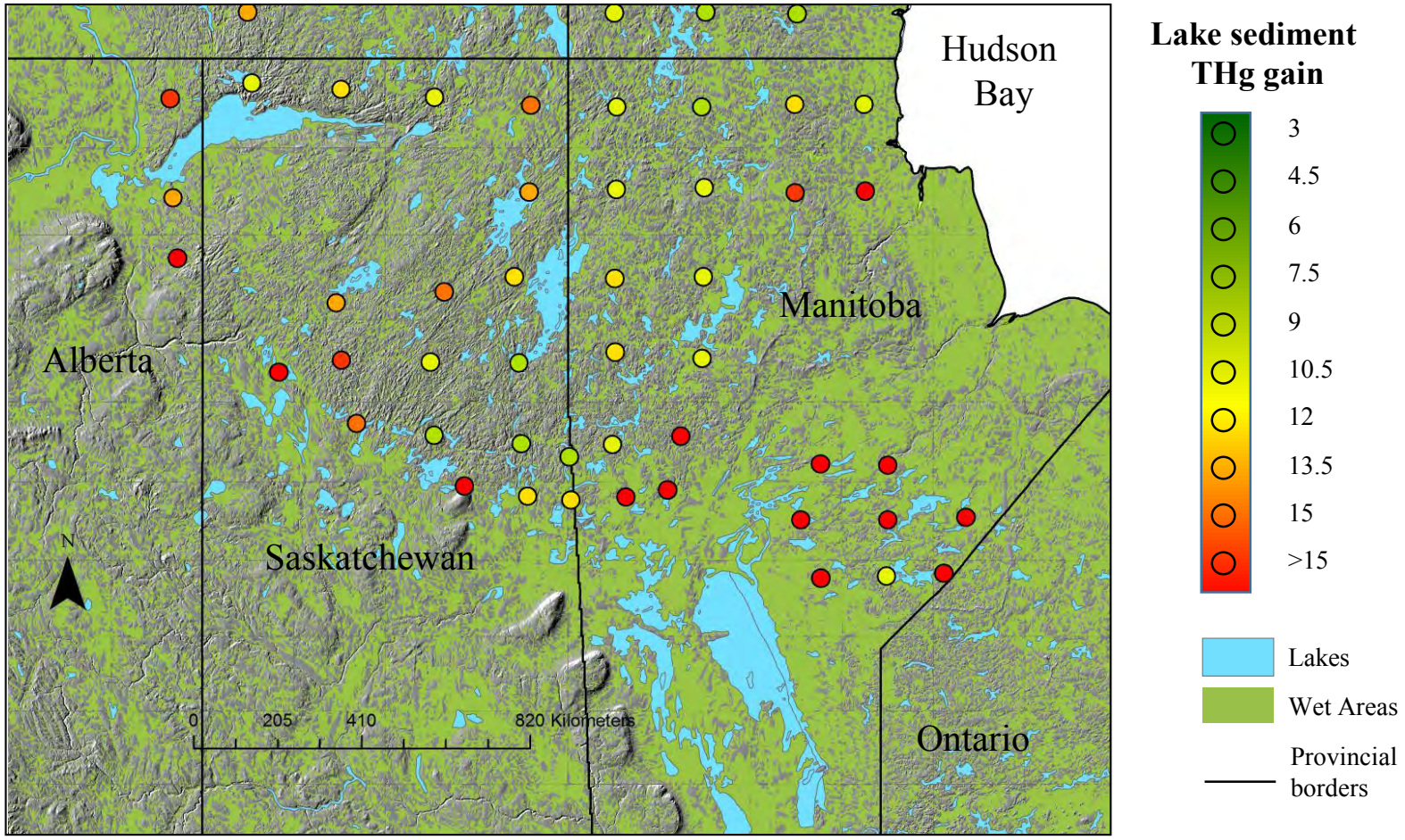

Figure 6.13 Box A of Figure 6.12: Locations with higher lake sediment THg gain expectations based on using Eq. 6.4 and the mean annual net atmospheric Hg deposition rate and loss of ignition (LOI, %), by NTS tile (points). Background: national hill-shaded DEM (300 m resolution; gray), flat and mostly wet forest areas and wetlands (shaded green), and open water (blue).

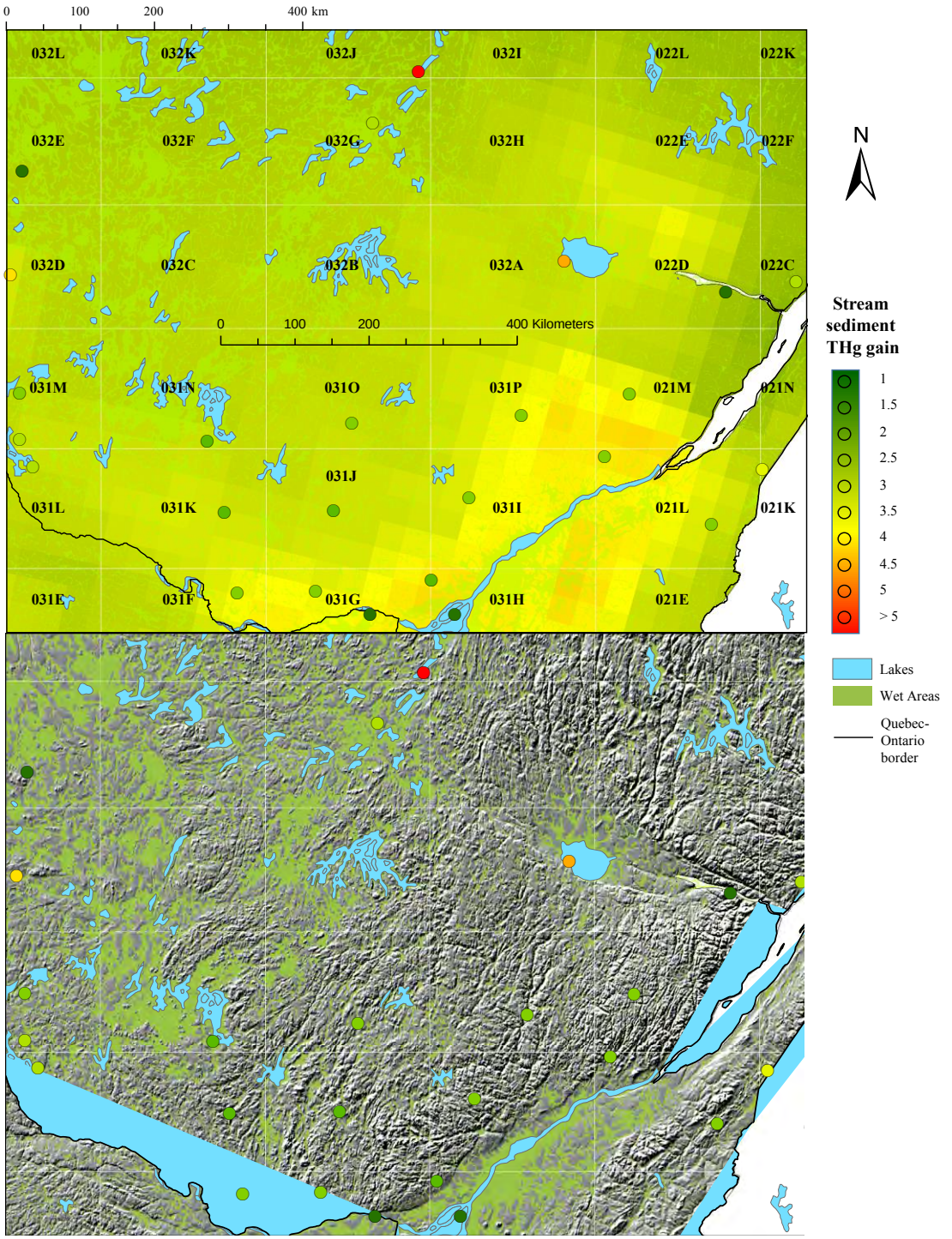

Figure 6.14 Box B of Figure 6.12: locations with lower and higher stream sediment THg gains (Eq. 6.4; points). Background: corresponding sediment THg gain estimates (top) and national hill-shaded DEM (300 m resolution; gray; bottom). Note flat areas next to streams and lakes shaded green (bottom), shaded grey rugged terrain, and the two low estimated sediment THg gains in the generally open field area of the Saint Lawrence floodplain along the lower right.

Conclusions

This Chapter establishes a strong cross-Canada link between stream and lake sediment THg, sediment LOI, and atmospheric variables pertaining to mean annual atmospheric Hg deposition, precipitation and January and July temperatures. This link is further affirmed by examining the 10^{th} to 90^{th} percentile distributions of log_{10}THg versus sediment LOI from 0 to 100 %, and using these to model the organic versus mineral contributions to sediment THg. The results by province/territory and QC geological survey zone demonstrate that the 10^{th} to 90^{th} percentiles of sediment log_{10}THg:

- are affected by regional difference in geogenic/anthropogenic Hg source strengths, as noted by the best-fit aij coefficients of Eq. 3.3 by province/territory and QC geological survey zone (Table 6.3);
- maintain the same shape for each province/territory and QC geological survey zone from LOI = 0 to 100 % (Figure 6.10);
- increase systematically in response to increasing mean annual atmospheric Hg deposition and precipitation rates by province/territory and by QC geological survey zone, as noted by the best-fit bij coefficients of Eq. 3.3 in Figure 6.11 and in Table 6.4;
- show that stream and lake sediments with high organic matter content (i.e. high LOI) accumulate more Hg with increasing atmospheric deposition than sediments with low LOI.

Chapter 7 Sediment THg versus other Elemental Concentrations and Stream and Lake Morphologies

Introduction

Sediment THg is also related to other heavy metal concentrations in sediments, and to morphological features of the waterbodies (Kainz and Lucotte, 2006). Chapter 5 already detailed how stream and lake sediment THg relates to LOI, with the organic contributions to sediment THg assumed to be due to atmospheric Hg sequestration, while the geogenic contributions would remain in mineral form. The objective of this chapter was to investigate how sediment THg relates to (i) some of the other total elemental concentrations in sediments (i.e. Cu, Zn, Mn, Cd, Fe, As, Ag, Ni, S), (ii) geographic location as represented by longitude and latitude, and (iii) stream and lake morphologies (lake area and depth, stream channel width, depth, and order). Since sediment THg varies by province/territory and survey zone (Chapter 4), the regression analyses of this chapter is done by province/and territory, and also informs on sediment THg in select NTS–tile specified areas with particularly high sediment THg.

Results

The best-fit regression models for stream and lake $\log_{10}$THg of across Canada and province/territory reveal that 42 to 49 % of the $\log_{10}$THg variations can be inferred from other stream and lake sediment variables of the open files (Table 7.1) as follows:

Table 7.1. **Table 7.1** Multiple regression analysis results for stream and lake sediment log_{10}THg (ppb) across Canada and by province/territory.

Location	Lake sediment log_{10}THg (ppb) regression summary						Stream sediment log_{10}THg (ppb) regression summary					
	n	Variable	Coeff.*	Std. Err.*	t-value	R^2	n	Variable	Coeff.	Std. Err.	t-value	R^2
Canada	102,582	Intercept	2.059	0.009	218.1	0.492	51,853	Intercept	0.876	0.014	62.2	0.415
		log_{10}LOI, %	0.300	0.002	130.9			log_{10}LOI	0.411	0.004	106.2	
		log_{10}Cu, ppm	0.237	0.002	97.8			log_{10}Cu	0.105	0.004	24.4	
		log_{10}Zn, ppm	0.134	0.003	41.6			log_{10}Zn	0.375	0.005	76.6	
		Lake area, km	-0.026	0.001	-25.5			Stream width, m	-0.0013	0.0001	-17.6	
		Lake depth, m	0.0028	0.0001	24.0			Stream depth, m	0.0038	0.0004	9.1	
		Longitude, °	0.0032	0.0001	78.4			Longitude	-0.001	0.0001	-14.2	
		Latitude, °	-0.0184	0.0002	-119.9			Latitude	-0.0093	0.0003	-31.7	
NB	315	Intercept	8.57	1.50	5.73	0.370	7,239	Intercept	0.83	0.01	58.71	0.630
		log_{10}LOI	0.47	0.04	11.63			log_{10}LOI	0.58	0.01	86.18	
		log_{10}Pb, m	0.19	0.02	8.79			log_{10}Pb	0.09	0.01	10.91	
		Longitude	0.11	0.02	4.95			log_{10}Mn	0.08	0.01	18.53	
								Stream flow rate**	-0.01	0.00	-5.30	
NS	3,187	Intercept	2.31	0.03	76.06	0.030	5,418	Intercept	1.45	0.08	19.07	0.020
Mainland		log_{10}LOI	0.09	0.02	5.06			log_{10}Pb	0.10	0.01	8.75	
		log_{10}Pb	0.10	0.01	8.64							
Cape	355	Intercept	0.93	0.07	14.07	0.450	2,654	Intercept	1.47	0.06	20.82	0.100
		log_{10}LOI	0.64	0.04	16.68			log_{10}Ag, ppm	0.25	0.04	6.90	
		log_{10}Pb	0.13	0.02	7.77			log_{10}Mn	0.14	0.02	8.90	
								log_{10}Pb	0.13	0.02	6.34	
NL	19,132	Intercept	2.84	0.060	43.75	0.510	1,065	Intercept	0.591	0.300	19.12	0.700
		log_{10}LOI	0.40	0.005	76.90			log_{10}LOI	0.425	0.014	30.86	
		log_{10}Cu	0.24	0.006	42.70			log_{10}Zn	0.204	0.022	9.42	
		log_{10}Zn	0.100	0.007	13.52			log_{10}Pb	0.174	0.020	8.92	
		Lattitude	0.050	0.001	-49.81							
		log_{10}Mn, ppm	0.040	0.004	10.82							
		Longitude	-0.010	0.001	-22.46							
		Lake depth	0.0047	0.000	15.86							
QC	55,020	Intercept	1.24	0.01	161.93	0.320	15,782	Intercept	2.54	0.02	109.50	0.590
		log_{10}LOI	0.39	0.00	126.23			log_{10}LOI	0.43	0.01	59.70	
		log_{10}Pb	0.23	0.00	52.45			log_{10}Sb	0.43	0.01	60.99	
		log_{10}Ni, ppm	0.15	0.00	5)5			log_{10}Ca	-0.33	0.01	-43.77	
		log_{10}Sb, ppm	0.14	0.00	42.96			log_{10}Ni	0.31	0.01	41.54	
								log_{10}Pb	0.10	0.01	11.78	
NU	5,808	Intercept	3.93	0.31	12.89	0.420	403	Intercept	-3.16	0.83	-3.83	0.520
		log_{10}LOI	0.34	0.01	37.30			log_{10}LOI	0.17	0.04	4.06	
		log_{10}Cu	0.24	0.01	19.07			Longitude	-0.04	0.01	-4.42	
		log_{10}Zn	0.11	0.01	7.51			log_{10}Zn	0.45	0.03	13.27	
		Latitude	-0.04	0.00	-13.02							
		Longitude	0.01	0.00	7.57							
		Lake depth	0.002	0.00	4.68							
NWT	4,058	Intercept	0.44	0.03	16.49	0.490	443	Intercept	1.20	0.10	12.16	0.410
		log_{10}LOI	0.35	0.01	39.06			log_{10}LOI	0.17	0.04	4.37	
		log_{10}Cu	0.36	0.01	32.03			log_{10}Zn	0.49	0.03	16.73	
		log_{10}Mn	0.05	0.01	5.28			log_{10}Mn	-0.22	0.04	-5.89	
		Lake depth	0.003	0.00	4.82							
YT	180	Intercept	0.51	0.12	4.13	0.640	19,388	Intercept	0.32	0.02	20.53	0.460
		log_{10}Cu	0.77	0.08	9.19			log_{10}LOI	0.35	0.01	47.92	
		log_{10}Cd, ppm	0.38	0.06	6.05			log_{10}Zn	0.44	0.01	53.54	
		log_{10}Mn	0.10	0.02	4.68			log_{10}Cu	0.23	0.01	25.61	
								Stream order**	-0.05	0.00	-15.61	
								Stream flow	-0.02	0.00	-6.71	

Table 7.1 Continued:

Location	Lake sediment log_{10}THg (ppb) regression summary					
	n	Variable	Coeff.*	Std. Err.*	t-value	R^2
ON	14,263	Intercept	2.36	0.05	45.04	0.360
		log_{10}LOI	0.25	0.01	41.03	
		log_{10}Cu	0.24	0.01	37.03	
		log_{10}Zn	0.24	0.01	25.58	
		Latitude	-0.03	0.00	-32.04	
MB	17,966	Intercept	0.15	0.05	3.20	0.230
		log_{10}LOI	0.30	0.01	65.28	
		log_{10}Cu	0.22	0.01	35.09	
		log_{10}Zn	-0.05	0.01	-6.63	
		Latitude	0.02	0.00	21.86	
		Lake depth	0.003	0.00	9.06	
SK	12,121	Intercept	3.22	0.12	27.51	0.370
		log_{10}LOI	0.37	0.01	56.59	
		log_{10}Cu	0.18	0.01	15.27	
		log_{10}Zn	0.13	0.01	19.00	
		Latitude	-0.030	0.000	-27.03	
		Longitude	0.010	0.000	8.09	
		Lake depth	0.002	0.000	5.77	
AB	960	Intercept	0.45	0.07	6.78	0.300
		log_{10}LOI	0.17	0.03	6.63	
		log_{10}Cu	0.36	0.03	13.59	
		log_{10}Zn	0.16	0.04	3.94	
		log_{10}Pb	0.14	0.03	5.08	

*Regression coefficient (Coeff.); standard error (Std. Err.).

**Numerical coding: stream flow rate: stagnant (1), slow (2), moderate (3), fast (4), torrential (5); stream order: primary (1), secondary (2), tertiary (3), quarterly (4).

Discussion

LOI - Across and within the provinces/territories, the most frequent and significant contributor to the $\log_{10}$THg variations is $\log_{10}$LOI when LOI is part of the data (Table7.1). Altogether, there are 19 $\log_{10}$LOI entries among the 22 best-fit models in dropping LOI from the list of the regression variables reduces the R^2 values considerably, e.g. from 0.51 to 0.35 for Labrador lake sediments, and from 0.70 to 0.45 for Labrador stream sediments (details not shown). Hence, the low R^2 values for the best-fit NS stream sediment THg models are, in part, due to the absence of NS stream LOI data. In addition, the extensive use of Hg as part of past Au prospecting activities throughout NS may have contributed to the high sediment THg values across the southern mainland lakes of NS, as suggested by Odumo *et al. (*2014).

Latitude and longitude - The negative latitude contributions to the $\log_{10}$THg variations from south to north reflect some of the climatic differences in atmospheric Hg deposition and subsequent accumulations in the sediments as presented and discussed in Chapters 5 and 6. The opposing east to west trends of streams and lakes reflect the differences in sample distribution, i.e. the number of surveyed lake locations decreases from east to west, while the number of surveyed stream locations increases from east to west, with no streams surveyed from AB, MB, ON, and SK (Figure 4.2). This decreasing trend from south to north is also reflected by the individual regression results for the lake sediment THg values in NU, ON and SK. In contrast, the lake sediment THg values of Labrador and MB follow the opposite trend.

Other total elemental concentrations - Across Canada, among the metals, $\log_{10}$Cu and $\log_{10}$Zn are the most significant contributors to $\log_{10}$THg variation. The presence of metals in the best-fit regression models by province/territory varies considerably owing to the mix of metals in local bedrock mineralization (Friske and Coker, 1995). By province/territory, among the metals, $\log_{10}$Zn, $\log_{10}$Cu, and $\log_{10}$Pb occur most ffrequently as significant contributors to $\log_{10}$THg variations: 12, 11 and 9 times, respectively (Table 7.1). In detail, Hg and Cu are related more frequently towards the west (AB, MB, SK, YT), north (NWT, NU). In the east (Labrador, NS, NB, QC) and AB, Hg and Pb occur more frequently. Also frequently occurring are the strong relationship between Hg and Mn in Labrador, MB, NB, NS, NWT, and YT. Occasionally, significant relationships are obtained between sediment THg and sediment Ni, Cd, Ag, and Sb. For QC streams with Ca data, $\log_{10}$THg decreases with increasing $\log_{10}$Ca, likely due to an enhanced precipitation of DOM in Ca-enriched surface water (Leenheer and Reddy, 2008).

Stream and lake morphologies - Log_{10}THg increases with increasing lake depth and decreases with increasing lake area or stream channel width, stream flow rate, stream order, the wet-area to basin area ratio (see also Chapter 9).

Examining the sediment THg data of some of the NTS tiles within the provincial/territorial surveys reveals that LOI remains as the strongest THg regression variable (Table 7.2). Since the THg-LOI dependency is curvilinear (Chapter 6), the best-fitted THg results improves further by transforming LOI into $\sin(\pi\ \text{LOI} / 100)^{0.5}$ or $\sin(\pi\ \text{LOI} / 100)^{0.75}$ at a number of locations, i.e. the selected NTS tiles for the La Ronge and

Flin Flon areas (MB), Sudbury (ON), and Kenora (ON). In comparison to the provincial/territorial regression results for THg (Table 7.1), Cu remains as the most frequent metal contributor to the THg variations, while Zn and Pb become less frequent within the select areas of Table 7.2. For the QC geological survey zones, Sb becomes a frequent regression variable (Labrador Trough, Témiscamingue and Sakami). Among the non-metals, F tends to be negatively related to sediment THg. For lakes with S data (QC Sakami area only), $\log_{10}$S replaces LOI as the more significant regression variable.

Table 7.2 Multiple regression analysis results for stream and lake sediment THg/log_{10}THg (ppb), by selected NTS tile.

	Location	n	Variable	Coeff.*	Std. Err.*	t-value	R^2		Location	n	Variable	Coeff.	Std.	t-value	R^2
log_{10}THg (ppb)	**Témiscamingu Grenville A, QC**	1,621	Intercept	1.66	0.03	48.8	0.467	log_{10}THg	**Selwyn Basin, YT** 105M-N, 105K-L	1,606	Intercept	2.12	0.043	49.6	0.590
			log_{10}LOI, %	0.33	0.02	20.2					log_{10}Cd, ppm	0.22	0.013	16.3	
			logNi, ppm	0.15	0.03	5.1					log_{10}Ag, ppm	0.26	0.019	13.6	
			log_{10}Sb, ppm	0.12	0.02	6.0					Rock type: era [a]	0.15	0.013	18.7	
			log_{10}Cu, ppm	0.20	0.03	7.3					log_{10}LOI	0.17	0.02	8.5	
			log_{10}Zn, ppm	0.13	0.03	4.9					$(A_W/A_B)^{0.5}$ [b]	-0.40	0.091	-4.3	
log_{10}THg	**Sneagamook Lake area, Labrador** 13K	957	Intercept	1.191	0.1	13.0	0.655	log_{10}THg	**Greater Sudbury, ON** 31M, 41I-J, 41O-P	4,698	Intercept	0.95	0.026	37.1	0.487
			log_{10}LOI	0.441	0.03	15.1					$\sin(\pi LOI/100)^{0.75}$	0.52	0.012	43.0	
			log10Cu, ppm	0.432	0.02	20.3					log_{10}Pb	0.12	0.007	17.6	
			log_{10}Pb, ppm	0.247	0.0	10.4					log_{10}Cu	0.13	0.01	12.8	
			log_{10}F, ppm	-0.247	0.0	-10.2					log_{10}Zn	0.02	0.016	12.4	
THg	**Great Bear Lake area, NWT** 86K,L	1,296	Intercept	17.3	2.26	7.7	0.462	log_{10}THg	**Schefferville, Churchill A, QC** 23I-J, 23N-P	3,576	Intercept	2.11	0.02	98.7	0.685
			LOI	0.53	0.04	14.2					log_{10}LOI	0.14	0.008	17.4	
			Cu	0.33	0.01	23.4					log_{10}Sb	0.30	0.011	27.4	
			Lake area, km^2	-3.08	0.11	6.8					log_{10}Ag	0.27	0.01	26.2	
			Lake depth, m	0.75	0.16	6.8					log_{10}Cr, ppm	0.16	0.008	21	
log_{10}THg	**Sakami, Opatica, QC** (Lakes wirh S data) 34A-C, 33F-H	218	Intercept	1.98	0.11	17.7	0.526	log_{10}THg	**Sakami, Opatica, QC** (Stream & lake) 34A-C, 33F-H	1,772	Intercept	1.54	0.04	40.8	0.385
			log_{10}S, %	0.26	0.03	7.6					log_{10}LOI	0.12	0.02	7.68	
			log_{10}Cu	0.35	0.05	7.1					log_{10}Cu	0.52	0.02	25.6	
			log_{10}Sb	0.15	0.02	5.9					log_{10}Sb	0.15	0.02	5.9	
log_{10}THg	**La Ronge–Flin Flon, MN** 63K-N, 73P,74A	4,908	Intercept	0.91	0.02	41.3	0.243	log_{10}THg	**Murdochville, Gaspé, QC** 22A-B	4,350	Intercept	0.04	0.003	12.4	0.635
			$\sin(\pi LOI/100)^{0.5}$	0.55	0.02	30.2					log_{10}LOI	0.13	0.002	71.5	
			log_{10}Cu	0.17	0.02	10.9					log_{10}Cu	0.06	0.002	25.1	
			log_{10}Co, ppm	0.12	0.02	7.0					log_{10}Pb	0.02	0.002	8.0	
log_{10}THg	**Kenora–Dryden, ON** 52E-F	1,913	Intercept	0.71	0.07	9.9	0.535	THg	**Bathurst Island, NU** 69A-B, 69H-G	418	Intercept	1.70	1.20	1.4	0.425
			$\sin(\pi LOI/100)^{0.5}$	0.70	0.02	29.6					LOI	0.50	0.072	7.0	
			log_{10}Pb	0.27	0.02	15.7					Zn, ppb	0.12	0.006	16.0	
			log_{10}Co	0.25	0.02	11.4					Co, ppb	1.44	0.16	8.8	
			log_{10}F	-0.28	0.02	-14.0									

[a] Rock type coding: Mezozoic & Paleozoic (1); Cenozoic & upper Proterozoic; Plaeozoic/Upper Proterozoic (0). [b]Area of basin (A_B, ha) devided by area of wet-area of each basin (A_W, ha); A_W referred to DTW < 0.5 m, including surface water.* Regression coefficient (Coeff.); standard error (Std. Err.).

Conclusions

The regression results of this chapter affirm that approximately 50 % of the sediment $\log_{10}$THg variations in stream and lake sediments are related to sediment LOI and other metal concentrations. In some cases, the best-fit R^2 values for the $\log_{10}$THg relationships increase up to 0.64 (YT streams) and 0.70 (Labrador streams), but in some other cases these values decrease towards near zero (NS).

In comparison to Hg, other heavy metals such as Cd, Cu, Ni, Pb, and Zn are not as strongly bound by organic matter (Thomas *et al.,* 1998; Han *et al.,* 2007; Xunyi, 2009). Within sediments, Hg is bound to organic S groups, attached to mineral surfaces, and also exists in mineral form, such as cinnabar, or HgS (Dmytriw *et al.,*1995; Gray *et al.,* 2000; Shuman, 2003; Ramasamy *et al.,* 2012).

Geographic location, stream and lake morphologies, and areas with high geogenic Hg sources also contribute to the sediment THg variations. Exceptions occur where anthropogenic sources dominate, and these would then become the main source of sediment THg. This would be the case for the stream and lake sediments in NS, where LOI and other heavy elements only explain a minor part of the overall THg variations.

Chapter 8 Regional Illustrations

Introduction

The objective of this chapter is to expand on the regression results summarized in Chapter 7 through geogenic interpretations and region-specific illustrations (Table 7.2). These illustrations overlay the point-by-point data for sediment THg on the broad geographic, geological, historical, and climatic context for the selected areas. The geological context refers to age and type of bedrock formation, with bedrock type classified as igneous extrusive (volcanic) and intrusive, metamorphic, and sedimentary. Heavy metal mineralizations occur when hydrothermal fluids from deep magma sources protrude into fractured bedrock formations. Of particular importance are the processes that have led to the occurrence of surface-exposed heavy metal mineralization. These processes may range from ancient to fairly recent orogenic uplift of mountain ranges, tectonic movements and related faults, volcanic extrusions, meteoric impacts, gradual surface erosion of mountain ranges over the course of billions of years, and recent to current mining activities.

Selected Areas

Maritimes and adjacent areas - Figure 8.1 provides an overview of the main bedrock types and associated faults for the Maritimes and Gaspé area in Appalaches B survey zone in QC. Across this region, high THg levels are associated with certain bedrock formations and these vary depending on the geological processes that gave rise to these formations. In detail, stream and lake sediment THg values are high (> 500 ppb), very high (> 1000 ppb), low (<50 ppb), or very low (< 20 ppb) for any of the four bedrock types (plutonic, metamorphic, volcanic, or sedimentary).

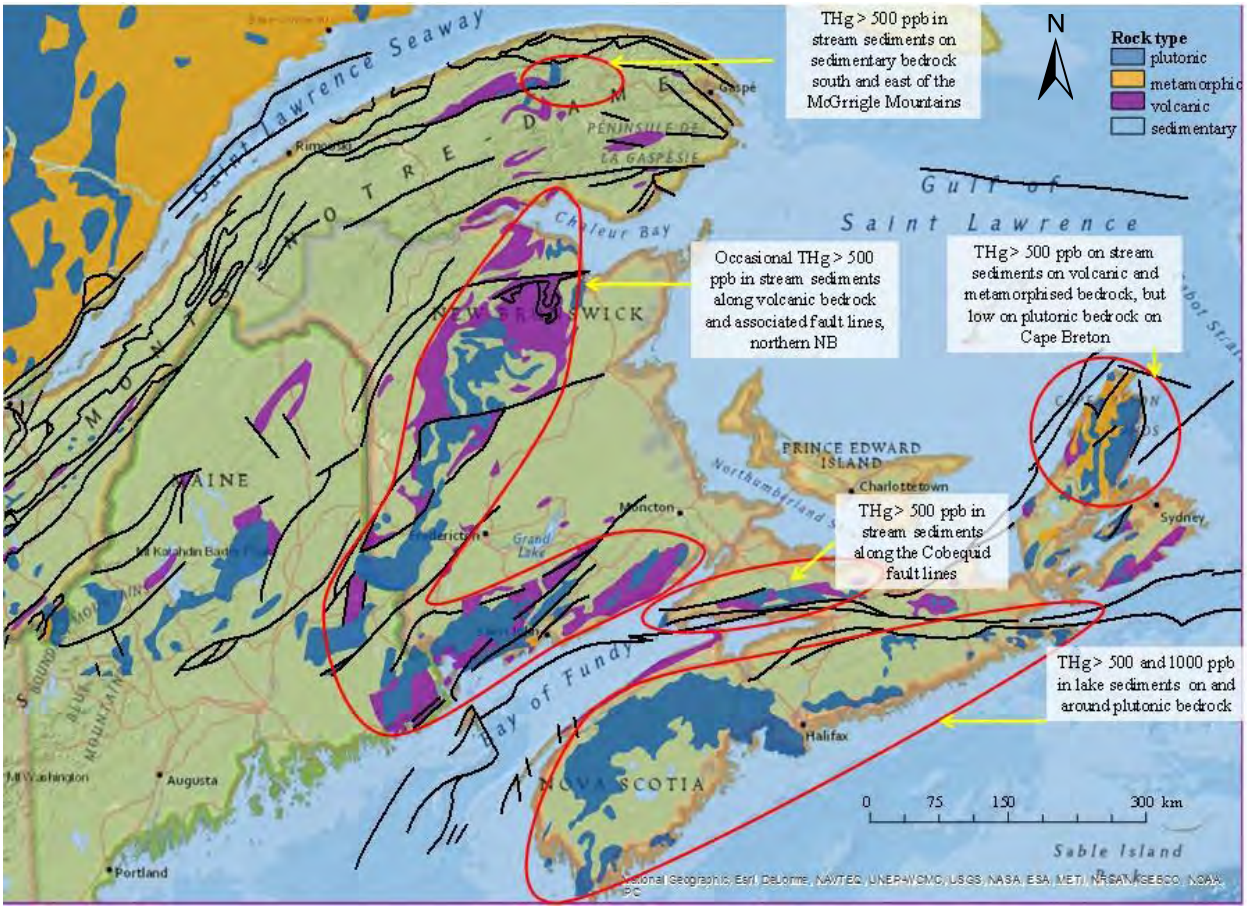

Figure 8.1 Main bedrock types and faults (black) for the Maritime.

Typically, sediment THg is generally higher on and along granitoid plutons with metal mineralization exposures in southern NS (lakes) and along the Cobequid faults in northern NS (streams). Lowest values occur in the stream sediments on sedimentary bedrock north and south of the Cobequid Range, and on the plutonic bedrock formation on northern Cape Breton.

NS - Settlements, forestry, mining, and agriculture have a long history in NS. The north western region has become a particular Hg bioaccumulation concern because of reported aquatic and terrestrial ecosystem sensitivities to Hg and high acid deposition rates (O'Driscoll *et al.*, 2005; Wyn *et al.*, 2010). In comparison, mean lake sediment THg across southern NS is

approximately 3 times higher than mean lake sediment THg in southern QC and ON, and approximately 10 times or higher than mean stream and lake sediment THg in northern Canada and high alpine areas (Tables 4.1, 4.2).

The terrain across northwestern NS consists of an intricate network of lakes, streams and wetlands interspersed by coarse- textured, shallow till-derived soils on tectonically- and magmatically-influenced greywacke (Cambrian) and slate (Ordovician) sedimentary bedrock formations, interspersed by biotite-rich granitoids (Upper Devonian plutons). The uplifting of the granitoids tends to elevate originally deep-seated heavy metal mineralizations to the surface, including Au and Hg (Figure A.3; Province of Nova Scotia, Department of Natural Resources, 2013, 2012). These mineralizations are, once surface exposed, more readily erodible and exploitable. In turn, these exploitations led to widespread Au prospecting and mining across NS since 1861, with Hg used to increase the efficiency of the Au extraction process (Little, 2006).

Sediment THg varies widely (5-36,000 ppb) across the province (Figure 8.2). Lakes of southern NS have higher THg than streams. Comparing the best-fit regression models for THg in Table 7.2 reveal a strong dependence of THg on LOI in the Cape Breton lakes but only a weak dependence in the mainland lakes. It is therefore suggested that the practice of Au extraction via Hg amalgamation has not only contributed to above mean sediment THg across many of the northwestern NS lakes, but also weakened the generally strong relationship between sediment THg and sediment LOI.

Across NS, high and low sediment THg values are associated with specific bedrock formations as follows:

- Cambrian – Ordovician slates and the granitoid Devonian South Mountain Batholith of the Goldenville formation contain S-rich and Hg-containing minerals such as biotite and pyrites occur across the NS mainland (Daughney *et al*., 2005). Hence, the weathering of the Hg-containing and surface-exposed minerals would be a major contributor to Hg in bedrock-covering soils, till and sediments (Garrett, 1974; Page and Murphy, 2005; Daughney *et al.,* 2005).

- The geologically-complex Precambrian-Devonian Cobequid Range was further enriched by mineral deposits along late Paleozoic sheer zones (Pe-Piper *et al.,* 2004), and along the inland cliff north of the Cobequid Bay fault. Here, sediment THg is generally low in the streams that drain the non-marine Carboniferous to Permian-Triassic sedimentary bedrock formations north and south of the Cobequid Range. These formations vary from reddish, soft sandstones and siltstones to hard and coarse-textured sandstones, or contain conglomerates of both formations (Keppie, 2000).

- In the northern mainland, the formation of Precambrian-Devonian and lower Carboniferous of the Avelon terrane resulted in a wide range of rock types, with black limestone having the highest in Hg content (mean value of 202 ppb; Daughney *et al.,* 2005). The mineral deposits along the sheer zones and the presence of late Paleozonic (younger) plutons within the Cobequid Highlands are of special concern in terms of high heavy metal mineralizations, including Hg (Pe- Piper *et al.,* 2004). Figure 8.2 presents the close-up of Cobequid Range and sediment THg range.

- The Precambrian Proterozoic-Paleozoic Cambrian bedrock formations on Cape Breton include exposures of Hg-enriched black shales and granites with Hg-containing biotite (Barr and Raeside, 1989).
- The late Neoproterozoic metamorphic and plutonic rocks are surrounded by younger Carboniferous sedimentary units (e.g. the Whycocomagh Mountain and Aberdeen Ridge) contain heavy metal deposits referring to Hg, Au, Pb, Cu, Zn, etc. (Swanton et al., 2009);
- The heavy metal veins within the carbonate formations (limestone and dolomite) with inter-bed shales and siltstones throughout central Cape Breton Island are known as the Lamey Brook and Glen Carbonate deposits (DeMont, 2002).
- The Stirling Zn-Pb-Cu mine in northeastern Cape Breton that is located on a volcano-massive sulphide (VMS) deposit. This mine achieved high levels of Au and metal production during 1935-1938 and 1952-1956. Stream sediments downstream from the mine tailings still contain THg up to 3,000 ppb (Hulshof and MacDonald, 1998).
- Hg containing coal seams occur along the **Sydney-Glace Bay area** (Birk *et al.*, 1986; Gregory *et al.*, 1978).

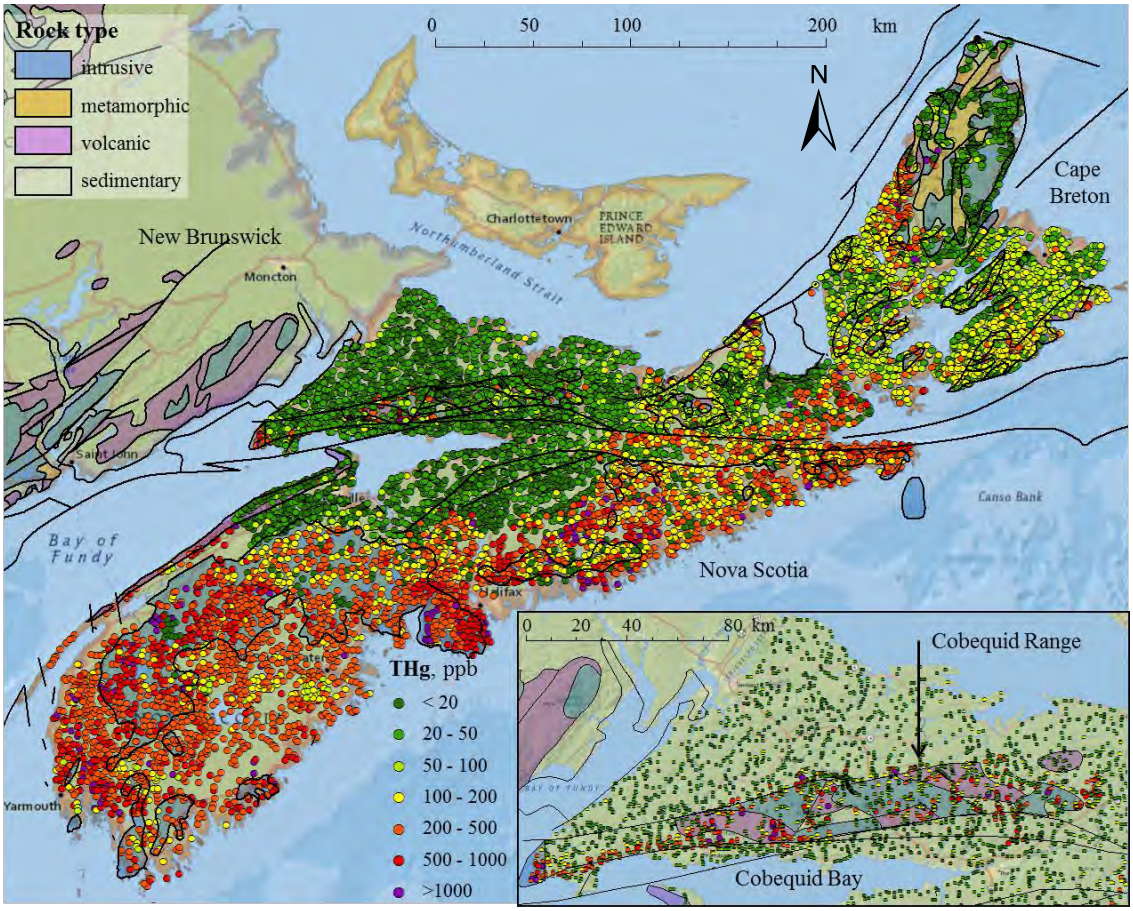

Figure 8.2 Stream and lake sediment THg (ppb) from low (green) to high (purple) in NS. Background: bedrock type and faults.

NB - On average, the THg levels in NB sediments are lower and less variable than in NS (Table 4.1; Figure 8.3). Across NB, THg rarely exceeds 500 ppb, and only so on Cambrian-Ordovician plutonic and volcanic formations that reach from Bathurst towards the southwestern border, and from there turning eastward the southern Neoproterozoic to Cambrian stretch of plutonic and volcanic formations north of the Bay of Fundy (Wilson *et al.*, 2005; Al *et al.*, 2006). The highest THg occurs downstream from the cyanide-containing Au mine tailing at Murray Brook in northern NB (Al *et al.*, 2006), and downwind from the lead smelter at Belledune, Chaleur Bay (Parsons and Cranston, 2006).

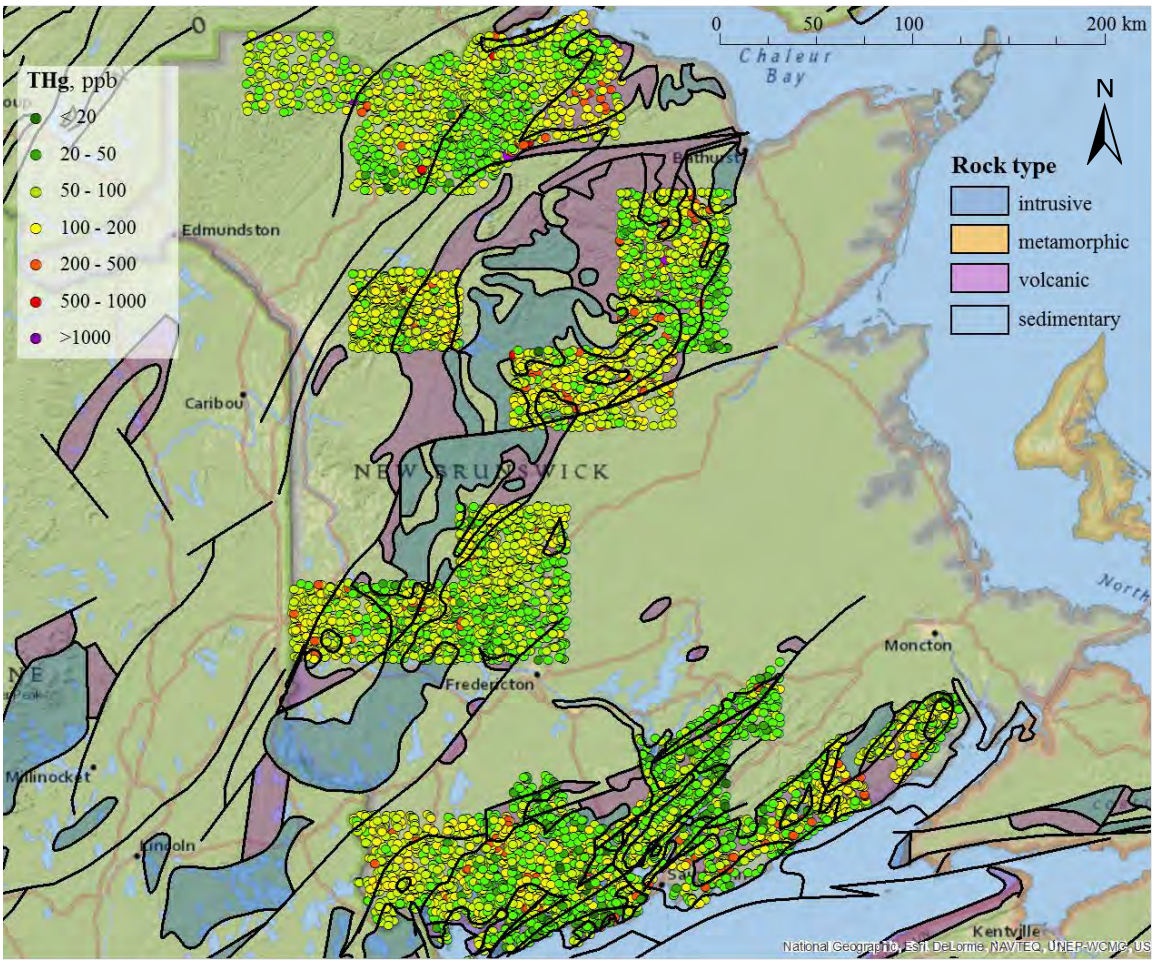

Figure 8.3 Stream and lake sediment THg (ppb) from low (green) to high (purple) in NB. Background: bedrock type and faults.

Overall, LOI, Pb and Mn account for 63 % of the stream sediment THg variations in NB, with LOI being the strongest contributor. The Carboniferous to Permian plain that extends across parts of eastern NB, all of PEI, and northern NS yields low values for sediment THg (Figure 8.1), but the same plain contains localized and generally deep-seated coal deposits with particularly high S and Hg concentrations. Hence, elevated S and Hg concentrations were noted in the air and in biological receptors downwind from the now demolished coal burning power generator at Grand Lake in central NB (Bourque *et al.*, 1996; Jardine *et al.*, 2009). Compared to the flat Carboniferous-Permian plain in the east,

sediment THg is more variable on the hummocky Ordovician-Devonian sedimentary bedrock formations in northwestern NB.

QC - There are as many stream and lake sediment sampling locations in QC as there are for the rest of Canada (Table 4.1). These locations fall across the geological regions of sub-provinces of QC (Figures 8.4). Some of THg variations of these regions are illustrated below for the Gaspé, Témiscamingue, Sakami, and Schefferville areas, where stream and lake sediment THg ranged from < 20 to > 1,000 ppb ppb:

Appalaches B: McGarrigle Mountains - Murdochivlle, Gaspé Peninsula - The area stretches over 150 km east-south to east of the Devonian plutonic invasion of the granitic McGarrigle mountains through the older Cambrian-Ordovician bedrock (Jones and Wiley, 2012). This intrusion is also flanked by south to east volcanic extrusions into the Early Devonian calcareous bedrock. The exposure of the Hg containing units has resulted from the Devonian orogenic uplift that occurred north to northwest across the peninsula.

For the streams of this area, sediment THg decreases from low to high stream order, as evident by the strings of red to green points along some of the flow channels in this area (Figure 8.5). The Hg sources likely originate along slopes and flow channels of surface-exposed bedrock, till and soil. The regression analysis for this area (Table 7.2) indicates that THg is highly correlated with LOI (mostly due to organic matter), but only moderately correlated with Cu and Pb. This confirms that organic matter of the streambed sediments preferentially binds Hg in relation to the other metals. Some of the high THg outliers maybe due to mining activities. The emissions from the Cu smelter at Murdochville, however, drifted eastwards where sediment THg is in comparison low (Aznar *et al.*, 2008).

Hence, downstream sediment THg from the geoenic sources to the west of Murdochville are considerably higher than downwind sediment THg to the east).

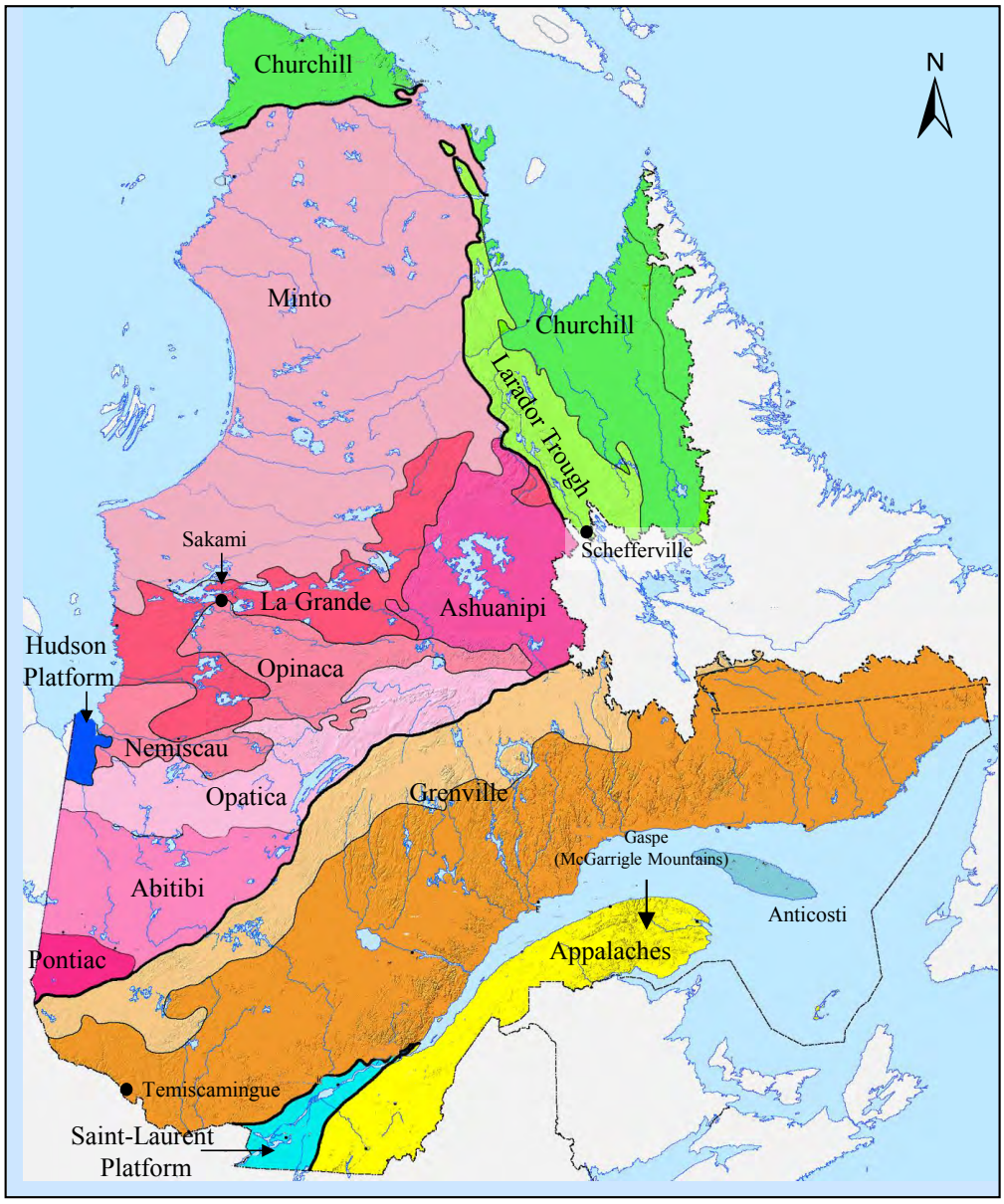

Figure 8.4 Geological provinces of QC, with sub-provinces for the Superior Province (pink; mostly Neoarchean), Grenville (brown, mostly Mesoproterozoic) and Churchill (green; mostly Paleoproterozoic). The other geological provinces refer to the Appalachian Orogen and Appalaches (yellow, varying from Cambrian to Ordovician to Devonian), the Hudson Platform (dark blue, Silurian), and the Saint Lawrence Platform (light blue, Cambrian to Ordovician). Adapted from Card and Ciesielski (1986).

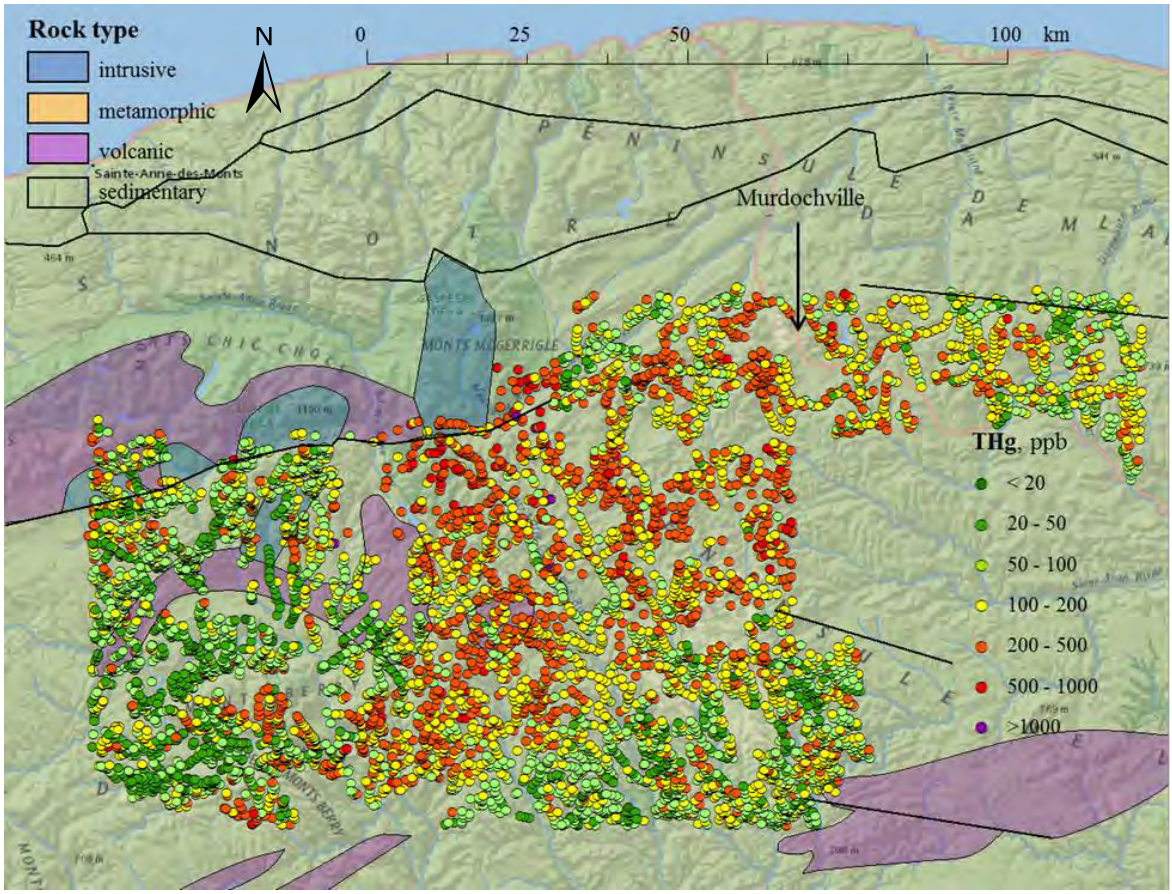

Figure 8.5 Stream sediment THg (ppb) in the Gaspé area of QC from low (green) to high (purple). Background: bedrock type and faults.

Grenville A: Temiscaming/Témiscamingue, QC and ON - The mostly pristine Témiscamingue area east of the Ottawa River from the town of Temiscaming northward to the southern portion of Lake Timiskaming (Cloutier, 2012) is underlain by plutonic bedrock (Neoarchean gneiss) that was subject to intense metamorphic processes approximately 2.6 Bya (Davis, 2002). After a prolonged period of erosion, this was followed by a succession of Paleoproterozoic upheaval and magmatic intrusions, which

resulted in substantive heavy metal mineralization (notably Ag and Co) in the igneous units, conglomerates, and sediments, most noticeably in the west of Lake Timiskaming (Wilson, 1910). Subsequent oceanic submersion produced fossil bearing Ordovician-Silurian limestone deposits 460 Mya to 420 Mya across the wider area, with the area around the northern part of Lake Timiskaming and beyond being an outlying remnant (Dix *et al.*, 2007).

The Jurassic break-up of the Pangean supercontinent approximately 180 Mya led to the sediment-filled Timiskaming Graben along the Ottawa River forming the northern component of the Ottawa-Bonnechere Graben complex. Altogether, periodic tectonic uplifting, rifting and continuing erosion brought originally deep-seated heavy metal mineralization to the surface.

The terrain east of Lake Timiskaming (Figure 8.6) shows many low to exceptionally high stream sediment THg (mean = 488 ± SD 588, min. = 10, max. = 9,392 ppb, n = 3 530), where THg is significantly correlated with Ni, Cu, Zn, Sb, and Sn, and with LOI also remaining as a significant component of the best-fit $\log_{10}$ THg model (Table 7.2). In contrast, mean stream sediment THg just south and west of Lake Simard on Neoarchean syenite-monzodiorite is much lower and less variable (THg = 26 ± 20 SD, min. = 5, max. = 160 ppb; n = 471). In comparison, stream sediment THg = 120 ± 53 SD ppb (min. = 35, max. = 271 ppb, n = 101) on the Paleoproterozic intrusive bedrock formations west of Lake Timiskaming (Figures 8.6, 8.7).

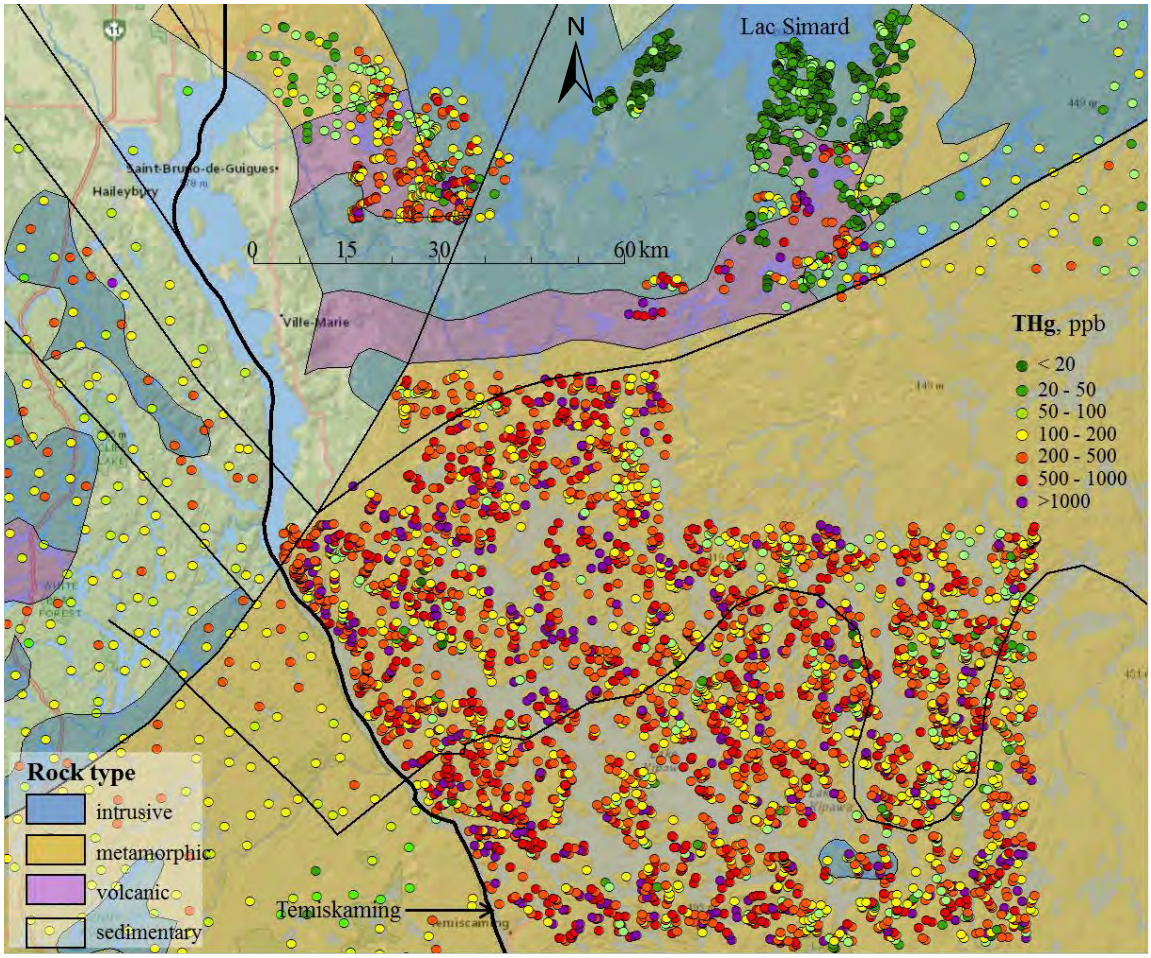

Figure 8.6 Stream sediment THg (ppb) from low (green) to high (purple) of the Témiscamingue area, east and west of Ottawa River along the ON-QC border (thick black line). Background: bedrock type.

Opatica: Sakami - High stream and lake sediment THg values occur on the La Grande volcanic belt north and immediate southwest of Sakami in Opatica La Grande Opinaca Nemiscau (Figure 8.7). These high values likely originate from early Proterozoic faulting, volcanic extrusions and subsequent mineralization (approximately 2.2 Bya; Mercier-Langevin *et al.*, 2012; Ciesielski, 1991). This is consistent with the strong correlation between sediment THg and sediment Cu (Table 6.2). LOI cease to be a significant variable when the regression analysis is restricted to only include samples with S inclusion.

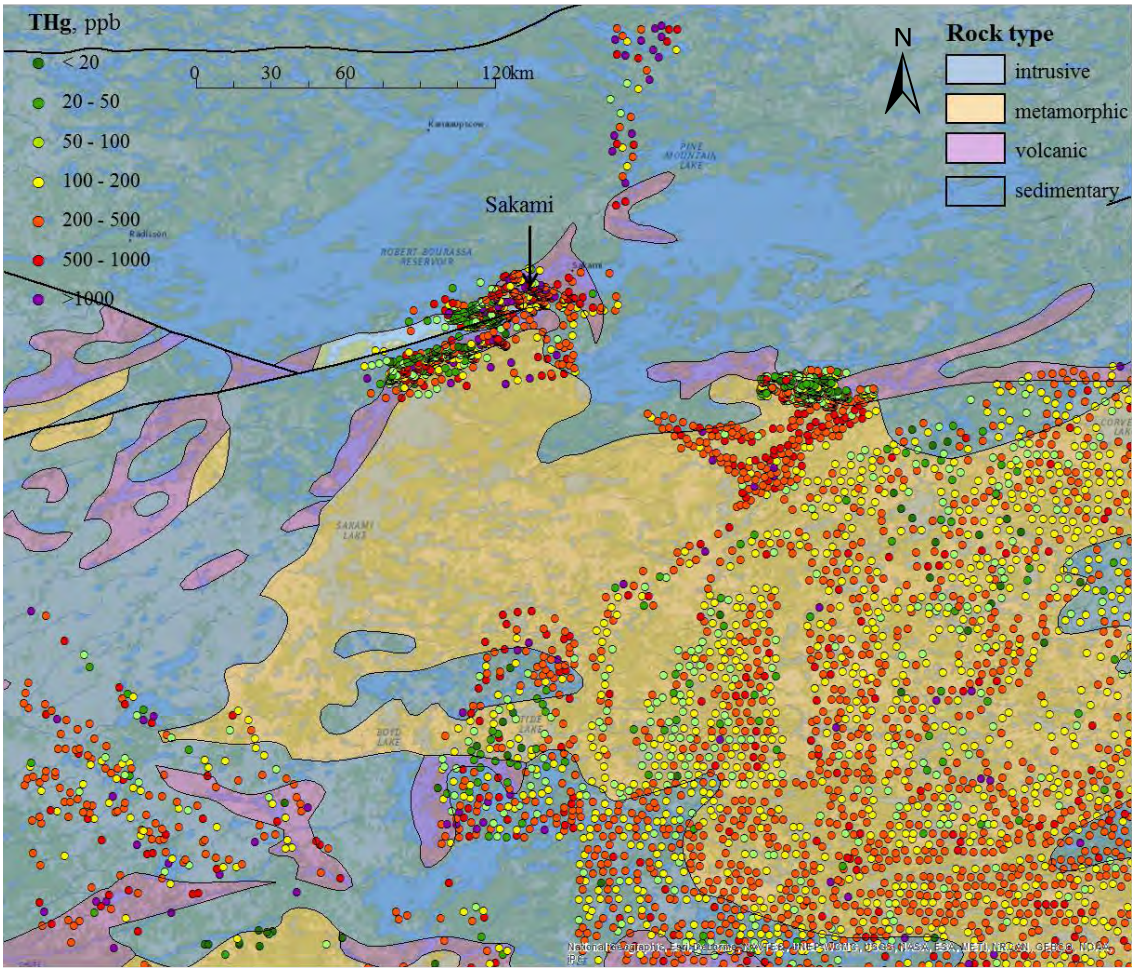

Figure 8.7 Sediment THg (ppb) from low (green) to high (purple) at Sakami and along the Opinaca basin to the south. Background: bedrock type and faults.

The Hg-S correlation is particularly strong where mineral sulfides dominate and where LOI is low. Within the generally barren and older Opinaca Basin to the south and northeast of Sakami, lake sediment THg commonly varies from 100 to 1,000 ppb, with occasional occurrences above and below these values. This range may be due to surface exposure of bedrock Hg-containing mineralizations in general and to Au mining activities at and around Sakami.

Churchill A: Schefferville, Labrador Trough, Labrador and QC- The Labrador Trough stretches south to northeast from west of Ungava Bay towards Schefferville (Figure 8.8; Churchill A) and Labrador City, and then turns southwest to the Lake Manicouagan impact crater, formed 214 Mya ago (Ramezani *et al.*, 2005). The Labrador Trough is a tectonic rift containing highly metamorphosed sedimentary and early Proterozoic volcanic rocks that were further influenced by upwelling magma 2.2 and 1.9 Mya (Poirier, 1989).

Geochemical exploration in this area has been intensive, as demonstrated by the closely spaced survey in Figure 8.9. Local mining interests have mostly focused on source of Fe (Government of Quebec, 2012). THg of the lake sediments north of Schefferville have a mean value of 190 ppb, with a maximum at 1,400 ppb. High THg are present but scattered, thereby suggesting that heavy metal mineralization exposures are local. The best-fit regression analysis relates THg to LOI, Sb, Ag, and Cr (Table 6.2). Densely sampled sediments in the southern area with low THg (66.7 ± 34 SD ppb, n = 255; Figure 8.9) are located on a plutonic Neoarchean tonalite (granodiorite) formation (close-up in Figure 8.9). This indicates that the exposed portion of this rock formation is contributing little Hg mineralization to the surrounding environment.

.

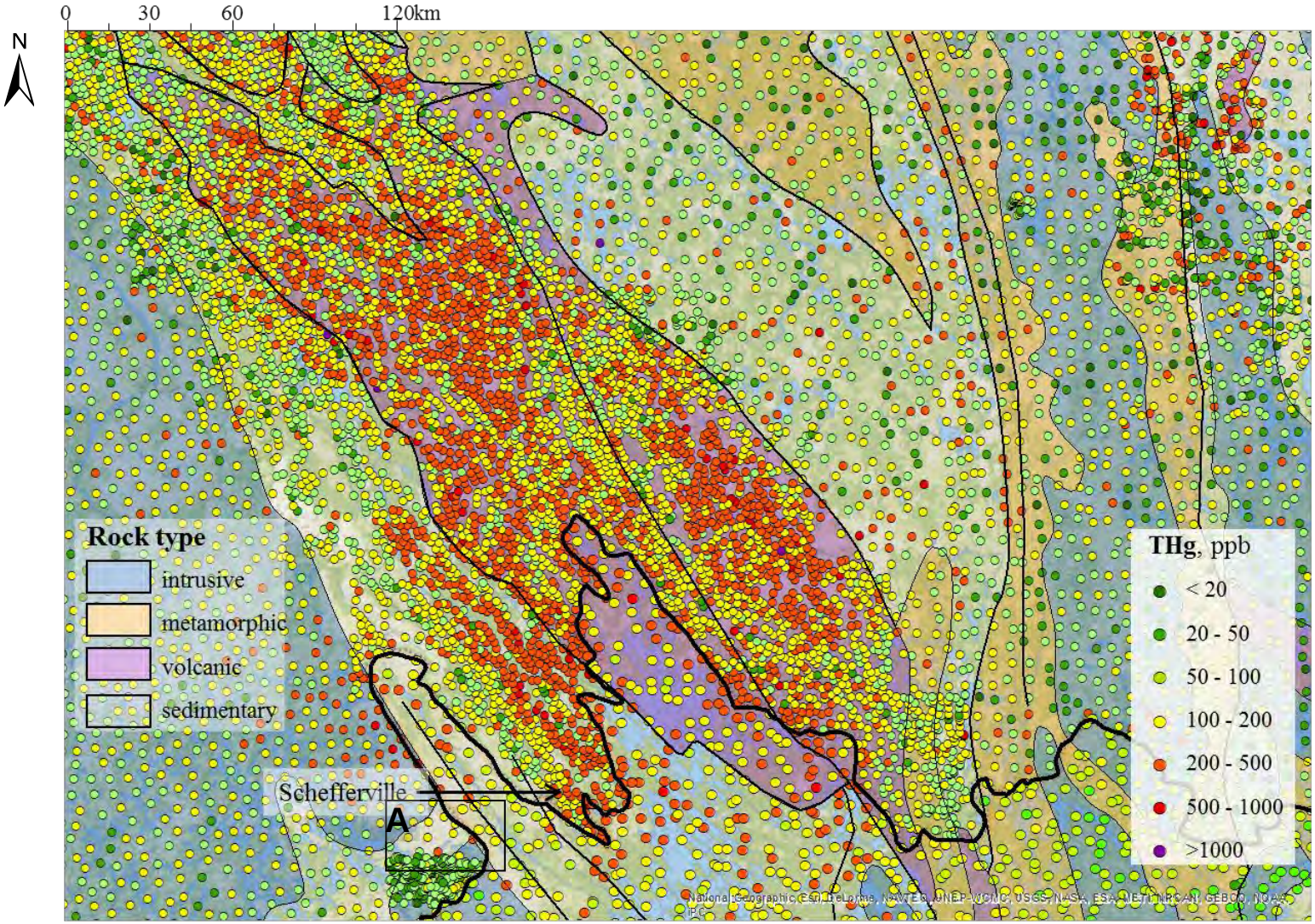

Figure 8.8 Lake sediment THg (ppb) from low (green) to high (purple) in the Labrador Trough area at Schefferville, QC. A: the densely sampled low THg locations expanded in Figure 8.9. Background: bedrock type and faults. Black line: QC-Labrador border.

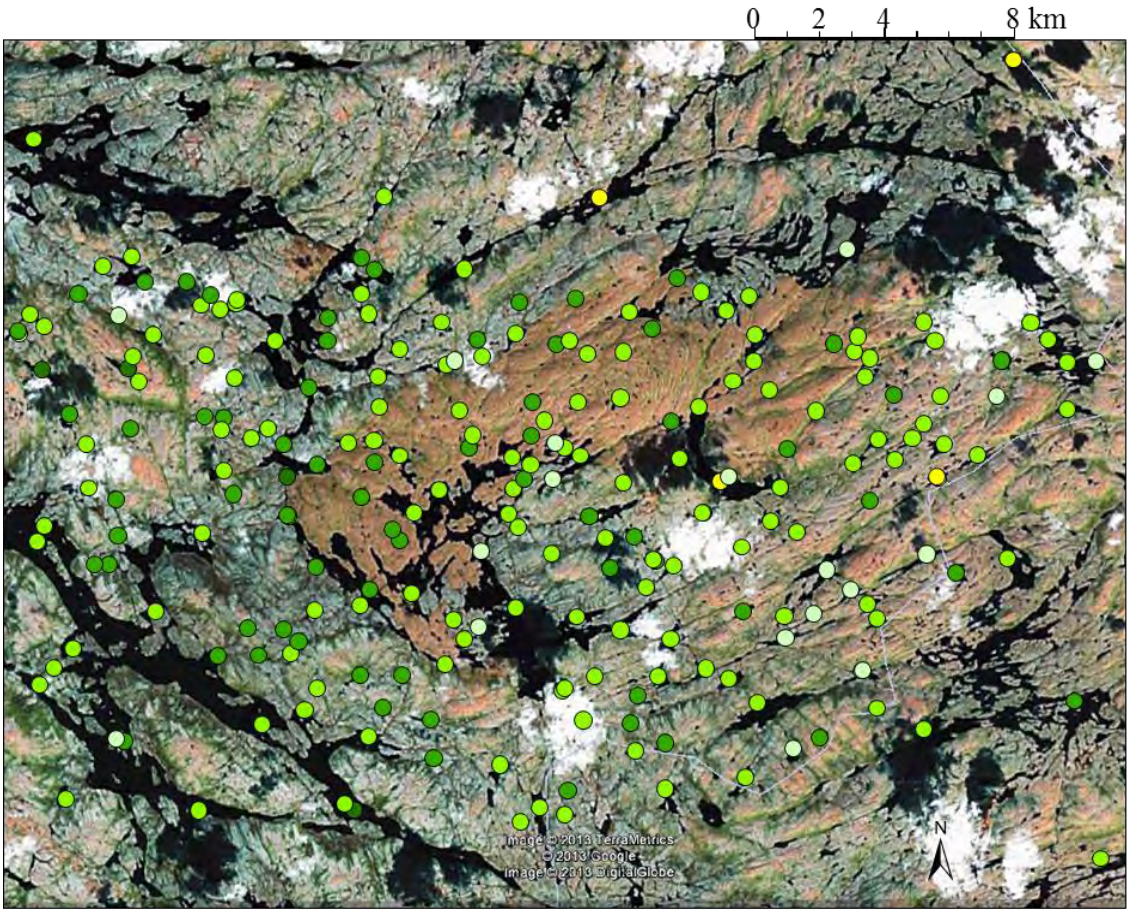

Figure 8.9 Close-up of the densely sampled low THg area (A) in Figure 8.8. Background: surface image (Googlemap). Legend for points: same as in Figure 8.8.

Sneagamook Lake area, Labrador - The Central Mineral Belt in Labrador (Figure 8.10) was formed by multiple Archean to Proterozoic mineralization events (2.7 to 1.2 Bya) that led to rhyolite-dominated metavolcanic rocks interspersed by intrusive rocks. The highest mineralization clusters containing Cu, Ni, U, Fe, Pb and F occur north and south of the Kanairiktok River as it flows eastwards from Snegamook Lake (McCuaig and Taylor, 2005). The best-fit regression analysis for the lake sediments in area of Figure 8.10 relate THg to LOI, Cu, Pb and F (Table 6.2). The mean and maximum THg

levels amount to 116 and 700 ppb, respectively, i.e. considerably lower than north of the Schefferville area.

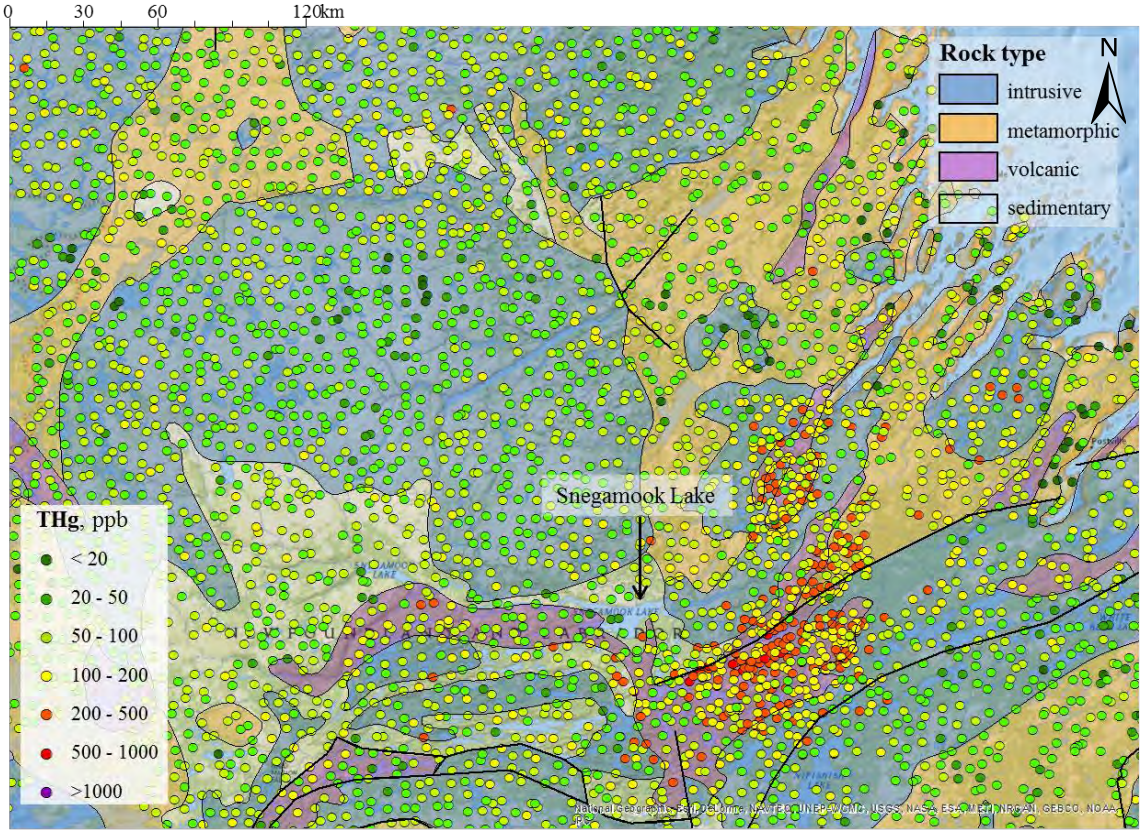

Figure 8.10 Stream ediment THg (ppb) from low (green) to high (purple) for the Snegamook Lake area in northeastern Labrador. Background: bedrock type and faults.

Greater Sudbury areas, ON - The Sudbury impact crater, stemming from a bolide (10-15 km diameter) collision 1.8 Bya, incurred several tectonic deformation thrusts over the course of 850 million years (Kettles and Shilts, 1996). This crater is filled with sedimentary bedrock, and is surrounded by tonalite and diorite-gabbro bedrock formations containing deep-seated heavy metal mineralization containing Ni, Cu, Pt, Pd, and Au. The wider area around this crater consists of a mix of extrusive, intrusive,

metamorphosed and sedimentary bedrock (Doreen *et al.*, 2009). Lake sediment THg across the area depicted in Figure 8.11 varies from < 20 ppb to > 1,000 ppb. From this figure, it is apparent that that the high and low values are moderately related to bedrock type, i.e. generally lower on granitoids and tonalites, and higher on and near mafic and diorite-gabbro formations and some of the faults. The mix of low and high THg is strongly correlated with LOI, i.e. $[\sin(\pi LOI\&/100)]^{0.7}$, and is weakly correlated with other metals (Chapter 7).

Across northeastern ON, metal mineralization is generally found in the supracrustal and intrusive rocks of the central meta-sedimentary belt (Kettles and Shilts, 1996). This belt stretches westward in the southern Grenville province of ON. In these areas, glaciofluvial sand deposits have generally higher Hg concentrations than the glaciomarine sandy deposits in the St Lawrence River floodplain on the east. The sediment THg of this region are relatively low (with most samples up to 200 ppb). For the Sudbury basin and surrounding areas and to the north of Lake Huron, sediment THg increases to approximately 500 ppb, with a few anomalies up to 21,000 ppb. Between Sault Ste. Marie and Lake Temagami, numerous metallic occurrences (Cu-Ni-Co-Pb-Ge-Ag-Au) are present, and most notably so at Cobalt (Takats and Dyer, 2004).

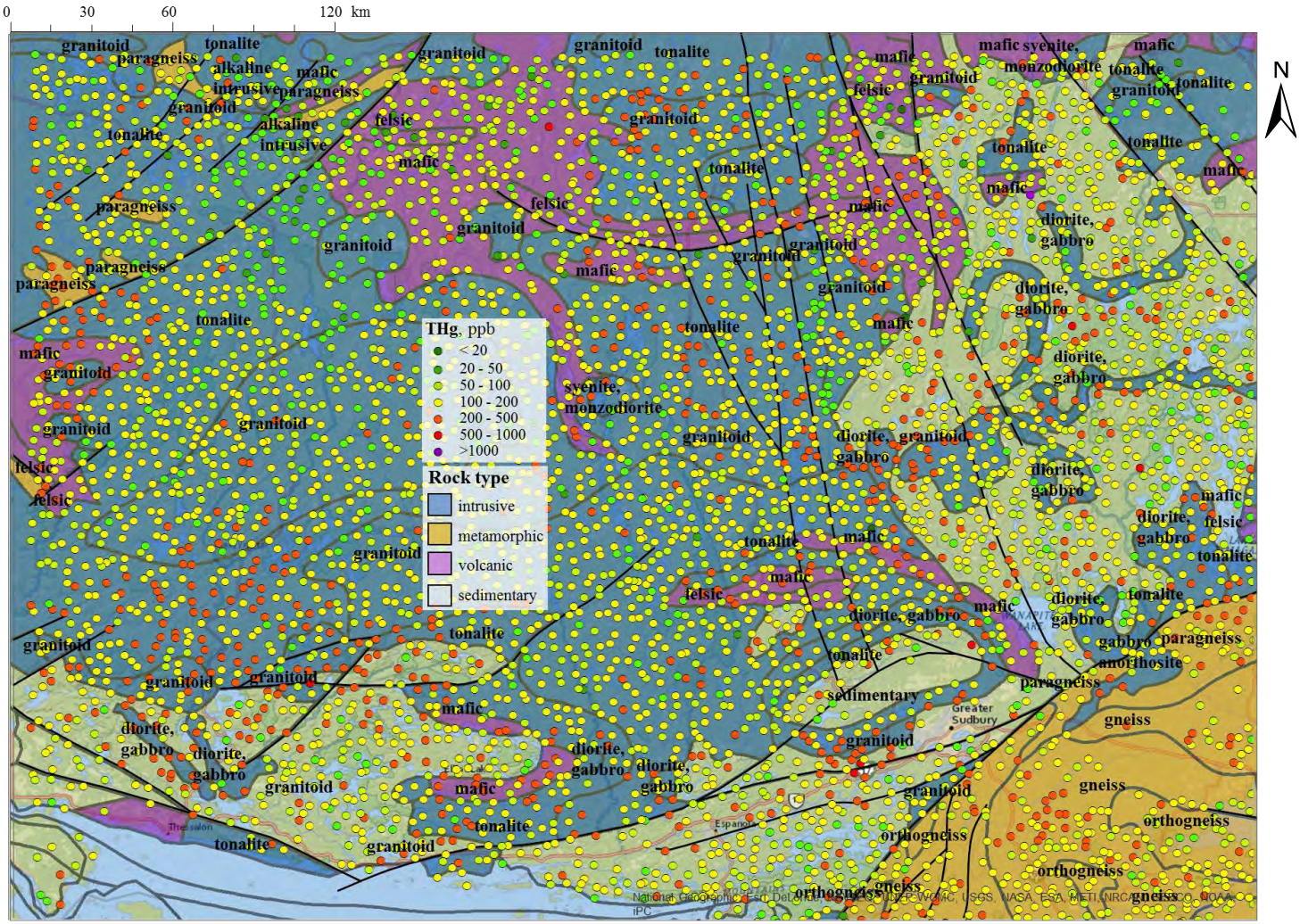

Figure 8.11 Lake sediment THg (ppb) from low (green) to high (purple). Background: bedrock type and faults for the greater Sudbury area north of Lake Huron. The Sudbury crater, visible in the southeast section by way of the elliptical sedimentary bedrock formation, is surrounded by tonalite-granitoid and diorite-gabbro formations.

Kenora-Dryden, ON - The Neoarchean bedrock formations in the sediment survey area from west of Kenora to east of Dryden (Figure 8.13) vary from granitic intrusions to mafic and felsic volcanic extrusions (Wheeler *et al.*, 1997). Heavy metal mineralization is present but are generally contained within a deep-seated mineral matrix. Lake sediment THg was low, rarely exceeding 200 ppb with no specific relationship to bedrock type or fault. The highest value occurred in the northeastern branch of the Lake of the Woods, near Cedar Island. The multivariate analysis of Chapter 7 showed THg is strongly correlated with LOI, i.e. [sin(πLOI&/100)]0.5], and less so with other metals. Mining activities have focused on Au and U extraction (Davies and Smith, 1988).

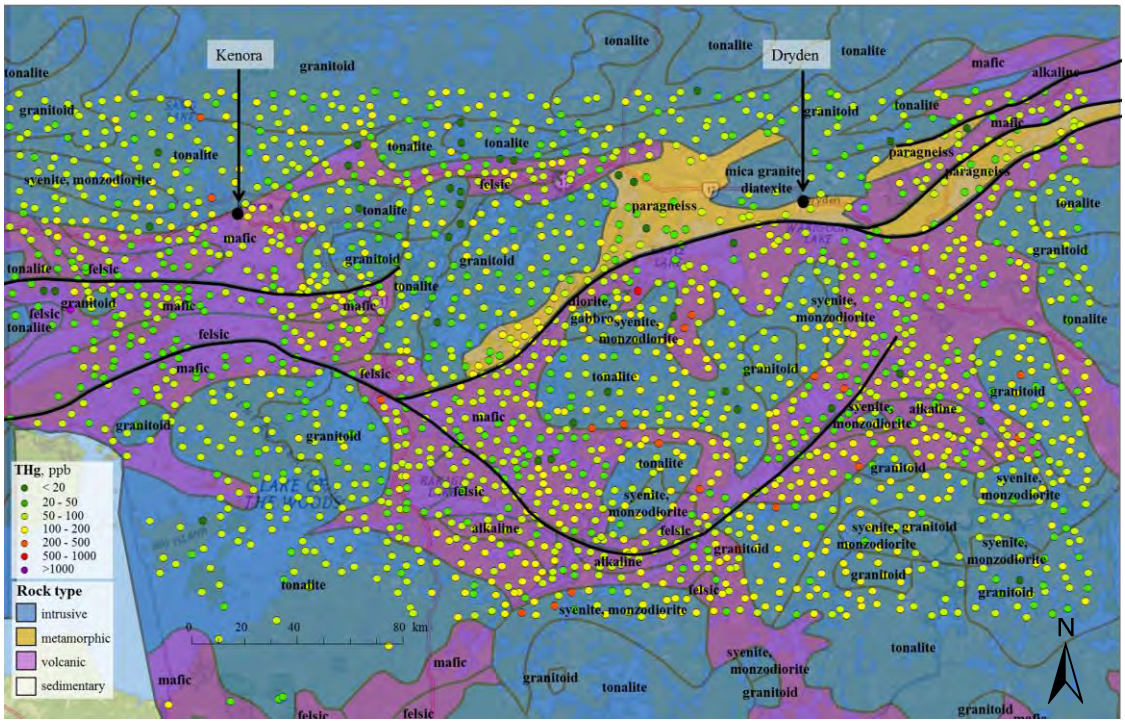

Figure 8.12 Lake sediment THg (ppb) from low (green) to high (purple) for Kenora-Dryden area west of Lake Superior. Background: bedrock type and faults. Note fairly low THg values throughout the area, with only a few locations with THg > 200 ppb.

La Ronge-Flin Flon, Northern MB and SK – Here, the sampled lakes are all located on Neoarchean to Paleoproterozic fault lines, shear zones and bedrock formations, ranging from ocean floor metabasalt and felsic-mafic plutons to metamorphosed granites (gneiss) and sedimentary bedrocks, with scattered VMS occurrences (Maxeiner *et al.*, 2004; Dunn, 1998; Syme *et al.*, 1996; Figure 8.13). Here, the higher sediment THg values (red to yellow points in Figure 8.13) are generally associated with lake catchments on meta- to ultra-mafic bedrock.

The higher THg values north of La Ronge (orange to red points in Figure 8.15) occur on the adjacent Paleoproterozoic formation. From this, it appears that some of the sedimentary bedrock formations produce Hg- carrying sediments more easily than the

nearby volcanic formations, granitoids and gneisses. The most significant contributors to the THg variations across this area are LOI, Pb, and Cu (Table 6.2). Mining activities have focused on Au extraction in the La Ronge area, and on Cu and Co in the greenstone belt east to west and south of Flin Fon.

The 80-year long Cu and Zn smelting activities at Flin Flon released up to approximately 1,000 kg of Hg per year but ceased in 2010 (Ma *et al.*, 2013). Downwind forest floor, open-area soils, peat, and lake sediment samples show historical and/or geospatial signatures of local Hg emission and deposition (Jones and Henderson, 2006; Outridge *et al.*, 2011; Eckley *et al.*, 2013; McMartin *et al.*, 2013). However, it is clear from Figure 8.13 that the 30 cm bulking of the collected lakes sediments obliterates this trend. Hence, this study's data are more useful for discerning large-scale sediment THg patterns rather than back-tracing anthropogenic contributions of bulk sediment Hg to local sources.

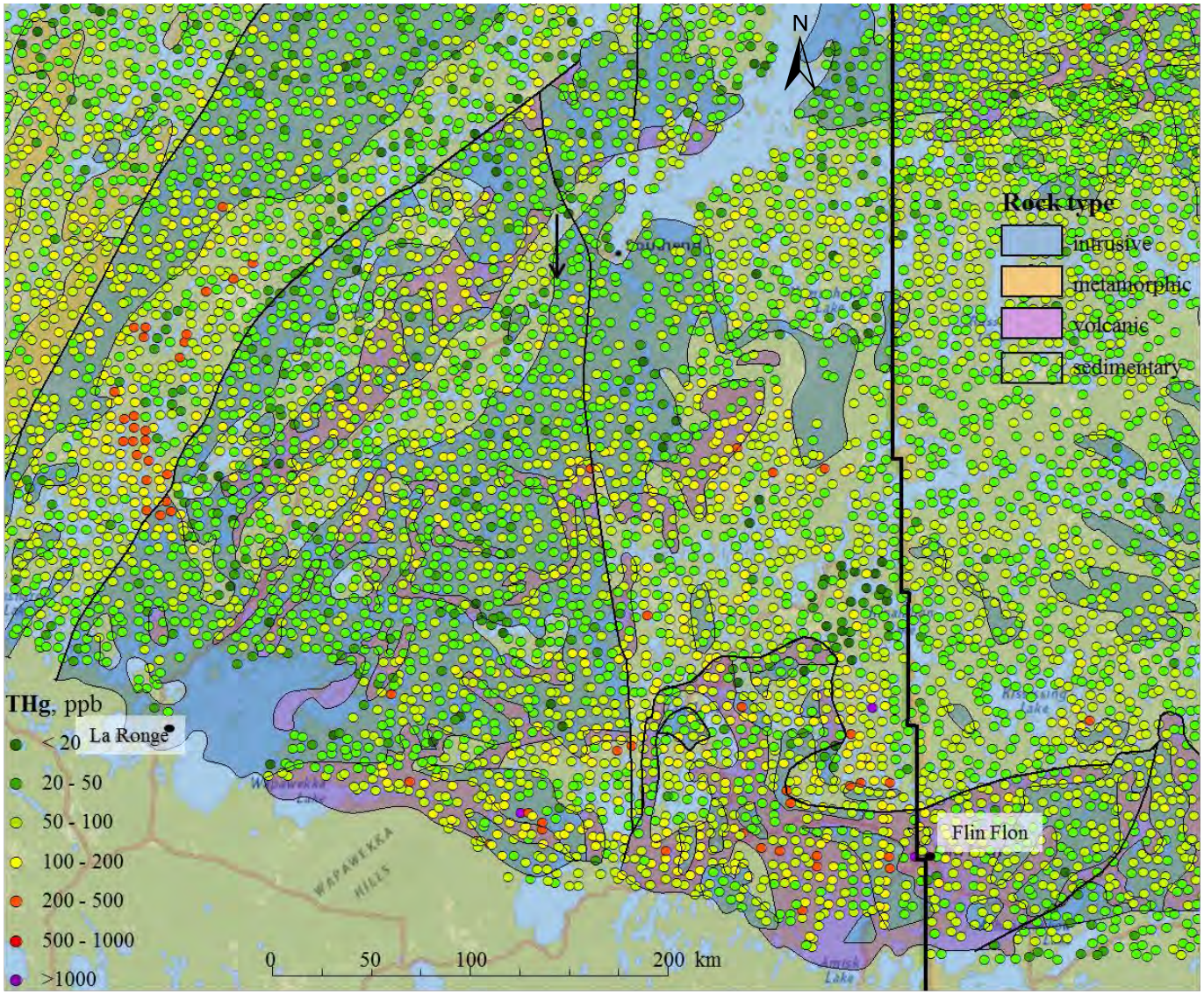

Figure 8.13 Stream sediment THg (ppb) from low (green) to high (purple) across the La Ronge to Flin-Flon area in northern SK and MB. Background: bedrock type and faults. Thick black line: provincial border.

Bathurst Island, NU - Bathurst Island is part of the Arctic Cordilleran Range. Most of the island is barren, only briefly sun-exposed during short summers, and partially to fully covered by snow and ice during long winters. The area is subject to high and annually recurring atmospheric Hg deposition episodes, but much of the deposited Hg leaves the area again prior to and during the time of snowmelt on account of photochemical Hg^{2+} reductions (Steffen *et al.*, 2008). The extent of rock weathering and erosion, and sediment production is low. Sediments THg levels are, on average, the lowest among the sediment sampling zones (Figure 8.14). Even at these low levels, there is a significant dependence of THg on sediment LOI, Co and Zn (Table 6.2). Sediment LOI would mostly be derived from tundra vegetation along valleys, from lichens that cover rocks, and from aquatic sources, especially algae.

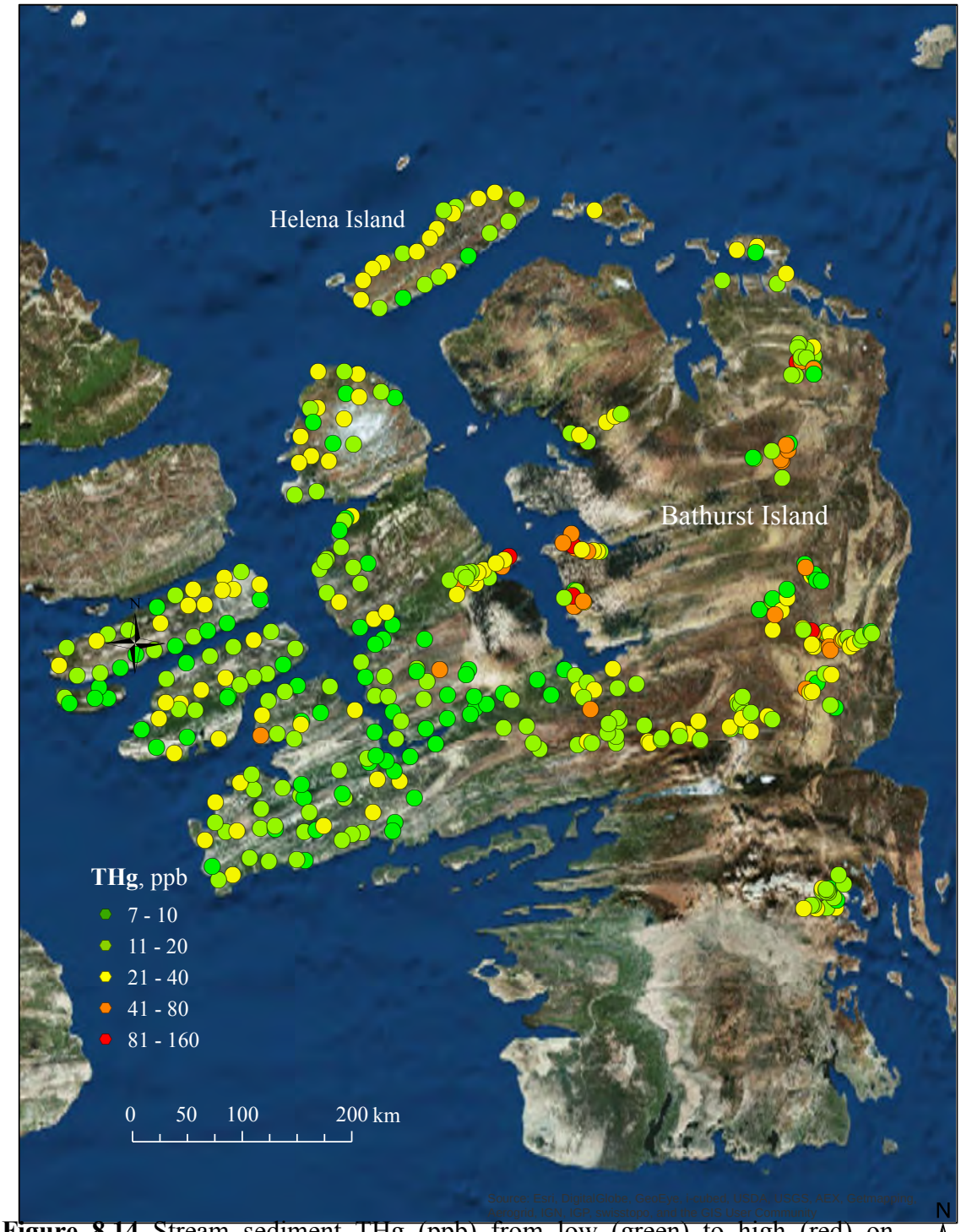

Figure 8.14 Stream sediment THg (ppb) from low (green) to high (red) on Bathurst Island, NU. Background: satellite image, sedimentary bedrock.

Great Bear Lake, NWT - The lake survey area in northeast of the Great Bear Lake is underlain by Precambrian sedimentary and metamorphic rocks interspersed by igneous intrusions, dikes and sills. Geochemical exploration and mining activities in this area focused on procuring nuclear fission materials since the 1940s. Other studies have also found that THg in Great Bear Lake sediments correlates with other heavy metals including U, and these correlations are amplified in Great Bear Lake estuaries downstream from mining locations (Moore and Sutherland, 1981; Lockhart *et al.*, 1998).

In this sampling zone, sediment THg varies from 10 to 400 ppb (Figure 8.15). Large, shallow, and clear lakes tend to have low sediment THg, while small, deep, turbid, and organically-enriched lakes tend to have high sediment THg. A regression analysis of the data from the Great Bear Lake survey area (Table 6.2) reveals that THg correlates positively with (i) LOI, (ii) Cu, and (iii) lake depth, but correlates negatively with lake size ($R^2 = 0.46$).

The highly significant Cu and LOI regression coefficients for THg imply strong geogenic as well as atmosphere-vegetation mediated Hg contributions, respectively. The latter contributions varied from one lake watershed to another, ranging from well vegetated (high LOI, high THg) to barren (low LOI, low THg). Lake size is important, resulting in lower THg and lower LOI with increasing size. Lake size itself is affected by the surrounding terrain, gradually increasing from high to low relief conditions. The amount of suspended material in the lake water also mattered, with LOI and THg increasing water turbidity, while turbidity decreases with increasing lake size.

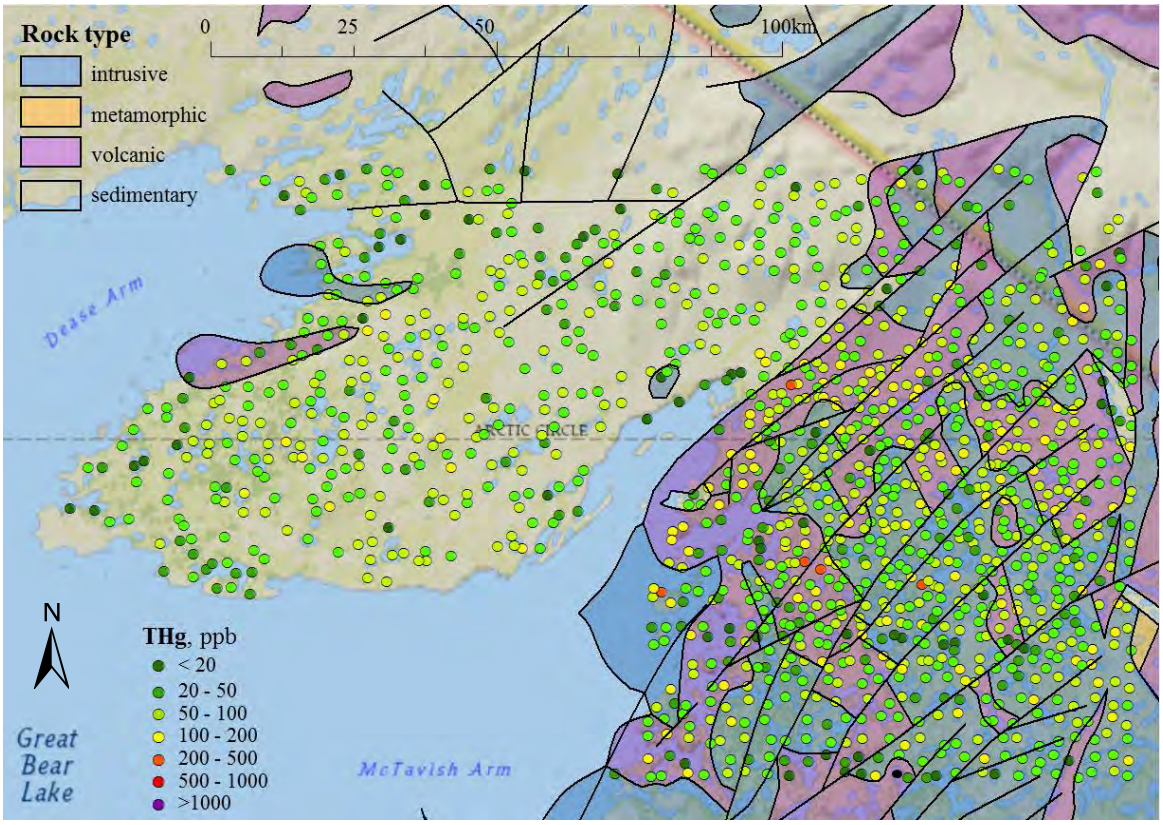

Figure 8.15 Stream sediment THg (ppb) from low (green) to high (purple) in northeast of the Great Bear Lake. Background: bedrock formations and faults.

Selwyn Basin, YT - The analysis of the THg containing GCS data for all of YT revealed the following (Nasr *et al.*, 2011):

- Mean sediment THg is slightly significantly higher in streams flowing through alluvial and organic soils than in streams flowing over bare rock and through outwash and till deposits; this trend is related to greater organic matter binding to sediment particles enriched with transition elements (Lu and Jaffe, 2001). As a result, dark coloured sediments had higher THg than light coloured sediments.
- Significantly elevated stream sediment THg occurs in swamps and active flood plains. This is in contrast to stream sediment THg from hilly and undulating terrain.

Sediments on peneplains (erosional surface-forming, nearly flat to broadly undulating plains) have the lowest mean THg.

- Terrains with trellis streams has significantly higher mean THg, on account of freshly exposed rock surfaces along steep ridges and stream channels. Sediments sampled from streams with basinal and herringbone flow patterns have lower THg.
- Sediment THg as well as Cd and Ag decrease with increasing stream order, presumably due to a gradual dilution of the trace element content in sediments with increasing distances from upland metallogenic sources and diluting contributions from other converging drainage basins.
- Sediment THg is lower in fast flowing streams because fine-grain sized and therefore more easily transported particles have higher metal content than coarse-grained particles (Table 7.2; Brandvold and McLemore, 1998).
- Upland to lowland stream organic matter transference and settling decreases from small to large stream orders due to decreasing litter input across the widening flow channels, and increasing Hg volatilization from sediments that accumulate in shallow streams (Byrnea et al., 2009).
- Including $\log_{10}$ values of metals other than Cu, Cd and Zn as additional independent variables further improved the regression results for $\log^{10}$THg but without increasing the resulting R^2 value substantially (details not shown).
- The stepwise backward regression analysis across YT indicates that bedrock type and lithology are significant variation contributors to sediment THg. This is mainly

due to the geospatial distribution and surface exposure of hydrothermal heavy metal mineralizations (Campbell, 2009; Goodfellow, 2007).

- The black shales of Mesozoic and Proterozoic bedrock formations (boxed area of Figure 8.16) were found to contribute significantly to sediment THg.
- Sediment Cd, Ag, and LOI were strongly associated with THg. THg decreases with increasing wet-area portion per drainage basin area of the sediments sampling locations. This is related to greater sediment, and therefore THg retention efficiency, as streams meander through wet-areas and wetlands of the sediment drainage basins.

The Selwyn Basin that crosses through YT from mid-west to northeast (Figure A1.2) contains high sediment THg and other heavy metals in the stream sediments (Figures 4.1, 4.2, 8.16). This is primarily due to the surface exposures of clastic Cambrian-Permian black shale formations. This widespread heavy metal bedrock anomaly has been attributed to the dispersal and settling of submarine volcanic plumes during the Precambrian-Devonian age. The Selwyn Basin was filled at this time with carbonate rich ocean water. Since then, this basin experienced repeated tectonic uplift and volcanic action, forming its mountainous terrain and geospatially scattered S mineralizations (Goodfellow, 2007; Yukon Government, 2014). Peaks and ridge tops are barren, while valleys are forest covered, thereby enriching the stream sediment with organic matter up to an LOI content of approximately 20 %. Gradual Hg evasion from barren black shales can be significant (Schroeder *et al,* 2005). Sediment THg is low downstream from the higher peaks of the granitoid plutons within this area (Garrett, 1974).

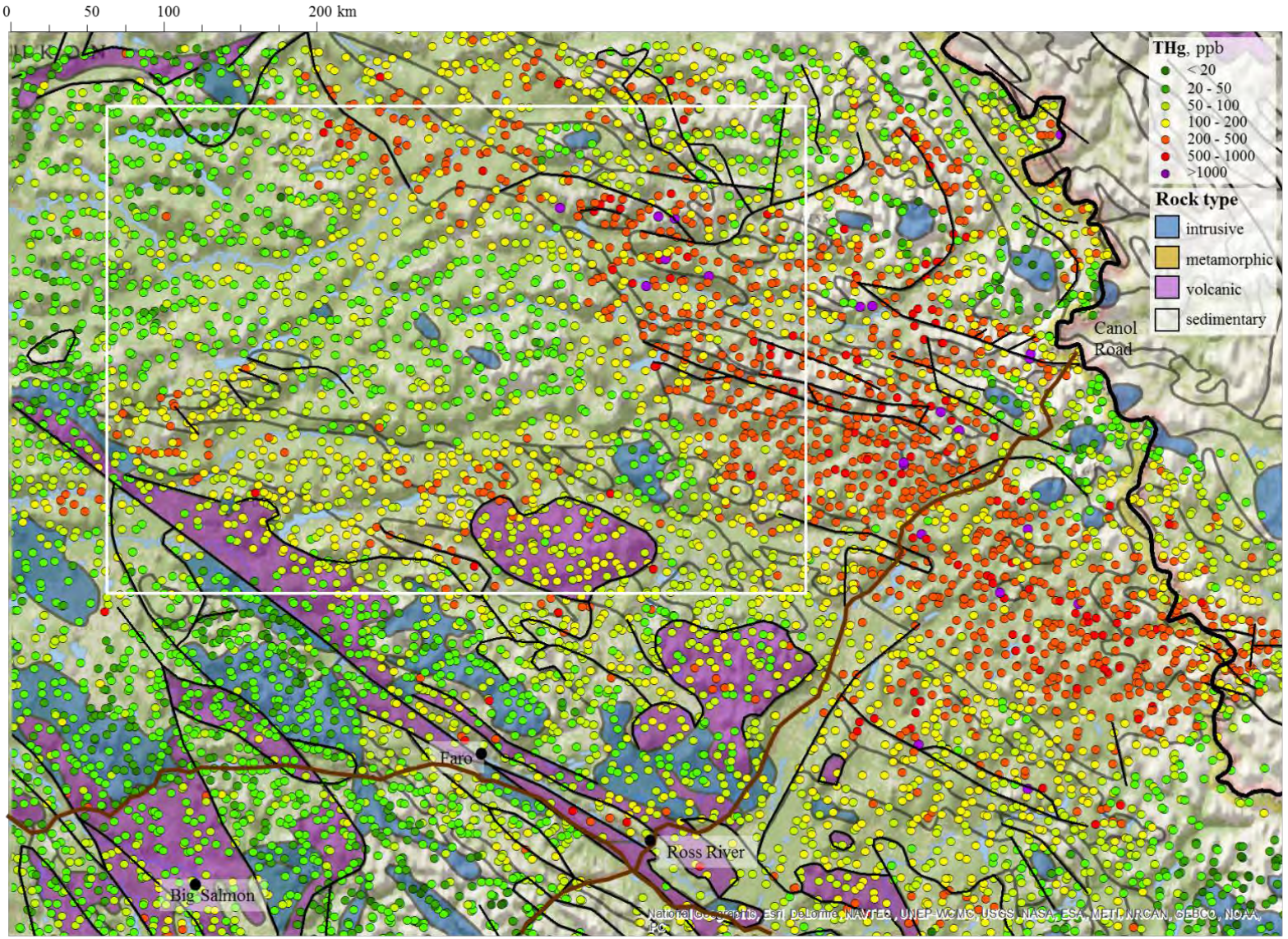

Figure 8.16 Stream sediment THg (ppb) from low (green) to high (purple) of central-east YT. Background: bedrock type and faults. Thick black line: YT-NWT border. White box: area used for basin geospatial analysis (Chapter 9).

BC - Stream sediments with THg > 1000 ppb occur in BC as follows: (i) on Vancouver Island (northwest to northwest, (ii) in the middle east section near Courtenay), (iii) on the mainland around Gold Bridge northwest of Lillooet, (iv) around Pinchi Lake (centre of past Hg mining activities northwest of Fort St. James), (v) west and northwest of Prince George, and (vi) on the Atlin Range in northwestern area (Figure 8.17). The higher values for sediment THg are associated with Triassic, Jurassic or Cretaceous mafic to ultramafic bedrock formations. Also of note are the fairly consistent sediment THg levels of approximately 100 to 200 ppb of the sediments of the sedimentary Skeena Range. In detail, sediment THg varies as follows:

- The THg levels of the stream sediments downslope from the alpine and ice-covered are consistently low at < 20 ppb.
- In the forest covered areas, stream sediment THg varies from approximately 50 to 500 ppb, and is higher on Vancouver Island than along the mainland coast.
- Stream sediment THg of the forest areas immediately north and east of Vancouver Island are as low as elsewhere along the mainland coast, thereby suggesting that the deposition of upwind urban Hg emissions is (i) generally low, and/or (ii) streambed scouring due to frequent high precipitation events disallows the gradual accumulation of Hg in sediments.
- Glacial drift moved Hg containing sediments away from their primary Hg source locations (Stevenson, 1940).

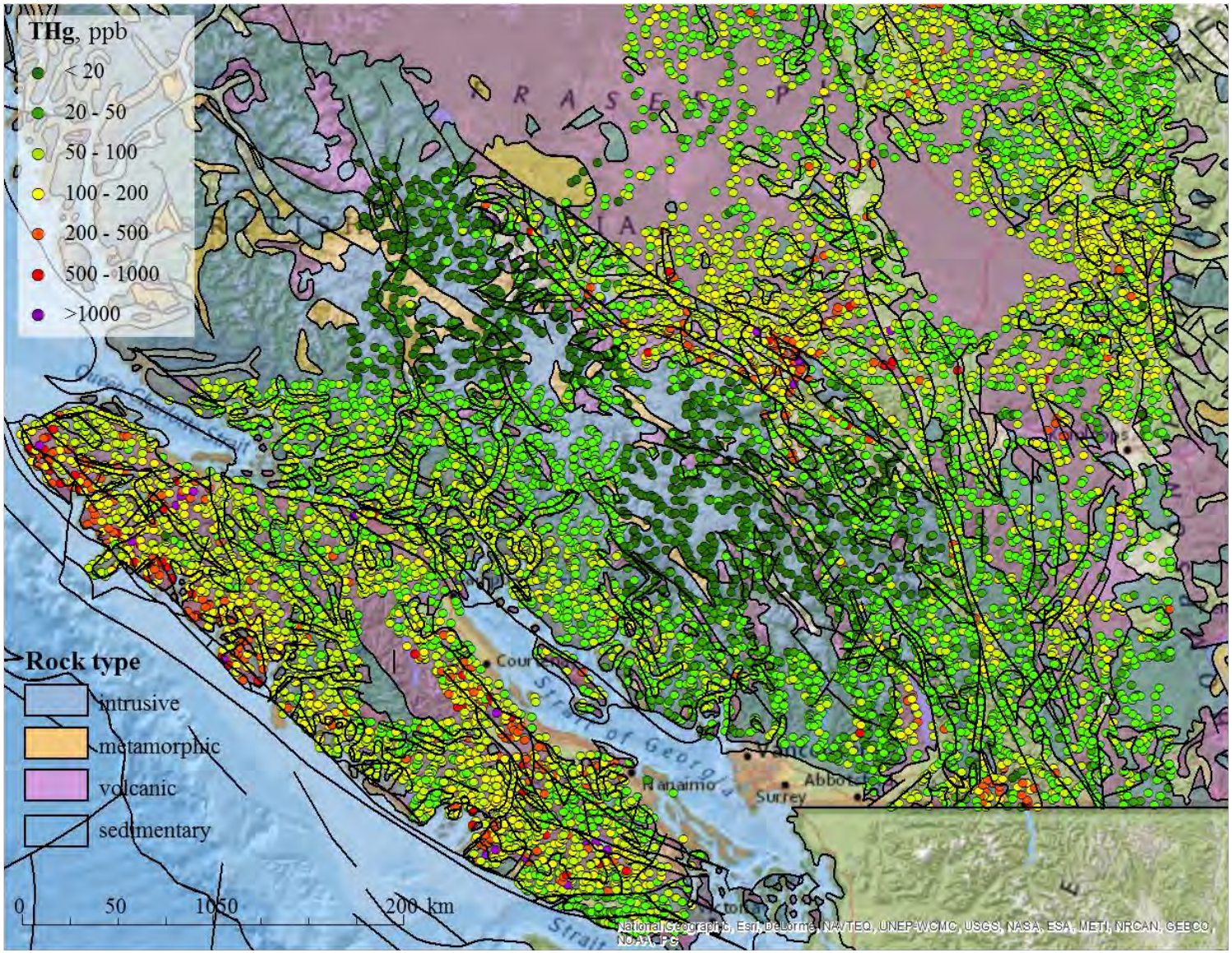

Figure 8.17 Stream sediment THg (ppb) from low (green) to high (purple) in northwestern BC. Background: bedrock type and faults.

- In some areas, stream sediment THg increases towards 2,000 ppb and higher, with some of the higher values associated with past and present mining locations. However, not all areas with major mining activities are part of the survey area database, notably the Myra Falls area west of the southern tip of Buttle Lake on Vancouver Island.

Conclusions

High sediment THg values generally occur in areas where geological processes have brought heavy metal deposits to the surface. Some of these processes refer to orogenic extrusion of magmatic rocks and uplifting of black shales, as is the case for the areas in BC and QC, and YT, respectively. Uplifting of intrusive rocks also bring heavy mineral deposits to the surface, as is the case for northern Gaspé (McGarrigle Mountains in Appalaches B), QC. Across the southern NS mainland, extensive ore deposits along fault/sheer zones (e.g. Tobeatic sheer zone) and between the rock formations of the Meguma terrane are additional significant Hg sources (Figure A1.3; Daughney *et al.*, 2005).

High sediment THg values occur on the volcanic belt formations east of the the James Bay region in northern QC (Opatica), the central mineral belt of Labrador (east of Snegamook Lake area), and the Labrador Trough at Schefferville, Labrador. Heavy meteor impacts may force magmatic flows to the surface as is sporadically the case around the heavily mined area of the Sudbury impact crater in ON. The presence of high subterranean heat and related shear strains may cause magmatic and geothermal outflows into metamorphosing bedrock, as occurred in the Témiscamingue area, QC. Faulting and

hydrothermal fluid along faults may bring heavy metals to the surface as well, and most notably so along the southern part of the Labrador Trough (QC), the Cobequid fault of northern NS (Figure A1.3) and the Pinchi Lake fault in BC (Paterson, 1977).

While high THg values in sediments, soils and till can be used as an indicator to locate heavy metal deposits in the sediment drainage basins. Once such locations are mined, sediment THg may increase further once Hg containing mine tailings settle in downstream streams and lakes. For upslope non-magmatic and non-faulted intrusive bedrock formations, sediment THg is low to very low. This is also the case for sedimentary bedrock formations. Exceptions refer to black shale formations (e.g. Selwyn basin, YT), and coal and oil bearing seams in, e.g. AB, SK, NB, and NS. Otherwise, sediment THg is generally low downstream from sedimentary bedrock formations, and where the sedimentary rocks are impacted by uplift, volcanic activities, and large meteor collisions.

Chapter 9 Sediment THg versus Upslope Wet-Area Coverage

Introduction

This chapter demonstrates how increasing wet–area plus water surfaces (denoted as A_W) per basin area (denoted as A_B) affect sediment THg numerically. It was hypothesized that A_W/A_B affects sediment THg negatively because of:

- increasing sediment retention in poorly drained areas,
- progressive Hg volatilization as water–carried Hg remains near the surface and is therefore subject to photochemical reduction processes (Nriagu, 1994), and
- progressive intermingling of the Hg containing particles with increasing amount of organic matter derived from wetland and aqueous vegetation. The latter dilutes the mineral portion of sediment THg (Chapter 6).

The sediment $\log_{10}$THg versus A_W/A_B analysis involved the nine cross–Canada case studies outlined in Chapter 3, with sediment sample sizes varying from 351 to 2,936. This analysis also involved the geospatial delineation of 12,655 upslope basin areas and their combined wet plus water areas (Table 1; Chapter 3). The regression analysis involved stream and lake sediment THg as dependent variable, and A_W/A_B as independent variable.

Results

The sediment THg versus A_W/AB plots show a negative trend with increasing A_W/A_B by case study (Figure 9.1). Notable exceptions are the three NS case studies, and the case study for Bathurst Island, NU. Table 9.1 provides a basic statistics summary for sediment $\log_{10}$THg (ppb) and A_W/A_B, and the best-fit regression results and the associated R^2 values for $\log_{10}$THg versus $0 < A_W/A_B < 0.4$, by study area and by medium type (stream, lake).

The A_W/A_B coefficients are - apart from the above exceptions - consistently negative, thereby affirming the hypothesized trend of decreasing sediment THg with wet-area coverage. This is further demonstrated by plotting the mean $\log_{10}$THg values per 0.025 A_W/A_B class against A_W/A_B in Figure 9.2. Here, the sharpest declined can be noted for Selwyn Basin, YT (Coeff. = -1.87, $R^2 = 0.884$), followed by Grenville A, QC (stream coeff. = -0.68, $R^2 = 0.783$) and Opatica, QC (lake, Coeff. = -0.56, $R^2 = 0.631$), while the overall trends for the NS and NU case studies remain demonstratively insignificant.

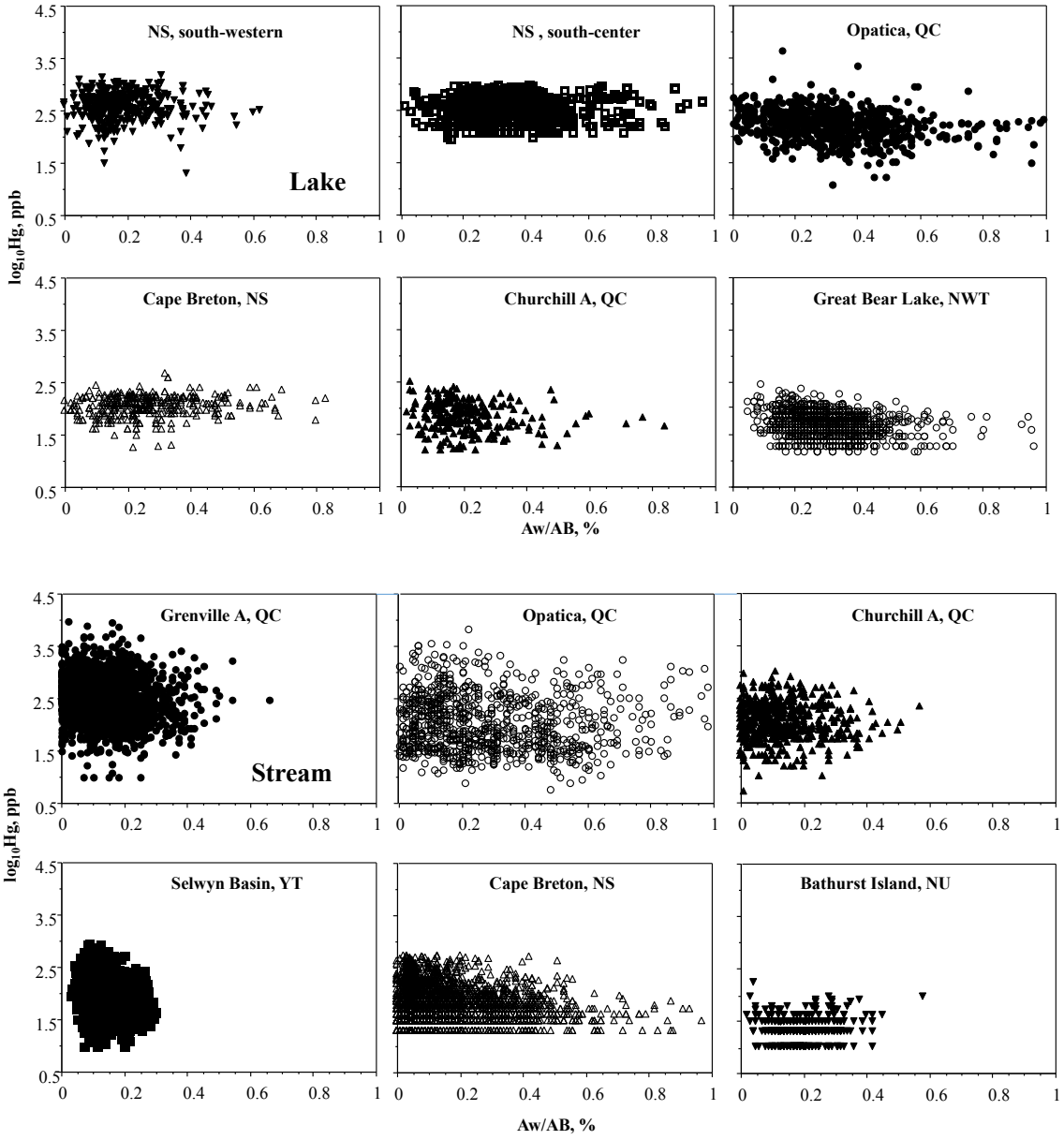

Figure 9.1 Scatterplots sediment $\log_{10}$THg (ppb) versus the ratio of area of wet-area to total area of basin (A_W/A_B), by study location. Top: lakes. Bottom: streams.

Table 9.1 Sediment log_{10}THg (ppb), ratio of area of wet-area to total area of sediment basin (A_W/A_B), and best-fit regression results for mean log_{10}THg versus $0 < A_W/A_B < 0.4$, by study location and medium type (stream, lake).

Location	Medium	Sediment log_{10}THg, ppb					A_W/A_B*					Regression summary**		
		n	Mean	Min.	Max.	Std. Dev.***	n	Mean	Min.	Max.	Std. Dev.	Intercept	Coeff.***	R^2
NS, south-west (16)	Lake	431	**2.55**	1.0	3.2	0.30	431	**0.19**	0.0	0.6	0.10	2.53	0.15	0.095
NS, south-center (16)		913	**2.36**	1.0	3.0	0.49	911	**0.33**	0.0	1.0	0.15	2.57	-0.03	0.004
Opatica, QC (27)		690	**2.23**	1.1	3.6	0.29	690	**0.33**	0.0	1.0	0.18	2.40	-0.56	0.631
Cape Breton, NS (17)		351	**2.04**	1.2	2.7	0.20	351	**0.28**	0.0	1.0	0.17	2.00	0.14	0.104
Churchill A, QC (30)		252	**1.81**	0.7	2.5	0.31	252	**0.22**	0.0	0.8	0.13	1.93	-0.51	0.403
Great Bear Lake, NWT (5)		1,081	**1.67**	1.0	2.5	0.28	1,081	**0.32**	0.0	1.0	0.14	1.79	-0.34	0.350
Grenville A, QC (22)	Stream	2,936	**2.52**	1.0	4.0	0.40	2,936	**0.14**	0.0	0.7	0.09	2.61	-0.68	0.783
Opatica, QC (27)		881	**2.05**	0.8	3.8	0.54	881	**0.28**	0.0	1.0	0.22	2.22	-0.61	0.496
Churchill A , QC (30)		510	**2.02**	0.7	3.0	0.37	510	**0.13**	0.0	0.6	0.11	1.96	-0.45	0.344
Selwyn Basin, YT (3)		1,581	**1.95**	1.0	3.0	0.36	1,581	**0.13**	0.0	0.3	0.04	2.21	-1.87	0.884
Cape Breton, NS (17)		2,627	**1.81**	1.0	2.7	0.33	2,627	**0.17**	0.0	1.0	0.17	1.89	-0.46	0.599
Bathurst Island, NU (4)		402	**1.34**	1.0	2.2	0.23	402	**0.19**	0.0	0.6	0.08	1.38	-0.20	0.076

*Area of basin (A_B, ha) devided by area of wet-area of each basin (A_W, ha); A_W referred to DTW < 0.5 m, including surface water. **Regression summary for log_{10}THg (ppb) versus A_W/A_B class (Figure 9.2). *** Standard deviation (Std. Dev.); regression coefficient (coeff.).

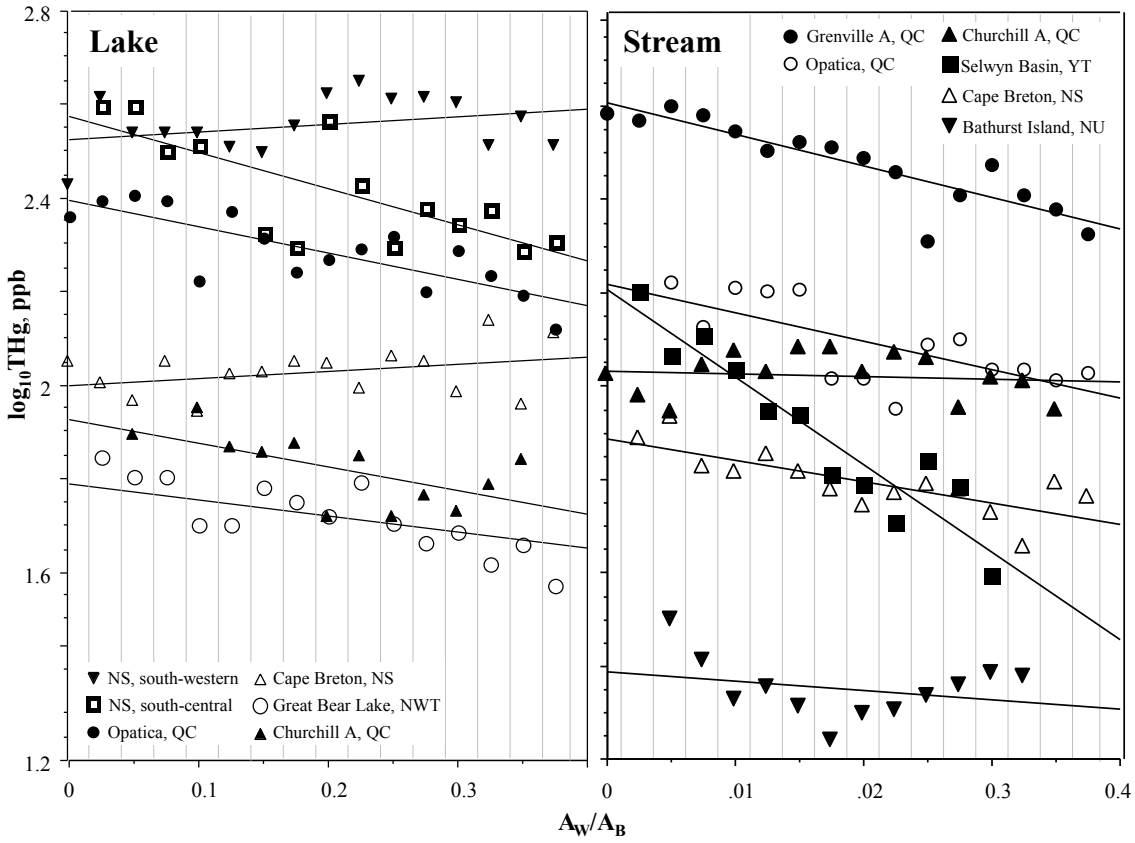

Figure 9.2 Scatterplots of mean stream and lake sediment log_{10}THg (ppb) per each 0.025 class of A_W/A_B = 0 to 0.4, by study location. A_W referred to DTW < 0.5 m, including surface water.

Discussion and Conclusions

Analyzing the log_{10}THg versus A_W/A_B trend lines revealed that sediment THg decreases with increasing basin wetness above the sediment sampling locations in most of the selected case studies. The streams of Selwyn Basin, YT, have the sharpest decline of log_{10}THg with increasing wet-area portion per basin. This is due to (i) the extensive geogenic Hg source contributions on the uplands above the tree line and (ii) increasing dense vegetation cover with downslope valley elevations. The latter refers to the surface-

exposed black shale formations especially in the steep high altitude terrain of the Selwyn basin (Chapter 8).

The release of Hg from uplands by way of weathering, soil erosion, and subsequent stream transport (Driscoll *et al.*, 1998; Scherbatskoy *et al.*, 1998; Shanley *et al.*, 2005; Schuster *et al.*, 2008) has a dominant influence on the downslope THg variations in stream and lake sediments (Rasmussen *et al.*, 1998a, b; Daughney *et al.*, 2005). This trend is also noticeable in the Figure 9.3 illustration for the YT study area, and this is similarly realized for the Grenville A, Churchill A, Opatica, and the Great Bear Lake study areas in Figure 9.2. Here THg decreases strongly with increasing A_W/A_B values. On Bathurst Island, NU, the geogenic Hg source contributions to stream sediment THg would be low due to low weathering rates, and long periods of seasonal frost coupled with extensive snow and ice-cover (Appendix 3). Figure 9.4 shows how the individual sediment THg sampling locations are situated below their upslope basins on Helena Island north of Bathurst Island during partial ice– and snow-cover conditions.

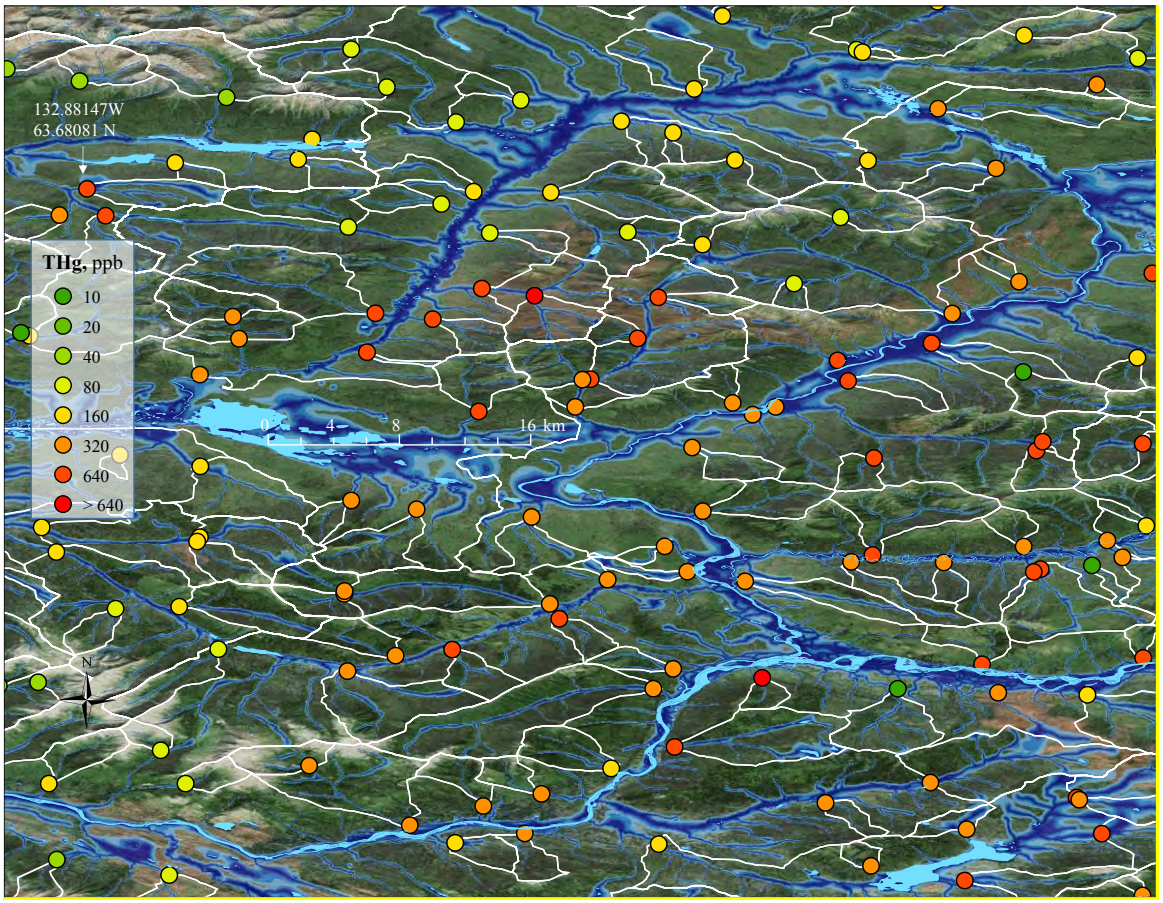

Figure 9.3 Stream sediment DEM derived basin borders (white lines) and THg (ppb; low: green to high: red points) for an area, part of NTS tile 105n in the central-east study location of YT. Background: Satellite image, wet-areas (shaded dark blue), and lakes (light blue).

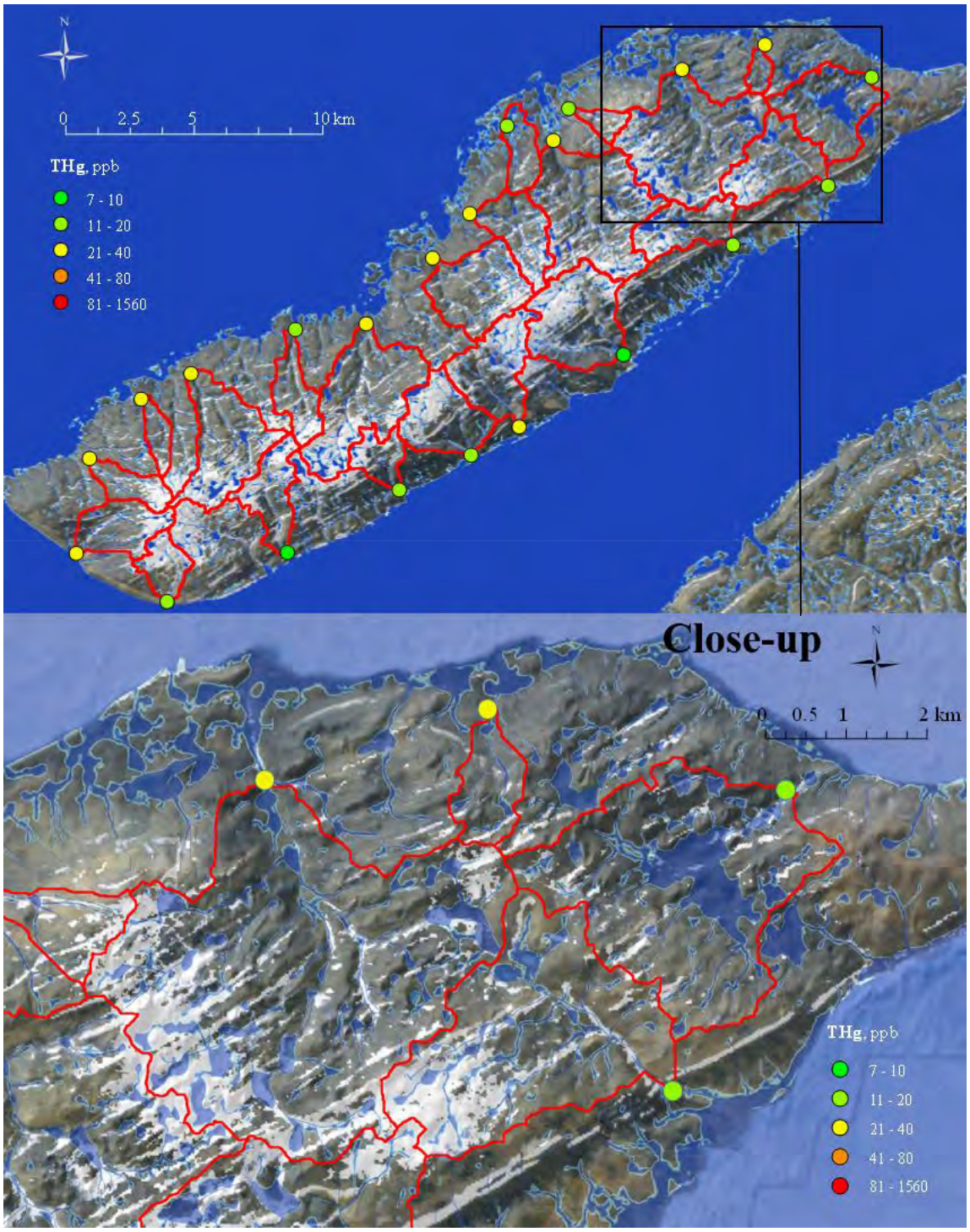

Figure 9.4 Helena Island, NU. Top: stream sediment DEM derived basin borders (red lines) and THg (ppb; low: green to high: red points). Background national DEM (300 m resolution), satellite image with ice-covered areas (white), and wet areas (shaded blue). Bottom: Close-up.

For the two NS mainland case studies, sediment THg is not related to A_W/A_B as is the case at the other study locations (excluding Bathurst Island, NU). In addition, the sediment THg values for NS are only weakly related to sediment LOI (Chapters 6, 7), even though total Hg concentrations in brown NS surface waters are strongly and positively correlated with total organic carbon (DOC; Meng *et al.*,2005; Clair *et al.*, 2008).

The exceptionally high sediment THg throughout NS are due to (i) high Hg concentrations within several bedrock formations across NS (Chapter 8), and (ii) the widespread Hg-contaminating Au-prospecting activities in NS of the past (Figure 9.5). These two factors would, by themselves and in principle, obscure the generally significant relationship between THg and A_W/A_B.

Sediments downstream from NS areas with exposed or thinly covered till bedrock have mean THg values of approximately 250 ppb. By dominant bedrock formations (THg values ≥ 1500 ppb excluded), downstream mean sediment THg varies as follows: Au- and S-bearing (358 ppb) > metamorphic (282 ppb) > intrusive (275 ppb) > volcanics (135 ppb) > clastic and organic (92 ppb) > evaporates (69 ppb) > unconsolidated glaciofluvial materials (20 ppb). For the Cape Breton case study, mean sediment THg is lower than for the mainland locations, and varies as follow (THg ≥ 1500 ppb excluded): clastic and organic (stream:117 ppb; lake:119 ppb) > intrusive (stream: 80 ppb, lake: 120 ppb).

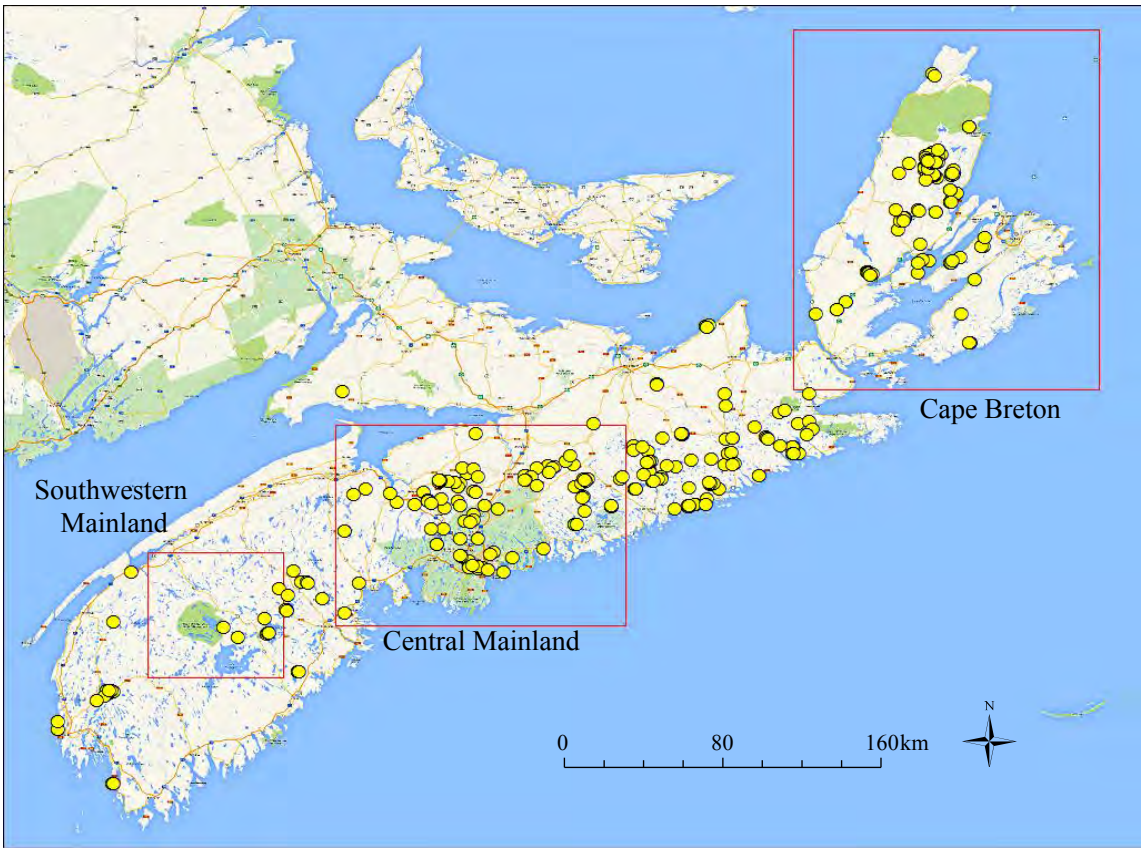

Figure 9.5 NS study locations (red boxes) and gold occurrence locations (yellow points). Data adapted from Province of Nova Scotia-Department of Natural Resources, 2013.

Further work could be done as follows:

- expanding the analysis of this chapter across the Canada-wide sediment surveys;
- using higher resolution DEMs for the wet-area and open-water delineation process;
- combining the wet-area delineations per basin with surface image analysis;
- gradual expansion of the geochemical surveys into as yet surveyed areas;
- collating the geochemical survey work with detailed profile studies for lake sediments;
- including vegetation cover extent and type per basin.

Chapter 10 Summary

Original Contribution

This study provided results aimed at a geospatial representation of how stream and lake sediment THg variations are affected by external and internal factors across Canada. This representation was achieved through compiling and analyzing the Canada-wide open files adapted from GSC, QC, and NS data sources (Chapter 4) within the context of other data layers pertaining to geology, topography, climate, and atmospheric Hg deposition (Chapters 5, 6, 7, 8, 9, and Appendices 2, 3, 4). The geospatial summations so obtained by province/territory, survey zone, and NTS tiles, generated simple yet numerically comprehensive models and maps that show how sediment THg varies geographically and climatically across Canada (Chapters 5, 6, 7, 9). The additional variability due to regional/local variations in topography (Chapters 4, 9), geology (Chapters 7, 8), ecological zonation, and terrestrial land cover (Appendices 2, 3) are also addressed by province/territory, survey zone, and NTS tile (Chapter 4-9, Appendices 2, 3, 4).

Matters that refer sediment THg to other topics such as (i) the concentrations of other heavy metals in sediments such as Cu, and (ii) the extent to which the lake sediment THg is related to total THg in fish are presented in Appendix 4 and 5. The following items summarize the analysis-, model-, and research-original realizations:

- Stream and lake sediment THg varies individually across Canada by four orders of magnitude, up to 36,000 ppb (Chapter 4). The majority of these values occur between 20 to 500 ppb THg range. Across the surveyed zones, mean sediment THg is generally higher in upland than in lowland streams and lakes. Mean lake

sediment THg is higher than in streams but is also less varied. These effects become more significant with increasing sample size per survey zone.

- Sediment THg varies by climate-geographic region and by local basin conditions as follows: sediment THg of Arctic Cordillera and southern Arctic ≈ alpine areas with ice-covered caps < Boreal Shield and Atlantic Maritimes < Taiga Shield < Hudson Bay (Chapter 4). Within these zones, sediment THg of snow/ice < frost-worked soil (sparse vegetation) < non-vegetated < wetland < graminoids Tundra < broadleaf < shrub Tundra < conifer and mixedwood (Chapter 4; Appendices 2, 3).

- Within the geography and climate context, there is a strong cross-regional link between sediment THg and atmospheric Hg deposition, with lake sediment THg being more significantly affected than stream sediment THg (Chapters 5, 6). In this, the loading of atmospherically-derived Hg increases as sediment organic matter increases, and this trend is substantially stronger for lake than for stream sediments, as quantified, modelled and mapped in Chapter 6.

- The wide THg variations are generally due to geogenic and anthropogenic clusters of very low and very high THg occurrences as elaborated in Chapter 8. High values occur in areas of past volcanic activities, e.g. (Snegamook Lake area, Labrador), tectonic uplift of black shales (e.g. the Selwyn Basin in YT), along faults (esp. Pinchi Lake, BC; the Cobequid Fault in NS), in troughs (Labrador Trough, Schefferville, QC), and around granitic and gneissic intrusions (Maguma Formation, northwestern NS; MacGarrigle Mountains, QC).

- Sediment THg are particularly high when upslope bedrock formations containing heavy metal deposits are surface exposed. Non-surface exposure keeps stream and lake sediment THg low. For example, THg is generally low in the erosion-filled Sudbury Crater, but high values occur in the surrounding rock-exposed areas. The area east of Temiskaming has many high THg values presumably due to frequent surface exposure of magmatic extrusions and hydrothermal fluid deposits within intrusive or metamorphosed intrusive bedrock formations (granites and gneiss; Chapter 8). Elsewhere in this area, stream and lake sediments have low THg values.

- Sediment THg values can also be elevated downstream from granite, gneiss and diorite formations with high biotite content and hence higher heavy metal contents including Hg. This appears to be the case across the Maguma Terrane in southern NS.

- LOI (or S if included in the data) is generally the strongest contributor to the sediment THg variations, followed by other sediment elements such as Cu and Zn (Chapter 7). The relationship between sediment THg and other sediment elements, however, varies from location to location, as summarized by province/territory, geological region and selected NTS tile areas.

- Lake sediment THg increases with increasing lake depth and decreasing lake area. Stream sediment THg would increase with increasing stream depth and decreasing flow rate, stream order, and width.

- Increasing the wet and open water area portions per upslope basin tends to decrease the downstream sediment THg, especially in swamp-dominated basins (Chapter 9; Appendix 3).
- While the organic matter contributions to THg stream and lake sediments generally increase from areas with low to high annual precipitation rate, this proves to be not the case for Cu (Appendix 4).
- Sediment THg accounts for approximately 40 % of the FIDMAC standardized THg variations in yellow perch (Appendix 5). Whether or not this association is causal remains to be seen since (i) Hg in fish is more directly related to the bio accumulation transfer of methyl Hg, (ii) the THg differences by climate region may not directly translate into corresponding climate change expectations, and (iii) the sediment sampling protocol addressed bulked Hg accumulations and concentrations of at least 100 years, while the fish surveys started in 1970.

Since the surveyed sediment sampling locations are generally widely spaced, the data cannot be used to discern small-scale variations in sediment THg downslope and downwind from mining, smelting and other Hg emitting/releasing activities (Feng *et al.*, 2010; Lockhart, 2003). For that purpose, sampling grids need to be smaller than the sediment-sampling grid. By intensifying the sampling grid Mills *et al. (*2009) were able to detect post-industrial THg enrichments in ON lake sediments (n = 171) on account of continued expansion and intensification of local Hg emissions and Hg-affecting landuse practices across southern ON.

Chapter 11 Knowledge Gaps and Recommendations for Further Research

While progress has been made in compiling and mapping THg across Canada, more work is required to integrate this progress into the wider Hg accumulation context as it pertains to estimating the total amounts of Hg locked up sediments, in wetlands, and upland vegetation and soils. Little information about this is currently available from local to regional and national scales. In this regard, the research of this study could be further expanded as follows:

- **Examining elements other than Hg in the sediment matrix -** Elements such as Fe, Mn and Cu are essentially non-volatile elements. Their sediment concentrations should therefore not change on account of climatic factors, or increase on account of long-range atmospheric deposition processes; however, sediment concentrations of elements that are or have been widely used as fuel additives, such as Pb, may also increase due to atmospheric deposition processes.

- **Relating fish Hg to sediment THg and other factors -** There has been much interest in knowing how fish Hg concentration is related to environmental factors such as atmospheric Hg deposition, local geogenic/anthropogenic Hg sources, and climate variations. All of this needs to be further researched, modelled and mapped within the context of prominent climate change expectation and landuse change across Canada, and across northern Canada in particular.

- **Building process models to determine Hg accumulation rates in streams and lakes -** From an ecological perspective, it is important to infer how much Hg enters

and leaves streams and lakes through various processes. Including atmospheric deposition and sequestration, upslope sediment transfer through soil weathering and erosion, the extent of organic matter binding of Hg in dissolved and particulate form, and the extent of Hg volatilization and re-processing during sediment transfer and after settling.

- **Special studies dealing with mining activities and processes -** Past and current mining activities generate downstream sediments with high THg. In this regard, watershed-specific studies are particularly useful to determine how much and how far Hg spreads downstream from past and present mining operations. Doing this involves building geospatial models that quantify sediment yields (i) from exposed soil surfaces per watershed in accordance with universal soil loss expectations, and (ii) from streambeds under periods of high stream discharge.

- **Geochemical prospecting** - The release of upstream heavy metal deposits can be further evaluated at the watershed level through fine-scale geospatial analysis based on DEM-generated watershed, flow-channel, and wet-areas mapping.

The following questions are particularly pressing in terms of quantifying Hg pools for stream and lake sediments and their upland pools in vegetation and soils:

- How can the surveyed THg database be used to estimate the overall Hg contents (kg/ha) in sediments across Canada as accumulated in stream and lake bottoms?

- How could such a database be expanded by integration into regional forest inventory databases and soil surveys to inform about total Hg contents of forest biomass and soil organic matter pools?

- How do Hg concentration and pools associated with upland vegetation, soils and wetlands compare with Hg pools in streams and lake sediments?
- How does the amount of net atmospheric Hg deposition transference of Hg from uplands to streams and lakes compare with the amount of Hg that is already stored in vegetation, soils, and sediments?
- To what extent can the new high-resolution DEMs be used in combination with the Universal Soil Loss Equation be used to comprehensively assess sediment and Hg loading to lakes, rivers and streams downstream from disturbed as well as undisturbed areas?

It is recommended that the next steps in terms of modelling and mapping sediment THg across Canada should involve examining how (i) geological formations (see Chapter 8), (ii) watershed and stream and lake watershed morphologies (Chapter 9), and (iii) surface cover type referring ice, barrens, forests, wetlands, grasslands, and drainage conditions (Appendix 2, 3) all contribute to the sediment THg variations across Canada, at higher resolution. Doing so requires:

- A geochemical Hg analysis of existing GSC produced soil and till surveys with special emphasis of estimating the extent of soil weathering and erosion in the watershed areas above each sediment sampling location.
- A systematic investigation of anthropogenic contributions to stream and lake sediment Hg at past and present mining activities in their respective historical and watershed specific contexts, as referred to above.

- Further investigations to quantify the difference between short and long-range atmospheric transport and deposition of Hg (Rutter *et al.,* 2008). In this, the short-range context is not easily quantified due to (i) historical variations in terms of actual Hg emissions and (ii) case by case challenges in modelling the recapture of smoke stack released Hg and other pollutants (Bourque and Arp 1996).

References

Al T.A., Leybourne M.I., Maprani A.C., MacQuarrie K.T., Dalziel J.A., Fox D., Yeasts P.A. Effects of acid-sulfate weathering and cyanide-containing gold tailings on the transport and fate of mercury and other metals in Gossan Creek: Murray Brook mine, New Brunswick, Canada. Applied Geochemistry 2006; 21: 1969-1985.

Amyot M., Arp P., Blais J., Depew D., Dorn S., Emmerton C., Evans M., Gamberg M., (Klaus) Gantner N., Girard C., Graydon J., Kirk J., Lean D., Lehnherr I., Muir D., Nasr M., Poulain A., Power M., Rencz A., Roach P., Stern G., Swanson H. Freshwater Environment. In: Canadian arctic contaminants assessment report III. Mercury in Canada's North. Eds.: Chételat J., Braune B. Northern contaminant program. Indian and Northern Affairs Canada, Minister of Aboriginal Affairs and Northern Development 2012; 100-157. http://emrlibrary.gov.yk.ca/INAC_Mercury_Report.pdf.

Ashley R.P., Rytuba J.J. Mercury geochemistry of gold placer tailings, sediments, bedrock, and waters in the Lower Clear Creek Area, Shasta County, California - Report of Investigations, 2001-2003. Open-file report 2008-1122. U.S. Geological Survey, Reston, Virginia 2008; 65 p.

Aznar J.C., Richer-Lafleche M., Cluis D. Metal contamination in the lichen *Alectoria sarmentosa* near the copper smelter of Murdochville, Quebec. Environmental Pollution 2008; 156: 76-81.

Bagnatoa E., Aiuppaa A., Parelloa F., D'Alessandrob W., Allardc P., Calabresea S. Mercury concentration, speciation and budget in volcanic aquifers: Italy and Guadeloupe (Lesser Antilles). Journal of Volcanology and Geothermal Research 2009; 179: 96-106.

Barr, S.M., Raeside R.P. Tectono-stratigraphic terranes in Cape Breton Island. Nova Scotia: Implications for the configuration of terranes in the northern Appalachian Orogen, Geology 1989; 17: 822-825.

Barrow E., Maxwell, Barrie M., Gachon, P. Climate variability and change in Canada, past, present and future. ACSD Science Assessment Series No. 2. Meteorological Service of Canada, Environment Canada, Toronto, Ontario 2004; 114 p.

Bash J.O., Bresnahan P., Miller D.R. Dynamic surface interface exchanges of mercury: a review and compartmentalized modeling framework. Journal of Applied Meteorology and Climatology 2007; 46: 1606-1618.

Bash J.O., Miller D.R. A note on elevated total gaseous mercury concentrations downwind from an agriculture field during tilling. Science of the Total Environment 2007; 388: 379-388.

Bayer H.L. Geospatial Modelling Environment (GME) software (2001-2002). http://www.spatialecology.com/gme/.

Bengtsson G., Picado F. Mercury sorption to sediments: dependence on grain size, dissolved organic carbon, and suspended bacteria. Chemosphere 2008; 73: 526-531.

Bidleman T.F., Macdonald R.W., Stow J. Canadian arctic contaminants assessment report II, sources, occurrence, trends and pathways in the physical environment. Canadian Arctic Contaminants Assessment Report II - Physical Environment 2003; 332 p.

Birk D., Pilgrim, J., Zodrow, E. Trace element contents of coals and associated rocks of Sydney basin Nova Scotia. Open file 2090. Geological Survey of Canada, Sydney, Nova Scotia 1986; 260 p.

Boszke L., Kawalski, A., Glosifiska G. Szarek, R., Siepak, J. Environmental factors affecting mercury speciation in the bottom of sediments; an overview. Polish Journal of Environmental Studies 2003; 12: 5-13.

Bourque C.P., Arp P.A. Simulating sulfur dioxide plume dispersion and subsequent deposition downwind from a stationary point source: a model. Environ Pollution1996; 91: 363-380.

Brandvold L.A., McLemore V.T. A study of the analytical variation of sampling and analysis of stream-sediments from areas contaminated by mining and milling. Journal of Geochemical Exploration 1998; 64: 185-196.

Braune B., Chételat J., Amyot M., Brown T., Claydon M., Evans M., Fisk A., Gaden A., Girard C., Hare A., Kirk J., Lehnherr I., Letcher R., Loseto L., Macdonald R., Mann E., McMeans B., Muir D., O'Driscoll N., Poulain A.J., Reimer K., Stern G. Mercury in the marine environment of the Canadian Arctic: review of recent findings. Science of the Total Environment 2014. DOI: 10.1016/j.scitotenv.2014.05.133.

Broster B.E., Daigle A.E., Burtt G. Engineering properties of fine-grained estuarine sediments in the Saint John River Valley at Fredericton, New Brunswick, Canada, Atlantic Geology 2013; 49, 179-193.

Broster B.E., Dickson M.L., Parkhill M.A. Comparison of humus and till as prospecting material in areas of thick overburden and multiple ice-flow events: an example from northeastern New Brunswick. Journal of Geochemical Exploration 2009; 103, 115-132.

Bubb J.M., Williams T.P., Lester J.N. The Behaviour of mercury within a contaminated tidal river system. Water Science & Technology 1994; 28: 329-338.

Byrnea H.E., Borelloa A., Bonzongoa J.C., Mazyck D.W. Investigations of photochemical transformations of aqueous mercury: Implications for water effluent treatment technologies. Water Research 2009; 43: 4278-4284.

Caldwell C.A., Canavan C.M., Bloom N.S. Potential effects of forest fire and storm flow on total mercury and methylmercury in sediments of an arid-lands reservoir. Science of the Total Environment 2000; 260: 125-133.

Campbell H., Broster B.E., Parkhill M., Susak Y., Arp P.A. Glacial dispersal from the Mount Fransac north massive sulphide deposit, Bathurst Mining Camp, New Brunswick, Canada. In: Proceedings of the 24th international applied geochemistry symposium. Eds.: Lentz D., Thorne K.G., Beal K.L. The Association of Applied Geochemistry (AAG), Fredericton, New Brunswick, Canada 2009; 545-548.

Canuel R., Lucotte M., de Grosbois S.B. Mercury cycling and human health concerns in remote ecosystems in the Americas. Sapiens 2009; 2, 13 p.

Card K.D., Ciesielski A. Subdivisions of the Superior Province of the Canadian Shield (DNAG 1). Geoscience Canada 1986; 13:5-13.

Caron S., Lucotte M., Teisserenc R. Mercury transfer from watersheds to aquatic environments following the erosion of agrarian soils: A molecular biomarker approach. Canadian Journal of Soil Science 2008; 88: 801-811.

Chadwick S.P., Babiarz C.L., Hurley J.P., Armstrong D.E. Influences of iron, manganese, and dissolved organic carbon on the hypolimnetic cycling of amended mercury. Science of the Total Environment 2006; 368: 177-188.

Chen C.Y., Borsuk M.E., Bugge D.M., Hollweg T., Balcom P.H. Benthic and pelagic pathways of methylmercury bioaccumulation in estuarine food webs of the Northeast United States. PLoS ONE 9: e89305 2014. DOI:10.1371/journal.pone.0089305.

Chen C.Y., Stemberger R.S., Kamman N.C., Mayes B.M., Folt C.L. Patterns of Hg bioaccumulation and transfer in aquatic food webs across multi-lake studies in the northeast US. Ecotoxicology 2005; 14: 135-147.

Chételat J., Amyot M., Arp P., Blais J.M., Depew D., Emmerton C.A., Evans M., Gamberg M., Gantner N., Girard C., Graydon J., Kirk J., Lean D., Lehnherr I., Muir D., Nasr M., Poulain A.J., Power M., Roach P., Stern G., Swanson H., Van der Velden S. Mercury in freshwater ecosystems of the Canadian Arctic: Recent advances on its cycling and fate. Science of the Total Environment 2014. DOI: 10.1016/j.scitotenv.2014.05.151.

Ciesielski A. Geology of the eastern Superior Province, James Bay and Bienville subprovinces, Quebec. Open file 2398, 1-8. Geological Survey of Canada 1991.

Clair T.A., Dennis I.F., Vet R., Laudon H. Long-term trends in catchment organic carbon and nitrogen exports from three acidified catchments in Nova Scotia, Canada. Biogeochemistry 2008; 87: 83-97.

Cloutier M. Parc national d'Opémican project. Provisional master plan. Ministère du Développement durable, de l'Environnement et des Parcs Direction du patrimoine écologique et des parcs. Bibliothèque et Archives nationales du Québec 2012. http://www.mddelcc.gouv.qc.ca/parcs/opemican/plan-directeur-en.pdf.

Coker W.B., Kettles I.M., Shilts W.W. Comparison of mercury concentrations in Modern lake-sediments and glacial drift in the Canadian Shield in the region of Ottawa Kingston to Georgian Bay, Ontario, Canada. Water, Air, and Soil Pollution 1995; 80: 1025-1029.

Cook T.L., Bradley R.S. Stoner J S., Francus P. Five thousand years of sediment transfer in a high arctic watershed recorded in annually laminated sediments from Lower Murray Lake, Ellesmere Island, Nunavut, Canada. Journal of Paleolimnology 2008. DOI 10.1007/s10933-008-9252-0.

Corriveau M.C., Jamieson H.E., Parsons M.B., Hall G.E.M. Mineralogical characterization of arsenic in gold mine tailings from three sites in Nova Scotia. Geochemistry: Exploration, Environment, Analysis 2011; 11: 179-192.

Dai Z.H., Feng X-.B., Zhang C., Qui G.L., Shang L.H. Surface soil mercury translocation in Wanshan mercury mining area of Southwest China. Chinese Journal of Ecology 2012; 31: 2103-2111.

Daly C., Gibson W.P., Taylor G.H., Johnson G.L., Pasteris P. A knowledge-based approach to the statistical mapping of climate. Climate Research 2002; 22: 99-113.

Dastoor A.P., Larocque Y. Global circulation of atmospheric mercury: A modelling study. Atmospheric Environment 2004; 38: 147-161.

Dastoor A.P., Moran M. 2005 Global/Regional Atmospheric Heavy Metals Model (GRAHM2005) estimates of atmospheric mercury deposition rates at sites in northern Canada, unpublished data. Air Quality Research Division, Environment Canada 2010.

Dastoor A.P., Davignon D., Theys N., Van Rosendael M., Steffen A., Ariya P.A. Modelling dynamic exchange of gaseous elemental mercury at polar sunrise. Environmental Science & Technology 2008; 42: 5183-5188.

Dastoor A.P., Davignon D. Global mercury modelling at Environment Canada. In: mercury fate and transport in the global atmosphere. Eds.: Pirrone N., Mason R. Springer, New York 2009; 519-532.

Daughney C.J., Siciliano S.D., Rencz A.N., Lean D.R.S., Fortin D. Bedrock mercury at Kejimkujik National Park. In: mercury cycling in a wetland-dominated Ecosystem: a multidisciplinary study. Eds.: O'Driscoll N.J., Rencz A.N., Lean D.R.S. The Society of Environmental Toxicology and Chemistry (SETAC), Pensacola, Florida, 2005; 131-195.

Davies J.C., Smith P.M. The geological setting of gold occurrences in the lake of the Woods area. Open file report 5695. Mines and Mineral Divisions, Ontario Geological Survey 1988; 381 p.

Davis D.W. U-Pb geochronology of Archean metasedimentary rocks in the Pontiac and Abitibi subprovinces, Quebec, constraints on timing, provenance and regional tectonics. Precambrian Research 2002; 115, 97-117.

Demers J.D., Driscoll C.T., Fahey T.J., Yavitt J.B. Mercury cycling in litter and soil in different forest types in the Adirondack region, New York, USA. Ecological Applications 2007; 17: 1341-1351.

Demers J.D., Driscoll C.T., Shanley J.B. Mercury mobilization and episodic stream acidification during snowmelt: Role of hydrologic flow paths, source areas, and

supply of dissolved organic carbon. Water Resources Research 2010; 46 W01511. DOI: 10.1029/2008WR007021.

DeMont G.J. Mineral inventory studies in Cape Breton Island. Report of activities 33. Province of Nova Scotia 2002.

Depew D.C., Burgess N.M., Anderson M.R., Baker R., Bhavsar S.P., Bodaly R.A., Eckley C.S., Evans M.S., Gantner N., Graydon J.A., Jacobs K., LeBlanc J.E., St. Louis V.L., Campbell L.M. An overview of mercury concentrations in freshwater fish species: a national fish mercury dataset for Canada. Canadian. Journal of Fisheries and Aquatic Sciences 2013a; 70: 436-451. DOI: http://dx.doi.org/10.1139/cjfas-2012-0338.

Depew D.C., Burgess N.M., Campbell L.M. Modeling mercury concentrations in prey fish: Derivation of a national scale common indicator of dietary mercury exposure for piscivorous fish and wildlife. Environmental Pollution 2013b; 176: 234-243. DOI: http://dx.doi.org/10.1016/j.envpol.2013.01.024.

Diamond M., Helm, P., Semkin R., Law S. Mass balance and modelling of contaminants in lakes. In: Sources, occurrence, trends, and pathways in the physical environment. Eds.: Bidleman, T.F., Lucotte M., and Stow, J. Canadian Arctic Contaminants Assessment Report II. Northern contaminant program. Indian and Northern Affairs Canada, Minister of Aboriginal Affairs and Northern Development 2003; 191-224.

Dick J., Tetzlaff D., Birkel C., Soulsby C. Modelling landscape controls on dissolved organic carbon sources and fluxes to streams. Biogeochemistry 2015; 122 (2-3): 361-374. DOI: 10.1007/s10533-014-0046-3.

Dittman J.A., Shanley J.B., Driscoll C.T., Aiken G.R., Chalmers A.T., Towse J.E., Selvendiran P. Mercury dynamics in relation to dissolved organic carbon concentration and quality during high flow events in three northeastern U.S. streams. Water Resources Research 2010; 46: W07522, doi:10.1029/2009WR008351.

Dix G.R., Coniglio M., Riva J.F., Achab A. The Late Ordovician Dawson Point formation (Timiskaming outlier, Ontario): key to a new regional synthesis of Richmondian-Hirnantian carbonate and siliciclastic magnafacies across the central Canadian craton. Canadian Journal of Earth Sciences 2007; 44, 1313-1331.

Dmytriw R., Mucci A., Lucotte M., Pichet P. The partitioning of mercury in the solid components of dry and flooded forest soils and sediments from a hydroelectric reservoir, Quebec (Canada). Water, Air, and Soil Pollution 1995; 80: 1099-1103.

Donovan P.M., Blum J.D., Demers J.D., Gu B., Brooks S.C., Peryam J. Identification of multiple mercury sources to stream sediments near Oak Ridge, TN, USA. Environmental Science & Technology 2014; 48 (7): 3666-74. DOI: 10.1021/es4046549. Epub 2014 Mar 14.

Ames D.E., Brown G.H., Card K.D., Fedorowich J.S., Golightly J.P., Gray M.J., James R.S., Scott Jobin-Bevans S., Long D.G.F., Naldrett A.J., Paakki J.J., Pattison E.F., Riller U., Rousell D.H., Stoness J.A., Koziol B. A field guide to the geology of

Sudbury, Ontario. Eds.: Rousell, D.H., Brown, G.H. Open file report 6243. Ontario Geological Survey 2009; 14-30.

Driscoll C.T., Holsapple J., Schofield C.L., Munson R. The chemistry and transport of mercury in a small wetland in the Adirondack region of New York, USA. Biogeochemistry 1998; 40: 137-146.

Dunn C.E. Geochemistry of humus from the southern La Ronge domain Saskatchewan (NTS 73P/7). Open file 3345. Geological Survey of Canada 1998.

Eckley C.S, Parsons M.T., Mintz R., Lapalme M., Mazur M., Tordon R., Elleman R., Graydon J.A., Blanchard P., St Louis V. Impact of closing Canada's largest point-source of mercury emissions on local atmospheric mercury concentrations. Environmental Science & Technology 2013; 47: 10339-48.

Ecological Stratification Working Group. A national ecological framework for Canada. Agriculture and Agri-Food Canada, Research Branch, Centre for Land and Biological Resources Research and Environment Canada, State of the Environment Directorate, Ecozone Analysis Branch, Ottawa/Hull.Report and national map at 1:7500 000 scale 1995.

El Bilali L., Rasmussen P.E., Hall G.E.M., Fortin D. Role of sediment composition in trace metal distribution in lake sediments. Applied Geochemistry 2002; 17, 1171-1181.

Environment Canada Atlantic Region. Mercury in Atlantic Canada: A progress report. Mercury team regional science coordinating committee 1998.

Environment Canada Atlantic Region. Mercury in Atlantic Canada: A progress report. Mercury team regional science coordinating committee 2011.

Ericksen J.A., Gustin M.S., Schorran D.E., Johnson D.W., Lindberg S.E., Coleman J.S. Accumulation of atmospheric mercury in forest foliage. Atmospheric Environment 2003; 37: 1613-1622.

Feng X., Foucher D., Hintelmann H., Yan H., He T., Qiu G. Tracing mercury contamination sources in sediments using mercury isotope compositions. Environmental Science & Technology 2010; 44: 3363-3368.

Fleck J.A., Alpers C.N., Marvin-DiPasquale M., Hothem R.L., Wright S.A., Ellett K., Beaulieu E., Agee J.L., Kakouros E., Kieu L.H., Eberl D.D., Blum A.E., and May J.T. The effects of sediment and mercury mobilization in the south Yuba river and Humbug creek confluence area, Nevada County, California: concentrations, speciation, and environmental fate - Part 1: field characterization. Open-file report 2010-1325A U.S. Geological Survey 2011; 104 p.

Fleming E.J., Mack E.E., Green P.G., Nelson D.C. Mercury methylation from unexpected sources: molybdate-inhibited freshwater sediments and an iron-reducing bacterium. Applied and Environmental Microbiology 2006; 72: 457-464.

Forest Watershed Research Center, University of New Brunswick University 2015. http://watershed.for.unb.ca/research/wet-areas-mapping/.

Franzen C., Kilian R., Biester H. Natural mercury enrichment in a minerogenic fen--evaluation of sources and processes. Journal of Environmental Monitoring 2004; 6: 466-472.

Friske P.W.B., Coker W.B. The Importance of geological controls on the natural distribution of mercury in stream and lake. Water, Air, and Soil Pollution 1995; 80: 1047-1051.

Friske P.W.B., Hornbrook E.H.W. Canada's national geochemical reconnaissance programme. Transactions of the Institution for Mining and Metallurgy, Section B: Applied Earth Science 1991; 100: B47-B56.

Fulton R.J. Surficial materials of Canada. Map 1880A, Scale 1:5000000. Geological Survey of Canada, Natural Resources Canada 1995.

Garrett R.G. mercury in some granitoid rocks of the Yukon and its relation to gold - tungsten mineralization. Journal of Geochemical Exploration 1974; 3: 277-289.

Gbor P.K., Wen D., Meng F., Yang F., Sloan J.J., 2007. Modeling of mercury emission, transport and deposition in North America. Atmospheric Environment 2007; 41: 1135-1149.

Gelinas Y., Lucotte M., Schmit J.P. History of the atmospheric deposition of major and trace elements in the industrialized St, Lawrence Valley, Quebec, Canada. Atmospheric Environment 2000; 34: 1797-1810.

Geobase, Natural Resources Canada. Canadian Digital Elevation Data 2011. http://www.geobase.ca/geobase/en/data/cded/.

Geobase, Natural Resources Canada. GeoBase Web Mapping Service (WMS). Canada, Minister of Natural Resources Canada 2006.

Geological Survey of Canada (GSC), Natural Resources Canada (NRCAN), Government of Canada. Canadian Geochemicl Surveys 2008. http://geochem.nrcan.gc.ca/cdogs/content/main/home_en.htm.

Givelet N., Roos-Barraclough F., Shotyk W. Predominant anthropogenic sources and rates of atmospheric mercury accumulation in southern Ontario recorded by peat cores from three bogs: comparison with natural "background" values (past 8000 years). Journal of Environmental Monitoring 2003; 5: 935-949.

Goodfellow W.D. Base metal metallogeny of the Selwyn Basin, Canada. Special publication no. 5: mineral deposits of Canada: A synthesis of major deposit-types, district metallogeny, the evolution of geological provinces, and exploration methods. Ed. Goodfellow W.D. Mineral Deposits Division, Geological Association of Canada 2007; 553-579.

Ghorpade S.; Heyes A.; Gilmour C.C.; Oswald C.J. The relationship between dissolved organic carbon quality and mercury transport in a boreal watershed. American Geophysical Union, Fall Meeting 2009; abstract #H53K-03.

Government of Quebec. Gouvernement du Québec, Ressources naturelles et de la Faune Québec, Geoscience Databases. 2012. http://www.mrn.gouv.qc.ca/english/mines/geology/geology-databases.jsp.

Government of Canada, Agriculture and Agri-Food Canada. National Ecological Framework for Canada 1999. http://sis.agr.gc.ca/cansis/nsdb/ecostrat/index.html.

Government of Canada, Environment Canada. Canadian Arctic Northern Contaminats Program (CANCP) 2013a. https://www.ec.gc.ca/natchem/default.asp?lang=En&n=CFCA273C-1.

Government of Canada, Environment Canada. The Clean Air Regulatory Agenda programs (CARA-2006). Government of Canada 2013b. http://www.ec.gc.ca/default.asp?lang=En&n=56D4043B-1&news=295B1964-9737-4F80-B064-B3088D9910BE.

Government of Canada, Environment Canada. Releases of mercury to the Environment 2014. https://www.ec.gc.ca/indicateurs-indicators/default.asp?lang=en&n=2E4A71BD-1.

Government of Yukon, Department of Environment GIS (ENVY GIS). 30 Meter Yukon Digital Elevation Model 2014. http://www.env.gov.yk.ca/publications-maps/geomatics/data/30m_dem.php.

Gray J.E., Theodorakos P.M., Bailey E.A., Turner R.R. Distribution, speciation, and transport of mercury in stream-sediment stream-water, and fish collected near abandoned mercury mines in southwestern Alaska, USA. Science of the Total Environment 2000; 60: 21-33.

Gregory D.J., Richardson J.M., Bisson B.M. A history of coal mining in Nova Scotia. Information Series No. 2. Nova Scotia Department of Mines 1978.

Grigal D.F. Inputs and outputs of mercury from terrestrial watersheds: a review. Environmental Review 2002; 10: 1-39.

Gustin M.S. Are mercury emissions from geologic sources significant? A status report. Science of the Total Environment 2003; 153-167.

Guy H.P. Fluvial sediment concepts. US Government Printing Office: Washington, DC. US Geological Survey Techniques of Water- Resources Investigations 03-C1. 1970; 55.

Han Y., Jin Z., Cao J., Posmentier E.S., An Z. Atmospheric Cu and Pb deposition and transport in lake sediments in a remote mountain area, northern China. Water, Air, and Soil Pollution 2007: 179: 167-181.

Haschenburger J.K. Observations of event-based streambed deformation in a gravel bed channel. Water, Air, and Soil Pollution 2006; 42 W11412. DOI: 10.1029/2006WR004985.

He T., Lu J., Yang F., Feng X. Horizontal and vertical variability of mercury species in pore water and sediments in small lakes in Ontario. Science of the Total Environment 2007; 386: 53-64.

Herschy R.W. Lake Sediments. Encyclopedia of lakes and reservoirs, Encyclopedia of Earth Sciences Series 2012; 458-463.

Hintelmann H., Harris R., Heyes A., Hurley J.P., Kelly C.A., Krabbenhoft D.P., Lindberg S., Rudd J.W., Scott K.J., St Louis V.L. Reactivity and mobility of new and old mercury deposition in a boreal forest ecosystem during the first year of the METAALICUS study. Environmental Science & Technology 2002; 36: 5034-5040.

Hintelmann, H., Harris R. Application of multiple stable mercury isotopes to determine the adsorption and desorption dynamics of Hg(II) and MeHg to sediments. Marine Chemistry. 2004; 90: 165- 173.

Hissler C., Probst J.-L. Impact of mercury atmospheric deposition on soils and streams in a mountainous catchment (Vosges, France) polluted by chlor-alkali industrial activity: the important trapping role of the organic matter. Science of the Total Environment 2006; 361:163-78.

Hulshof A.H.M., MacDonald A.S. Dispersion of tailings from the stilling Zn-Pb-Cu mine site, Cape Breton Island, Nova Scotia. Atlantic Geology 1998; 34: 159-170.

Indian and Northern Affairs Canada. Contaminated sites in the Northwest Territories, Northern Contaminated Sites Program 2006. http://www.aadnc-aandc.gc.ca/eng/1100100035301/1100100035302.

International Conference on Mercury as a Global Pollutant (ICMGP) 2011. http://mercury2011.org/.

International Conference on Mercury as a Global Pollutant (ICMGP) 2013. http://www.mercury2013.com/full-program/.

Jackson T.A., Muir D.C.G., Vincent W.F. Historical variations in the stable isotope composition of mercury in Arctic lake sediments. Environmental Science & Technology 2004; 38: 2813-2821.

Jardine T.D., Kidd K.A., Cunjak R.A., Arp P.A. Factors affecting water strider (Hemiptera: Gerridae) mercury concentrations in lotic systems. Environmental Toxicology and Chemistry 2009; 28: 1480-1492.

Jebrak M., Higueras P.L., Marcoux E., Lorenzo S. Geology and geochemistry of high-grade, volcanic rock-hosted, mercury mineralisation in the Nuevo Entredicho deposit, Almaden district, Spain. Mineralium Deposita 2002; 37: 421-432.

Jones M., Willey L. Eastern Alpine Guide, Chapter 10. Beyond Ktaadn Inc. 2012. http://easternalpine.org/eag/guide.html.

Jones G., Henderson V. Metal concentrations in soil and produce from gardens in Flin Flon, Manitoba, 2002. Habitat Management and ecosystem Monitoring Section, Wildlife and Ecosystem Protection Branch, Manitoba Conservation, Manitoba Conservation Report No. 2006-01, Winnipeg, Manitoba 2006; 81 p.

Jutras M.F., Nasr M., Castonguay M., Pit C., Pomeroy J.H., Smith T.P., Zhang C.F., Ritchie C.D., Meng F.R., Clair T.A., Arp P.A. Dissolved organic carbon concentrations and fluxes in forest catchments and streams: DOC-3 model. Ecological Modelling 2011; 222: 2291-2313.

Jutras M.-F., Castonguay M., Nasr M., Ogilvie J., Bhatti J. S., Arp P.A. Modeling and mapping hydrothermal regimes and potential impacts of climate change on

permafrost within the South Mackenzie Plain, Northwest Territories, Canada. Ecoscience 2014; 21: 1–14.

Kainz M., Arts M.T., Mazumder A. Essential versus potentially toxic dietary substances: a seasonal comparison of essential fatty acids and methyl mercury concentrations in the planktonic food web. Environmental Pollution 2008; 155: 262-270.

Kainz M., Lucotte M. Mercury concentrations in lake sediments - revising the predictive power of catchment morphometry and organic matter composition. Water, Air, and Soil Pollution 2006; 170: 173-189.

Kainz M., Lucotte, M., Parrish, C.C. Relationships between organic matter composition and methyl mercury content of offshore and carbon-rich littoral sediments in an oligotrophic lake. Canadian Journal of Fisheries and Aquatic Sciences 2003; 60: 888-896.

Kainz M., Mazumder A. Effect of algal and bacterial diet on methyl mercury concentrations in zooplankton. Environmental Science & Technology 2005; 39: 1666-1672.

Keppie J.D. Geological map of the Province of Nova Scotia, Map ME 2000-1 (1:500 000). Nova Scotia Department of Natural Resources 2000. http://novascotia.ca/natr/meb/download/mg/map/htm/map_2000-001.asp.

Kerin E.J., Gilmour C.C., Roden E., Suzuki M.T., Coates J.D., Mason R.P. Mercury methylation by dissimilatory iron-reducing bacteria. Applied and Environmental Microbiology 2006; 72: 7919-7921.

Kettles I.M., Shilts W.W. Geochemical and lithological composition of surficial sediments, southeastern Ontario. Open file 3175. Geological Survey of Canada 1996.

Kirk J.L., Muir D.C., Antoniades D., Douglas M.S., Evans M.S., Jackson T.A., Kling H., Lamoureux S., Lim D.S., Pienitz R., Smol J.P., Stewart K., Wang X., Yang F. Climate change and mercury accumulation in Canadian high and subarctic lakes. Environmental Science & Technology 2011; 45: 964-970.

Kolker A., Olson M.L., Krabbenhoft D.P., Tate M.T., Engle M.A. Patterns of mercury dispersion from local and regional emission sources, rural Central Wisconsin, USA. Atmospheric Chemistry and Physics 2010; 10: 4467-4476.

Lahoutifard N., Poissant L., Scott S.L. Scavenging of gaseous mercury by acidic snow at Kuujjuarapik, northern Quebec. Science of the Total Environment 2006; 355: 118-126.

Lahoutifard N., Sparling M., Lean D. Total and methyl mercury patterns in Arctic snow during springtime at Resolute, Nunavut, Canada. Atmospheric Environment 2005; 39: 7597-7606.

Lalonde J.D., Poulain A.J., Amyot M. The role of mercury redox reactions in snow on snow-to-air mercury transfer. Environmental Science & Technology 2002; 36: 174-178.

Landis M.S., Ryan J.V., Ter Schure A.F.H., Laudal D. The behavior of mercury emissions from a commercial coal-fired power plant: the relationship between stack speciation and near-field plume measurements. Environmental Science & Technology 2014; 48 (22):13540-13548. DOI: 10.1021/es500783t.

Leenher J.A., Reddy M.M. Co-precipitation of dissolved organic matter by calcium carbonate in pyramid lake, Nevada. Annals of Environmental Science 2008; 2: 11-25.

Lin Y., Larssen T., Vogt R.D., Feng X., Zhang H. Modelling transport and transformation of mercury fractions in heavily contaminated mountain streams by coupling a GIS-based hydrological model with a mercury chemistry model. Science of the Total Environment 2011; 409: 4596-605. DOI: 10.1016/j.scitotenv.2011.07.033.

Little L.E. Distribution of arsenic and mercury in terrestrial and marine environments impacted by gold mine tailings, Win Harbour, Nova Scotia 2006; 161 p.

Little M.; Burgess, N.M.; Campbell L. Metadata: Fish Mercury Data layer for Canada (FIDMAC) 2014. DOI: http://dx.doi.org/10.6084/m9.figshare.1210773.

Lockhart W.L., Macdonald R.W., Outridge P.M., Wilkinson P., DeLaronde J.B., Rudd J.W.M. Tests of the fidelity of lake sediment core records of mercury deposition to known histories of mercury contamination. The Science of the Total Environment 2000; 260: 171-180.

Lockhart W.L., Wilkinson P., Billeck B.N., Danell R.A., Hunt R.V., Brunskill G.J., DeLaronde J., St Louis V. Fluxes of mercury to lake sediments in central and northern Canada inferred from dated sediment cores. Biogeochemistry 1998; 40: 163-173.

Lockhart W.L. Mercury in sediments. In: Sources, occurrence, trends, and pathways in the physical environment. Canadian Arctic Contaminants Assessment Report II. Eds.: Bidleman T.F., R.W. Macdonald and J. Stow. Aboriginal Affairs and Northern Development Northern Contaminants Program. 2003; 143-147.

Lodenius M., Tulisalo E., Soltanpour-Gargagari A. Exchange of mercury between atmosphere and vegetation under contaminated conditions. Science of the Total Environment 2003; 304: 169-174.

Louchouarn P., Lucotte M., Mucci A., Pichet P. Geochemistry of mercury in 2 hydroelectric reservoirs in Quebec, Canada. Canadian Journal of Fisheries and Aquatic Sciences 1993; 50: 269-281.

Loukola-Ruskeeniemi K., Kantola M, Halonen T., Seppänen K., Henttonen P., Kallio E., Kurki P., Savolainen H. Mercury-bearing black shales and human Hg intake in eastern Finland: impact and mechanisms. Environmental Geology 2003; 43: 283-297.

Lu X., Jaffe R. Interaction between Hg(II) and natural dissolved organic matter: a fluorescence spectroscopy based study. Water Research 2001; 35: 1793-1803.

Ma J., Hintelmann H., Kirk J.L., Muir D.C.G. Mercury concentrations and mercury isotope composition in lake sediment cores from the vicinity of a metal smelting facility in Flin Flon, Manitoba. Chemical Geology 2013; 336: 96-102.

Macdonald D.D., Levy D.A., Czarnecki A., Low G., Riche N. State of the aquatic knowledge of Great Bear watershed. Macdonald Environmental Science LTD. 2004; 191 p.

Madsen J.D, Chambers P.A., James W.F., Koch E.W., Westlake D.F. The interaction between water movement, sediment dynamics and submersed macrophytes. Hydrobiologia 2001; 444: 71-84.

Mann E., Ziegler S.E., Mallory M.L. O'Driscoll N.J. Mercury photochemistry in snow and implications for Arctic ecosystems. Environmental Reviews 2014; 22 (4): 331-345.

Marvin-Dipasquale M., Lutz M.A., Brigham M.E., Krabbenhoft D.P., Aiken G.R., Orem W.H., Hall B.D. Mercury cycling in stream ecosystems: 2. Benthic methylmercury production and bed sediment-pore water partitioning. Environmental Science & Technology 2009; 43: 2726-32.

Maxeiner R.O., Harper C.T., Corrigan D., MacDougall D.G. La Ronge-Lynn lake Bridge project: geology of the southern Reindeer lake area (1996-2001, 2004). Open file report (Saskatchewan Geological Survey) 2003-1. Saskatchewan Geological Survey, Saskatchewan Industry and Resources 2004.

McCuaig S.J., Taylor D.M. till geochemistry of the Snegamook lake area (NTS map areas 13K/3, 13K/6 and 13K/11). Open file 013K/0283, 1-134. St. John's, Newfoundland, Government of Newfoundland and Labrador, Department of Natural Resources, Geological Survey 2005.

McCurdy M.W., Anglin C.D., Friske P.W.B., Balma R.G., Day S.J.A. National geochemical reconnaissance, stream sediment and water survey, Bathurst Island, Northwest Territories (Parts of NTS 68G, 68H, 69A and 69B), Geological Survey of Canada Open file 3292 1997. http://geogratis.gc.ca/api/en/nrcan-rncan/ess-sst/f1f3a9d6-ec9a-5389-92d8-9a0eb3b2c855.html.

McMartin I., Henderson P.J., Plouffe A., Knight R.D. Comparison of Cu-Hg-Ni-Pb concentrations in soils adjacent to anthropogenic point sources: examples from four Canadian sites. Geochemistry-exploration Environment Analysis 2013; 2: 57-73.

Mei Y., Hornberger G.M., Kaplan L.A. Newbold J.D., Aufdenkampe A.K. The delivery of dissolved organic carbon from a forested hillslope to a headwater stream in southeastern Pennsylvania, USA. Water Resources Research 2014; 50, (7): 5774-5796. DOI: 10.1002/2014WR015635.

Meng F.R., Arp P.A., Sangster A., Brun G.L., Rencz A.N., Hall G.E., Holmes J., Lean D.R.S., Clair T.A. Modeling dissolved organic carbon, total and methyl mercury in Kejimkujik freshwaters. In: mercury cycling in a wetland-dominated ecosystem: a multidisciplinary study. Eds.: O'Driscoll N.J., Rencz A.N., Lean D.R.S. The

Society of Environmental Toxicology and Chemistry (SETAC), Pensacola, Florida 2005; 267-282.

Mercier-Langevin P., Daigneault R., Goutier J., Dion C., Archer P. Geology of the Archean intrusion-hosted La-Grande-Sud Au-Cu prospect, La Grande Subprovince, James Bay region, Québec. Economic Geology 2012; 107, 935-962.

Miller E.K., Vanarsdale A., Keeler G.J., Chalmers A., Poissant L., Kamman N.C., Brulotte R. Estimation and mapping of wet and dry mercury deposition across northeastern North America. Ecotoxicology 2005; 14: 53-70.

Mills R.B., Paterson A.M., Lean D.R., Smol J.P., Mierle G., Blais J.M. Dissecting the spatial scales of mercury accumulation in Ontario lake sediment. Environmental Pollution 2009; 157: 2949-2956.

Moore J.W., Sutherland D.J. Distribution of heavy metals and radionuclides in sediments, Water, and fish in an area of Great Bear Lake contaminated with mine wastes. Archives of Environmental Contamination and Toxicology 1981; 10: 329-338.

Moore T.R., Bubier J.L., Heyes A., Flett R.J. Methyl and total mercury in boreal wetland plants, Experimental Lakes Area, Northwestern Ontario. Journal of Environmental Quality 1995; 24: 845-850.

Moore C.W., Obrist D., Steffen A., Staebler R.M., Douglas T.A., Richter A., Nghiem S.V. Convective forcing of mercury and ozone in the Arctic boundary layer induced by leads in sea ice. Nature 2014; 506: 81-84. DOI:10.1038/nature12924.

Morrison H. 2011. The Canadian Clean Air Regulatory Agenda Mercury Science Program. Ecotoxicology 2011; 20: 1512-1519. DOI: 10.1007/s10646-011-0714-1.

Muir D.C.G., Wang X., Yang F., Nguyen N., Jackson T.A., Evans M.S., Douglas M., Köck G., Lamoureux S., Pienitz R., Smol J.P., Vincent W.F., Dastoor A. Spatial trends and historical deposition of mercury in eastern and northern Canada inferred from lake sediment cores. Environmental Science & Technology 2009; 43: 4802-4809.

Munthe J., Wängberg I., Rognerud S., Fjeld E., Verta M., Porvari P., Meili M. Mercury in Nordic ecosystems. IVL Report B1761. IVL Swedish Environmental Research Institute Ltd, Göteborg, Sweden, 2007; 43 p.

Murphy P.N.C., J. Ogilvie, K. Connor, Arp P.A. Mapping wetlands: a comparison of two different approaches for New Brunswick, Canada. Wetlands 2007; 27: 846-854.

Murphy P.N.C., Ogilvie J., Castonguay M., Zhang C.F., Meng F.R., Arp P.A. Improving forest operations planning through high-resolution flow-channel and wet-areas mapping. Forestry Chronicle 2008; 84: 568-574.

Murphy P.N.C., Ogilvie J., Meng F.R., White B., Bhatti J.S., Arp P.A. Modelling and mapping topographic variations in forest soils at high resolution: A case study. Ecological Modelling 2011; 222: 2314-2332.

Nasr M. Mercury levels in fungal fruiting bodies from interior and coastal forests in the Bay of Fundy region, New Brunswick, Canada. Master of Science in Forestry and

Environmental Science Thesis. University of New Brunswick. New Brunswick 2007; 195 p.

Nasr M., Arp P.A. Hg concentrations and accumulations in fungal fruiting bodies, as influenced by forest soil substrates and moss carpets. Applied Geochemistry 2011; 26: 1905-1917.

Nasr M., Arp, P.A. 2015a. Mercury in forest soils and vegetation, including mosses and mushrooms. Environment. Canada Report: Canadian Mercury Science Assessment. Chapter 3c; In Print.

Nasr M., Arp P.A. 2015b. Total mercury concentrations in stream and lake sediments across Canada. Environment. Canada Report: Canadian Mercury Science Assessment. Chapter 3b; In Print.

Nasr M., Ogilvie J., Castonguay M., Rencz A., Arp P.A. Total Hg concentrations in stream and lake sediments: discerning geospatial patterns and controls across Canada. Applied Geochemistry 2011; 26: 1818-1831.

Natural Resources of Canada (NRCAN), Canada3D - Digital elevation model of the Canadian landmass. 2007. http://www.geogratis.ca/geogratis/en/collection/detail.doid=8880.

Nova Scotia Department of Natural Resources. DP ME 132, Version2, regional lake sediment geochemical survey by the Nova Scotia Department of Natural Resources over southern Nova Scotia, (1977-1978) 2006; http://novascotia.ca/NATR/meb/download/dp132.asp.

Nova Scotia Department of Natural Resources. DP ME 133, Version2, regional lake sediment and water geochemical survey by the Nova Scotia Department of Natural Resources over eastern Cape Breton, (1983-1985) 2006. http://novascotia.ca/natr/meb/download/dp133.asp.

Nova Scotia Department of Natural Resources. DP ME 136, Version2, regional stream sediment and water surveys by the Nova Scotia Department of Natural Resources over the northern mainland Nova Scotia and Cape Breton Island, (1982-1983) 2006. http://novascotia.ca/NATR/meb/download/dp136.asp.

Nriagu J.O. Mechanistic steps in the photoreduction of mercury in natural waters. The Science of the Total Environment 1994; 154: 1-8.

O`Driscoll, N.J., Poissant, L., Canário, J., Ridal, J., Lean, D. Continuous analysis of dissolved gaseous mercury and mercury volatilization in the upper St. Lawrence River; Exploring temporal trends and UV attenuation. Environmental Science & Technology 2007; 41: 5342-5348.

O'Driscoll N.J., Rencz A.N., Lean D.R.S. Mercury cycling in a wetland-dominated ecosystem: a multidisciplinary study. The Society of Environmental Toxicology and Chemistry (SETAC), Pensacola, Florida 2005; 392p.

Odumo B.O., Carbonell G., Angeyo H.K., Patel J.P., Torrijos M., Rodríguez Martín J. A. Impact of gold mining associated with mercury contamination in soil, biota

sediments and tailings in Kenya. Environmental Science and Pollution Research 2014. DOI: 10.1007/s11356-014-3190-3.

Olubunmi F.E., Olorunsola O.E. Evaluation of the status of heavy metal pollution of sediment of Agbabu bitumen deposit area, Nigeria. European Journal of Scientific Research 2010; 41: 373-382.

Otorowski C.A. Mercury in gulls of the Bay of Fundy. Master of Science in Forestry and Environmental Science Thesis. University of New Brunswick. New Brunswick 2005; 187 p.

Outridge P.M., Rausch N., Percival J.B., Shotyk W., McNeely R. Comparison of mercury and zinc profiles in peat and lake sediment archives with historical changes in emissions from the Flin Flon metal smelter, Manitoba, Canada. Science of the Total Environment 2011; 409: 548-563.

Outridge P.M., Sanei L.H., Stern G.A., Hamilton P.B., Goodarzi F. Evidence for control of mercury accumulation rates in Canadian High Arctic lake sediments by variations of aquatic primary productivity. Environmental Science & Technology 2007; 41: 5259-5265.

Page K.D., Murphy J.B. Mercury concentrations in the bedrock of southwestern Nova Scotia: a reconnaissance study. Atlantic Geology [S.l.] 2005; 31-40. DOI: http://dx.doi.org/10.4138/657.

Parameter-elevation Regressions on Independent Slopes Model (PRISM) Climate Group. PRISM (1961-1990) 2014. http://www.prism.oregonstate.edu/.

Parsons M.B., Cranston R.E. Influence of lead smelter emissions on the distribution of metals in marine sediments from Chaleur Bay, eastern Canada. Geochemistry: Exploration Environment, Analysis 2006; 6: 259-276.

Parsons M.J., Long D.T., Giesy J.P., Kannan K. Inferring sources for mercury to inland lakes using sediment chronologies of polycyclic aromatic hydrocarbons. Environmental Science: Processes & Impacts 2014; 16 (9): 2108-16. DOI: 10.1039/c4em00127c. Epub 2014.

Paterson I.A. The geology and evolution of the Pinchi fault zone at Pinchi Lake, central British Columbia. Canadian Journal of Earth Sciences 1977; 14: 1324-1342.

Paulson A.J. Sources of mercury in sediments, water, and fish of the lakes of Whatcom County, Washington, Scientific Investigating Report. Open-file report 2004-5084. U.S. Geological Survey, Washington, U.S. U.S. Geological Survey 2004; 98 p.

Pe-Piper G., Reynolds P.H., Nearing J., Piper D.J.W. Early Carboniferous deformation and mineralization in the Cobequid shear zone, Nova Scotia: an 40Ar/39Ar geochronology study. Canadian Journal of Earth Sciences 2004; 41: 1425-1436.

Pirrone N., Cinnirella S., Feng X., Finkelman R.B., Friedli H.R., Leaner J., Mason R., Mukherjee A.B., Stracher G.B., Streets D.G., Telmer K. Global mercury emissions to the atmosphere from anthropogenic and natural sources. Atmospheric Chemistry and Physics 2010; 10: 5951-5964.

Plouffe A. Physical partitioning of mercury in till: an example from central British Columbia, Canada. Journal of Geochemical Exploration 1997; 59: 219-232.

Poirier G.G. Structure and metamorphism of the eastern boundary of the Labrador Trough near Kuujjuaq, Quebec, and its tectonic implications. MSc Thesis, McGill University 1989; 229 p.

Poissant L., Martin Pilote M., Yumvihoz E., Lean D. foliage/atmosphere fluxes in a maple forest ecosystem in Québec, Canada 2008; 13 (D10). DOI: 10.1029/2007JD009510.

Power M. Klein G.M., Guiguer K.R.R.A., Kwan M.K.H. Mercury accumulation in the fish community of a sub-Arctic lake in relation to trophic position and carbon sources. Applied Ecology 2002; 39: 819-830.

Province of Nova Scotia. Historic gold mine tailings. 2012. http://www.novascotia.ca/nse/contaminatedsites/goldmines.asp.

Province of Nova Scotia. Mineral Resources Branch. Geochemistry digital products 2006. http://www.gov.ns.ca/natr/meb/one/mea-home.asp.

Province of Nova Scotia. Nova Scotia's Wetlands 2014. http://www.novascotia.ca/nse/wetland/.

Province of Nova Scotia. Enhanced Digital Elevation Model (2006), Nova Scotia, Canada 2013. http://novascotia.ca/natr/MEB/download/dp055.asp.

Province of Nova Scotia, Department of Natural Resources. Nova Scotia Mineral Occurrence Database DP ME 2, Version 10 (2009). Nova Scotia Mineral Occurrence Database 2013. http://novascotia.ca/natr/meb/download/dp002dds.asp.

Qinghua C., Mingcai Y. Abundances of chemical elements in rocks, sediments, and the continental crust of China. In: Proceedings of the 24th International Applied Geochemistry Symposium. Eds.: Lentz D.R., Throne K.G., Beal K.L. The Association of Applied Geochemistry (AAG) 2009; 947-951.

Rada R.G., Wiener J.G., Winfrey M.R., Powell D.E. Recent increases in atmospheric deposition of mercury to north-central Wisconsin lakes inferred from sediment analyses. Archives of Environmental Contamination and Toxicology 1989; 18: 175-181.

Ramasamy E.V., Toms A., Shylesh C.M., Jayasooryan K.K., Mahesh M. Mercury fractionation in the sediments of Vembanad wetland, west coast of India. Environmental Geochemistry and Health. 2012; 34: 575-586. DOI: 10.1007/s10653-012-9457-z.

Ramezani J.S.A., Bowring M.S., Pringle F.D. Winslow III, Rasbury E.T. The Manicouagan impact melt rock: a proposed standard for intercalibration of U-Pb and 40Ar/39Ar isotopic systems. 15th V.M. Goldsmidt Conference Abstract Volume, 2005; p. A321.

Rasmussen P.E., Friske P.W.B., Azzaria L.M., Garrett R.G. Mercury in the Canadian environment: current research challenges. Geological Survey of Canada

contribution no. 1997256. Journal of Geological Association of Canada, Geoscience Canada 1998a; 25: 1-13.

Rasmussen P.E., Villard D.J., Gardner H.D., Fortescue J.A.C., Schiff S.L., Shilts W.W. Mercury in lake sediments of the Precambrian Shield near Huntsville, Ontario, Canada Environmental Geology 1998b; 33: 170-182.

Rencz A.N., O'Driscoll N.J., Hall G.E.M., Peron T., Telmer K., Burgess N.M. Spatial variation and correlations of mercury levels in the terrestrial and aquatic components of a wetland dominated ecosystem: Kejimkujik Park, Nova Scotia, Canada. Water, Air, and Soil Pollution 2003; 143: 271-288.

Rennie M.D., Gary Sprules W., Vaillancourt A. Changes in fish condition and mercury vary by region, not Bythotrephes invasion: a result of climate change? Ecography 2010; 33: 471-482.

Ressources naturelles et de la Faune Québec, Gouvernement du Québec. Geoscience databases. 2012. http://sigeom.mrn.gouv.qc.ca/signet/classes/I1102_index.

Riscassi A.L., Hokanson K.J., Scanlon T.M. Streamwater particulate mercury and suspended sediment dynamics in a forested headwater catchment. Water, Air, & Soil Pollution 2011 (1-4); 220: 23-26.

Riscassi A.L, Scanlon T.M. Controls on stream water dissolved mercury in three mid-Appalachian forested headwater catchments. 2011; 47 (12). DOI: 10.1029/2011WR010977.

Rutter, A.P., Schauer, J.J., Lough, G.C., Snyder, D.C., Kolb, C.J., Klooster, S.V., Rudolf, T., Manolopoulos, H., and Olson, M.L. A comparison of speciated atmospheric mercury at an urban center and an upwind rural location. Journal of Environmental Monitoring 2008; 10:102-8.

Rydberg J., Rosén P., Lambertsson L., De Vleeschouwe F., Tomasdotter S., Bindler R. Assessment of the spatial distributions of total- and methyl-mercury and their relationship to sediment geochemistry from a whole-lake perspective. Journal of Geophysical Research: Biogeosciences 2012; 117.

Sanei H., Goodarzi F. relationship between organic matter and mercury in recent lake sediments: The physical geochemical aspects. Applied Geochemistry 2006; 21: 1900-1912.

Sanei H., Outridge P.M., Goodarzi F., Wang F., Armstrong D., Warren K., Fishback L. Wet deposition mercury fluxes in the Canadian sub-Arctic and southern Alberta, measured using an automated precipitation collector adapted to cold regions. Atmospheric Environment 2010; 1672-1681.

Scherbatskoy T., Shanley J.B., Keeler G.J. Factors controlling mercury transport in an upland forested catchment. Water, Air, and Soil Pollution 1998; 105: 427-438.

Schroeder W.H., Beauchamp S., Edwards G., Poissant L., Rasmussen P., Tordon R., Dias G., Kemp J., Van Heyst B., Banic C.M. Gaseous mercury emissions from natural

sources in Canadian landscapes. Journal of Geophysical Research: Atmospheres 2005; 110: D18.

Scudder B.C., Chasar L.C., Wentz D.A., Bauch N.J., Brigham M.E., Moran P.W., Krabbenhoft D.P. Mercury in fish, bed sediment, and water from streams across the United States, 1998-2005: U.S. Geological survey scientific investigations report 2009-5109 2009; 74 p.

Schuster P.F., Shanley J.B., Marvin-Dipasquale M., Reddy M.M., Aiken G.R., Roth D.A., Taylor H.E., Krabbenhoft D.P., Dewild J.F. Mercury and organic carbon dynamics during runoff episodes from a northeastern USA watershed. Water, Air, and Soil Pollution 2008; 187: 89-108.

Shanley J.B., Kamman N.C., Clair T.A., Chalmers A. Physical controls on total and methylmercury concentrations in streams and lakes of the northeastern USA. Ecotoxicology 2005; 14: 125-134.

Shuman B. Controls on loss-on-ignition variation in cores from two shallow lakes in the northeastern United States. Journal of Paleolimnology 2003; 30: 371-385.

Sichingabula H.M. Factors controlling variations in suspended sediment concentration for single-valued sediment rating curves, Fraser River, British Columbia, Canada. Hydrological Processes 1998; 12: 1869-1894.

Skyllberg U. Competition among thiols and inorganic sulfides and polysulfides for Hg and MeHg in wetland soils and sediments under suboxic conditions: Illumination of controversies and implications for MeHg net production. Journal of Geophysical Research: Biogeosciences 2008; 113 (G2): G00C03, 1-14.

Smith C.N., Kesler S.E., Blum J.D., Rytuba J.J. Isotope geochemistry of mercury in source rocks, mineral deposits and spring deposits of the California Coast Ranges, USA. Earth and Planetary Science Letters 2008; 269: 398-406.

Spencer S.H., Shutler D., O'Brien M.S. Correlates of mercury in female river otters (*Lontra Canadensis*) from Nova Scotia, Canada. Environmental Toxicology and Chemistry 2011; 30 (8): 1879-1884.

St Louis V.L., Rudd J.W., Kelly C.A., Hall B.D., Rolfhus K.R., Scott K.J., Lindberg S.E., Dong W. Importance of the forest canopy to fluxes of methyl mercury and total mercury to boreal ecosystems. Environmental Science & Technology 2001; 35: 3089-3098.

Stamenkovic J., Gustin M.S. Nonstomatal versus stomatal uptake of atmospheric mercury. Journal of Environmental Science & Technology 2009; 43: 1367-1372.

Steedman R.J., France R.L. Origin and transport of aeolian sediment from new clearcuts into boreal lakes, northwestern Ontario, Canada. Water, Air, & Soil Pollution 2000; 122, 139-152.

Steffen A., Douglas T., Amyot M., Ariya P., Aspmo K., Berg T., Bottenheim J., Brooks S., Cobbett F., Dastoor A., Dommergue A., Ebinghaus R., Ferrari C., Gardfeldt K., Goodsite M.E., Lean D., Poulain A.J., Scherz C., Skov H., Sommar J., Temme C. A

synthesis of atmospheric mercury depletion event chemistry in the atmosphere and snow. Atmospheric Chemistry and Physics 2008; 8: 1445-1482.

Stevenson J. Mercury deposits of British Columbia. Bulletin No 5, British Colombia Department of Mines 1940; 1-93p.

Stokes P.M., Dreier S.I. Mercury accumulation by filamentous algae: A promising biological monitoring system for methyl mercury in acid-stressed lakes. Environmental Pollution Series B, Chemical and Physical 1983; 5: 255-271.

Strode S., Jaeglé L., Noelle E., Selin N.E. Impact of mercury emissions from historic gold and silver mining: global modeling. Atmospheric Environment 2009; 43: 2012-2017.

Swanton D.A., White C.E., Barr M. Bedrock Geology in the Whycocomagh Mountain-Aberdeen Ridge Area (11F/14 and 11K/03), Central Cape Breton Island, Nova Scotia. Report of Activities113. Province of Nova Scotia, 2009; 113-123 p.

Syme E.C., Bailes A.H., Lucas S.B. Tectonic assembly of paleoproterozoic Flin Flon belt and setting of VMS deposits, Field trip B1. Geological Association of Canada, Winnipeg section; Mineralogical Association of Canada Annual Meeting, Winnipeg, Manitoba, 1996; 1-130 p.

Takats P.A., Dyer R.D. Temagami area lake sediment geochemical survey, northeastern Ontario. Open file report 6144. Ontario Geological Survey 2004; 1-113.

Teisserenc R., Lucotte M., Houel S. Terrestrial organic matter biomarkers as tracers of Hg sources in lake sediments. Biogeochemistry 2011; 103: 235-244.

ten Hulscher T.E.M., Mol G.A.J., Luers F. Release of metals from polluted sediments in a shallow lake: quantifying resuspension. Hydrobiologia 1992; 235/236: 97-105.

The Geological Society of America. Geological Time Scale 2012. http://www.geosociety.org/science/timescale/.

Thomas C.A., Bendell-Young L.I. Linking the sediment geochemistry of an intertidal region to metal bioavailability in the deposit feeder *Macoma balthica*. Marine Ecology Progress Series 1998; 173: 197- 213.

University of New Brunswick, Forest Watershed Research Center. Wet areas mapping (WAM) 2015. http://watershed.for.unb.ca/research/wet-areas-mapping/.

Université du Québec à Montréal. Collaborative Mercury Research Network (COMERN) 2001. http://www.unites.uqam.ca/comern/index.html.

US Department of the Interior, US Geological Survey. Mercury experiment to assess atmospheric loadings in Canada and the US (METAALICUS) project 2013, wi.water.usgs.gov/mercury/metaalicus-project.html.

US Environmental Protection Agency (USEPA). Mercury environmental effects 2009. http://www.epa.gov/mercury/eco.htm.

Vaidya O.C., Howell G.D., Leger D.A. Evaluation of the distribution of mercury in lakes in Nova Scotia and Newfoundland (Canada). Water, Air, and Soil Pollution 2000; 117: 353-369.

Vernet J.P., Thomas R.L. The occurrence and distribution of mercury in the sediments of the Petit Lac (western Lake Geneva). Ecologae Geologicae Helvetiae 1972; 65: 307-316.

von Wachenfeldt E., Eddie, Sobek S., Bastviken D., Tranvik L.J. Linking allochthonous dissolved organic matter and boreal lake sediment carbon sequestration: The role of light-mediated flocculation. Limnology and Oceanography 2008; 53(6): 2416-2426.

Watras C.J., Morrison K.A., Kent A., Price N., Regnell O., Eckley C., Hintelmann H., Hubacher T. Sources of methylmercury to a wetland-dominated lake in northern Wisconsin. Environmental Science & Technology 2005; 39: 4747-4758.

Wentz D.A., Brigham M.E., Chasar L.C., Lutz M.A., Krabbenhoft, D.P. Mercury in the Nation's streams—Levels, trends, and implications: U.S. Geological Survey Circular 1395, 2014; 90 p. DOI: http://dx.doi.org/10.3133/cir1395.

Wheeler J.O., Hoffman P.F., Card K.D., Davidson A., Sanford B.V., Okulitch A.V., Roest, W.R. Geological Map of Canada (CD-ROM) Map D1860A. Geological Survey of Canada 1997.

Wilson M.E. Geology of the Area Adjoining the east side of lake Timiskaming, Quebec. Canada Department of Mines. Geological Survey Branch. Government Printing Bureau, Ottawa 1910; 90 p.

Wilson, R.A., Parkhill, M.A., and Carroll, J.I. New Brunswick Appalachian Transect: Bedrock and Quaternary geology of the Mount Carleton - Restigouche River Area. New Brunswick Department of Natural Resources, Noranda-Falconbridge Inc. 2005.

Wong A.H.K., McQueen D.J., Williams D.D., Demers E. Transfer of mercury from benthic invertebrates to fishes in lakes with contrasting fish community structures. Canadian Journal of Fisheries and Aquatic Sciences 1997; 54: 1320-1330.

Wu F., Xu L., Liao H., Guo F., Zhao X., Giesy J.P. Relationship between mercury and organic carbon in sediment cores from Lakes Qinghai and Chenghai, China. Journal of Soils and Sediments 2013; 13: 1084-1092.

Wu Y., Jiang X., Liu E., Yao S., Zhu Y., Sun Z. The enrichment characteristics of mercury in the sediments of Dongjiu and Xijiu, Taihu Lake catchment, in the past century. Science in China Series D: Earth Sciences 2008; 51: 848-854.

Wyn B., Kidd K.A., Burgess N.M., Curry R.A., Munkittrick K.R. Increasing mercury in yellow perch at a hotspot in Atlantic Canada, Kejimkujik National Park. Environmental Science & Technology 2010; 44: 9176-9181.

Xia K., Skyllberg U.L., Bleam W.F., Bloom P.R., Nater E.A., Helmke P.A. X-ray absorption spectroscopic evidence for the complexation of Hg (II) by reduced sulfur in soil humic substances. Journal of Environmental Science & Technology 1999; 33: 257-261.

Xunyi J. Atmospheric transport and deposition of trace metals in remote reservoirs of the south china coastal region. Master of Philosophy. The Hong Kong Polytechnic University, Hong Kong 2009; 222 p.

Yang C.T. Sediment transport—theory and practice. McGraw-Hill Companies, New York (reprint by Krieger Publishing Company, Malabar, Florida, 2003) 1996; 396 p.

Yu K.W., DeLaune R.D., Devai I., Tao R., Jugsujinda A. Total and methyl mercury in wetland soils and sediments of Louisiana's Pontchartrain Basin (USA). Journal of Environmental Science and Health Part A-Toxic/Hazardous Substances & Environmental Engineering 2008; 43:1657-1662.

Yu X., Driscoll C.T., Huang J., Holsen T.M., Blackwell B.D. Modeling and mapping of atmospheric mercury deposition in Adirondack Park, New York. PLoS ONE 2013; 8 (3): e59322.

Yukon Government, Energy, Mines and Resources. 2014. http://www.geology.gov.yk.ca/.

Yukon Government. Energy, Mines and Resources. 2012. http://www.geology.gov.yk.ca/.

Zhang L., Paige Wright L., Blanchard P. A review of current knowledge concerning dry deposition of atmospheric mercury. Atmospheric Environment 2009; 43: 5853-5864.

Zhang X., Rygwelski K.R., Kreis Jr R.G., Rossmann R. A mercury transport and fate model (LM2-Mercury) for mass budget assessment of mercury cycling in Lake Michigan. Journal of Great Lakes Research 2014; 40 (2): 347-359.

Appendices

Appendix 1 Supplementary Materials

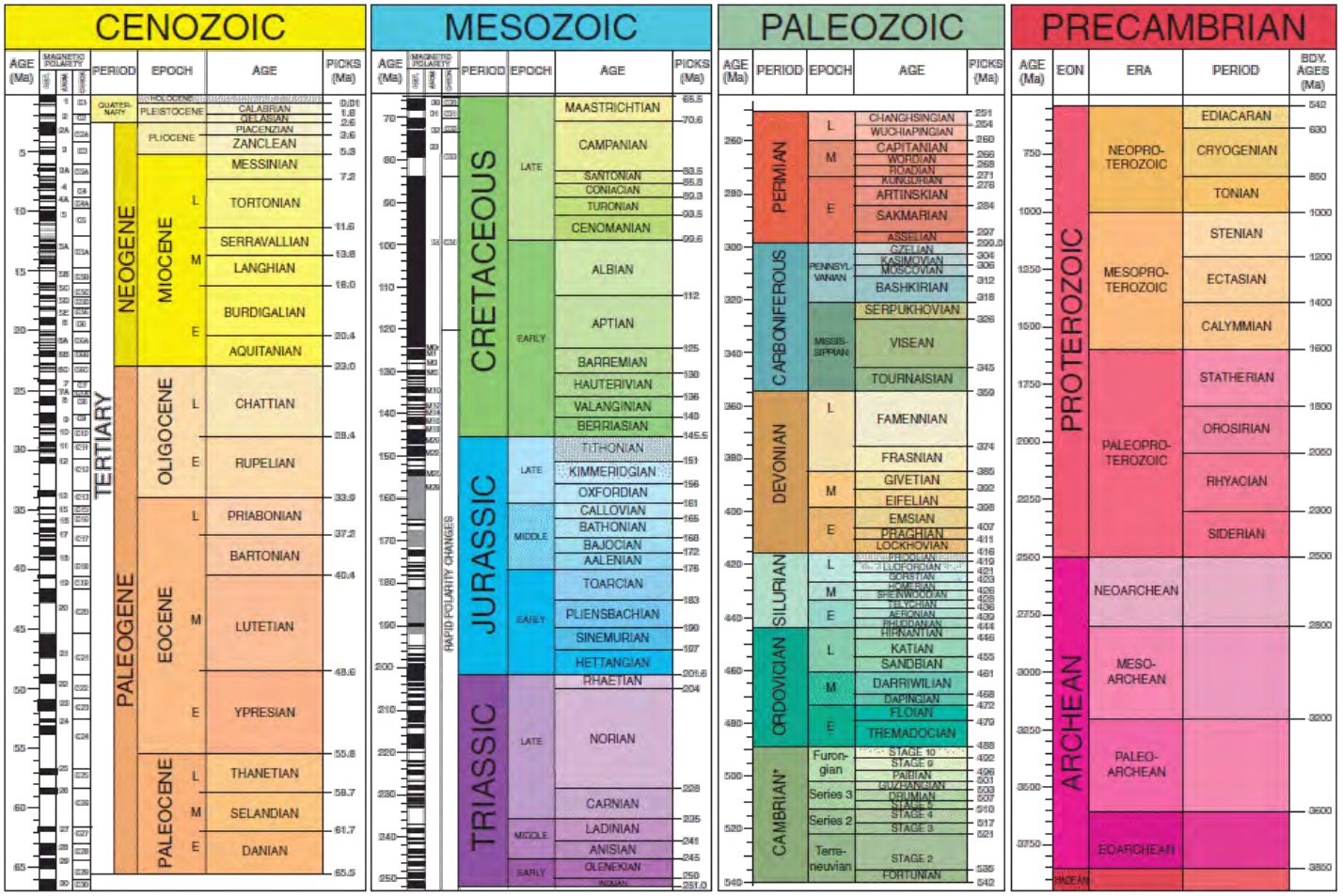

Figure A1.1 Geological time scale (The Geological Society of America, 2012).

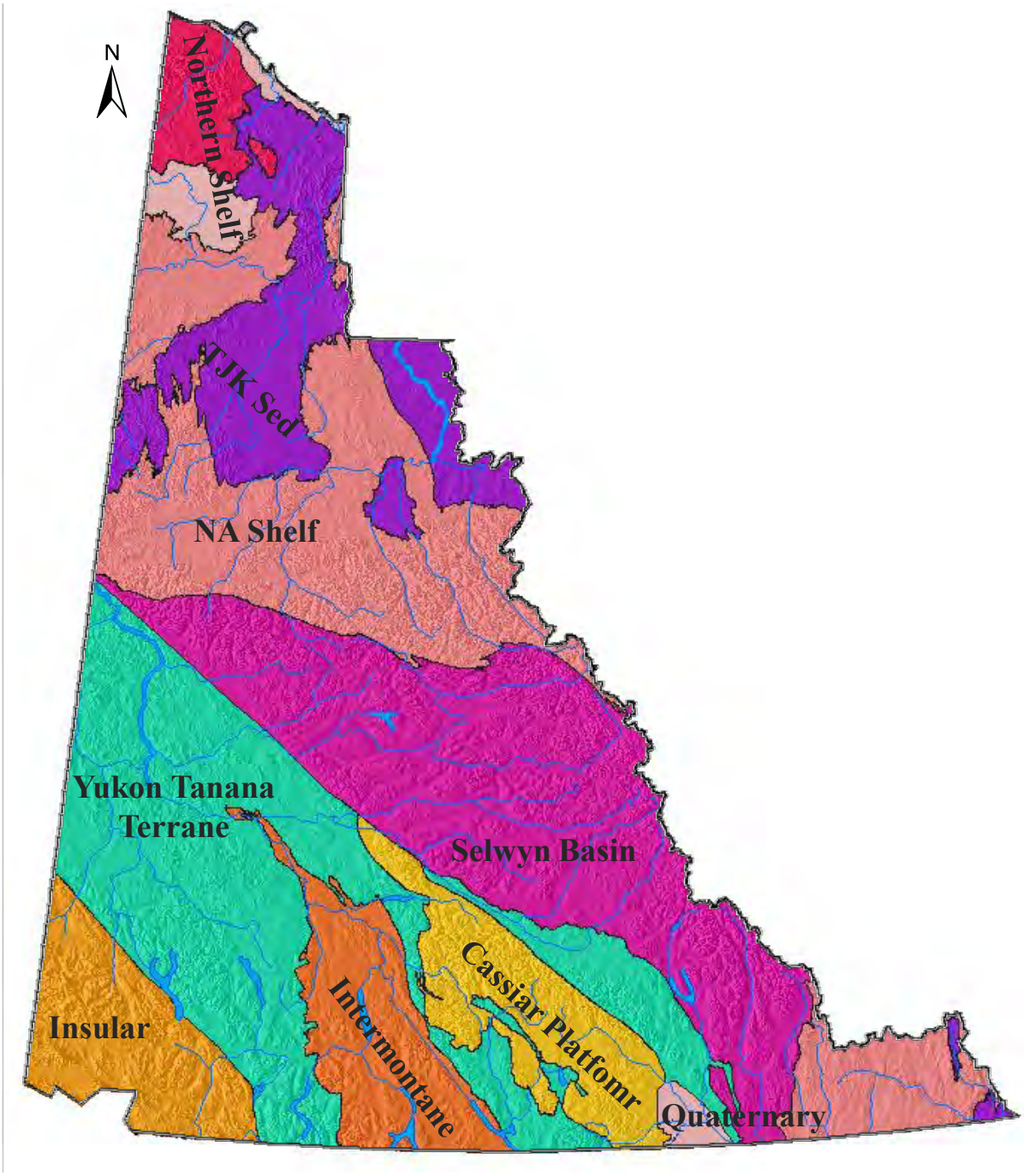

Figure A1.2 Geological division of YT, by terrain type (Yukon Government, 2012).

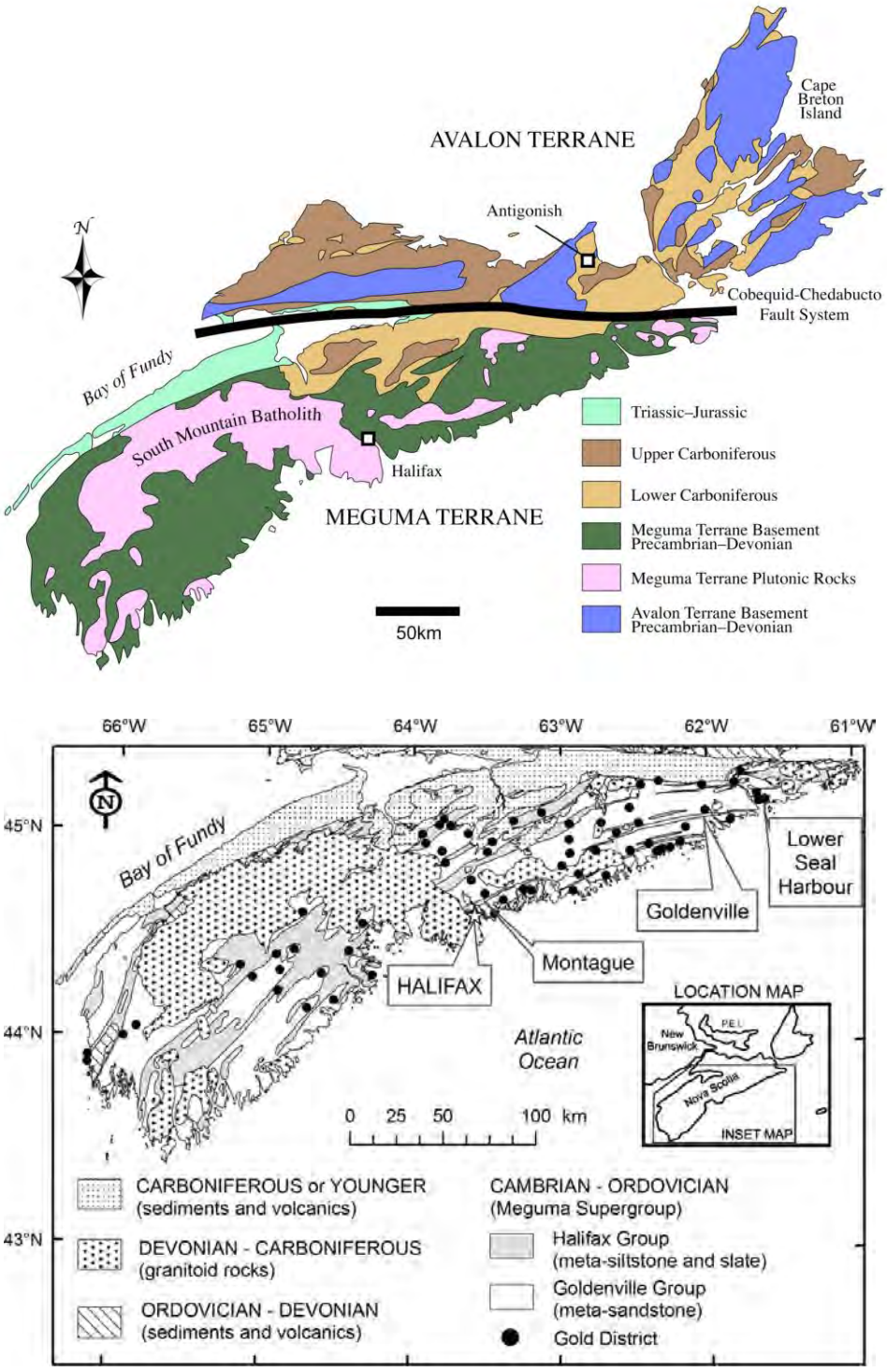

Figure A1.3 Geological map of NS (Top) and southern mainland NS with places of gold districts and detailed rock formations of the Meguma Terrane (bottom). Adopted from Corriveau *et al. (*2011).

Appendix 2 Sediment THg versus Land Cover Type, Northern Canada

The objective of this Appendix is to summarize how sediment THg values vary across Northern Canada by land cover type. Generally, sediment THg is lowest in streams and lakes when surrounded by ice and frost-worked mineral soils, and increases gradually to higher values as the vegetation cover increased from tundra and cryptogam covered barrens to wetlands, shrub lands, and forests. This analysis uses all the stream and lake sediment surveys north of 60˚ latitude, with land cover type specified according to the ecological land classification data layer and annual July air temperature (Chapter 3).

For northern Canada, stream and lake sediment THg ranges from 5 to 5,950 ppb with overall mean value of 65 ± SE 0.5 (n = 36,310; Figures A2.1, A2.2). The majority of the sediment samples (99.6 %) ranges between 5 and 600 ppb, with 112 values over 600 ppb (Figure. A2.2). There are 20 THg values > 1500 ppb in YT streams. Notable are the generally higher sediment THg (mean 110 ± SE 1.4, ppb) in the Selwyn Basin (zone 3, YT), and the generally lower THg (mean 25.4 ± SE 0.8, ppb) on Bathurst Island, NU (zone 4).

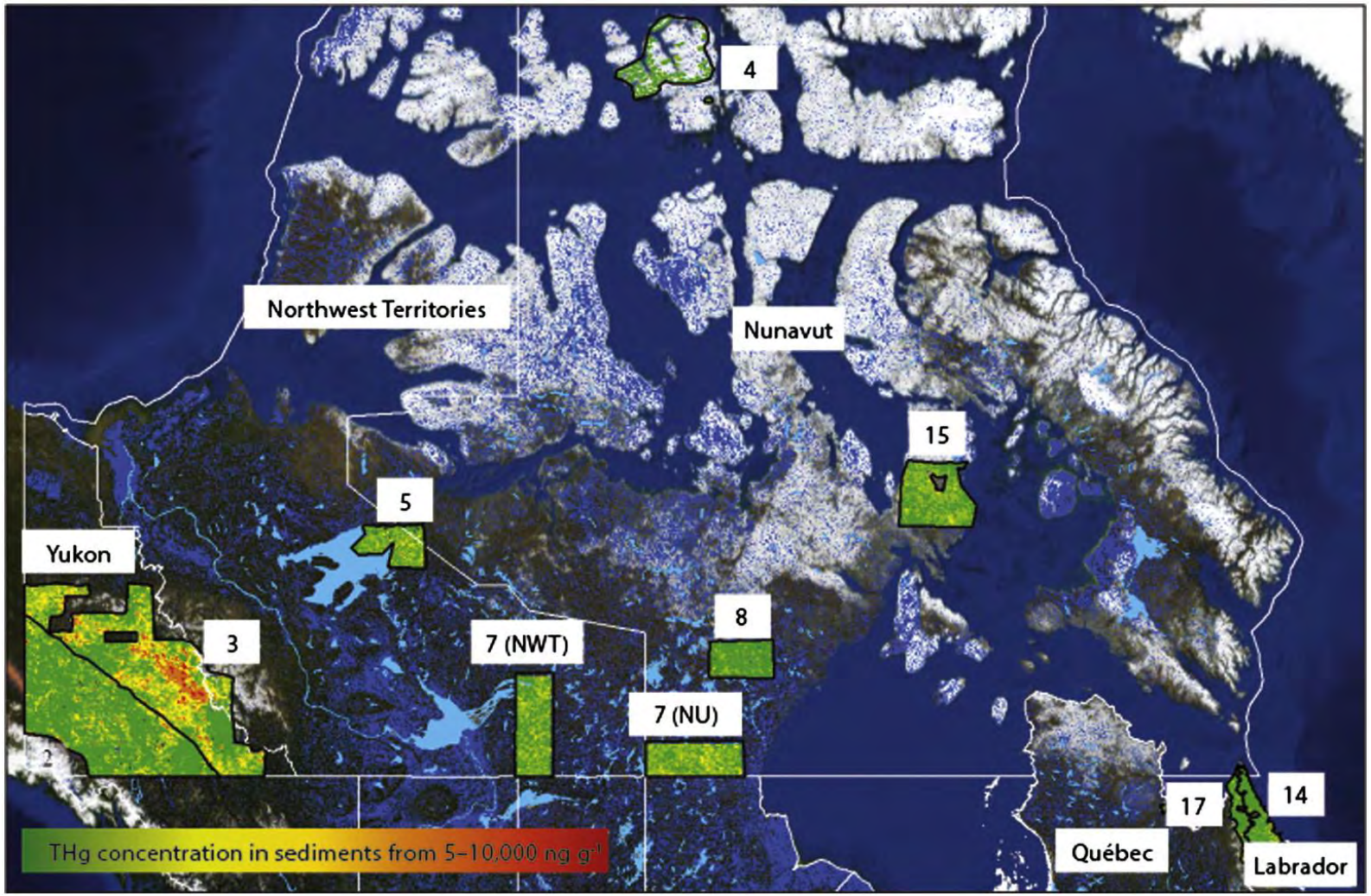

Figure A2.1 Overview of data compiled for stream and lake sediment THg (ppb) from low (green) to high (red) across northern Canada, by survey zone. Background: DEM derived lowlands (dark blue) and main surface water features (light blue), based on the national DEM (300 m resolution), also showing provincial/territorial borders.

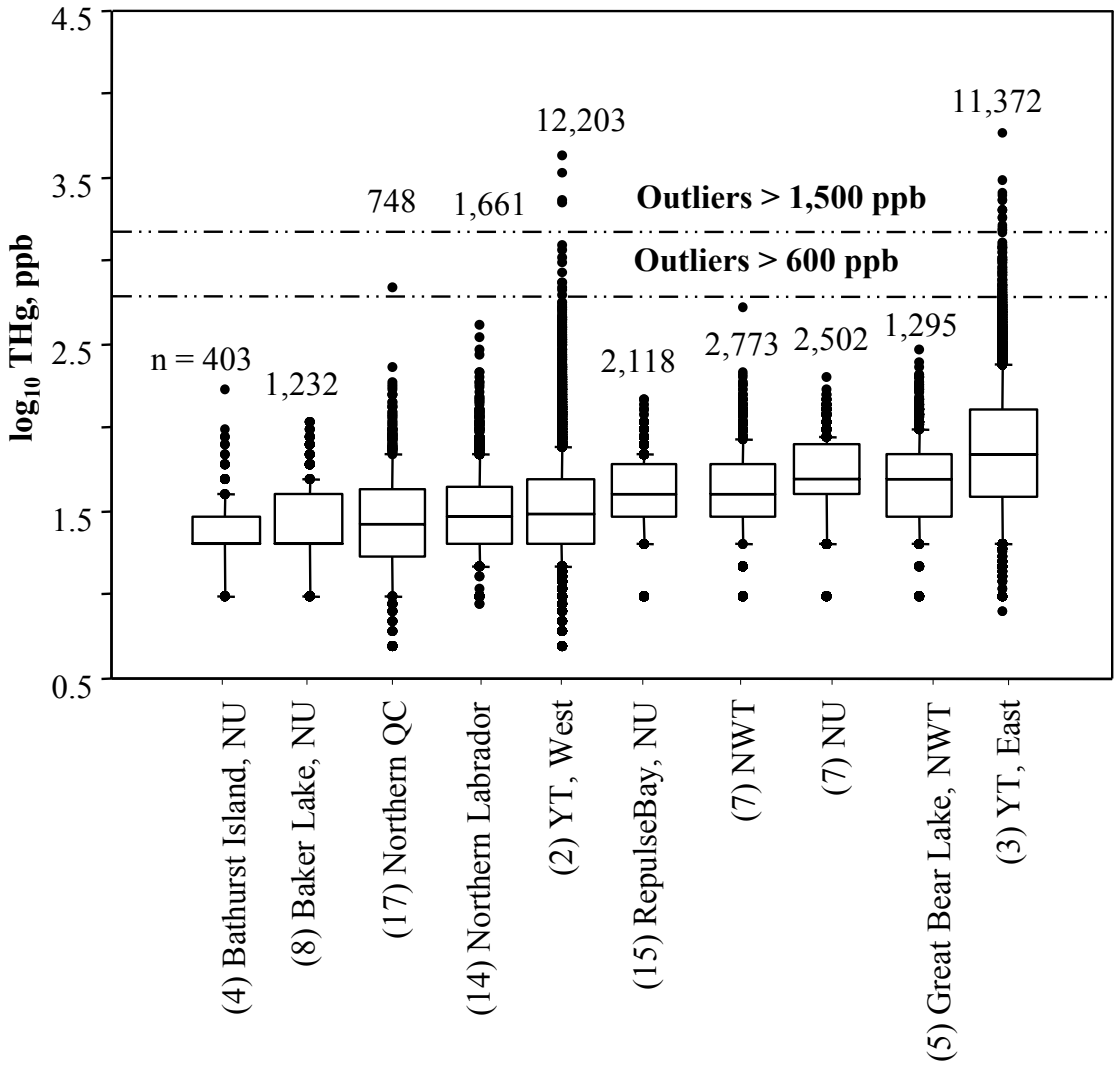

Figure A2.2 Box plots for stream and lake sediment log_{10}THg (ppb) across northern Canada, by survey zone (Figure A2.1). The line inside each box is the median, the upper and lower edges of the box are the 75th and 25th percentiles, and the upper and lower error bars are the 90th and 10th percentiles. Highly elevated outliers (THg ≥ 600 and 1,500 ppb) for the entire dataset are presented with dashed horizontal line. The boxes are arranged from low to high mean THg, by survey zone.

In each survey zone with both stream and lake data (YT, Labrador), mean THg was lower in streams than in lake sediments (p-value <0.0001). To this effect, the sediment content of Hg binding organic matter was also lower for streams (mean: LOI = 8 %) than for lakes (mean: LOI = 28 %). However, mean stream sediment THg easily exceeded mean lake sediment and vice versa in areas with high upstream THg sources.

Differentiating upland from lowland sediment sampling locations (Chapter 3) produces results that are similar to the national survey results in Chapter 4 (Table 2A.1). For the northern survey zones, overall mean THg is higher for upland lakes (48.5 ± 1.0 SE, ppb) and streams (77.9 ± 0.9 SE, ppb) than for lowland lakes (38.8 ± 1.0 SE, ppb) and streams (64.7 ± 1.6 SE, ppb).

There is a significant drop in mean THg from lake to stream (crit. mean = 2.2, p-value < 0.0001), from upland to lowland lakes (crit. mean = 1.2, p-value < 0.0001), and from upland to lowland streams (crit. mean = 4.1, p-value < 0.0001). These upland versus lowland trends are also found in specific survey zones, namely Great Bear Lake, NWT (zone 5: 60 vs. 50 ppb), Baker Lake, NU (zone 8: 33 vs. 26 ppb), the southern NWT (zone 7: 52 vs. 42 ppb), and southern NU (zone 7: 62 vs. 51 ppb).

Upland streams have significantly higher THg compared to lowland locations in the east-central YT (Selwyn Basin, zone 3; 113 vs. 96 ppb) and west YT (zone 2: 43 vs. 37 ppb). This trend can be explained by upland sediments being closer to geogenic Hg sources. As a result, sediment THg decreases towards the more distant lowlands on account of gradual Hg volatilization and en-route filtration and settling of Hg-carrying particles.

Average GRAHM2005 mean annual net atmospheric Hg deposition rates for survey zones vary from 6 to 12 μg m^{-2} a^{-1} (Table 2A.2). In each survey zone, sediment THg is not related to the large-scale GRAHM projections (grid cells of 25 × 25 km). Likewise, sediment THg is not related to the modeled atmospheric deposition across the survey zones. The lack of correspondence may be due to:

- the importance of watershed transport processes that occur following deposition;
- the 1970 to 1990 THg data predate the 2005 model for atmospheric Hg deposition;
- the sediment sampling depth of up to 30 cm, which weakens detection of accelerated atmospheric Hg deposition over recent times;
- the relatively narrow range of net atmospheric Hg deposition and sediment THg flux rates across the Arctic region.

Table A2.1 Sediment THg (ppb) of northern Canada (above 60˚ north), by survey zone, upland/lowland location, and medium type (stream, lake).

Northern Canada Survey zone	Terrain	Lake sediment THg, ppb					
		n	Mean	Std. Dev.	Std. Err.	Crit. Diff.*	p-value*
Baker Lake, NU (8)	Upland	546	**32.9**	19.4	0.8	2.0	<0.0001
	Lowland	686	**25.9**	16.7	0.6		
QC, north (17)	Upland	635	**35.9**	38.7	1.5	7.6	0.7555
	Lowland	113	**37.1**	33.1	3.1		
Labrador, north, NL (14)	Upland	453	**49.3**	26.3	1.2	6.2	0.0654
	Lowland	78	**43.4**	23.7	2.7		
YT, west (2)	Upland	80	**58.6**	48.9	5.5	19.8	0.1922
	Lowland	28	**45.5**	34.0	6.4		
Melville Peninsula, NU (15)	Upland	1,539	**44.7**	19.8	0.5	1.9	0.0700
	Lowland	579	**42.9**	21.7	0.9		
NWT (7)	Upland	1,780	**52.1**	29.3	0.7	2.3	<0.0001
	Lowland	993	**42.3**	30.4	1.0		
NU (7)	Upland	1,300	**61.9**	27.2	0.8	3.6	<0.0001
	Lowland	1,202	**50.9**	26.9	0.8		
Great Bear Lake north-east, NWT (5)	Upland	906	**59.7**	36.7	1.2	4.2	<0.0001
	Lowland	392	**50.0**	32.2	1.6		
YT, east (3)	Upland	72	**123.2**	111.3	13.1	47.8	0.4700
	Lowland	24	**105.8**	66.7	13.6		
Zones with stream & lake data	Upland	605	**59.3**	39.4	3.2	26.4	0.2373
	Lowland	130	**55.4**	33.8	5.5		
Total **		735	**58.6**	38.4	3.6		
All zones	Upland	7,311	**48.5**	27.3	1.0	1.2	<0.0001
	Lowland	4,095	**38.8**	23.4	1.0		
Total **		11,406	**45.0**	25.9	1.0		

TableA2.1 Continued:

Northern Canada	Stream sediment THg, ppb						Lake versus stream	
Survey zone	**n**	**Mean**	**Std. Dev.**	**Std. Err.**	**Crit. Diff.***	**p-value***	**Crit. Diff.**	**p-value**
Bathurst Island, NU (4)	311	**25.7**	16.4	0.9	1.6	0.4210	-	-
	92	**24.1**	16.3	1.7			-	-
Labrador, north, NL (14)	997	**32.1**	32.0	1.01	5.5	0.0737	3.0	<0.0001
	133	**27.0**	17.8	1.55				
YT, West (2)	10,212	**44.9**	79.1	0.8	3.6	<0.0001	17.1	0.10
	1,883	**37.8**	34.4	0.8			12.7	0.20
YT, east (3)	9,557	**112.7**	153.4	1.6	7.7	<0.0001	35.5	0.56
	1,719	**95.7**	127.4	3.1			51.1	0.70
Zones with stream & lake data	20,766	**76.9**	124.7	0.9	4.2	<0.0001	1.9	<0.0001
	3,735	**64.4**	95.0	1.6			2.9	<0.0001
Total **	24,501	**75.0**	120.2	1.0			2.1	<0.0001
All zones	20,130	**77.9**	114.5	0.9	4.1	<0.0001	2.2	<0.0001
	3,701	**64.7**	77.3	1.6				
Total **	23,831	**75.8**	108.8	1.0				

* Critical difference (Crit. Diff.) by Fisher's Probable Least Squares Difference (PLSD).

** Weighted mean, standard deviation (Std. Dev.), and standard error (Std. Err.).

No lake samples: Bathurst Island, NU (4). No stream samples: Baker Lake, NU (8), QC, north (17), Melville Peninsula, NU (15), NWT (7), NU (7), Great Bear Lake north-east, NWT (5).

Northern sediment THg varies by vegetation cover type (Tables 2A.2, 2A.3). Areas with dominant snow and ice and sparse to non-vegetative surface cover have the lowest sediment THg, while coniferous and mixedwood locations have significantly higher values (p-value < 0.0001). On average, stream sediment THg remains higher when derived from areas covered by conifer, mixedwood, wetlands, and graminoid and shrub tundra than from other land types.

For lake sediments, the THg range is narrower than for streams, and is highest when derived from areas with coniferous, mixedwood and broadleaf canopy covers. Highest sediment THg therefore occurs downstream from forested areas in the Churchill region of QC, Labrador, YT, and close to southern boreal shield in NWT and NU, northeast of the Great Bear Lake, NWT, and Baker Lake, NU.

Re-analyzing the sediment THg values by excluding the YT samples (because of its generally alpine conditions and the black shale THg anomaly of the Selwyn Basin) produces a statistically well-defined profile for mean sediment THg by land cover type (Tables A2.4, A2.5; Figure A2.3). This analysis shows, once again, a strong positive relationship between sediment THg, mean annual July temperature and land cover type (Figure A2.4). In this grouping, sediment THg is lowest downstream from frost-worked soils (cryptogam crust-frost boils with sparsely graminoids and cryptogam plants). Sediment THg values would be somewhat higher downstream from barrens than tundra vegetation due to long-lasting bedrock-covering Hg-retaining lichens relative to the short-lasting annual vegetation comprised of grasses, herbs, mosses, and shrubs.

Table A2.2 Ecozones and dominant vegetation/land cover type by sediment survey zone across northern Canada (above 60˚ north), with corresponding mean GRAHM2005 annual net atmospheric Hg deposition rate ($atmHg_{dep}$; µg m^{-2} a^{-1}).

Northern Canada survey zone	**Ecozone ***	**Dominant vegetation/land cover ***	**atm.$Hg_{dep.}$ ** µg m^{-2} a^{-1}**
Bathurst Island, NU(4)	North Arctic	Barren, none/sparsely vegetation, mostly coveed by snow/ice	7.4
Baker Lake, NU (8)	South Arctic	Tundra, wetland, shrubs, Barren, none/sparsely vegetation, Bryoids	9.1
QC, north (17)	Arctic Cordillera	Barren, none/sparsely vegetation, shrubs, open and sparse coniferous	12.3
Labrador, north, NL (14)	Arctic Cordillera	Barren, none/sparsely vegetation, shrubs	10.0
YT, west (2)	Taiga Cordillera	Mixedwood, broadleaf, coniferous, shrub, herb, exposed land and rock, wetland	8.3
Melville Peninsula, NU (15)	North Arctic	Barren, bare soil with cryptogam crust, none/sparsely vegetative colluvium till,	9.8
NWT (7)	Taiga Arctic	Mixedwood, broadleaf, coniferous, shrub, exposed land, wetland (treed, herb, shrub)	10.9
NU (7)	Taiga Shield	Bryoids, shrub, exposed rock with none/sparsely vegetation, dense coniferous	9.9
Great Bear Lake north-east, NWT (5)	Taiga Shield & Taiga plain	Bryoids, Mixedwood, broadleaf, coniferous, shrub, exposed land, wetland	6.4
YT, east (3)	Taiga Cordillera & Boreal cordillera	Mixedwood, broadleaf, coniferous, shrub, herb, exposed land and rock, wetland	8.3

* Obtained by geospatial analysis (Chapter 3) from GIS data of Canada ecological map framework, adapted from Ecological Stratification Working Group, 1996. **GRAHM2005 mean annual net atmospheric Hg deposition rate (atm.Hgdep., µg m^{-2} a^{-1}).

Table A2.3 Stream and lake sediment THg (ppb) of northern Canada (above 60˚ north), by vegetation/land cover type.

Northern Canada	Sediments THg, ppb						Crit. Diff. **		
vegetation/land cover	n	Mean	Min.	Max.	Std. Dev.	Std. Err.	Conifer[a]	Mixedwood[b]	p-value
Snow/ice *	109	**28.6**	10	217	26.8	2.6	20.6	23.6	<0.0001
Sparse vegetation	2,134	**41.9**	5	232	23.7	0.5	5.1	12.6	<0.0001
no-vegetation	1,364	**50.4**	5	2,280	77.9	2.1	6.1	13.1	<0.0001
Wetlands	494	**55.7**	7	680	61.4	2.8	9.8	15.2	<0.0001
Graminoid Tundras	2,300	**57.9**	5	3,018	88.8	1.9	4.9	12.6	<0.0001
Broadleaves	329	**64.1**	6	615	77.0	4.3	12.0	16.6	0.0032[a] 0.0002[b]
Shrub Tundras	10,690	**64.3**	5	4,350	98.6	1.0	2.9	11.9	<0.0001
Conifers	11,440	**82.1**	5	5,950	133.5	1.3	11.9		0.0306
Mixedwoods	333	**95.2**	9	2,050	165.0	9.0			
Total	29,193	**68.5**	5	5,950	110.0	0.6			

* Glacial or non-glacial

** Critical difference (Crit. Diff.) and p-value by Fisher's Probable Least Squares Difference (PLSD).

Table A2.4 stream and lake sediment THg (ppb) of northern Canada (above 60˚ north), by vegetation/land cover type.

Northern Canada, excluding YT	n	log_{10}THg, ppb					atm. Hg_{dep} **	T_{July} **	$T_{Jan.}$ **	ppt **
vegetation/land cover		Mean	Min.	Max.	Std. Dev.*	Std. Err.*	µg m^{-2} a^{-1}	˚C	˚C	m a^{-1}
Frost-worked soil	404	25.8	10	170	18.0	1.2	8.2	6.5	-31.3	0.418
Tundras	2,374	36.0	5	696	30.0	0.6	9.6	9.7	-29.2	0.355
Barrens	2,533	43.9	5	300	26.5	0.5	10.0	8.4	-28.5	0.369
Shrubs	824	54.4	5	727	63.1	2.2	9.5	11.4	-24.8	0.478
Welands	533	50.2	5	525	38.0	1.6	9.7	11.5	-28.8	0.355
Conifers	554	75.5	5	712	67.4	2.9	9.0	15.1	-26.2	0.333
Broadleaves	33	76.6	15	215	51.2	8.9	8.8	14.8	-26.6	0.306

* Critical difference (Crit. Diff.) and p-value by Fisher's Probable Least Squares Difference (PLSD). **GRAHM2005 mean annual net atmospheric Hg deposition rate (atm.Hgdep., µg m^{-2} a^{-1}); mean annual July temprature (T_{July}, ˚C) and January Temprature ($T_{Jan.}$ ˚C); mean annual precipitation rate (ppt, m a^{-1}).

Table A2.5 Mean differences for stream and lake sediment log_{10}THg (ppb) of northern Canada (above 60˚ north, excluding YT), by vegetation/land cover type.

Northern Canada, excluding YT vegetation/land cover	Frost-worked soil	Tundras	Barrens	Shrubs	Welands	Conifers	Broadleaves
Frost-worked soil	0						
Tundras	**0.130**	0					
Barrens	**0.237**	**0.107**	0				
Shrubs	**0.236**	**0.106**	0.000	0			
Welands	**0.275**	**0.145**	**0.038**	0.039	0		
Conifers	**0.429**	**0.299**	**0.192**	**0.192**	**0.154**	0	
Broadleaves	**0.474**	**0.344**	**0.237**	**0.238**	**0.199**	0.045	0

Bold: significant at p-value < 0.0001

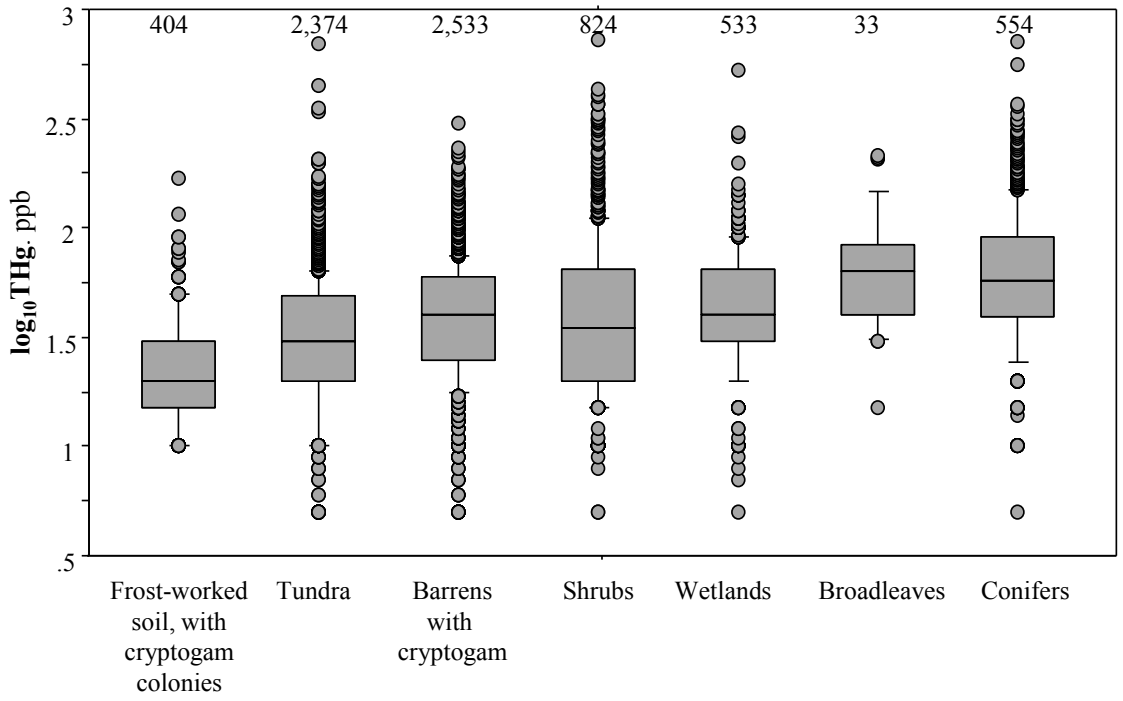

Figure A2.3 Box plots for stream and lake sediment log_{10}THg (ppb) across northern Canada (above 60˚ north, excluding YT), by vegetation/land cover type. The line inside each box is the median, the upper and lower edges of the box are the 75th and 25th percentiles, and the lower and upper error bars are the 10th and 90th percentiles. The boxes are arranged from low to high mean THg, by vegetation/land cover type.

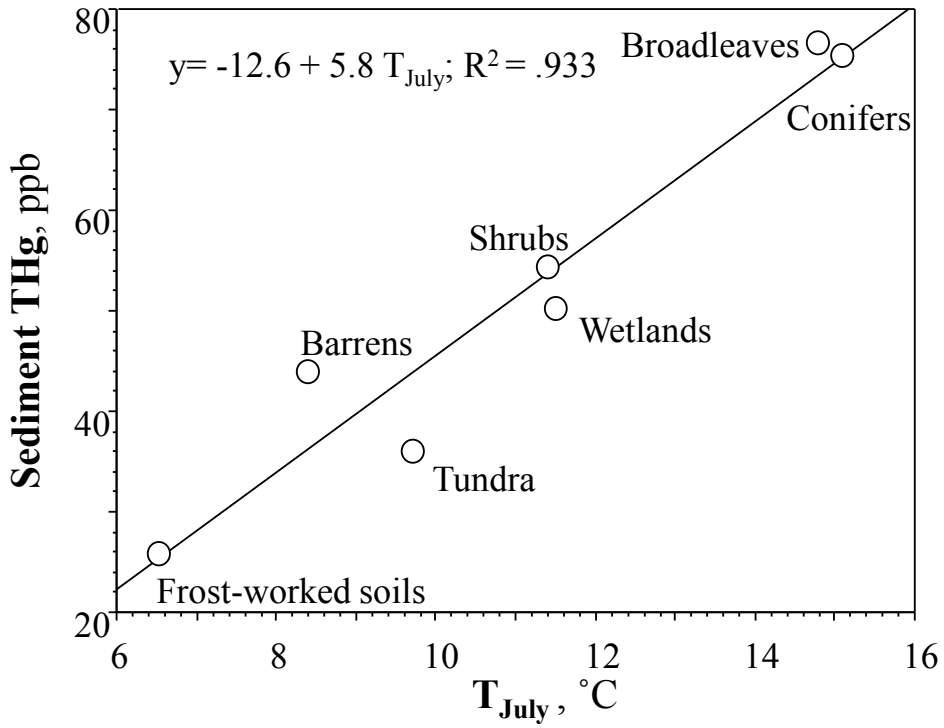

Figure A2.4 Scatterplots of stream and lake sediment THg (ppb) versus T_{July} (˚C), by vegetation land cover type across northern Canada (above 60˚ north excluding YT).

The strong correlation between THg and July temperature (R^2= 0.93; Figure A2.4) suggests the following:

- Frost-worked mineral soil as they occur across cold northern floodplains (mean July temperatures at a 6.5 ± 2.2 SD, ˚C) produce sediments with low THg values, possibly on account of low Hg retention by sparse crypotogamic vegetation cover (average season with T > 0 ˚C ≈ 2 to 3 months). The sediment THg value of 25.8 ppb is similar to the average THg value for glacial tills (Chapter 6), hence the sediments derived from frost-worked soils are essentially till derived, hence mostly geogenic, with little if any atmospheric THg added.
- Barren landscapes produce sediment with appreciably higher sediment THg than landscapes with frost-worked soils, because cryptogamic vegetation (mostly lichens) lasts long, grows slowly across especially on exposed rock surfaces, and remains essentially remains undisturbed from year to year. With T_{July} = 8.4 ± 2.1 SD ˚C across the barren landscapes, the T > 0 ˚C season lasts approximately 2.5 to 3.5 months.
- Compared to barren dominated areas, tundra areas produce sediments with somewhat lower THg values due to its vegetation mix, which - apart from lichens - includes faster growing shrubs, grasses, and mosses in varying proportions. With T_{July} = 9.7 ± 2.0 SD 2.0 ˚C across the tundra landscapes, the T > 0 ˚C season lasts for approximately 3 to 4 months.
- As mean July temperatures increase towards 11.57 ± 3.0 SD ˚C, and the season with T > 0 ˚C lasts from 3.5 to 5 months, shrubs become taller on uplands and wetlands, and with that, atmospheric THg sequestration increases as well. At the

- same time, overall Hg retention increases because of increased shading of Hg containing litter below the shrub canopies.
- As mean July temperatures increase towards 15 ± 1.7 SD ˚C, and the season with T 0 ˚C lasts from 4 to 6 months, there is a gradual transition from tall shrubs to forest. With that, overall atmospheric Hg sequestration and retention increases further because of an increased leaf duration and production per ground area, and increased shading of the Hg containing forest litter.

Due to the law of central tendency, the correlation coefficient between sediment Hg and mean July temperature increases strongly from 0.230 (R^2 = 0.053) by sampling location to 0.966 (R^2 = 0.933) by cover type. This suggests that increasing summer temperatures across northern Canada not only enhance vegetative growth across northern Canada (as to be expected), but also enhance the atmospherically-derived Hg component in sediments. Note that a positive relationship between sediment THg and mean July temperature also exist across all of Canada as documented in Chapter 6, but that result is not as direct because of the additional correlations between sediment THg, mean annual precipitation rates, and atmospheric Hg deposition.

Appendix 3 Sediment THg versus Land Cover Type, Cape Breton, NS

The objective of this Appendix is to demonstrate how sediment THg varies by land cover type. This is done by selecting Cape Breton stream and lake sediments on (n = 2,978) as a case study. Within this selection, stream sediment THg decreases as the wet-area percentage of the basin area above each sampling location increased (Table 3A.1). In this analysis, wet-area refers to DTW < 0.5 m, with surface water features for which DTW = 0 excluded. In addition:

- the sediment THg is higher in the stream basins with swamps than basins with marshes, bogs or fens (p-value < 0.0001; Figure A3.1);
- sediment THg is generally lower for non-forested than forested watersheds;
- wetter watersheds have less sediment THg than drier watersheds (Table 3A.2);
- mean sediment THg is higher in watersheds with no wetlands (141 ± 13 SE, ppb) than watersheds with wetland inclusions (96 ± 3 SE, ppb; p-value < 0.0001);
- stream sediment THg is higher at 143 ± SE 14 ppb for the smaller non-wetland watersheds with large forest (74 %) areas but low surface water (0.2 %) and wet-area (4 %) coverages;.
- in contrast, sediment is lower at 92 ± 4 SE ppb for the larger watersheds with smaller forest (45 %) but larger surface water (22 %), and wet-area (15 %) coverages (p-value < 0.0001).

Table A3.1 Stream sediment log_{10}THg (ppb), basin area (A_B, ha), wet-area (A_W, ha) and mean wet-area to basin-area ratios (A_W/AB; %), by log_{10}THg range of Cape Breton, NS.

Sediment log_{10}THg, ppb	n	Mean area, ha		A_B/A_W, %*	
Range		A_B	A_W	per basin	Across basin
1.0-1.70	934	889	158	15.0	17.8
1.70-1.95	797	553	90	11.3	16.3
1.95-2.20	563	444	54	8.3	12.2
2.20-2.52	256	616	59	6.9	9.5
2.52-2.70	66	671	60	7.2	8.9
2.70-2.73	11	259	19	6.3	7.1

*Area of basin (A_B, ha) devided by area of wet-area of each basin (A_W, ha). A_W referred to (DTW < 0.5 m, excluding surface water).

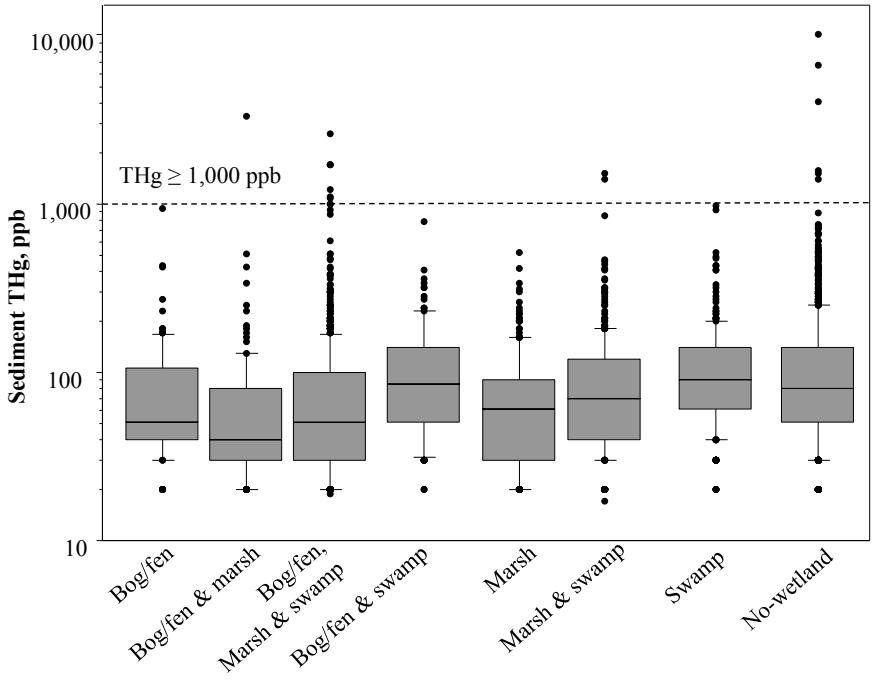

Figure A3.1 Boxplot of stream sediment THg (ppb) for Cape Breton, NS, by upstream wetland type. The line inside each box is the median, the upper and lower edges of the box are the 75th and 25th percentiles, and the lower and upper error bars are the 10th and 90th percentiles. Highly elevated outliers (THg ≥ 1,000 ppb) for the entire dataset are presented with dashed horizontal line. The boxes are arranged from low to high mean THg, by wetland type.

Table A3.2 Stream and lake sediment THg (ppb) of Cape Breton, NS, by wetland, water body, and forest areas (ha; %), by non-wetland and wetland-dominated basins.

Basin	n	Sediment THg, ppb			A_B	Forest	Surface water	Wetland	A_W/A_B*
		mean	Std. Dev.	Std. Err.	ha		ha		%
No-wetland	982	**141**	419	13	101	75	0.4	0	4
Forested	962	**142**	423	14	103	76	0.4	0	4
Stream	935	**143**	429	14	105	78	0.2	0	4
Lake	27	**104**	36	7	44	21	7.8	0	8
Non-forested	20	**81**	60	13	4	0	0.0	0	26
Stream	16	**75**	64	16	5	0	0.0	0	13
Lake	4	**103**	39	19	0.1	0	0.0	0	74
Wetland	1,996	**96**	154	3	1,299	580	54	152	17
Forested	1,968	**97**	155	3	1,317	588	55	154	16
Stream	1,651	**92**	166	4	1,025	467	23	123	15
Lake	317	**122**	56	3	2,916	1,248	227	329	21
Non-forested	28	**62**	45	9	22	0	0.1	9	65
Stream	23	**49**	37	8	26	0	0.0	10	59
Lake	5	**122**	26	12	4	0	0.6	2	91

*Area of basin (AB, ha) devided by area of wet-area of each basin (AW, ha). A_W referred to (DTW < 0.5 m, excluding surface water). Standard deviation (Std. Dev.). Standard error (Std. Err.).

Appendix 4 Sediment Cu versus LOI

The objective of this Appendix is to show that the total sediment concentrations for Cu increase with respect to increasing sediment LOI content in the same way that sediment THg did. This is done by plotting and modelling the 10^{th} and 90^{th} $\log_{10}$Cu percentiles of the open file data for sediment Cu per each 10 % LOI class, by province/territory and QC geological survey zones. The model for the 10^{th} and 90^{th} $\log_{10}$Cu percentiles, in analogy to Eqs. 3.1 and 3.2, is given by:

$$\log_{10}Cu_{i,j}\,(ppb) = a_{ij}\,(1 - LOI\,(\%) / 100) + b_{ij}\,[1 - \exp(- c_j\,LOI\,(\%) / 100)] \qquad \text{Eq. 4A.1}$$

The best-fit results produced with the above equation are overlaid on the actual percentile values in Figure 4A.1. Based on the corresponding best-fit a_{ij} and b_{ij} coefficients (Table A4.1) and Table 6.3, it follows that the mean (%) value for a_{ij} is approximately 500 times larger for $\log_{10}$Cu than for $\log_{10}$THg, i.e. 0.67 ppm versus 1.12 ppb, respectively. Hence, the mineral-based contributions to sediment Cu are approximately 500 times larger than for sediment THg. Nevertheless, the organic matter contributions to THg and Cu asymptotically approach their upper ppb and ppm b_{ij} values at approximately the same rate as LOI increased towards 100 %. This means that the c_j coefficients are approximately the same for sediment THg and sediment Cu.

This similarity between THg and Cu is due to the generally strong affiliation between humified organic matter and heavy metal ions. The best-fit Cu b_{ij} coefficients, however, do not correlate with mean annual precipitation rates by province/territory and QC geological survey zone (Table A4.1). This result is undoubtedly due to the Hg versus Cu difference in volatility, and hence the lower availability of Cu for long-range

atmospheric transport and deposition. As a consequence, the Cu contributions to sediment organic matter remain unchanged or decrease somewhat with increasing atmospheric deposition, as follows:

- for the stream and lake sediments, the $\log_{10}$Cu b_{ij} coefficients for the 10^{th} and 90^{th} percentiles do not change significantly with increasing mean annual precipitation rates (R^2 = 0.059 and 0.001 for lakes, and at R^2 = 0.022 and 0.037 for streams, respectively);
- for stream $\log_{10}$Cu a_{ij} coefficients:

$$\log_{10}\text{Cu}\ (a_{ij}, \text{ppm}) = 0.851 - 0.335\ \text{ppt}\ (\text{m a}^{-1}) \qquad R^2 = 0.121 \qquad \text{Eq. 4A.2}$$

Hence, the stream $a_{ij,}$ coefficients for $\log_{10}$Cu decrease slightly with increasing precipitation rate, due to increased Cu solubilisation and leaching from soils. This leaching would increase further with increasing soil acidity, and would therefore be strongest in areas and watersheds with coniferous forest cover. For the lake $\log_{10}$Cu a_{ij} coefficients, any changes from areas with low to increasing precipitation rates remain insignificant (R^2 = 0. 013).

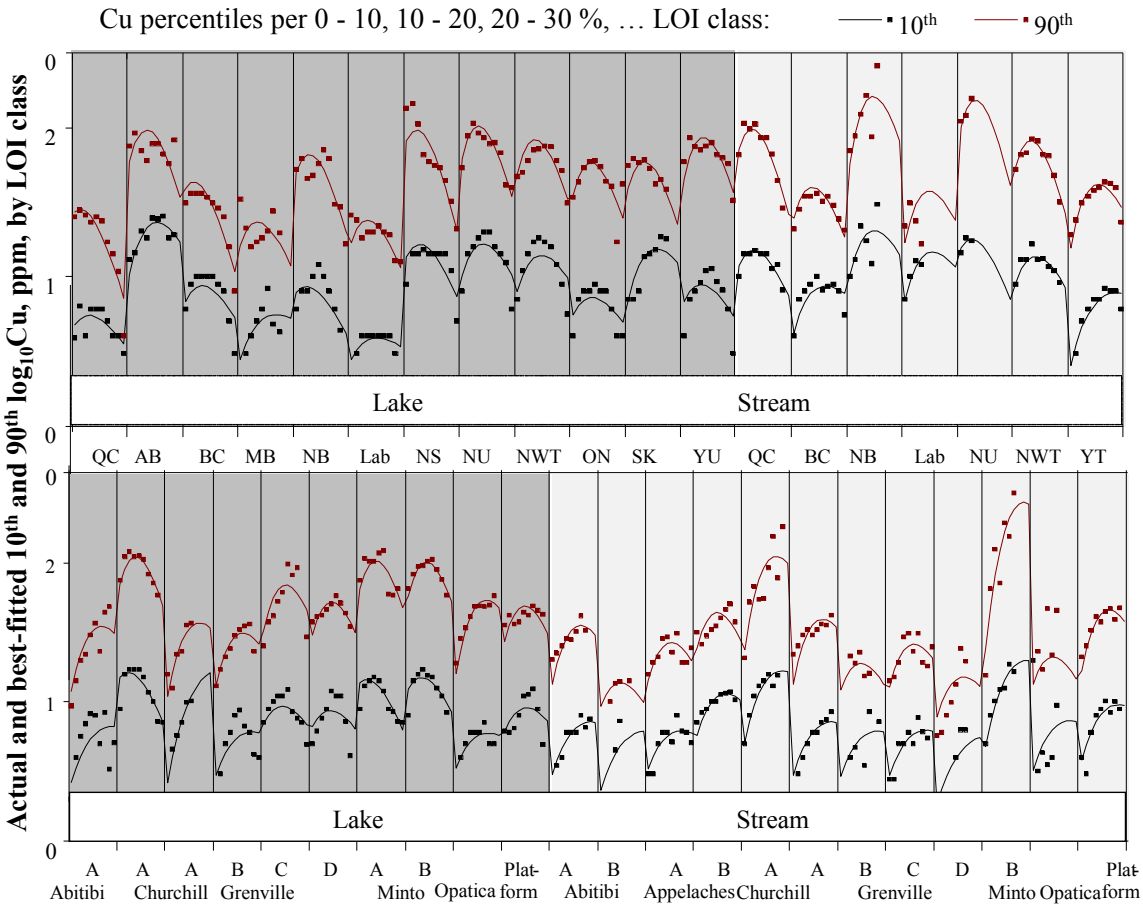

Figure A4.1 Plots of actual versus best-fit (Eq. 4A.1) 10th and 90th percentiles for stream and lake sediment log_{10}Cu (ppm) versus LOI (%), by province/territory (top) and QC geological survey zone (18-30; bottom).

Table A4.1 Best-fit a_{ij} and b_{ij} parameter values and sediment Cu concentration (ppm) for the 10th and 90th percentiles of Cu for LOI = 0 versus 100 %, by province/territory and QC geological survey zone (18-30), and medium type (stream, lake; Eq. 4A.1: Figure 4A.1).

Location	Medium	ppt*	Subscript		$\log_{10}$Cu (ppm) Parameters		
					a_{ij}	b_{ij}	
		m a^{-1}	i	j	10th	10th	90th
Abitibi A	**Lake**	0.95	1	1	0.35	1.02	1.82
Churchill A	QC	0.64	3		1.15	1.01	2.02
Grenville A		0.96	6		0.31	1.51	1.87
Grenville B		0.98	7		0.41	0.96	1.72
Grenville C		0.97	8		0.80	1.01	2.01
Grenville D		1.05	9		0.78	0.97	1.80
Minto A		0.76	10		1.11	0.94	2.01
Minto B		0.61	11		1.05	1.11	2.07
Opatica		0.82	12		0.47	0.93	2.05
Plate-forme		1.09	13		0.73	1.05	1.79
QC	Canada	0.85	14		0.65	0.58	0.89
AB		0.40	15		0.92	1.34	1.64
BC		0.79	16		0.79	0.78	1.08
MB		0.47	17		0.38	0.79	1.15
NB		1.28	18		0.87	0.65	1.38
NL		0.88	19		0.46	0.43	1.10
NS		1.39	20		1.09	0.91	1.38
NU		0.30	21		0.94	1.09	1.65
NWT		0.31	22		0.82	1.07	1.62
ON		0.86	23		0.69	0.74	1.49
SK		0.46	24		0.75	1.19	1.44
YT		0.36	25		0.79	0.79	1.68
Abitibi A	**Stream**	0.88	1	2	0.41	1.05	1.80
Abitibi B	QC	0.95	2		0.20	0.98	1.19
Appalaches A		1.16	3		0.46	0.95	1.57
Appalaches B		0.95	4		0.69	1.24	1.75
Churchill A		0.69	5		0.62	1.50	2.44
Grenville A		1.00	6		0.41	1.05	1.87
Grenville B		1.08	7		0.41	0.97	1.35
Grenville C		1.08	8		0.41	0.97	1.59
Grenville D		1.05	9		0.20	0.93	1.35
Minto B		0.58	11		0.58	1.60	2.98
Opatica		0.75	12		0.45	1.06	1.41
Plate-forme		1.07	13		0.48	1.22	1.89
QC	Canada	0.96	14		1.03	0.93	1.50
BC		1.09	16		0.55	0.97	1.36
NB		1.15	18		0.99	1.17	2.14
NL		0.63	19		0.72	1.22	1.54
NU		0.30	21		1.15	0.89	1.71
NWT		0.32	22		0.90	1.00	1.51
YT		0.36	25		0.31	0.99	1.59

a_{ij} (90th) = a_{ij} (10th) + (0.648 ± SE 0.027); a_{ij} and b_{ij} standard error (Std. Err.: SE) = ± 0.15; cj = 0.0178± SE 0.0011. * mean annual precipitation rate (ppt, m a^{-1}).

Appendix 5 Sediment THg versus Fish Hg across Canada

Introduction

This Appendix documents the extent to which Hg in fish and in lake sediments is related to the variations in atmospheric Hg deposition rate and climate across Canada. This analysis was enabled by the recent release of the FIMDAC (Chapter 3).

Results and Discussion

Regressing the standardized values for fish $\log_{10}$Hg against lake sediment $\log_{10}$THg, mean annual GRAHM2005 estimated atmospheric Hg deposition rate, mean annual precipitation rate, and mean July air temperature per NTS tile generated the following equation:

Yellow perch $\log_{10}$Hg (ppb) = (1.32 ± 0.02 SD) Sediment $\log_{10}$THg (ppb; lake)

- (0.031 ± 0.002 SD) T_{July} (˚C) $R^2 = 0.382$ Eq. A5.1

where Sediment $\log_{10}$THg refers to the best-fisted model acquired from Eq. 6.5 (Chapter 6), based on mean annual precipitation and GRAHM-estimated atmospheric Hg deposition rates as follows:

$\log_{10}$THg(ppb; lake) = (1.380 ± 0.048 SD) + (0.406± 0.059 SD) ppt (m a^{-1})

+ (0.012± 0.004 SD) $atm.Hg_{dep}$ (μg m^{-2} a^{-1}) $R^2 = 0.432$ Eq. 6.5

According to the best-fit model of Eq. 5.1 (Chapter 5) for GRAHM estimates for atmospheric Hg deposition, 80 % of the GRAHM estimates for atmospheric Hg deposition relate to climate and geographic locations as follows:

$atm.Hg_{dep.}$ ($\mu g\ m^{-2}\ a^{-1}$) = - (24.7 ± 0.8 SD) + (26.8 ± 1.0 SD) ppt $(m\ a^{-1})^{0.5}$

+ (0.80 ± 0.06 SD) T_{July} ˚C) - (0.25 ± 0.03 SD) $T_{Jan.}$ (˚C)

- (7.7 ± 0.7 SD) Pacific Rim + (7.5 ± 1.0 SD) Bathurst Island $R^2 = 0.803$ Eq. 5.1

with Pacific Rim and Bathurst locations coded 1, and 0 otherwise. The non-linear precipitation term accounts for at least some of the wet deposition component of atmospheric Hg deposition. The mean annual temperature terms may in part account for:

- the geographical distribution of Hg emissions and deposition, which - in Canada - are highest along southeast and the Pacific Rim, and least in the High Arctic and on ice-covered alpine areas;
- the lower Hg volatility at low temperatures.

The location-specific adjustments compensate for:

- a precipitation-induced atmospheric Hg deposition rate over- estimations for the Pacific Rim;
- temperature-induced under-estimations for the atmospheric Hg deposition rates on Bathurst Island.

By climate variables, the regression analysis generate the following best-fit results for yellow perch $log_{10}Hg$:

Yellow perch $log_{10}Hg$ (ppb) = (1.54 ± 0.07 SD) + (0.77 ± 0.02 SD) ppt $(m\ a^{-1})$

- (0.022 ± 0.003 SD) T_{July} (˚C) - (0.007 ± 0.001 SD) $T_{Jan.}$ (˚C) $R^2 = 0.385$ Eq. A5.2

Interpreting the yellow perch data layer in terms of atmospheric deposition alone produces the following equation:

Yellow perch $\log_{10}$Hg (ppb) = (1.47±0.01 SD) + (0.030±0.001 SD) atm.Hg_{dep} (μg m^{-2} a^{-1})

$R^2 = 0.206$ Eq. A5.3

i.e. atmospheric deposition, by itself, accounted for only 20.6 % of the yellow perch Hg concentration variations. Adding mean annual July and January air temperatures to the regression analysis leads to a 10 % improvement as follows:

Yellow perch $\log_{10}$Hg(ppb) = (2.67± 0.06SD) + (0.025±0.001 SD) atm.Hg_{dep} (μg m^{-2} a^{-1})

- (0.050 ± 0.003 SD) T_{July} (°C) + (0.016 ± 0.01 SD) $T_{Jan.}$ (°C) $R^2 = 0.303$ Eq. A5.4

Hence, fish Hg concentration are more effectively relatable to the cross-Canada climate variations than to the corresponding atmospheric Hg deposition rate variations. Table A5.1 provides a summary of all the variables that were used in deriving the above Equations.

Checking the correlations among the above equations' variables reveals that fish Hg only has a weak correlation with T_{July} (Table 5A.2). However, factor analyzing this matrix reveals that T_{July} is nevertheless an important albeit indirect and geographically-independent co-variant of the overall fish Hg variations (Factor 2, Table 5A.3).

Table A5.1 Yellow perch log_{10}Hg concentration (ppb), lake sediment THg (ppb), GRAHM2005 mean annual net atmospheric Hg deposition rate ($atmHg_{dep}$; μg m^{-2} a^{-1}), mean annual precipitation rate (ppt, m a^{-1}), July and January air temperatures (T_{July}, $T_{Jan.}$; ˚C), and latitude and longitude (˚) of Eqs. A5.1-A5.6.

Variable	Mean	Min.	Max.	Std. Dev. **
Yellow perch log_{10}Hg, ppb (wet weight) *	1.8	1.3	2.9	0.3
Lake sediment log_{10}THg, ppb (dry weight)	1.8	1.5	2.7	0.1
ppt, m a^{-1} **	0.7	0.1	2.8	0.3
atm.Hg_{dep}, μg m^{-2} a^{-1} **	11.3	2.5	31.1	4.5
$T_{january}$, ˚C **	16.6	6.2	20.9	1.8
T_{july}, ˚C **	-19.6	-33.0	4.6	5.8
Latitude, ˚	53.4	43.9	69.4	4.6
Longitude, ˚	-93.9	-138.7	-53.8	17.0

* Fish Mercury Datalayer for Canada (FIMDAC), adopted from Depew et al. (2013 a, b) and Little et al., 2014; excluded: fish Hg concentration ≤ 10 ppb and data from the Great Lakes, rivers, and other water courses; remaining sample size: n = 3,180.

** Standard deviation (Std. Dev.); GRAHM2005 mean annual net atmospheric Hg deposition rate (atm.Hgdep., μg m^{-2} a^{-1}); mean annual precipitation rate (ppt, m a^{-1}); mean annual July temprature (T_{July}, ˚C) and January Temprature ($T_{Jan.}$ ˚C).

Table A5.2 Correlation coefficients for the variables used in the fish Hg analysis of Eqs. A5.1-A5.6.

Variable	Mean	Min.	Max.	Std. Dev. **
Yellow perch $\log_{10}$Hg, ppb (wet weight) *	1.8	1.3	2.9	0.3
Lake sediment $\log_{10}$THg, ppb (dry weight)	1.8	1.5	2.7	0.1
ppt, m a^{-1} **	0.7	0.1	2.8	0.3
atm.Hg_{dep}, μg m^{-2} a^{-1} **	11.3	2.5	31.1	4.5
$T_{january}$, °C **	16.6	6.2	20.9	1.8
T_{july}, °C **	-19.6	-33.0	4.6	5.8
Latitude, °	53.4	43.9	69.4	4.6
Longitude, °	-93.9	-138.7	-53.8	17.0

* Fish Mercury Datalayer for Canada (FIMDAC), adopted from Depew et al. (2013 a, b) and Little et al., 2014; excluded: fish Hg concentration ≤ 10 ppb and data from the Great Lakes, rivers, and other water courses; remaining sample size: n = 3,180.

** Standard deviation (Std. Dev.); GRAHM2005 mean annual net atmospheric Hg deposition rate (atm.Hgdep., μg m^{-2} a^{-1}); mean annual precipitation rate (ppt, m a^{-1}); mean annual July temprature (T_{July}, °C) and January Temprature ($T_{Jan.}$, °C).

Table A5.3 Factor analysis of the correlations of variables of fish analysis of Eqs. A5.1 to A5.6 (Table A5.2).

Variable	Factor 1	Factor 2	Communality
Yellow perch $\log_{10}$Hg, ppb (wet weight)	**0.64**	**0.47**	0.63
Lake sediment $\log_{10}$THg, ppb (dry weight)	**0.97**	0.09	0.95
ppt, m a^{-1} **	**0.95**	0.11	0.92
atm.$Hg_{dep,}$ µg m^{-2} a^{-1} **	**0.84**	0.00	0.70
$T_{Jan.,}$ $^{\circ}C$ **	**0.81**	-0.32	0.76
$T_{july,}$ $^{\circ}C$ **	0.38	**-0.86**	0.88
Latitude, $^{\circ}$ **	**-0.92**	0.25	0.91
Longitude, $^{\circ}$ **	**0.80**	0.40	0.80

* Fish Mercury Datalayer for Canada (FIMDAC), adopted from Depew et al. (2013 a, b) and Little et al., 2014; excluded: fish Hg concentration ≤ 10 ppb and data from the Great Lakes, rivers, and other water courses; remaining sample size: n = 3,180.

** GRAHM2005 mean annual net atmospheric Hg deposition rate (atm.Hgdep., µg m^{-2} a^{-1}); mean annual precipitation rate (ppt, m a^{-1}); mean annual July temprature ($T_{July,}$ $^{\circ}C$) and January Temprature ($T_{Jan.,}$ $^{\circ}C$).

Projecting the Eq. A5.1 results across Canada and overlaying the fork-length standardized yellow perch fish Hg data produces the map in Figure A5.1. The corresponding map-to- data conformance is plotted in Figure A5.2. This plot indicates that approximately 80 % of the standardized yellow perch Hg concentrations can be mapped within a conformance of factor of two, 6 times out of 10. This is somewhat lower than the mapping conformance of using Eq. 6.5 (Chapter 6) for lake sediment $\log_{10}$THg, hence fish Hg is somewhat less predictable than sediment THg. This difference would be due to additional factors that affect fish Hg uptake and retention, i.e., trophic lake–to–lake variations and related Hg uptake dynamics (Rennie *et al.,* 2009; Power *et al.*, 2002). In Figure 4.1, these differences are most noticeable from northwestern ON, across northern MB, and SK to NWT. 2002).

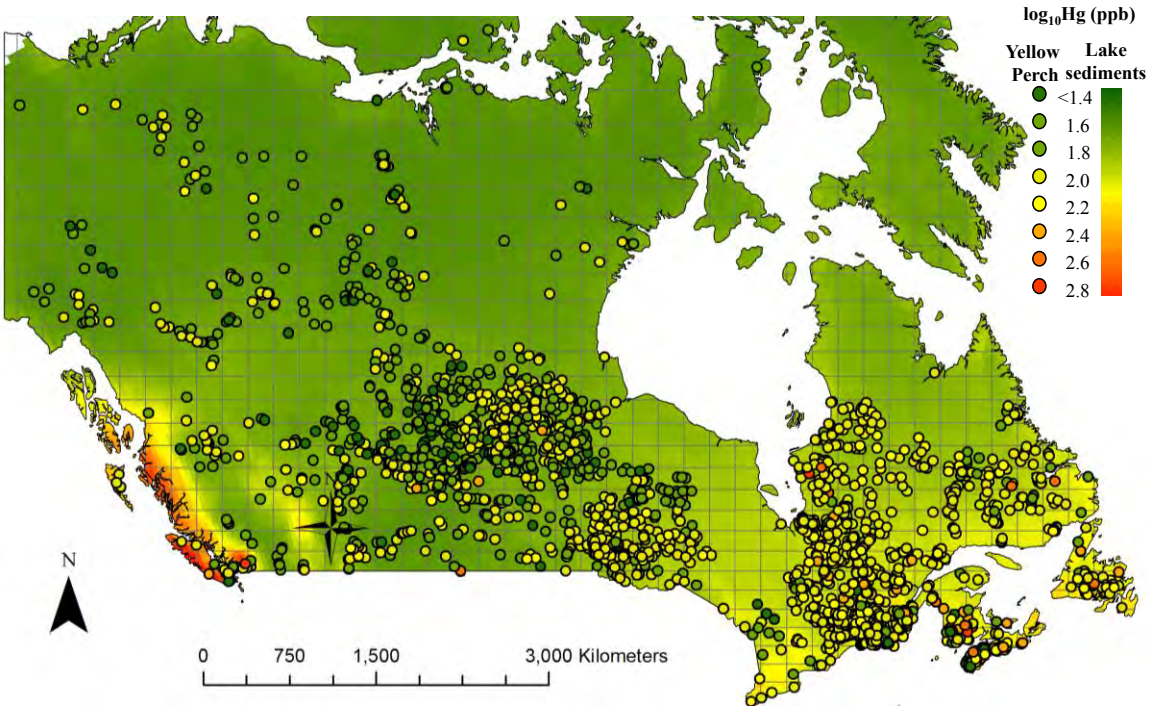

Figure A5.1 Overlaying standardized yellow perch Hg concentrations (ppb, wet weight; obtained from Fish Mercury Data layer for Canada (FIMDAC) on the corresponding Eq. A5.1 estimated map.

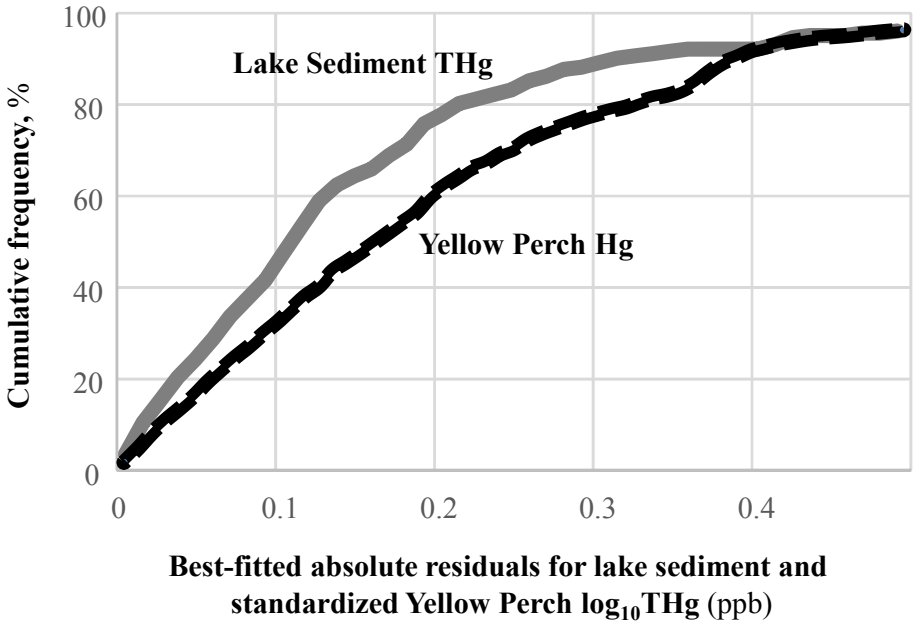

Figure A5.2 Standardized yellow perch $\log_{10}$Hg concentration (ppb) map-to-data conformance plot based on Eq. A5.1: x-axis: best-fit $\log_{10}$Hg (ppb) residuals; y-axis: cumulative frequency of the residuals. Also overlaid: the corresponding conformance plot for lake sediment $\log_{10}$THg (ppb).

2009; Power *et al.*, 2002). In Figure 4.1, these differences are most noticeable from northwestern ON, across northern MB, and SK to NWT.

Eqs. A5.1 to A5.4 account for approximately 40 % of the variations in sediment Hg and the standardized Hg concentrations in yellow perch due to combined effects of mean annual precipitation rate, mean annual temperature and/or atmospheric Hg deposition. However, it remains to be seen what part of these sediment and fish Hg affecting associations are causative. Note that the sediment THg data were generated from bulked 30 cm depth lake sediment samples. This amounts to approximately 100 years of sediment accumulation, and disregards any historical implied THg changes from the top 5 cm to the bottom 30 cm of lake sediments, as reported by Munthe *et al.* (2007).

Hence, the fish data are not aligned in time with either the sediment data or the mapped climate and atmospheric Hg deposition variations. A significant time dependency, however, is not reflected by the standardized fish data:

Yellow perch $\log_{10}$Hg(ppb) = (1.78 ± 0.01 SD) + (0.0020 ± 0.0005 SD)

$R^2 = 0.0047$ Eq. A5.7

The slight positive trend implied by Eq. A5.7 is in fact opposite to what could have been expected from the significant drop in atmospheric Hg emission and deposition since 1970 (Butler *et al.,* 2008; Environment Canada, 2014). In some areas, gradual declines in fish Hg have occurred (Rennie *et al.,* 2010). That would be in agreement with Eqs. A5.1 and A5.2 which indicate that fish and lake sediment THg should both decrease with decreasing atmospheric Hg deposition rates.

For lakes, sediment THg increases with increasing atmospheric Hg deposition have been reported by Munthe *et al.* (2007) and Muir *et al.* (2009). Concurrent increases in July temperatures, however, could compensate for at least some of increased Hg loadings on fish. Detailed studies have shown that increasing water temperatures increase the production and uptake of methyl Hg in sediments and in epilimnic and hypolimnic waters (Watras *et al*., 2005). There is also a concurrent if not sustained increase in Hg demethylation according to Trudel and Rasmussen (1997).

Declining to non–declining trends of fish Hg with respect to climate warming have been reported and discussed by French *et al. (*2006) and Rennie *et al. (*2010). These varying trends may stem from complex interactions involving changes in trophic Hg transferences, fish predation, and reductions in atmospheric and terrestrial Hg inputs into lakes. These reductions, as implied by Eqs. A5.3 and A5.4, occurred in areas that

experienced reductions in annual precipitation rate. So, while Eqs. A5.1, A5.4, A5.5 and A5.6 reveal spatial variations for fish Hg, sediment THg, atmospheric Hg deposition and precipitation rates, and air temperatures, it is not yet transparent how these variations translate into climate–induced fish Hg concentration variations over time. A major reason for this refers to the short–term difference between direct effects of climate change on atmospheric Hg deposition versus the long–term accumulation and release of atmospherically–sequestered Hg from vegetation, soils and sediments (Ter Meulen 1997; Tessrenc *et al.,* 2011; UNEP 2013 a, b; Nasr, 2014).

Conclusions

All of the above suggests that both sediments as well as fish are subject to increasing Hg accumulations with increasing atmospheric Hg deposition rates, and these accumulations are further affected by mean annual precipitation rates as well as mean annual July and January temperatures. For lake sediments, increasing mean annual July temperatures would increase sediment THg due to increased atmospheric Hg sequestration by terrestrial vegetation and aquatic organisms per upslope basin. In contrast, decreasing mean annual January temperatures would reduce the rate of loss of sequestered Hg from land and water. For fish, some of the increased Hg uptake may not necessarily lead to increased Hg concentrations due to temperature-enhanced growth rates (growth dilution) and metabolic processes that involve Hg demethylization.

For the purpose of predicting and mapping, it is shown that the NTS-tile standardized and averaged Hg concentrations in fish are more closely aligned to the

corresponding sediment THg values than to the modelled atmospheric Hg deposition values. In principle, external Hg loading factors lead to concurrent Hg accumulations in fish and in lake sediments, but sediments are generally Hg retaining, while fish experience additional external and internal Hg uptake and loss processes.

Curriculum Vitae

Mina Nasr

Education

Esfahan University
BSc, Chemistry 1999

University of New Brunswick
MSc, Forestry and Environmental Management 2007

Selected Publications

Nasr M., Arp P.A. Total mercury concentrations in stream and lake sediments across Canada. Environment. Canada Report: Canadian Mercury Science Assessment 2015; Chapter 3b. In Print.

Nasr M., Arp, P.A. Pools of mercury in forest soils, a New Brunswick case study. Environment. Canada Report: Canadian Mercury Science Assessment 2015; Chapter 3c. Submitted, In Print.

Nasr M., Arp P.A. Biomonitoring and assessing total mercury concentrations and pools in forested areas. Biomonitoring 2015. Accepted.

Nasr M., Campbell L., Depew D., Dastoor A.P., Burgess N.M., Rencz A., Arp P.A. Relating sediment Hg to fish Hg across Canada. To be submitted, subject to revisions.

Nasr M., Arp P.A. Spatial analysis of Hg levels in bulk sediment from Arctic streams and lakes. In book: Mercury in Canada's North, Chapter 5: Freshwater Environment. Editors: Chételat J., Braune. Aboriginal Affairs and Northern Development 2011; 110-111.

Nasr M., Malloch D.W., Arp P.A. Quantifying Hg within ectomycorrhizal fruiting bodies, from emergence to senescence. Fungal Biology 2012; 116: 1163-1177.

Nasr M., Ogilvie J., Castonguay M., Rencz A., Arp P.A. Total Hg concentrations in stream and lake sediments: discerning geospatial patterns and controls across Canada. Applied Geochemistry 2011; 26: 1818-1831.

Nasr M., Arp P.A. Hg concentrations and accumulations in fungal fruiting bodies, as influenced by forest soil substrates and moss carpets. Applied Geochemistry 2011; 26: 1905-1917.

Nasr M., Castonguay M., Ogilvie J., Arp P.A. Critical Loads and exceedences of acid deposition for the Georgia Basin, British Columbia. Journal of Limnology 2010; 69 (suppl. 1) 181-192.

Jutras M.F., Castonguay M., **Nasr M.**, Ogilvie J., Bhatti J. S., Arp P.A. Modeling and mapping hydrothermal regimes and potential impacts of climate change on

permafrost within the South Mackenzie Plain, Northwest Territories, Canada. Ecoscience 2014; 21: 1-14.

Jutras M.F., **Nasr M**., Castonguay M., Pit C., Pomeroy J.H., Smith T.P., Zhang C. F., Ritchie C.D., Meng F.R., Clair T.A., Arp P.A. Dissolved organic carbon concentrations and fluxes in forest catchments and streams: DOC-3 model. Ecological modelling 2011; 222: 2291-2313.

Murphy P.N.C., Castonguay M., Ogilvie J., **Nasr M.**, Hazlett P.W., Bhatti J., Arp A.P. A geospatial and temporal framework for modeling gaseous N and other N losses from forest soils and basins, with application to the Turkey Lakes Watershed Project, in Ontario, Canada. Forest Ecology and Management 2009; 258: 2304-2317. DOI:10.1016/j.foreco.2008.12.006.